INSTITUTE OF AERONAUTICAL ENGINEERING

(Autonomous)

Dundigal, Hyderabad -500 043

AERONAUTICAL ENGINEERING

COURSE LECTURE NOTES

Course Name	**AIRCRAFT STABILITY AND CONTROL**
Course Code	AAE014
Programme	B.Tech
Semester	VI
Course Coordinator	Dr. Yagya Dutta Dwivedi
Course Faculty	Dr. Yagya Dutta Dwivedi , Professor, AE Mr. S. Devraj, Assistant Professor, AE
Lecture Numbers	1-60
Topic Covered	All

COURSE OBJECTIVES:

I	Demonstrate concept of stability and application to dynamic systems like Aircraft, and the role of primary controls and secondary controls in longitudinal stability.
II	Understand the concept of slide slip angle, roll angle and yaw angle their concepts related to lateral-directional stability.
III	Learn about the mathematical modeling of an aircraft in longitudinal, lateral and directional cases.
IV	Estimate the longitudinal and directional parameters with the help of the linearized equations of aircraft motion.
V	Analyze the different type of modes in longitudinal, lateral and directional motion of aircraft, and recovery from those modes.

COURSE LEARNING OUTCOMES (CLOs):

CLO Code	CLO	Description
AAE11.01	CLO 1	Apply concept of stability, controllability and maneuverability in an aircraft.
AAE11.02	CLO 2	Use and interpret the basic mathematics, science and engineering for solving problems of longitudinal, lateral and directional static stability.
AAE11.03	CLO 3	Describe stick fixed and stick free conditions for neutral point.

Source from Yechout, T.R. "Introduction to Aircraft Flight Mechanics", AIAA education Series, 2003

AAE11.04	CLO 4	Demonstrate different methods for finding static margin, control force and CG limitation.
AAE11.05	CLO 5	Organize total stability parameters in order of merit of flight conditions.
AAE11.06	CLO 6	Locate the cause of instability in an aircraft and solve the issue.
AAE11.07	CLO 7	Identify aircraft different types of stability for different categories of aircraft
AAE11.08	CLO 8	Demonstrate the aircraft component contribution for different stability.
AAE11.09	CLO 9	Discuss and identify the stability problems of aircraft in different phases.
AAE11.10	CLO 10	Relate different stability criteria and do the comparative study.
AAE11.11	CLO 11	Interpret the concept behind equations of motions in different frame of references.
AAE11.12	CLO 12	Appraise the factors that enhance the stability of aircraft during different flight regime.
AAE11.13	CLO 13	Create new concept of the stability in new configuration and type of aircrafts.
AAE11.14	CLO 14	Describe the effects of forces and moments in disturbed or perturbed conditions on the stability.
AAE11.15	CLO 15	Discuss the concept of linearization of equation of motion and aerodynamic forces and moments.

SYLLABUS

UNIT I	**INTRODUCTION AND LONGITUDINAL STABILITY-I**
Aircraft axes system, Definition: Equilibrium, stability, controllability, & maneuverability. Examples from simple mechanical systems for stability. Longitudinal static stability and dynamic stability for un accelerated flight. Criteria for longitudinal static stability and trim condition. Contribution of Principle components. Equations of equilibrium- stick fixed neutral point, elevator angle required to trim. Definition-static margin. Equations of motion in steady, symmetric pull-up maneuver, elevator effectiveness, elevator hinge moment, neutral point, maneuver point, static margin for stick fixed and stick free conditions, control force and control gradient. Trim tabs and types of trim tabs, Aerodynamic and mass balancing of control surfaces, forward and aft most limits of CG.	
UNIT II	**LATERAL-DIRECTIONAL STATIC STABILITY**
Introduction to lateral-direction stability- aerodynamic forces and moments, aircraft side force due to side slip, aircraft rolling moment due to side slip, and aircraft yawing moment due to side slip. Aircraft component contribution, directional static stability, Aircraft component contribution for lateral-directional stability, rudder requirements.	
UNIT III	**AIRCRAFT EQUATION OF MOTION**
UNIT IV	**LINEARIZATION OF EQUATIONS OF MOTION AND AERODYNAMIC FORCES AND MOMENTS DERIVATIVES**
Description of state of motion of vehicle, forces and moments as perturbations over prescribed reference flight condition. Equation of motion in perturbation variables. Assumption of small perturbations, first order approximations-linearization equations of motion. Linearised of force and moment equation of motion Linearised longitudinal and lateral-directional equations of perturbed motion. Significance of aerodynamic derivatives. Derivatives of axial, normal force components	

Source from Yechout, T.R. "Introduction to Aircraft Flight Mechanics", AIAA education Series, 2003

and pitching moment with respect to the velocity, angle of attack, angle of attack rate, pitch rate, elevator angle.

UNIT V	AIRCRAFT DYNAMIC STABILITY

Principle modes of motion characteristics, mode shapes and significance, time constant, undamped natural frequency and damping ratio- mode shapes- significance. One degree of freedom, two degree of freedom approximations- constant speed (short period), constant angle of attack (long period) approximations- solutions. Determination of longitudinal and lateral stability from coefficients of characteristic equation- stability and lateral stability from coefficients of characteristics equation- stability criteria, Aircraft spin- entry, balance of forces in steady spin, recovery, pilot techniques.

Text Books

1. Yechout, T.R.et al., "Introduction to Aircraft Flight Mechanics", AIAA education Series, 2003, ISBN 1-56347-577-4.
2. Nelson, R.C., "Flight Stability and Automatic Control", 2nd Edn., Tata McGraw Hill, 2007, ISBN 0-07-066110-3.
3. Etkin, B and Reid, L.D., "Dynamics of Flight", 3rd Edn., John Wiley, 1998, ISBN0-47103418-5.

UNIT –I

INTRODUCTION AND LONGITUDINAL STABILITY

1.1 Aircraft Axes System

An aircraft in flight is free to rotate in three dimensions: *yaw*, nose left or right about an axis running up and down; *pitch*, nose up or down about an axis running from wing to wing; and *roll*, rotation about an axis running from nose to tail. The axes are alternatively designated as *vertical*, *transverse*, and *longitudinal* respectively. These axes move with the vehicle and rotate relative to the Earth along with the craft. These definitions were analogously applied to spacecraft when the first manned spacecraft were designed in the late 1950s.

The definition of military aircraft mission payloads may cover a wide range of possibilities including personnel, troops, support equipment and supplies in transport aircraft and internally carried stores, externally carried stores and sensor pods on combat aircraft.

These rotations are produced by torques (or moments) about the principal axes. On an aircraft, these are intentionally produced by means of moving control surfaces, which vary the distribution of the net aerodynamic force about the vehicle's center of gravity. Elevators (moving flaps on the horizontal tail) produce pitch, a rudder on the vertical tail produces yaw, and ailerons (flaps on the wings that move in opposing directions) produce roll. On a spacecraft, the moments are usually produced by a reaction control system consisting of small rocket thrusters used to apply asymmetrical thrust on the vehicle.

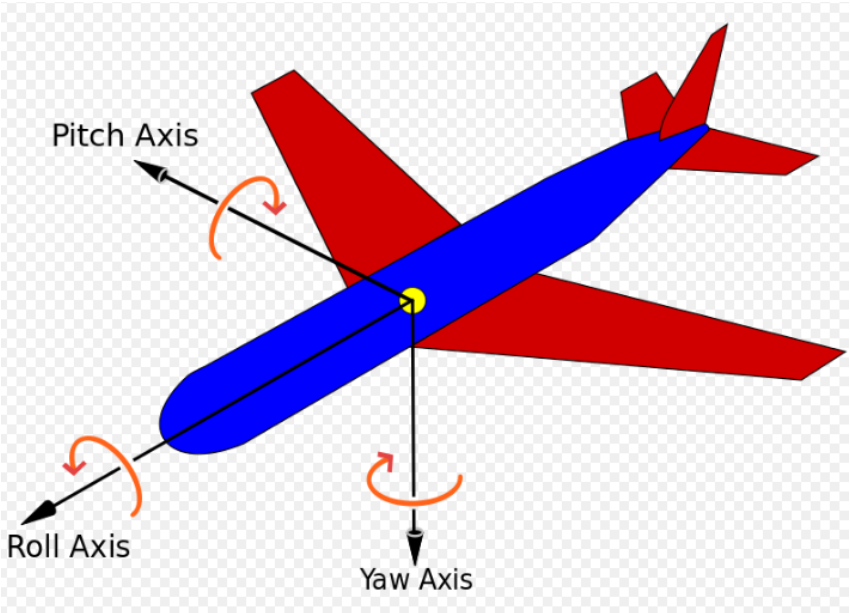

Fig1.1 Aircraft Axes System

Source from Yechout, T.R. "Introduction to Aircraft Flight Mechanics", AIAA education Series, 2003

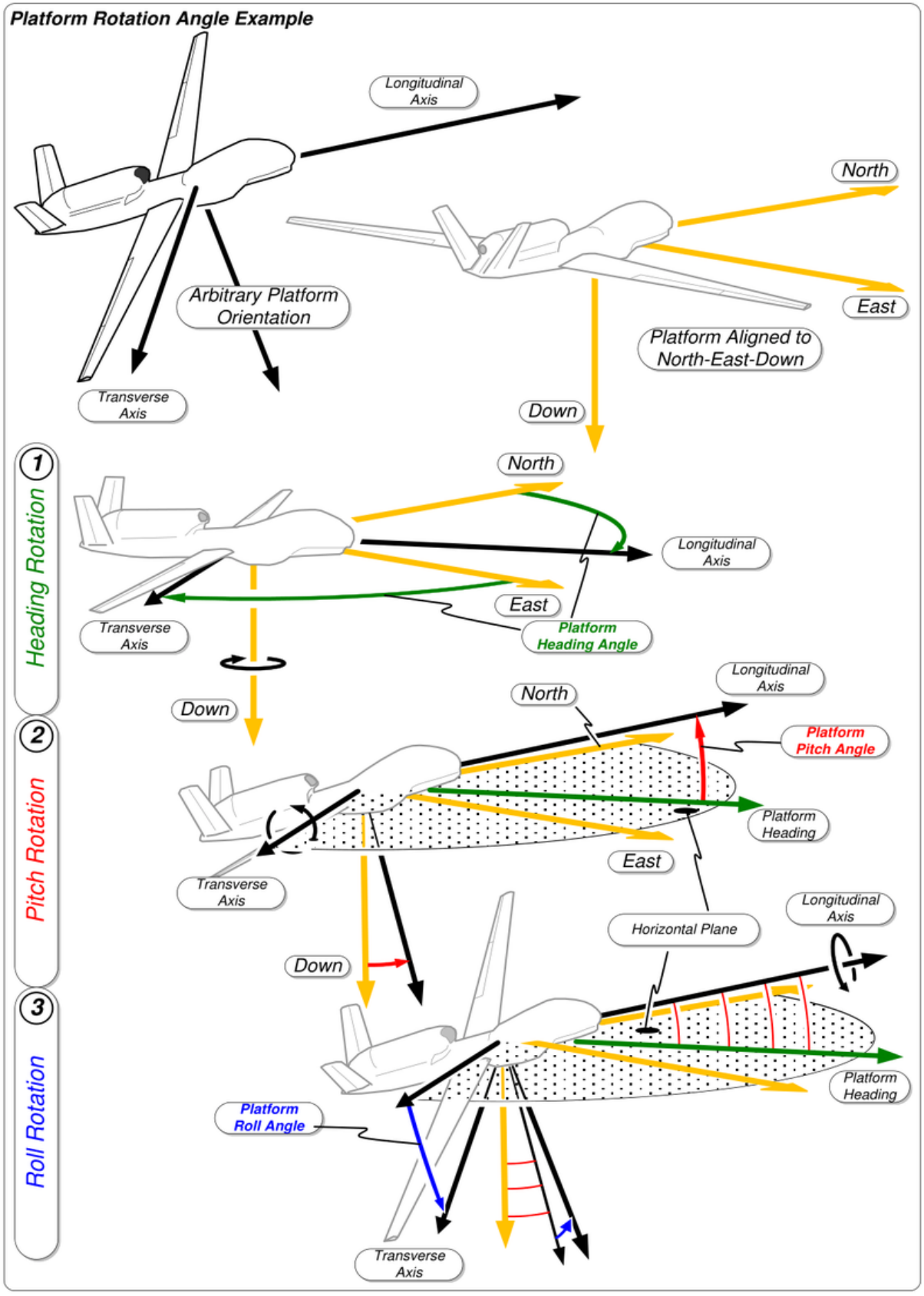

Fig 1.2 Axes system in different rotation of aircraft

Source from Yechout, T.R. "Introduction to Aircraft Flight Mechanics", AIAA education Series, 2003

1.2 Principle Axes

- **Normal axis,** or yaw axis — an axis drawn from top to bottom, and perpendicular to the other two axes. Parallel to the *fuselage station*.

- **Transverse axis**, lateral axis, or pitch axis — an axis running from the pilot's left to right in piloted aircraft, and parallel to the wings of a winged aircraft. Parallel to the *buttock line*.

- **Longitudinal axis**, or roll axis — an axis drawn through the body of the vehicle from tail to nose in the normal direction of flight, or the direction the pilot faces. Parallel to the *waterline*.

Normally, these axes are represented by the letters X, Y and Z in order to compare them with some reference frame, usually named x, y, z. Normally, this is made in such a way that the X is used for the longitudinal axis Fig 1.1.

1.2.1 Vertical axis (yaw)

The position of all three axes, with the right-hand rule for its rotations

The yaw axis has its origin at the center of gravity and is directed towards the bottom of the aircraft, perpendicular to the wings and to the fuselage reference line. Motion about this axis is called yaw. A positive yawing motion moves the nose of the aircraft to the right.[1][2] The rudder is the primary control of yaw.[3]

The term *yaw* was originally applied in sailing, and referred to the motion of an unsteady ship rotating about its vertical axis. Its etymology is uncertain.

1.2.2 Transverse axis (pitch)

The **pitch axis** (also called **transverse** or **lateral axis** has its origin at the center of gravity and is directed to the right, parallel to a line drawn from wingtip to wingtip. Motion about this axis is called **pitch**. A positive pitching motion raises the nose of the aircraft and lowers the tail. The elevators are the primary control of pitch.

1.2.3 Longitudinal axis (roll)

Source from Yechout, T.R. "Introduction to Aircraft Flight Mechanics", AIAA education Series, 2003

The **roll axis** (or **longitudinal axis)** has its origin at the center of gravity and is directed forward, parallel to the fuselage reference line. Motion about this axis is called **roll**. An angular displacement about this axis is called **bank**. A positive rolling motion lifts the left wing and lowers the right wing. The pilot rolls by increasing the lift on one wing and decreasing it on the other. This changes the bank angle. The ailerons are the primary control of bank. The rudder also has a secondary effect on bank.

1.3 Definitions

1.3.1 Equilibrium

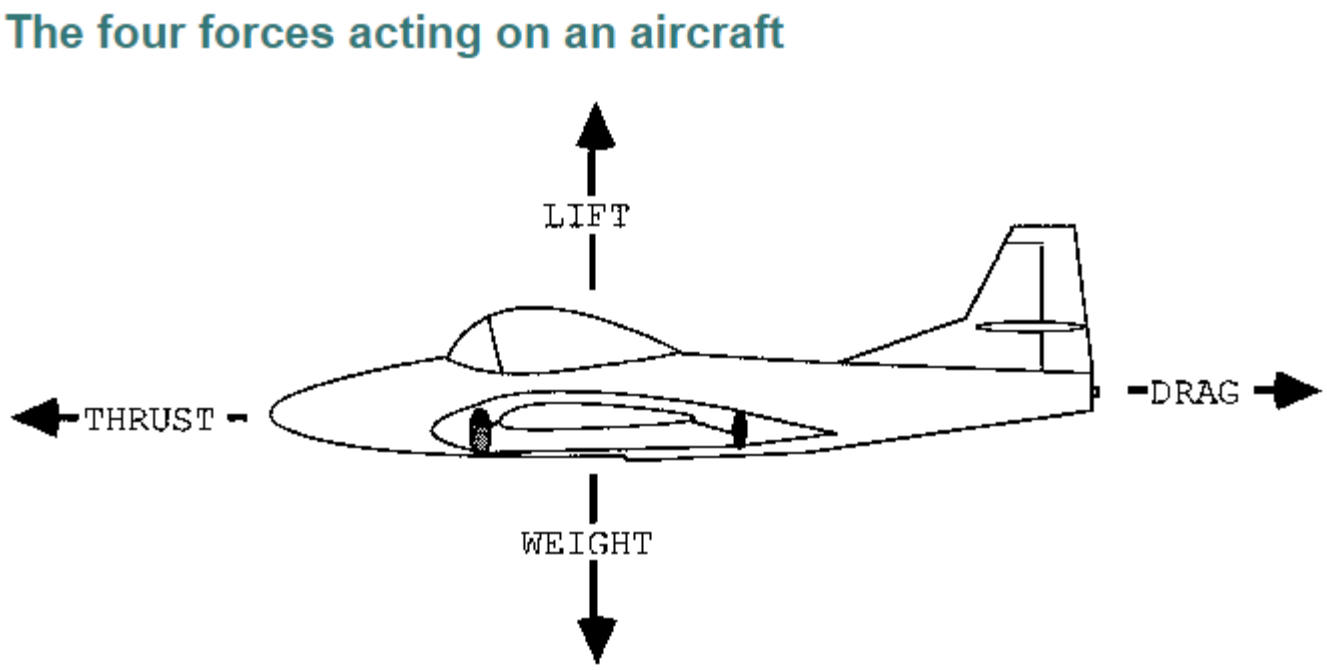

Fig 1.3 Four forces acting on an aircraft for equilibrium

Introduction

Kinds of Equilibrium

There are three types of equilibrium, namely stable, neutral and unstable equilibrium. Prof. Schumpeter explains the three positions with a simple illustration of a ball placed in three different states. According to Schumpeter, “A ball that rests at the bottom of a bowl

Source from Yechout, T.R. “Introduction to Aircraft Flight Mechanics”, AIAA education Series, 2003

illustrates the first case; a ball that rests on a billiard table, the second case, and a ball that is perched on the top of an inverted bowl, the third case."

Figure 1

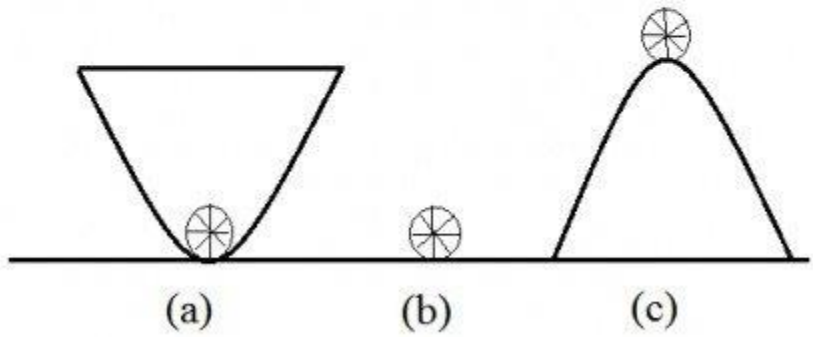

in figure 1(a), the ball is comfort at the base of the bowl. It remains in stable equilibrium. If interfered, the ball is going to rest at its original position again. In figure 1(b), the ball is located on a billiard table. It shows neutral equilibrium. If perturbed, the ball is going to find its balance at another new position. In figure 1(c), the ball is stabilized on top of the upturned bowl. It is basically in unstable equilibrium. If interrupted, the ball will certainly move down either side of the bowl and fails to get back to its original position.

Conditions for equilibrium

Maintaining a steady flight requires a balance and is often described as an equilibrium of all the forces acting upon an aircraft.

In a steady flight, the sum of all the opposing forces equals to zero. There can be no unbalance forces when the aircraft is flying level or when it is climbing or descending (Newton's Third Law). This does not mean that all the four forces are equal. It means that the opposing forces are equal.

- **L = W**
- **D = T**

If the lift is greater then the lift, the aircraft will accelerate downward. When the thrust is greater than drag, the aircraft will accelerate forward. If the drag is greater then the thrust, a deceleration will occur.

Source from Yechout, T.R. "Introduction to Aircraft Flight Mechanics", AIAA education Series, 2003

An aircraft in powered flight can be said to be under the influence of the four main forces:

Lift (L)

Lift of main planes, acting vertically upwards through the Centre of Pressure. The main purpose of lift is to keep the aircraft airborne.

Lift is a mechanical force whereby it is generated by the interaction and contact of a solid body with a fluid (liquid or gas). In order for lift to be generated, its solid body must be in contact with the fluid. When there is no fluid, there is no lift. It does not apply for a Space Shuttle.

Lift is generated by different velocity between the solid object and the fluid. There must be motion between the fluid and the object. If there is no motion, there will be no lift. Lift acts perpendicular to the motion whereas drag acts in the direction opposite to the motion. (National Aeronautics and Space Administration)

1.2 Weight (W)

Weight , acting vertically downwards through the Centre of Gravity of aircraft.

Drag (D)

Drag, acting horizontally backwards opposing forward motion.

There are 2 components under drag:

- **Induced drag**, which is caused from the creation of lift and increases with the angle of attack. When the wing is not producing lift, induced drag is zero and it decreases with airspeed.

- **Parasite drag**, which is all drag not caused from the production of lift. Parasite drag is created by displacement of air by the aircraft, turbulence generated by the airfoil, and the hindrance of airflow as it passes over the surface of the aircraft or components. It increases with the speed and includes skin friction drag, interference drag and form drag.

Thrust (T)

Thrust, of engine(s) pulling(or pushing) the aircraft horizontally forwards. It is a force provided by the engines which is required to overcome drag (D).

Source from Yechout, T.R. "Introduction to Aircraft Flight Mechanics", AIAA education Series, 2003

Understanding the difficulties in balancing the four forces

While weight always acts vertically downwards, lift acts vertically upwards only during level (horizontal) flight. Lift is inclined backwards during climb and forwards during descent. Furthermore, the centre of pressure and centre of gravity also change in the course of flight. Line of action of thrust and drag are also similarly affected by the attitude of aircraft.

The role intended for the aircraft determines the relative position of its main planes, engines, etc. Consider a low-winged aircraft with fixed landing gear and engine mounted on its nose. It is very likely to have its drag centreline below that of thrust, resulting in nose down pitch (moment) during level flight. Lift and weight are deliberately coupled to provide nose down pitch for safety reasons.

Stable equilibrium

Definition of stable equilibrium. :

A state of equilibrium of a body (such as a pendulum hanging directly downward from its point of support) such that when the body is slightly displaced it tends to return to its original position — compare unstable equilibrium.

Definition of **unstable equilibrium**

A state of equilibrium of a body (as a pendulum standing directly upward from its point of support) such that when the body is slightly displaced it departs further from the original position

Source from Yechout, T.R. "Introduction to Aircraft Flight Mechanics", AIAA education Series, 2003

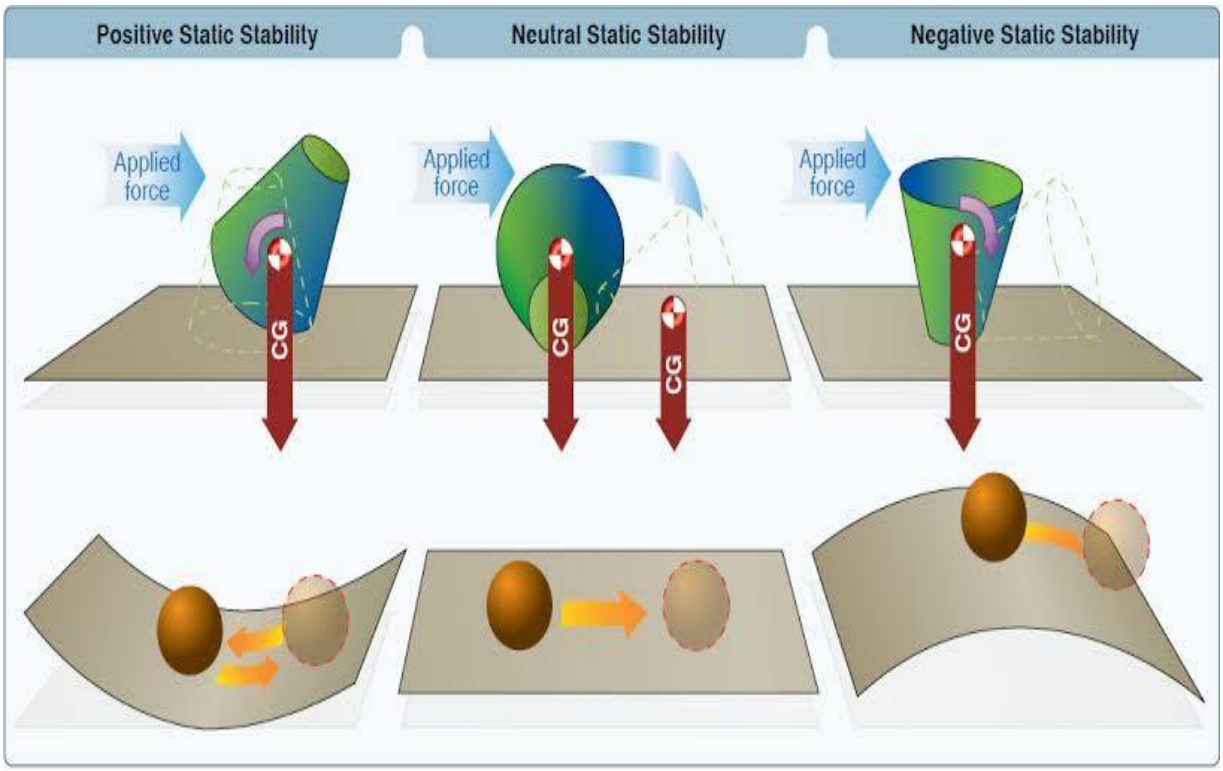

Definition of Maneuverability

Maneuverability

Airplanes are not limited to being a relatively fast means of getting somewhere. Long ago thrill-seeking pilots discovered that aircraft have the potential for providing loads of fun while getting nowhere fast. Aerobatics are an essential skill for fighter pilots; and the training that it gives to pilots in position orientation and judgment is considered so vital that a great deal of time is spent teaching these maneuvers. Maneuverability is defined as the ability to change the speed and flight direction of an airplane. A highly maneuverable airplane, such as a fighter, has a capability to accelerate or slow down very quickly, and also to turn sharply. Quick turns with short turn radii place high loads on the wings as well as the pilot. These loads are referred to as "g forces" and the ability to "pull g's" is considered one measure of maneuverability. One g is the force acting on the airplane in level flight imposed by the gravitational pull of the earth. Five g in a maneuver exerts 5 times the gravitational force of the earth

Source from Yechout, T.R. "Introduction to Aircraft Flight Mechanics", AIAA education Series, 2003

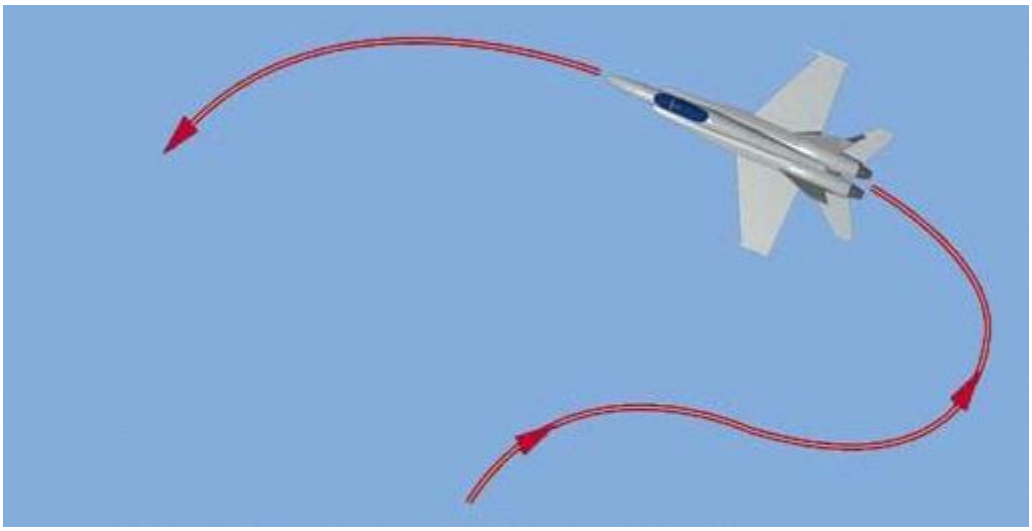

Fig: Maneuvarability

Aileron Roll

The aileron roll is simply a 360 degree roll accomplished by putting in and maintaining coordinated aileron pressure. The maneuver is started slightly nose high because, as the airplane rolls, its lift vector is no longer countering its weight, so the nose of the airplane drops significantly during the maneuver. Back stick pressure is maintained throughout so that even when upside down, positive seat pressure (about 1 G) will be felt. As the airplane approaches wings-level at the end of the maneuver, aileron pressure is removed and the roll stops.

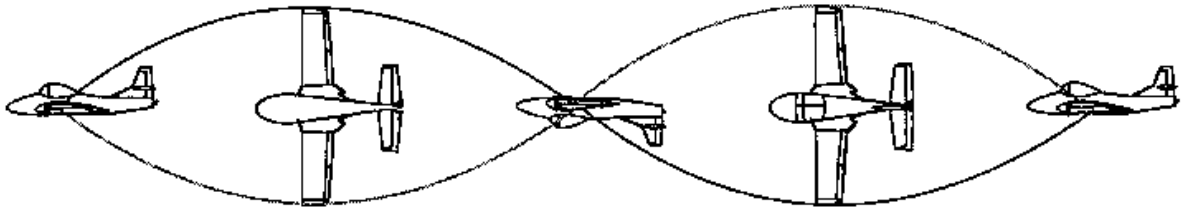

Fig: Aileron roll

Loop

A loop is simply a 360 degree change in pitch. Because the airplane will climb several thousand feet during the maneuver, it is started at a relatively high

Source from Yechout, T.R. "Introduction to Aircraft Flight Mechanics", AIAA education Series, 2003

airspeed and power setting (if these are too low, the airspeed will decay excessively in the climb and the maneuver will have to be discontinued.) The pilot, once satisfied with the airspeed and throttle setting, will pull back on the stick until about three Gs are felt. The nose of the airplane will go up and a steadily increasing climb will be established. As the maneuver continues, positive G is maintained by continuing to pull. The airplane continues to increase its pitch until it has pitched through a full circle. When the world is right-side-up again, the pilot releases the back stick pressure and returns the aircraft to level flight.

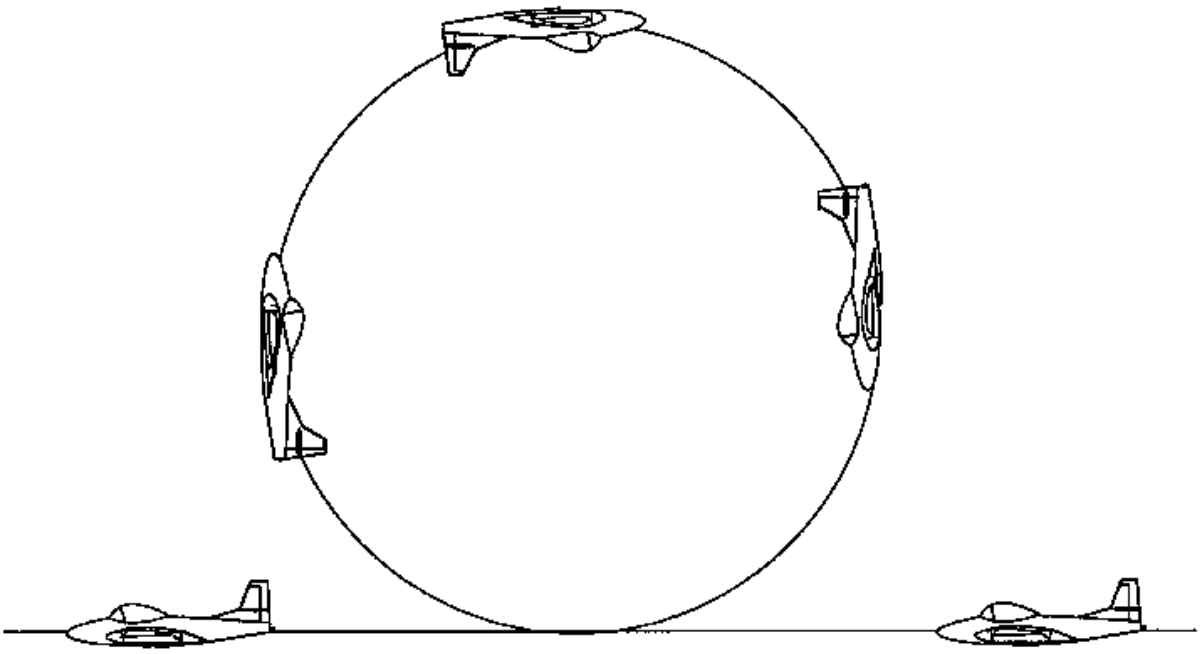

Fig: Loop

Controllability

Controllability: the response of an aircraft in steady flight, on pilot control inputs. For instance deflecting the ailerons: a high resulting roll rate means a fast response. Generally, an aircraft becomes less controllable, especially at slow flight speeds, as the CG is **moved further aft (my emphasis).** An aircraft that cleanly recovers from a prolonged spin with the CG at one position may fail completely to respond to normal recovery attempts when the CG is moved aft by one or two inches.

Source from Yechout, T.R. "Introduction to Aircraft Flight Mechanics", AIAA education Series, 2003

Aerodynamic maneuverability vs supermaneuverability

Traditional aircraft maneuvering is accomplished by altering the flow of air passing over the control surfaces of the aircraft—the ailerons, elevators, flaps, air brakes and rudder. Some of these control surfaces can be combined—such as in the "ruddervators" of a V-tail configuration—but the basic properties are unaffected. When a control surface is moved to present an angle to the oncoming airflow, it alters the airflow around the surface, changing its pressure distribution, and thus applying a pitching, rolling, or yawing moment to the aircraft.

The angle of control surface deflection and resulting directional force on the aircraft are controlled both by the pilot and the aircraft's inbuilt control systems to maintain the desired attitude, such as pitch, roll and heading, and also to perform aerobatic maneuvers that rapidly change the aircraft's attitude. For traditional maneuvering control to be maintained, the aircraft must maintain sufficient forward velocity and a sufficiently low angle of attack to provide airflow over the wings (maintaining lift) and also over its control surfaces.

As airflow decreases so does effectiveness of the control surfaces and thus the maneuverability. If the angle of attack exceeds its critical value, the airplane will stall. Pilots are trained to avoid stalls during aerobatic maneuvering and especially in combat, as a stall can permit an opponent to gain an advantageous position while the stalled aircraft's pilot attempts to recover.

The speed at which an aircraft is capable of its maximum aerodynamic maneuverability is known as the corner airspeed; at any greater speed the control surfaces cannot operate at maximum effect due to either airframe stresses or induced instability from turbulent airflow over the control surface. At lower speeds the redirection of air over control surfaces, and thus the force applied to maneuver the aircraft, is reduced below the airframe's maximum capacity and thus the aircraft will not turn at its maximum rate. It is therefore desirable in aerobatic maneuvering to maintain corner velocity.

Contribution of the aircraft Components for longitudinal stability

Wing Contribution:

Aerodynamic properties of airfoils

The basic features of a typical airfoil section are sketched in Fig. 2.2. The longest straight line from the trailing edge to a point on the leading edge of the contour defines the chord line. The length of this line is called simply the chord c. The locus of points midway between the upper and lower surfaces is called the mean line, or camber line. For a symmetric airfoil, the camber and chord lines coincide. 2.3. For low speeds (i.e., Mach numbers $M << 1$), and at high Reynolds numbers $Re = V c/\nu >> 1$, the results of thin-

Source from Yechout, T.R. "Introduction to Aircraft Flight Mechanics", AIAA education Series, 2003

airfoil theory predict the lifting properties of airfoils quite accurately for angles of attack not too near the stall. Thin-airfoil theory predicts a linear relationship between the section lift coefficient and the angle of attack α of the form

$$c\ell = a0\ (\alpha - \alpha 0)$$

as shown in Fig. 2.3. The theory also predicts the value of the lift-curve slope

$$a0 = \partial c\ell\ \partial\alpha = 2\pi \qquad (2.15)$$

Thickness effects (not accounted for in thin-airfoil theory) tend to increase the value of a0, while viscous effects (also neglected in the theory) tend to decrease the value of a0. The value of a0 for realistic conditions is, as a result of these counter-balancing effects, remarkably close to 2π for most practical airfoil shapes at the high Reynolds numbers of practical flight. The angle α0 is called the angle for zero lift, and is a function only of the shape of the camber line. Increasing (conventional, sub-sonic) camber makes the angle for zero lift α0 increasingly negative. For camber lines of a given family (i.e., shape), the angle for zero lift is very nearly proportional to the magnitude of camber – i.e., to the maximum deviation of the camber line from the chord line. A second important result from thin-airfoil theory concerns the location of the aerodynamic center . The aerodynamic center of an airfoil is the point about which the pitching moment, due to the distribution of aerodynamic forces acting on the airfoil surface, is independent of the angle of attack. Thin-airfoil theory tells us that the aerodynamic center is located on the chord line, one quarter of the way from the leading to the trailing edge – the so-called quarter-chord point. The value of the pitching moment about the aerodynamic center can also be determined from thin-airfoil theory, but requires a detailed calculation for each specific shape of camber line. Here, we simply note that, for a given shape of camber line the pitching moment about the aerodynamic center is proportional to the amplitude of the camber, and generally is negative for conventional subsonic (concave down) camber shapes. It is worth emphasizing that thin-airfoil theory neglects the effects of viscosity and, therefore, cannot predict the behavior of airfoil stall, which is due to boundary layer separation at high angles of attack. Nevertheless, for the angles of attack usually encountered in controlled flight, it provides a very useful approximation for the lift.

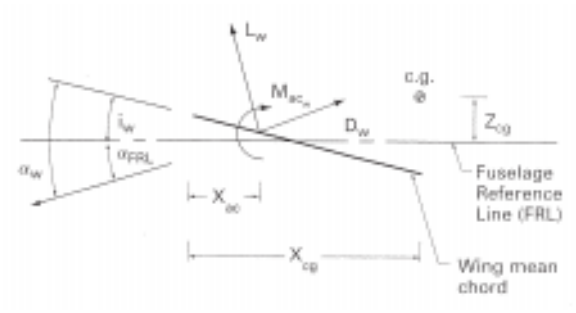

The wing is a lifting surface which produces both **Lift** and **Drag**.

- Lift is perpendicular to free-stream velocity.
  - If $\alpha_{FRL} > 0$, then lift vector pitches forward (nose-down direction) in the body-fixed frame.
- Drag is parallel to free-stream velocity.
  - If $\alpha_{FRL} > 0$, then drag also rotates in the nose-down direction.

To determine the contributions of Lift and drag in the body-fixed frame, these forces must be *rotated* by the angle of attack and any additional wing inclination.

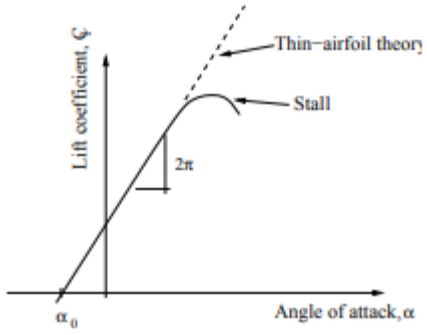

Fig: Airfoil section lift coefficient as a function of angle of attack.

Source from Yechout, T.R. "Introduction to Aircraft Flight Mechanics", AIAA education Series, 2003

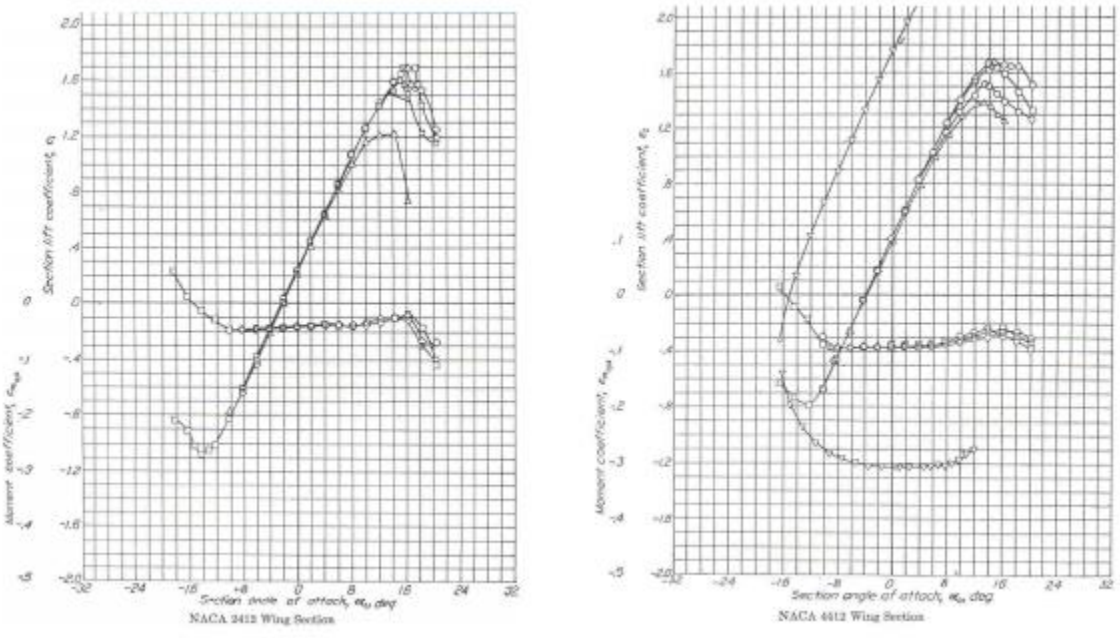

Fig: Airfoil lift and moment coefficients as a function of angle of attack; wind tunnel data for two cambered airfoil sections. Data from Abbott & von Doenhoff [1].

Finally, wind tunnel data for two cambered airfoil sections are presented in Fig. 2.4. Both airfoils have the same thickness distributions and camber line shapes, but the airfoil on the right has twice as much camber as the one on the left (corresponding to 4 per cent chord, versus 2 per cent for the airfoil on the left). The several curves correspond to Reynolds numbers ranging from Re = 3 × 106 to Re = 9×106 , with the curves having larger values of $c\ell max$ corresponding to the higher Reynolds numbers. The outlying curves in the plot on the right correspond to data taken with a 20 per cent chord split flap deflected (and are not of interest here). Note that these data are generally consistent with the results of thin-airfoil theory. In particular: 1. The lift-curve slopes are within about 95 per cent of the value of $a0 = 2\pi$ over a significant range of angles of attack. Note that the angles of attack in Fig. 2.4 are in degrees, whereas the $a0 = 2\pi$ is per radian; 2. The angle for zero lift of the section having the larger camber is approximately twice that of the section having the smaller camber; and 3. The moment coefficients measured about the quarter-chord point are very nearly independent of angle of attack, and are roughly twice as large for the airfoil having the larger camber.

Aerodynamic properties of finite wings

The vortex structures trailing downstream of a finite wing produce an induced downwash field near the wing which can be characterized by an induced angle of attack

$$\alpha i = CL\ \pi eAR \qquad (2.16)$$

For a straight (un-swept) wing with an elliptical spanwise loading, lifting-line theory predicts that the induced angle of attack αi is constant across the span of the wing, and the efficiency factor e = 1.0. For non-elliptical span loadings, e < 1.0, but for most practical wings αi is still nearly constant across the span. Thus, for a finite wing lifting-line theory predicts that

$$CL = a0\ (\alpha - \alpha0 - \alpha i) \qquad (2.17)$$

where a0 is the wing section lift-curve slope and α0 is the angle for zero lift of the section. Substituting Eq. (2.16) and solving for the lift coefficient gives

$$CL = a0\ 1 + a0\ \pi eAR\ (\alpha - \alpha0) = a(\alpha - \alpha0) \qquad (2.18)$$

whence the wing lift-curve slope is given by

$$a = \partial CL\ \partial\alpha = a0\ 1 + a0\ \pi eAR \qquad (2.19)$$

Lifting-line theory is asymptotically correct in the limit of large aspect ratio, so, in principle, Eq. (2.18) is valid only in the limit as AR → ∞. At the same time, slender-body theory is valid in the limit of vanishingly small aspect ratio, and it predicts, independently of planform shape, that the lift-curve slope is

$$a = \pi AR/\ 2 \qquad (2.20)$$

Note that this is one-half the value predicted by the limit of the lifting-line result, Eq. (2.19), as the aspect ratio goes to zero. We can construct a single empirical formula that contains the correct limits for both large and small aspect ratio of the form

$$a = \pi AR\ 1 + r\ 1 + {}^{3}\ \pi AR\ a0\ {}'2 \qquad (2.21)$$

A plot of this equation, and of the lifting-line and slender-body theory results, is shown in Fig. 2.5. Equation (2.21) can also be modified to account for wing sweep and the effects of compressibility. If the sweep of the quarter-chord line of the planform is Λc/4, the effective section incidence is increased by the factor 1/ cos Λc/4, relative to that of the wing,1while the dynamic pressure of the flow normal to the quarter-chord line is reduced by the factor cos2 Λc/4. The section lift-curve slope is thus reduced by the factor cos Λc/4, and a version of Eq. (2.21) that accounts for sweep can be written

$$a = \pi AR\ 1 + r\ 1 + {}^{3}\ \pi AR\ a0\ \cos\ \Lambda c/4\ {}'2 \qquad (2.22)$$

Source from Yechout, T.R. "Introduction to Aircraft Flight Mechanics", AIAA education Series, 2003

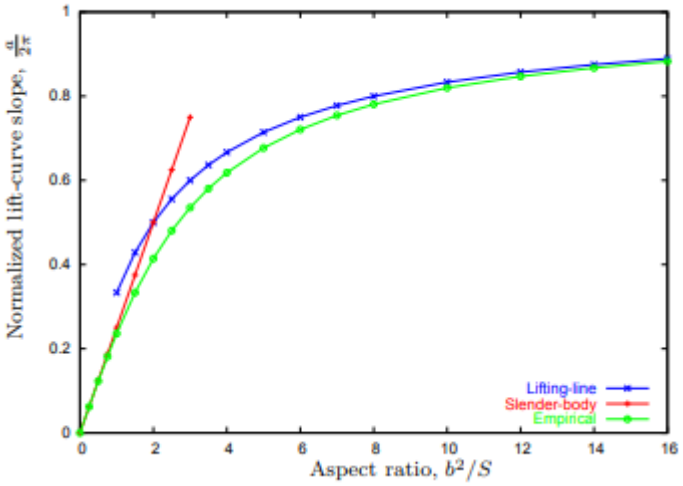

Fig**:** Empirical formula for lift-curve slope of a finite wing compared with lifting-line and slender-body limits. Plot is constructed assuming a0 = 2π.

Fuselage contribution

Fuselage contribution to pitch stiffness The contribution of the fuselage to the pitching moment is affected by interference effects with the wing flow field. These can be estimated using a simple strip theory (as described, for example, in Example 2.2 of the text by Nelson [4]), but here we will introduce a simple estimate for the destabilizing effect of the fuselage in the absence of interference effects. Slender-body theory predicts a distribution of lifting force given by

$$\frac{\mathrm{d}L}{\mathrm{d}x} = 2Q\alpha\frac{\mathrm{d}S_f}{\mathrm{d}x}$$

where Sf = πw2/4 is the equivalent cross-sectional area of the fuselage based on its width w as a function of the streamwise variable x. For a finite-length fuselage, Eq. (2.30) predicts positive lift on the forward part of the fuselage (where Sf is generally increasing), and negative lift on the rearward part (where Sf is generally decreasing), but the total lift is identically zero (since Sf (0) = Sf (ℓf) = 0, where ℓf is the fuselage length). Since the total lift acting on the fuselage is zero, the resulting force system is a pure couple, and the pitching moment will be the same, regardless of the reference point about which it is taken. Thus, e.g., taking the moment about the fuselage nose (x = 0), we have

Source from Yechout, T.R. "Introduction to Aircraft Flight Mechanics", AIAA education Series, 2003

$$M_f = -\int_0^{\ell_f} x\,\mathrm{d}L = -2Q\alpha\int_0^{\ell_f} x\,\mathrm{d}S_f = 2Q\alpha\int_0^{\ell_f} S_f\,\mathrm{d}x = 2Q\alpha\mathcal{V} \qquad (2.31)$$

where V is the volume of the "equivalent" fuselage (i.e., the body having the same planform as the actual fuselage, but with circular cross-sections). The fuselage contribution to the vehicle pitching moment coefficient is then

$$\mathbf{C}_m = \frac{M_f}{Q S \bar{c}} = \frac{2\mathcal{V}}{S\bar{c}}\alpha \qquad (2.32)$$

and the corresponding pitch stiffness is

$$\mathbf{C}_{m_\alpha} = \left(\frac{\partial \mathbf{C}_m}{\partial \alpha}\right)_{\text{fuse}} = \frac{2\mathcal{V}}{S\bar{c}} \qquad (2.33)$$

Note that this is always positive – i.e., destabilizing.

Wing-tail interference

The one interference effect we will account for is that between the wing and the horizontal tail. Because the tail operates in the downwash field of the wing (for conventional, aft-tail configurations), the effective angle of attack of the tail is reduced. The reduction in angle of attack can be estimated to be

$$\varepsilon = \kappa\frac{\mathbf{C}_L}{\pi e \mathbf{AR}} \qquad (2.34)$$

where $1 < \kappa < 2$. Note that $\kappa = 1$ corresponds to $\varepsilon = \alpha i$, the induced angle of attack of the wing, while $\kappa = 2$ corresponds to the limit when the tail is far downstream of the wing. For stability considerations, it is the rate of change of tail downwash with angle of attack that is most important, and this can be estimated as

$$\frac{\mathrm{d}\varepsilon}{\mathrm{d}\alpha} = \frac{\kappa}{\pi e \mathbf{AR}}\left(\mathbf{C}_{L\alpha}\right)_{\text{wing}} \qquad (2.35)$$

Control Surfaces

Source from Yechout, T.R. "Introduction to Aircraft Flight Mechanics", AIAA education Series, 2003

Aerodynamic control surfaces are usually trailing-edge flaps on lifting surfaces that can be deflected by control input from the pilot (or autopilot). Changes in camber line slope near the trailing edge of a lifting surface are very effective at generating lift. The lifting pressure difference due to trailing-edge flap deflection on a two-dimensional airfoil, calculated according to thin-airfoil theory, is plotted in Fig. 2.7 (a) for flap chord lengths of 10, 20, and 30 percent of the airfoil chord. The values plotted

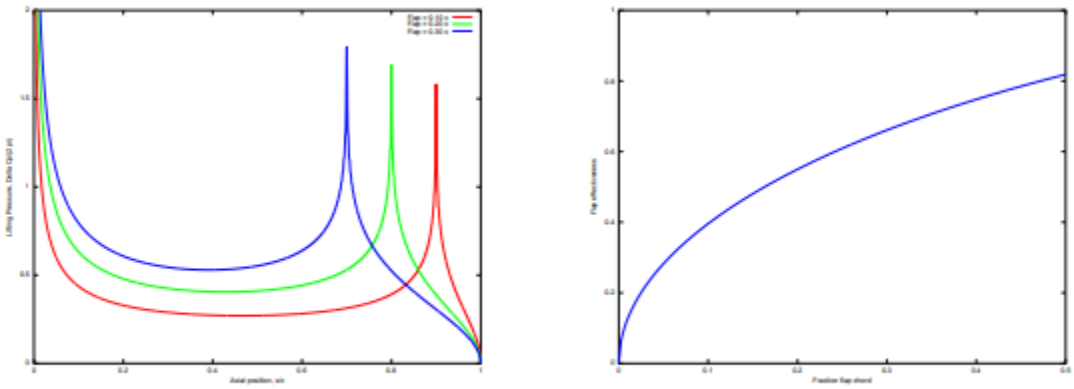

(a) Lifting pressure coefficient (b) Control effectiveness

Fig. Lifting pressure distribution due to flap deflection and resulting control effectiveness

are per unit angular deflection, and normalized by 2π, so their integrals can be compared with the changes due to increments in angle of attack. Figure 2.7 (b) shows the control effectiveness

$$\frac{\partial \mathbf{C}_\ell}{\partial \delta} \qquad (2.36)$$

also normalized by 2π. It is seen from this latter figure that deflection of a flap that consists of only 25 percent chord is capable of generating about 60 percent of the lift of the entire airfoil pitched through an angle of attack equal to that of the flap deflection. Actual flap effectiveness is, of course, reduced somewhat from these ideal values by the presence of viscous effects near the airfoil trailing edge, but the flap effectiveness is still nearly 50 percent of the lift-curve slope for a 25 percent chord flap for most actual flap designs. The control forces required to change the flap angle are related to the aerodynamic moments about the hinge-line of the flap. The aerodynamic moment about the hinge line is usually expressed in terms of the dimensionless hinge moment coefficient, e.g., for the elevator hinge moment He, defined as

Source from Yechout, T.R. "Introduction to Aircraft Flight Mechanics", AIAA education Series, 2003

$$\mathbf{C}_{h_e} \equiv \frac{H_e}{\frac{1}{2}\rho V^2 S_e c_e} \tag{2.37}$$

where Se and ce are the elevator planform area and chord length, respectively; these are based on the area of the control surface aft of the hinge line. The most important characteristics related to the hinge moments are the restoring tendency and the floating tendency. The restoring tendency is the derivative of the hinge moment coefficient with respect to control deflection; e.g., for the elevator,

$$\mathbf{C}_{h_{\delta_e}} = \frac{\partial \mathbf{C}_{h_e}}{\partial \delta_e} \tag{2.38}$$

The floating tendency is the derivative of the hinge moment coefficient with respect to angle of attack; e.g., for the elevator,

$$\mathbf{C}_{h_{e\alpha_t}} = \frac{\partial \mathbf{C}_{h_e}}{\partial \alpha_t} \tag{2.39}$$

where αt is the angle of attack of the tail.

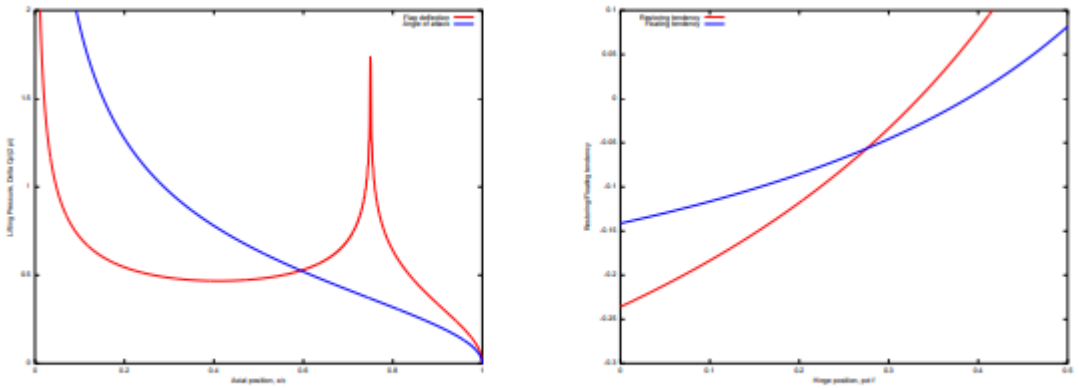

(a) Lifting pressure coefficient (b) Hinge moment derivatives

Fig. Lifting pressure distributions (normalized by 2π) due to flap deflection and to change in angle of attack, and resulting restoring and floating tendencies of control flap. Results of thin-airfoil theory for 25 percent chord trailing-edge flap.

The restoring and floating tendencies are due primarily to the moments produced about the control flap hinge line by the lifting pressures induced by changes in either control position or angle of attack. The thin-airfoil approximations to these lifting pressure distributions are illustrated in Fig. 2.8 (a) for a 25 percent chord trailing edge flap. The

Source from Yechout, T.R. "Introduction to Aircraft Flight Mechanics", AIAA education Series, 2003

plotted values of ΔCp are normalized by 2π, so the average value of the ΔCp due to angle of attack change is unity (corresponding to a lift curve slope of 2π). Figure 2.8 (b) illustrates the corresponding floating and restoring tendencies as functions of the hinge line location, measured in fraction of flap chord. It is seen that both tendencies are negative for hinge lines located ahead of approximately the 33 percent flap chord station. While these results, based on inviscid, thin-airfoil theory are qualitatively correct, actual hinge moment coefficients are affected by viscous effects and leakage of flow between the flap and the main lifting surface, so the results presented here should be used only as a guide to intuition.

1.2.1 EFFECTS OF CONTROL MOVEMENTS

Knowing what happens when the controls are operated is the most basic skill of piloting. It is also among the most misunderstood. When an airplane is flying, it has a good deal of forward speed and airflow over all of its surfaces. Control movements must be understood in terms of this airflow and its effects.

The Elevator

The elevator controls the Angle of Attack [AOA] of the wings, and subsequently the pitch. Pulling back on the stick results in a down force on the tail (the same thing is operating here that was operating on the wings, only in a different direction). If the controls are reversed, the opposite happens.

Backward stick movement forces the tail down and the nose up. This rotation occurs around the center of gravity of the airplane. Initially the airplane, even though its nose is up, is still headed in the same direction - the only thing that has changed is the angle of attack. But an increase in the angle of attack results in an increase in lift, so now the airplane starts to go up. Then, like an arrow, it points into the wind, increasing its pitch. This process continues, viewed from the cockpit as an increase in pitch, until the pilot moves the stick forward to a neutral position and stabilizes the pitch.

The temptation to think that the stick directly raises or lowers the nose is very strong, and most of the time, roughly correct. But if the stick is moved back when the airplane is very close to the stall the aircraft will not pitch up much, if at all. This back stick movement and increase in AOA will stall the wing, causing a loss of lift and acceleration downward: now the pitch moves opposite the stick movement.

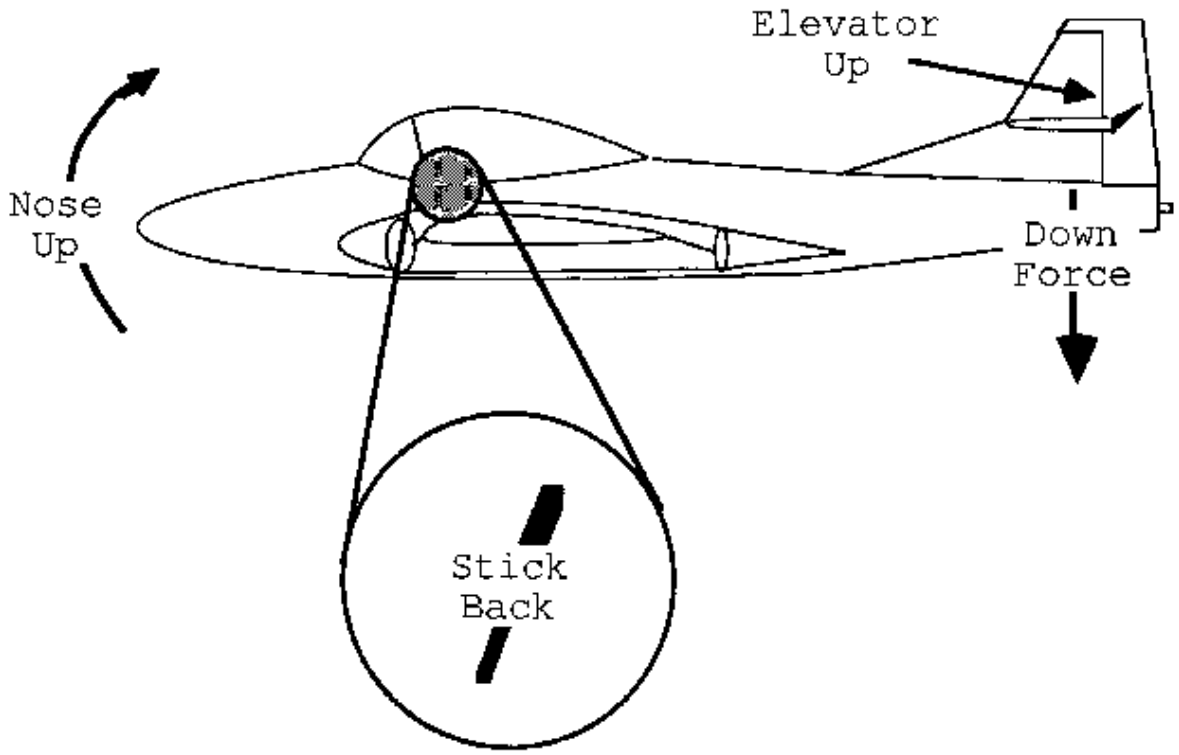

Effects of Back Stick Movement

Fig: Elevator effect

The Ailerons

The ailerons are a much simpler control than the elevator. Located near the wing tips on the trailing edge of the wing, they are used in unison to change the amount of lift each wing is producing and roll the airplane.

When the pilot moves the stick side-to-side from center, the ailerons move in opposite directions. In a roll to the right (as viewed from the cockpit), the right aileron goes up and the left aileron goes down. Each aileron serves to change how that part of the wing deflects the air and thus increases or decreases the amount of lift produced by each wing. The down aileron forces the air down harder, resulting in an increase in lift and the up aileron decreases the downward force, resulting in a decrease in lift. In the case of a right roll, the decreased lift on the right side and increased lift on the left side result in a roll to the right.

Operating the ailerons causes an effect called adverse yaw. Adverse yaw is the result of an increase in drag on the wing with the down aileron, or "upgoing" wing. This wing, since it is forcing the air down harder than the "downgoing" wing and producing more lift, also produces more drag. The drag pulls

the wing back and causes yaw. If this yaw is not corrected with rudder, the roll is said to be "uncoordinated."

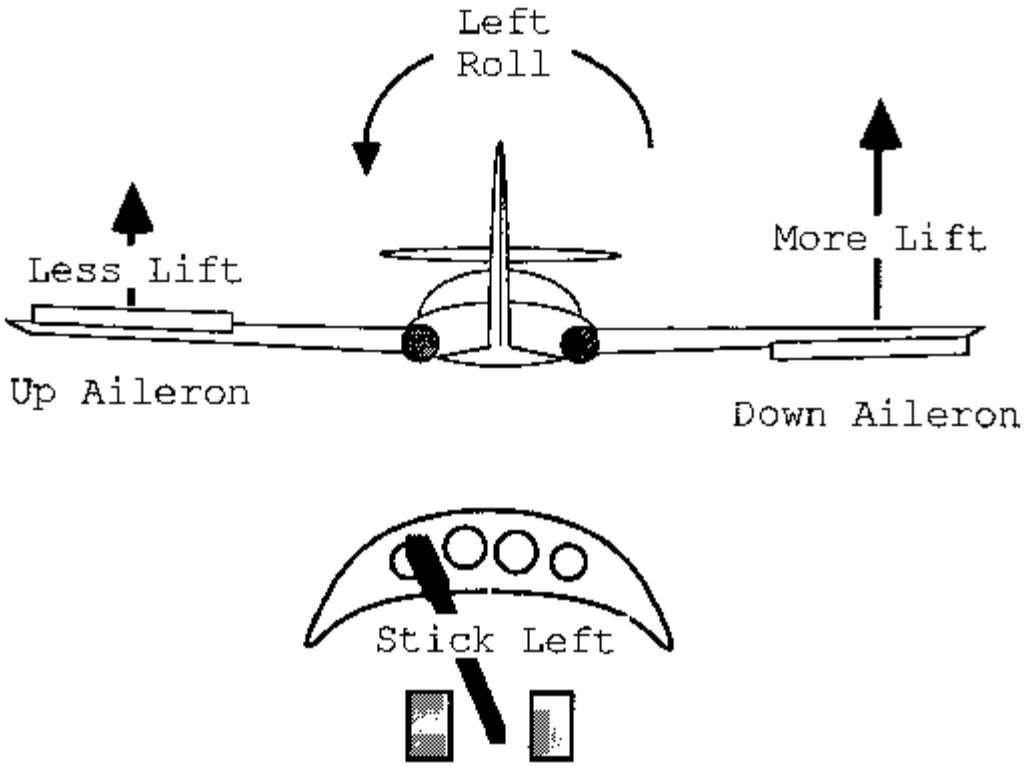

Fig: Aileron effect

The Rudder

The rudder is controlled by the "rudder pedals" located on the floor of the aircraft. They are both connected to the rudder so that when one or the other pedals is depressed, it moves the rudder in the desired direction. The rudder, connected to the vertical stabilizer, then starts to deflect air much like a wing, only the resulting force is to the side. This force causes a change in yaw. As mentioned earlier, the rudder is not used very often, but when it is needed (e.g., in a crosswind), its presence is appreciated.

Control Fixed Stability

Even for the controls-fixed case, our text is a bit careless with nomenclature and equations, so we review the most important results for this case here. We have seen that for the analysis of longitudinal stability, terms involving products of the drag coefficient and either vertical displacements of the vehicle center-of-gravity or sines of the angle of attack can be neglected. Then, with the axial locations as specified in Fig. 3.1 the pitching moment about the vehicle c.g. can be written

$$\mathbf{C}_{m_{cg}} = \mathbf{C}_{m0_w} + \mathbf{C}_{L_w}\left(\frac{x_{cg}}{\bar{c}} - \frac{x_{ac}}{\bar{c}}\right) - \eta\frac{S_t}{S}\mathbf{C}_{L_t}\left[\frac{\ell_t}{\bar{c}} - \left(\frac{x_{cg}}{\bar{c}} - \frac{x_{ac}}{\bar{c}}\right)\right] + \mathbf{C}_{m_f} \qquad (3.1)$$

where we assume that Cm0t = 0, since the tail is usually symmetrical. Note that, as is the usual convention when analyzing static longitudinal stability and control, the positive direction of the x-axis is taken to be aft; 1 thus, e.g., the second term on the right-hand side of Eq. (3.1) contributes to a positive (nose-up) pitching moment for positive lift when the c.g. is aft of the wing aerodynamic center.

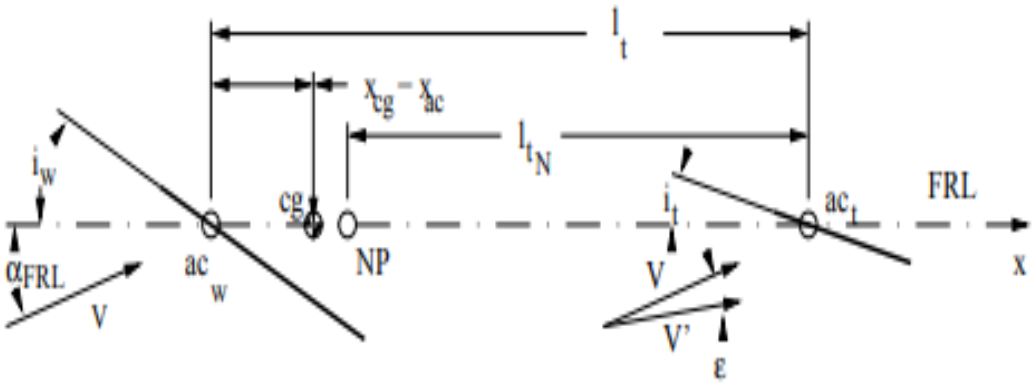

Fig: 3.1: Geometry of wing and tail with respect to vehicle c.g., basic neutral point, and wing aerodynamic center. Note that positive direction of the x-axis i

$$\mathbf{C}_{m_{cg}} = \mathbf{C}_{m0_w} + \left(\frac{x_{cg}}{\bar{c}} - \frac{x_{ac}}{\bar{c}}\right)\left[\mathbf{C}_{L_w} + \eta\frac{S_t}{S}\mathbf{C}_{L_t}\right] - \eta V_H \mathbf{C}_{L_t} + \mathbf{C}_{m_f} \qquad (3.2)$$

where VH = ℓtSt cS¯ is the tail volume parameter . Note that this definition is based on the distance between the aerodynamic centers of the wing and tail, and is therefore independent of the vehicle c.g. location. Note that the total vehicle lift coefficient.

Source from Yechout, T.R. "Introduction to Aircraft Flight Mechanics", AIAA education Series, 2003

$$\mathbf{C}_L = \frac{L_w + L_t}{QS} = \mathbf{C}_{L_w} + \eta \frac{S_t}{S} \mathbf{C}_{L_t} \tag{3.3}$$

where $\eta = Q_t/Q$ is the tail efficiency factor, and this total vehicle lift coefficient is exactly the quantity appearing in the square brackets in Eq. (3.2). Now, we can introduce the dependence of the lift coefficients on angle of attack as

$$\begin{aligned} \mathbf{C}_{L_w} &= \mathbf{C}_{L_{\alpha_w}} (\alpha_{FRL} + i_w - \alpha_{0_w}) \\ \mathbf{C}_{L_t} &= \mathbf{C}_{L_{\alpha_t}} \left(\alpha_{FRL} + i_t - \left[\varepsilon_0 + \frac{\mathrm{d}\varepsilon}{\mathrm{d}\alpha} \alpha_{FRL} \right] \right) \end{aligned} \tag{3.4}$$

Note that, consistent with the usual use of symmetric sections for the horizontal tail, we have assumed $\alpha_{0_t} = 0$. Introducing these expressions into Eq. (3.3), the latter can be expressed as

$$\mathbf{C}_L = \mathbf{C}_{L_{\alpha_w}} (i_w - \alpha_{0_w}) + \eta \frac{S_t}{S} \mathbf{C}_{L_{\alpha_t}} (i_t - \varepsilon_0) + \left(\mathbf{C}_{L_{\alpha_w}} + \eta \frac{S_t}{S} \left[1 - \frac{\mathrm{d}\varepsilon}{\mathrm{d}\alpha} \right] \mathbf{C}_{L_{\alpha_t}} \right) \alpha_{FRL} \tag{3.5}$$

This equation has the form

$$\mathbf{C}_L = \mathbf{C}_{L0} + \mathbf{C}_{L_\alpha} \alpha_{FRL} \tag{3.6}$$

where the *vehicle* lift curve slope is

$$\mathbf{C}_{L_\alpha} = \mathbf{C}_{L_{\alpha_w}} + \eta \frac{S_t}{S} \left(1 - \frac{\mathrm{d}\varepsilon}{\mathrm{d}\alpha} \right) \mathbf{C}_{L_{\alpha_t}} \tag{3.7}$$

and

$$\mathbf{C}_{L0} = \mathbf{C}_{L_{\alpha_w}} (i_w - \alpha_{0_w}) + \eta \frac{S_t}{S} \mathbf{C}_{L_{\alpha_t}} (i_t - \varepsilon_0) \tag{3.8}$$

is the vehicle lift coefficient at zero (fuselage reference line) angle of attack. Finally, if we define the vehicle angle of attack relative to the angle of attack for zero *vehicle* lift, i.e.,

$$\alpha \equiv \alpha_{FRL} - \alpha_0 \tag{3.9}$$

Source from Yechout, T.R. "Introduction to Aircraft Flight Mechanics", AIAA education Series, 2003

where

$$\alpha_0 = -\frac{\mathbf{C}_{L0}}{\mathbf{C}_{L\alpha}} \tag{3.10}$$

then

$$\mathbf{C}_L = \mathbf{C}_{L\alpha}\alpha \tag{3.11}$$

where $\mathbf{C}_{L\alpha}$ is the vehicle lift curve slope, given by Eq. (3.7).

Introducing the angle of attack into Eq. (3.2), the expression for the vehicle pitching moment coefficient becomes

$$\begin{aligned}\mathbf{C}_{m_{cg}} =& \mathbf{C}_{m0_w} + \left(\frac{x_{cg}}{\bar{c}} - \frac{x_{ac}}{\bar{c}}\right)\left[\mathbf{C}_{L\alpha_w}(i_w - \alpha_{0_w}) + \eta\frac{S_t}{S}\mathbf{C}_{L\alpha_t}(i_t - \varepsilon_0)\right] - \eta V_H \mathbf{C}_{L\alpha_t}(i_t - \varepsilon_0) + \\ & \left\{\left(\frac{x_{cg}}{\bar{c}} - \frac{x_{ac}}{\bar{c}}\right)\left[\mathbf{C}_{L\alpha_w} + \eta\frac{S_t}{S}\left(1 - \frac{d\varepsilon}{d\alpha}\right)\mathbf{C}_{L\alpha_t}\right] - \eta V_H\left(1 - \frac{d\varepsilon}{d\alpha}\right)\mathbf{C}_{L\alpha_t} + \mathbf{C}_{m\alpha_f}\right\}\alpha_{FRL}\end{aligned} \tag{3.12}$$

This can be expressed in terms of the angle of attack from zero vehicle lift as

$$\begin{aligned}\mathbf{C}_{m_{cg}} = & \mathbf{C}_{m0_w} + \left(\frac{x_{cg}}{\bar{c}} - \frac{x_{ac}}{\bar{c}}\right)\left[\mathbf{C}_{L\alpha_w}(i_w - \alpha_{0_w}) + \eta\frac{S_t}{S}\mathbf{C}_{L\alpha_t}(i_t - \varepsilon_0)\right] - \eta V_H \mathbf{C}_{L\alpha_t}(i_t - \varepsilon_0) \\ & + \mathbf{C}_{m\alpha}\alpha_0 + \left\{\left(\frac{x_{cg}}{\bar{c}} - \frac{x_{ac}}{\bar{c}}\right)\mathbf{C}_{L\alpha} - \eta V_H \mathbf{C}_{L\alpha_t}\left(1 - \frac{d\varepsilon}{d\alpha}\right) + \mathbf{C}_{m\alpha_f}\right\}\alpha\end{aligned} \tag{3.13}$$

This equation has the form

$$\mathbf{C}_m = \mathbf{C}_{m0} + \mathbf{C}_{m\alpha}\alpha \tag{3.14}$$

with the *vehicle* pitching moment coefficient at zero lift

$$\mathbf{C}_{m0} = \mathbf{C}_{m0_w} + \left(\frac{x_{cg}}{\bar{c}} - \frac{x_{ac}}{\bar{c}}\right)\left[\mathbf{C}_{L\alpha_w}(i_w - \alpha_{0_w}) + \eta\frac{S_t}{S}\mathbf{C}_{L\alpha_t}(i_t - \varepsilon_0)\right] - \eta V_H \mathbf{C}_{L\alpha_t}(i_t - \varepsilon_0) + \mathbf{C}_{m\alpha}\alpha_0 \tag{3.15}$$

and the vehicle pitch stiffness

$$\mathbf{C}_{m\alpha} = \left(\frac{x_{cg}}{\bar{c}} - \frac{x_{ac}}{\bar{c}}\right)\mathbf{C}_{L\alpha} - \eta V_H \mathbf{C}_{L\alpha_t}\left(1 - \frac{d\varepsilon}{d\alpha}\right) + \mathbf{C}_{m\alpha_f} \tag{3.16}$$

Note that Eq. (3.15) can be simplified (using Eq. (3.16)) to

$$\mathbf{C}_{m0} = \mathbf{C}_{m0_w} - \eta V_H \mathbf{C}_{L\alpha_t}\left[i_t - \varepsilon_0 + \left(1 - \frac{d\varepsilon}{d\alpha}\right)\alpha_0\right] + \mathbf{C}_{m\alpha_f}\alpha_0 \tag{3.17}$$

Note that Eq. (3.17) correctly shows that the pitching moment at zero net vehicle lift is independent of the c.g. location, as it must be (since at zero lift the resultant aerodynamic force must sum to a pure couple).

The basic (or control-fixed) *neutral point* is defined as the c.g. location for which the vehicle is neutrally stable in pitch – i.e., the c.g. location for which the pitch stiffness goes to zero. From Eq. (3.16) the neutral point is seen to be located at

$$\frac{x_{NP}}{\bar{c}} = \frac{x_{ac}}{\bar{c}} + \eta V_H \frac{\mathbf{C}_{L\alpha_t}}{\mathbf{C}_{L\alpha}}\left(1 - \frac{d\varepsilon}{d\alpha}\right) - \frac{\mathbf{C}_{m\alpha_f}}{\mathbf{C}_{L\alpha}} \tag{3.18}$$

Source from Yechout, T.R. "Introduction to Aircraft Flight Mechanics", AIAA education Series, 2003

Note that Eq. (3.16) for the pitch stiffness can be expressed as

$$\mathbf{C}_{m_\alpha} = \left\{ \frac{x_{\text{cg}}}{\bar{c}} - \left[\frac{x_{\text{ac}}}{\bar{c}} + \eta V_H \frac{\mathbf{C}_{L\alpha_t}}{\mathbf{C}_{L_\alpha}} \left(1 - \frac{\mathrm{d}\varepsilon}{\mathrm{d}\alpha} \right) - \frac{\mathbf{C}_{m_{\alpha_f}}}{\mathbf{C}_{L_\alpha}} \right] \right\} \mathbf{C}_{L_\alpha} \tag{3.19}$$

where the quantity in square brackets is exactly the location of the basic neutral point, as shown in Eq. (3.18). Thus, we can write

$$\mathbf{C}_{m_\alpha} = \left\{ \frac{x_{\text{cg}}}{\bar{c}} - \frac{x_{NP}}{\bar{c}} \right\} \mathbf{C}_{L_\alpha} \tag{3.20}$$

or, alternatively,

$$\frac{\partial \mathbf{C}_m}{\partial \mathbf{C}_L} = -\left(\frac{x_{NP}}{\bar{c}} - \frac{x_{\text{cg}}}{\bar{c}} \right) \tag{3.21}$$

Thus, the pitch stiffness, measured with respect to changes in vehicle lift coefficient, is proportional to the distance between the c.g. and the basic neutral point. The quantity in parentheses on the right-hand side of Eq. (3.21), i.e., the distance between the vehicle c.g. and the basic neutral point, expressed as a percentage of the wing mean aerodynamic chord, is called the vehicle *static margin*.[2]

Static Longitudinal Control

The elevator is the aerodynamic control for pitch angle of the vehicle, and its effect is described in terms of the *elevator effectiveness*

$$a_e = \frac{\partial \mathbf{C}_{L_t}}{\partial \delta_e} \tag{3.22}$$

where $\mathbf{C}_{L_t}$ is the lift coefficient of the horizontal tail and δ_e is the elevator deflection, considered positive trailing edge down. The horizontal tail lift coefficient is then given by

$$\mathbf{C}_{L_t} = \frac{\partial \mathbf{C}_{L_t}}{\partial \alpha_t} (\alpha + i_t - \varepsilon) + a_e \delta_e \tag{3.23}$$

and the change in *vehicle* lift coefficient due to elevator deflection is

$$\mathbf{C}_{L_{\delta_e}} = \eta \frac{S_t}{S} a_e \tag{3.24}$$

while the change in vehicle pitching moment due to elevator deflection is

$$\begin{aligned} \mathbf{C}_{m_{\delta_e}} &= -\eta \frac{S_t}{S} a_e \left[\frac{\ell_t}{\bar{c}} + \frac{x_{\text{ac}} - x_{\text{cg}}}{\bar{c}} \right] \\ &= -\mathbf{C}_{L_{\delta_e}} \left[\frac{\ell_t}{\bar{c}} + \frac{x_{\text{ac}} - x_{\text{cg}}}{\bar{c}} \right] \end{aligned} \tag{3.25}$$

The geometry of the moment arm of the tail lift relative to the vehicle c.g. (which justifies the second term in Eq. (3.25)) is shown in Fig. 3.1.

The vehicle is in equilibrium (i.e., is trimmed) at a given lift coefficient $\mathbf{C}_{L_{\text{trim}}}$ when

$$\begin{aligned} \mathbf{C}_{L_\alpha} \alpha + \mathbf{C}_{L_{\delta_e}} \delta_e &= \mathbf{C}_{L_{\text{trim}}} \\ \mathbf{C}_{m_\alpha} \alpha + \mathbf{C}_{m_{\delta_e}} \delta_e &= -\mathbf{C}_{m_0} \end{aligned} \tag{3.26}$$

Source from Yechout, T.R. "Introduction to Aircraft Flight Mechanics", AIAA education Series, 2003

These two equations can be solved for the unknown angle of attack and elevator deflection to give

$$\alpha_{\text{trim}} = \frac{-\mathbf{C}_{L_{\delta_e}}\mathbf{C}_{m0} - \mathbf{C}_{m_{\delta_e}}\mathbf{C}_{L\text{trim}}}{\Delta}$$
$$\delta_{\text{trim}} = \frac{\mathbf{C}_{L_\alpha}\mathbf{C}_{m0} + \mathbf{C}_{m_\alpha}\mathbf{C}_{L\text{trim}}}{\Delta} \tag{3.27}$$

where

$$\Delta = -\mathbf{C}_{L_\alpha}\mathbf{C}_{m_{\delta_e}} + \mathbf{C}_{m_\alpha}\mathbf{C}_{L_{\delta_e}} \tag{3.28}$$

Note that the parameter

$$\begin{aligned}\Delta &= -\mathbf{C}_{L_\alpha}\mathbf{C}_{m_{\delta_e}} + \mathbf{C}_{m_\alpha}\mathbf{C}_{L_{\delta_e}} \\ &= -\mathbf{C}_{L_\alpha}\left[-\mathbf{C}_{L_{\delta_e}}\left(\frac{\ell_t}{\bar{c}} + \frac{x_{\text{ac}} - x_{\text{cg}}}{\bar{c}}\right)\right] + \mathbf{C}_{L_\alpha}\left(\frac{x_{\text{cg}} - x_{NP}}{\bar{c}}\right)\mathbf{C}_{L_{\delta_e}} \\ &= \mathbf{C}_{L_\alpha}\mathbf{C}_{L_{\delta_e}}\left(\frac{\ell_t}{\bar{c}} + \frac{x_{\text{ac}} - x_{NP}}{\bar{c}}\right) = \mathbf{C}_{L_\alpha}\mathbf{C}_{L_{\delta_e}}\frac{\ell_{t_N}}{\bar{c}}\end{aligned} \tag{3.29}$$

where

$$\ell_{t_N} = \ell_t + x_{\text{ac}} - x_{NP} \tag{3.30}$$

is the distance from the basic neutral point to the tail aerodynamic center. Thus, the parameter Δ is independent of the vehicle c.g. location, and is seen to be positive for conventional (aft tail) configurations, and negative for canard (forward tail) configurations.

An important derivative related to handling qualities is the control position gradient for trim, which can be seen from the second of Eqs. (3.27) to be given by

$$\left(\frac{\mathrm{d}\delta_e}{\mathrm{d}\mathbf{C}_L}\right)_{\text{trim}} = \frac{\mathbf{C}_{m_\alpha}}{\Delta} \tag{3.31}$$

It is seen from Eq. (3.31) that the control position gradient, which measures the sensitivity of trimmed lift coefficient to control position, is negative for stable, aft tail configurations, and is proportional to the static margin (since Δ is independent of c.g. location and $\mathbf{C}_{m_\alpha}$ is directly proportional to the static margin). In fact, using Eq. 3.29, we can see that

$$\left(\frac{\mathrm{d}\delta_e}{\mathrm{d}\mathbf{C}_L}\right)_{\text{trim}} = \frac{-1}{\mathbf{C}_{L_{\delta_e}}}\frac{x_{NP} - x_{\text{c.g.}}}{\ell_{t_N}} \tag{3.32}$$

Control Surface Hinge Moments

Just as the control position gradient is related to the pitch stiffness of the vehicle when the controls are fixed, the control force gradients are related to the pitch stiffness of the vehicle when the controls are allowed to float free He = 0. The elevator hinge moment is usually expressed in terms of the hinge moment coefficient Che = He QSec¯e (3.59) where the reference area Se and moment arm ¯ce correspond to the planform area and mean chord of the control surface aft of the hinge line. Note that the elevator hinge moment coefficient is defined relative to Q, not Qt. While it would seem to make more sense to use Qt, hinge moments are sufficiently difficult to predict that they are almost always determined from experiments in which the tail efficiency factor is effectively included in the definition of Che (rather than explicitly isolated in a separate factor).

Source from Yechout, T.R. "Introduction to Aircraft Flight Mechanics", AIAA education Series, 2003

Assuming that the hinge moment is a linear function of angle of attack, control deflection, etc., we write

$$\mathbf{C}_{h_e} = \mathbf{C}_{h_{e_0}} + \mathbf{C}_{h_\alpha}\alpha + \mathbf{C}_{h_{\delta_e}}\delta_e + \mathbf{C}_{h_{\delta_t}}\delta_t \tag{3.60}$$

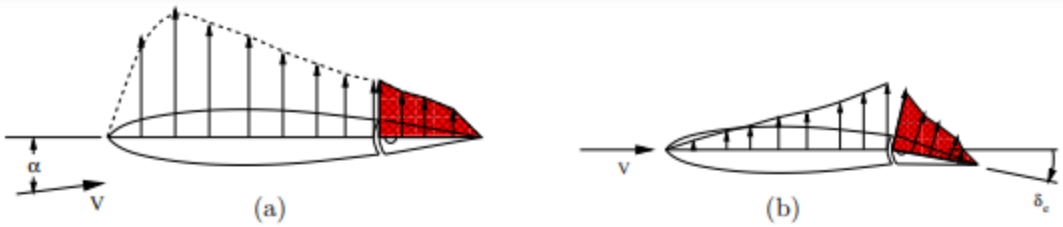

Figure 3.4: Schematic illustration of aerodynamic forces responsible for (a) floating and (b) restoring tendencies of trailing edge control surfaces. Floating (or restoring) tendency represents moment about hinge line of (shaded) lift distribution acting on control surface per unit angle of attack (or control deflection).

In this equation, α is the angle of attack (from angle for zero vehicle lift), δ_e is the elevator deflection, and δ_t is the deflection of the *control tab* (to be described in greater detail later).

The derivative $\mathbf{C}_{h_\alpha}$ characterizes the hinge moment created by changes in angle of attack; it is called the *floating tendency*, as the hinge moment generated by an increase in angle of attack generally causes the control surface to float upward. The derivative $\mathbf{C}_{h_{\delta_e}}$ characterizes the hinge moment created by a deflection of the control (considered positive trailing edge down); it is called the *restoring tendency*, as the nose-down hinge moment generated by a positive control deflection tends to restore the control to its original position. The floating tendency in Eq. (3.60) is referred to the vehicle angle of attack, and so it is related to the derivative based on tail angle of attack α_t by

$$\mathbf{C}_{h_\alpha} = \left(1 - \frac{\mathrm{d}\epsilon}{\mathrm{d}\alpha}\right)\mathbf{C}_{h_{\alpha_t}} \tag{3.61}$$

which accounts for the effects of wing induced downwash at the tail. The aerodynamic forces responsible for generating the hinge moments reflected in the floating and restoring tendencies are sketched in Fig. 3.4. Only the shaded portion of the lift distribution in these figures acts on the control surface and contributes to the hinge moment.

The angle at which the free elevator floats is determined by the fact that the hinge moment (and, therefore, the hinge moment coefficient) must be zero

$$\mathbf{C}_{h_e} = 0 = \mathbf{C}_{h_{e_0}} + \mathbf{C}_{h_\alpha}\alpha + \mathbf{C}_{h_{\delta_e}}\delta_{e\text{free}} + \mathbf{C}_{h_{\delta_t}}\delta_t$$

or

$$\delta_{e\text{free}} = -\frac{1}{\mathbf{C}_{h_{\delta_e}}}\left(\mathbf{C}_{h_{e_0}} + \mathbf{C}_{h_\alpha}\alpha + \mathbf{C}_{h_{\delta_t}}\delta_t\right) \tag{3.62}$$

The corresponding lift and moment coefficients are

$$\begin{aligned}\mathbf{C}_{L\text{free}} &= \mathbf{C}_{L_\alpha}\alpha + \mathbf{C}_{L_{\delta_e}}\delta_{e\text{free}} \\ \mathbf{C}_{m\text{free}} &= \mathbf{C}_{m_0} + \mathbf{C}_{m_\alpha}\alpha + \mathbf{C}_{m_{\delta_e}}\delta_{e\text{free}}\end{aligned} \tag{3.63}$$

which, upon substituting from Eq. (3.62), can be written

$$\begin{aligned}\mathbf{C}_{L\text{free}} &= \mathbf{C}_{L_\alpha}\left(1 - \frac{\mathbf{C}_{L_{\delta_e}}\mathbf{C}_{h_\alpha}}{\mathbf{C}_{L_\alpha}\mathbf{C}_{h_{\delta_e}}}\right)\alpha - \frac{\mathbf{C}_{L_{\delta_e}}}{\mathbf{C}_{h_{\delta_e}}}\left(\mathbf{C}_{h_{e_0}} + \mathbf{C}_{h_{\delta_t}}\delta_t\right) \\ \mathbf{C}_{m\text{free}} &= \mathbf{C}_{m_\alpha}\left(1 - \frac{\mathbf{C}_{m_{\delta_e}}\mathbf{C}_{h_\alpha}}{\mathbf{C}_{m_\alpha}\mathbf{C}_{h_{\delta_e}}}\right)\alpha + \mathbf{C}_{m_0} - \frac{\mathbf{C}_{m_{\delta_e}}}{\mathbf{C}_{h_{\delta_e}}}\left(\mathbf{C}_{h_{e_0}} + \mathbf{C}_{h_{\delta_t}}\delta_t\right)\end{aligned} \tag{3.64}$$

Source from Yechout, T.R. "Introduction to Aircraft Flight Mechanics", AIAA education Series, 2003

Thus, if we denote the control free lift curve slope and pitch stiffness using primes, we see from the above equations that

$$\mathbf{C}_{L_\alpha}{}' = \mathbf{C}_{L_\alpha}\left(1 - \frac{\mathbf{C}_{L_{\delta_e}}\mathbf{C}_{h_\alpha}}{\mathbf{C}_{L_\alpha}\mathbf{C}_{h_{\delta_e}}}\right)$$
$$\mathbf{C}_{m_\alpha}{}' = \mathbf{C}_{m_\alpha}\left(1 - \frac{\mathbf{C}_{m_{\delta_e}}\mathbf{C}_{h_\alpha}}{\mathbf{C}_{m_\alpha}\mathbf{C}_{h_{\delta_e}}}\right) \quad (3.65)$$

Inspection of these equations shows that the lift curve slope is always reduced by freeing the controls, and the pitch stiffness of a stable configuration is reduced in magnitude by freeing the controls for an aft tail configuration, and increased in magnitude for a forward tail (canard) configuration (in all cases assuming that the floating and restoring tendencies both are negative).

Control free Neutral Point

The c.g. location at which the control free pitch stiffness vanishes is called the control free neutral point. The location of the control free neutral point x'_{NP} can be determined by expressing the pitch stiffness in the second of Eqs. (3.65),

$$\mathbf{C}_{m_\alpha}{}' = \mathbf{C}_{m_\alpha} - \frac{\mathbf{C}_{m\delta_e}\mathbf{C}_{h_\alpha}}{\mathbf{C}_{h\delta_e}}$$

as

$$\begin{aligned}\mathbf{C}_{m_\alpha}{}' &= \left(\frac{x_{\text{cg}}}{\bar{c}} - \frac{x_{NP}}{\bar{c}}\right)\mathbf{C}_{L\alpha} + \frac{\mathbf{C}_{h\alpha}\mathbf{C}_{L\delta_e}}{\mathbf{C}_{h\delta_e}}\left(\frac{\ell_t}{\bar{c}} + \frac{x_{\text{ac}}}{\bar{c}} - \frac{x_{\text{cg}}}{\bar{c}}\right) \\ &= \left(\frac{x_{\text{cg}}}{\bar{c}} - \frac{x_{NP}}{\bar{c}}\right)\mathbf{C}_{L\alpha} + \frac{\mathbf{C}_{h\alpha}}{\mathbf{C}_{h\delta_e}}\eta\frac{S_t}{S}a_e\left(\frac{\ell_t + x_{\text{ac}} - x_{NP}}{\bar{c}} + \frac{x_{NP} - x_{\text{cg}}}{\bar{c}}\right) \\ &= \left(\frac{x_{\text{cg}}}{\bar{c}} - \frac{x_{NP}}{\bar{c}}\right)\left[\mathbf{C}_{L\alpha} - \frac{\mathbf{C}_{L\delta_e}\mathbf{C}_{h\alpha}}{\mathbf{C}_{h\delta_e}}\right] + \eta V_{H_N}\frac{\mathbf{C}_{h\alpha}a_e}{\mathbf{C}_{h\delta_e}}\end{aligned} \tag{3.66}$$

where $a_e = \partial\mathbf{C}_{Lt}/\partial\delta_e$ is the elevator effectiveness and

$$V_{H_N} = \left(\frac{\ell_t}{\bar{c}} + \frac{x_{\text{ac}}}{\bar{c}} - \frac{x_{NP}}{\bar{c}}\right)\frac{S_t}{S} \tag{3.67}$$

is the tail volume ratio based on ℓ_{t_N}, the distance between the tail aerodynamic center and the basic neutral point, as defined in Eq. (3.30). The quantity in square brackets in the final version of Eq. (3.66) is seen to be simply the control free vehicle lift curve slope $\mathbf{C}_{L_\alpha}{}'$, so we have

$$\mathbf{C}_{m_\alpha}{}' = \left(\frac{x_{\text{cg}}}{\bar{c}} - \frac{x_{NP}}{\bar{c}}\right)\mathbf{C}_{L_\alpha}{}' + \eta V_{H_N}\frac{\mathbf{C}_{h\alpha}a_e}{\mathbf{C}_{h\delta_e}} \tag{3.68}$$

Setting the control free pitch stiffness $\mathbf{C}_{m_\alpha}{}'$ to zero gives the distance between the control free and basic neutral points as

$$\frac{x_{NP}}{\bar{c}} - \frac{x'_{NP}}{\bar{c}} = \eta V_{H_N}\frac{a_e}{\mathbf{C}_{L_\alpha}{}'}\frac{\mathbf{C}_{h\alpha}}{\mathbf{C}_{h\delta_e}} \tag{3.69}$$

Finally, if Eq. (3.69) is substituted back into Eq. (3.68) to eliminate the variable x_{NP}, we have

$$\mathbf{C}_{m_\alpha}{}' = -\left(\frac{x'_{NP}}{\bar{c}} - \frac{x_{\text{cg}}}{\bar{c}}\right)\mathbf{C}_{L_\alpha}{}' \tag{3.70}$$

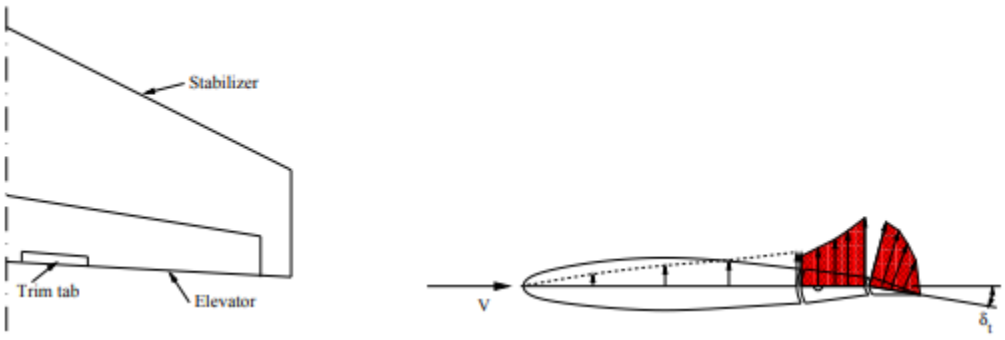

(a) (b)

Figure 3.5: (a) Typical location of trim tab on horizontal control (elevator), and (b) schematic illustration of aerodynamic forces responsible for hinge moment due to trim tab deflection.

showing that the control free pitch stiffness is directly proportional to the *control free static margin*

$$\left(\frac{x'_{NP}}{\bar{c}} - \frac{x_{\text{cg}}}{\bar{c}}\right)$$

static m

Source from Yechout, T.R. "Introduction to Aircraft Flight Mechanics", AIAA education Series, 2003

Trim Tab

gin μ x ′ NP c¯ − xcg c¯ ¶ 3.3.3 Trim Tabs Trim tabs can be used by the pilot to trim the vehicle at zero control force for any desired speed. Trim tabs are small control surfaces mounted at the trailing edges of primary control surfaces. A linkage is provided that allows the pilot to set the angle of the trim tab, relative to the primary control surface, in a way that is independent of the deflection of the primary control surface. Deflection of the trim tab creates a hinge moment that causes the elevator to float at the angle desired for trim. The geometry of

Source from Yechout, T.R. "Introduction to Aircraft Flight Mechanics", AIAA education Series, 2003

Zero control force corresponds to zero hinge moment, or

$$\mathbf{C}_{he} = 0 = \mathbf{C}_{he_0} + \mathbf{C}_{h\alpha}\alpha + \mathbf{C}_{h\delta_e}\delta_e + \mathbf{C}_{h\delta_t}\delta_t$$

and the trim tab deflection that achieves this for arbitrary angle of attack and control deflection is

$$\delta_t = -\frac{1}{\mathbf{C}_{h\delta_t}}\left(\mathbf{C}_{he_0} + \mathbf{C}_{h\alpha}\alpha + \mathbf{C}_{h\delta_e}\delta_e\right) \tag{3.71}$$

so the tab setting required for zero control force at trim is

$$\delta_{t_{\text{trim}}} = -\frac{1}{\mathbf{C}_{h\delta_t}}\left(\mathbf{C}_{he_0} + \mathbf{C}_{h\alpha}\alpha_{\text{trim}} + \mathbf{C}_{h\delta_e}\delta_{e\text{trim}}\right) \tag{3.72}$$

The values of α_{trim} and $\delta_{e\text{trim}}$ are given by Eqs. (3.27)

$$\begin{aligned} \alpha_{\text{trim}} &= \frac{-\mathbf{C}_{L\delta_e}\mathbf{C}_{m0} - \mathbf{C}_{m\delta_e}\mathbf{C}_{L\text{trim}}}{\Delta} \\ \delta_{e\text{trim}} &= \frac{\mathbf{C}_{L\alpha}\mathbf{C}_{m0} + \mathbf{C}_{m\alpha}\mathbf{C}_{L\text{trim}}}{\Delta} \end{aligned} \tag{3.73}$$

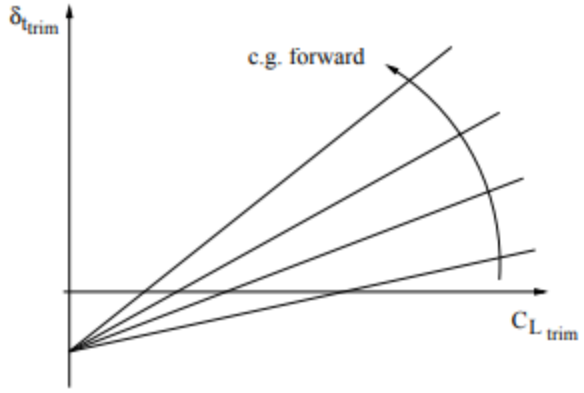

Figure 3.6: Variation in trim tab setting as function of velocity for stable, aft tail vehicle.

Substituting these values into Eq. (3.72) gives the required trim tab setting as

$$\delta_{t_{\text{trim}}} = -\frac{1}{\mathbf{C}_{h\delta_t}}\left(\mathbf{C}_{he_0} + \frac{\mathbf{C}_{m0}}{\Delta}\left(-\mathbf{C}_{h\alpha}\mathbf{C}_{L\delta_e} + \mathbf{C}_{h\delta_e}\mathbf{C}_{L\alpha}\right) + \frac{1}{\Delta}\left(-\mathbf{C}_{h\alpha}\mathbf{C}_{m\delta_e} + \mathbf{C}_{h\delta_e}\mathbf{C}_{m\alpha}\right)\mathbf{C}_{L\text{trim}}\right) \tag{3.74}$$

Note that the coefficient of $\mathbf{C}_{L\text{trim}}$ in this equation – which gives the sensitivity of the trim tab setting to the trim lift coefficient – can be written as

$$\frac{\mathrm{d}\delta_t}{\mathrm{d}\mathbf{C}_L} = -\frac{\mathbf{C}_{h\delta_e}}{\mathbf{C}_{h\delta_t}\Delta}\left(\mathbf{C}_{m\alpha} - \frac{\mathbf{C}_{h\alpha}\mathbf{C}_{m\delta_e}}{\mathbf{C}_{h\delta_e}}\right) = -\frac{\mathbf{C}_{h\delta_e}}{\mathbf{C}_{h\delta_t}\Delta}\mathbf{C}_{m\alpha}{}' = -\frac{\mathbf{C}_{h\delta_e}}{\mathbf{C}_{h\delta_t}\Delta}\left(\frac{x'_{NP}}{\bar{c}} - \frac{x_{\text{cg}}}{\bar{c}}\right)\mathbf{C}_{L\alpha}{}' \tag{3.75}$$

and Eq. (3.74) can be written

$$\delta_{t_{\text{trim}}} = -\frac{1}{\mathbf{C}_{h\delta_t}}\left[\mathbf{C}_{he_0} + \frac{\mathbf{C}_{m0}}{\Delta}\left(-\mathbf{C}_{h\alpha}\mathbf{C}_{L\delta_e} + \mathbf{C}_{h\delta_e}\mathbf{C}_{L\alpha}\right) + \frac{\mathbf{C}_{h\delta_e}}{\Delta}\mathbf{C}_{L\alpha}{}'\left(\frac{x'_{NP}}{\bar{c}} - \frac{x_{\text{cg}}}{\bar{c}}\right)\mathbf{C}_{L\text{trim}}\right] \tag{3.76}$$

Thus, the tab setting for trim is a linear function of trimmed lift coefficient whose slope is proportional to the control free static margin. This variation is shown schematically for a conventional (aft tail) configuration in Fig. 3.6.

Control Force for Trim

Source from Yechout, T.R. "Introduction to Aircraft Flight Mechanics", AIAA education Series, 2003

As mentioned earlier, the most important aspects of stability relating to handling qualities of the vehicle are related to control forces. For longitudinal control, the control force F is related to the elevator hinge moment He through a gearing constant G, so that

$$F = GH_e \qquad (3.77)$$

This equation defines a positive control force as a pull, corresponding to the force required to balance a positive (nose up) elevator hinge moment.4 The units of the gearing constant G are inverse length, which can be interpreted as a mechanical advantage corresponding to radians of control deflection per unit distance (foot) of control yoke displacement.

Source from Yechout, T.R. "Introduction to Aircraft Flight Mechanics", AIAA education Series, 2003

Expressing the hinge moment in terms of the corresponding dimensionless coefficient, we have

$$F = GS_e\bar{c}_eQ\mathbf{C}_{h_e} = GS_e\bar{c}_eQ\left(\mathbf{C}_{h_{e_0}} + \mathbf{C}_{h_\alpha}\alpha + \mathbf{C}_{h_{\delta_e}}\delta_e + \mathbf{C}_{h_{\delta_t}}\delta_t\right) \tag{3.78}$$

Since this equation is linear in tab deflection, the control force required for a tab setting other than the trim value is

$$F = GS_e\bar{c}_eQ\mathbf{C}_{h\delta_t}\left(\delta_t - \delta_{t_{\text{trim}}}\right) \tag{3.79}$$

and, substituting the tab setting required for trim from Eq. (3.76), we have

$$F = GS_e\bar{c}_eQ\left[\mathbf{C}_{h\delta_t}\delta_t + \mathbf{C}_{h_{e_0}} + \frac{\mathbf{C}_{m0}}{\Delta}\left(-\mathbf{C}_{h_\alpha}\mathbf{C}_{L\delta_e} + \mathbf{C}_{h\delta_e}\mathbf{C}_{L\alpha}\right) + \frac{\mathbf{C}_{h\delta_e}}{\Delta}\mathbf{C}_{L\alpha}'\left(\frac{x_{\text{cg}} - x'_{NP}}{\bar{c}}\right)\mathbf{C}_{L\text{trim}}\right] \tag{3.80}$$

Finally, substituting

$$\mathbf{C}_{L\text{trim}} = \frac{W/S}{Q} \tag{3.81}$$

for level flight with $L = W$, we have

$$\begin{aligned} F =& GS_e\bar{c}_e(W/S)\frac{\mathbf{C}_{h\delta_e}\mathbf{C}_{L\alpha}'}{\Delta}\left(\frac{x_{\text{cg}} - x'_{NP}}{\bar{c}}\right) + \\ & GS_e\bar{c}_e\left[\mathbf{C}_{h\delta_t}\delta_t + \mathbf{C}_{h_{e_0}} + \frac{\mathbf{C}_{m0}}{\Delta}\left(-\mathbf{C}_{h_\alpha}\mathbf{C}_{L\delta_e} + \mathbf{C}_{h\delta_e}\mathbf{C}_{L\alpha}\right)\right]\frac{1}{2}\rho V^2 \end{aligned} \tag{3.82}$$

The dependence of control force on velocity described by this equation is sketched in Fig. 3.7. Note from the equation that:

1. The control force $F \propto S_e\bar{c}_e$, i.e, is proportional to the *cube* of the size of the vehicle; control forces grow rapidly with aircraft size, and large aircraft require powered (or power-assisted) control systems.
2. The location of the c.g. (i.e., the control free static margin) affects only the constant term in the equation.
3. The vehicle weight enters only in the ratio W/S.
4. The effect of trim tab deflection δ_t is to change the coefficient of the V^2 term, and hence controls the intercept of the curve with the velocity axis.

4. The effect of trim tab deflection δ_t is to change the coefficient of the V^2 term, and hence controls the intercept of the curve with the velocity axis.

If we denote the velocity at which the control force is zero as V_{trim}, then Eq. (3.82) gives

$$\begin{aligned} & GS_e\bar{c}_e\left(\mathbf{C}_{h\delta_t}\delta_t + \mathbf{C}_{h_{e_0}} + \frac{\mathbf{C}_{m0}}{\Delta}\left(-\mathbf{C}_{h_\alpha}\mathbf{C}_{L\delta_e} + \mathbf{C}_{h\delta_e}\mathbf{C}_{L\alpha}\right)\right)\frac{1}{2}\rho V_{\text{trim}}^2 = \\ & -GS_e\bar{c}_e(W/S)\frac{\mathbf{C}_{h\delta_e}\mathbf{C}_{L\alpha}'}{\Delta}\left(\frac{x_{\text{cg}} - x'_{NP}}{\bar{c}}\right) \end{aligned} \tag{3.83}$$

so

$$F = GS_e\bar{c}_e(W/S)\frac{\mathbf{C}_{h\delta_e}\mathbf{C}_{L\alpha}'}{\Delta}\left(\frac{x_{\text{cg}} - x'_{NP}}{\bar{c}}\right)\left[1 - (V/V_{\text{trim}})^2\right] \tag{3.84}$$

and

$$\left.\frac{\mathrm{d}F}{\mathrm{d}V}\right)_{V_{\text{trim}}} = -\frac{2}{V_{\text{trim}}}GS_e\bar{c}_e(W/S)\frac{\mathbf{C}_{h\delta_e}\mathbf{C}_{L\alpha}'}{\Delta}\left(\frac{x_{\text{cg}} - x'_{NP}}{\bar{c}}\right) \tag{3.85}$$

These last two equations, which also can be interpreted in terms of Fig. 3.7, show that:

Source from Yechout, T.R. "Introduction to Aircraft Flight Mechanics", AIAA education Series, 2003

Control-force for Maneuver

Perhaps the single most important stability property of an aircraft, in terms of handling properties, describes the control force required to perform a maneuver. This force must not be too small to avoid over-stressing the airframe, nor too large to avoid making the pilot work too hard. We will again consider the steady pull-up. The change in control force required to effect the maneuver is

is

$$\Delta F = GS_e\bar{c}_e Q \Delta \mathbf{C}_{h_e} \tag{3.86}$$

where

$$\Delta \mathbf{C}_{h_e} = \mathbf{C}_{h_\alpha}\Delta\alpha + \mathbf{C}_{h_{\delta_e}}\Delta\delta_e + \mathbf{C}_{h_q}\hat{q} \tag{3.87}$$

where $\hat{q}$ is the dimensionless pitch rate, as defined in Section 3.2.1. It was also seen in that section that the dimensionless pitch rate for a pull-up could be related directly to the excess load factor $(n-1)$, so, using Eq. (3.48), we have

$$\Delta \mathbf{C}_{h_e} = \mathbf{C}_{h_\alpha}\Delta\alpha + \mathbf{C}_{h_{\delta_e}}\Delta\delta_e + \frac{(n-1)\mathbf{C}_W}{2\mu}\mathbf{C}_{h_q} \tag{3.88}$$

The derivative $\mathbf{C}_{h_q}$ arises from the change in hinge moment due to the change in tail angle of attack arising from the pitch rate. Thus

$$\Delta \mathbf{C}_{h_e} = \mathbf{C}_{h_{\alpha_t}}\Delta\alpha_t = \mathbf{C}_{h_{\alpha_t}}\frac{2\ell_t}{\bar{c}}\hat{q} \tag{3.89}$$

and

$$\mathbf{C}_{h_q} \equiv \frac{\partial \mathbf{C}_{h_e}}{\partial \hat{q}} = 2\frac{\ell_t}{\bar{c}}\mathbf{C}_{h_{\alpha_t}} \tag{3.90}$$

Source from Yechout, T.R. "Introduction to Aircraft Flight Mechanics", AIAA education Series, 2003

Now, we can use the solution for $\Delta\delta_e$ from Eq. (3.52)

$$\Delta\delta_e = \frac{(n-1)\mathbf{C}_W}{\Delta}\left[\left(1-\frac{\mathbf{C}_{Lq}}{2\mu}\right)\mathbf{C}_{m\alpha}+\frac{\mathbf{C}_{mq}}{2\mu}\mathbf{C}_{L\alpha}\right] \tag{3.91}$$

along with the lift coefficient equation, Eq. (3.49), which can be written

$$\Delta\alpha = \frac{1}{\mathbf{C}_{L\alpha}}\left[(n-1)\mathbf{C}_W\left(1-\frac{\mathbf{C}_{Lq}}{2\mu}\right)-\mathbf{C}_{L\delta_e}\Delta\delta_e\right] \tag{3.92}$$

in the hinge moment equation to give

$$\Delta\mathbf{C}_{he} = \mathbf{C}_{h\alpha}\frac{n-1}{\mathbf{C}_{L\alpha}}\left[\left(1-\frac{\mathbf{C}_{Lq}}{2\mu}\right)\mathbf{C}_W-\mathbf{C}_{L\delta_e}\frac{\Delta\delta_e}{n-1}\right]+\mathbf{C}_{h\delta_e}\Delta\delta_e+\frac{(n-1)\mathbf{C}_W}{2\mu}\mathbf{C}_{hq} \tag{3.93}$$

which can be rearranged into the form

$$\frac{\Delta\mathbf{C}_{he}}{n-1} = \frac{\mathbf{C}_W}{\mathbf{C}_{L\alpha}}\left[\left(1-\frac{\mathbf{C}_{Lq}}{2\mu}\right)\mathbf{C}_{h\alpha}+\frac{\mathbf{C}_{hq}}{2\mu}\mathbf{C}_{L\alpha}\right]+\frac{\Delta\delta_e}{n-1}\mathbf{C}_{h\delta_e}\frac{\mathbf{C}_{L\alpha}'}{\mathbf{C}_{L\alpha}} \tag{3.94}$$

Finally, using Eq. (3.57) for $\Delta\delta_e/(n-1)$, the equation for the hinge moment increment can be written

$$\frac{\Delta\mathbf{C}_{he}}{n-1} = \frac{\mathbf{C}_W\mathbf{C}_{L\alpha}'\mathbf{C}_{h\delta_e}}{\Delta}\left(1-\frac{\mathbf{C}_{Lq}}{2\mu}\right)\left[\frac{x_{cg}-x_{MP}}{\bar{c}}+\frac{\Delta}{\mathbf{C}_{L\alpha}'\mathbf{C}_{h\delta_e}}\left(\frac{\mathbf{C}_{h\alpha}}{\mathbf{C}_{L\alpha}}+\frac{\mathbf{C}_{hq}}{2\mu-\mathbf{C}_{Lq}}\right)\right] \tag{3.95}$$

The *control free maneuver point* is defined as the c.g. location for which the control force gradient (per g) (or, equivalently, the hinge moment coefficient gradient) vanishes. This is seen from Eq. (3.95) to give

$$\frac{x_{MP}-x_{MP}'}{\bar{c}} = \frac{\Delta}{\mathbf{C}_{L\alpha}'\mathbf{C}_{h\delta_e}}\left(\frac{\mathbf{C}_{h\alpha}}{\mathbf{C}_{L\alpha}}+\frac{\mathbf{C}_{hq}}{2\mu-\mathbf{C}_{Lq}}\right) \tag{3.96}$$

Note that this quantity is positive for aft tail configurations, and negative for forward tail (canard) configurations. Substitution of this expression back into Eq. (3.95) then gives

$$\frac{\Delta\mathbf{C}_{he}}{n-1} = \frac{\mathbf{C}_W\mathbf{C}_{L\alpha}'\mathbf{C}_{h\delta_e}}{\Delta}\left(1-\frac{\mathbf{C}_{Lq}}{2\mu}\right)\left(\frac{x_{cg}-x_{MP}'}{\bar{c}}\right) \tag{3.97}$$

Finally, the control force gradient (per g) is

$$\begin{aligned}\frac{\partial F}{\partial n} &= \frac{\Delta F}{n-1} = GS_e\bar{c}_eQ\frac{\Delta\mathbf{C}_{he}}{n-1}\\ &= GS_e\bar{c}_eQ\frac{\mathbf{C}_W\mathbf{C}_{L\alpha}'\mathbf{C}_{h\delta_e}}{\Delta}\left(1-\frac{\mathbf{C}_{Lq}}{2\mu}\right)\left(\frac{x_{cg}-x_{MP}'}{\bar{c}}\right)\end{aligned} \tag{3.98}$$

or, since $Q\mathbf{C}_W = W/S$,

$$\frac{\partial F}{\partial n} = GS_e\bar{c}_e(W/S)\frac{\mathbf{C}_{L\alpha}'\mathbf{C}_{h\delta_e}}{\Delta}\left(1-\frac{\mathbf{C}_{Lq}}{2\mu}\right)\left(\frac{x_{cg}-x_{MP}'}{\bar{c}}\right) \tag{3.99}$$

The distance $\frac{x_{MP}'-x_{cg}}{\bar{c}}$, seen from the above equation to be directly related to the sensitivity of normal acceleration of the vehicle to control force, is called the *control free maneuver margin*.

Note that the control force gradient (per g) is

Source from Yechout, T.R. "Introduction to Aircraft Flight Mechanics", AIAA education Series, 2003

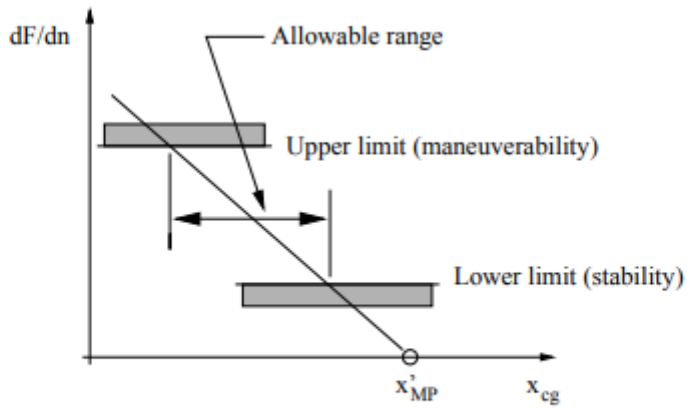

Figure 3.8: Allowable c.g. travel as imposed by limits on control force gradient (per g).

1. Directly proportional to the vehicle wing loading W/S;
2. Directly proportional to the *cube* of the linear size of the vehicle;
3. Directly proportional to the (control free) maneuver margin $(x'_{MP} - x_{cg})/\bar{c}$; and
4. Independent of airspeed.

The control force gradient should be neither too small nor too large. If the gradient is too small, the vehicle will be overly sensitive to small control inputs and it will be too easy for the pilot to over stress the airframe. At the same time, the control forces required for normal maneuvers must not be larger than the pilot can supply (or so large that the pilot becomes unduly tired performing normal maneuvers). The lower and upper limits on control force gradient (per g) determine allowable rearward and forward limits on c.g. travel, as sketched in Fig. 3.8. The values of these limits will depend on the vehicle mission; in general the limits will be higher for transport aircraft, and lower for vehicles which require greater maneuverability (such as military fighters or aerobatic aircraft).

Causes the lift curve slope to decrease as the angle of attack increases and a point is reached when the slope becomes zero; this is the point of maximum lift coefficient, C1 max, which denotes the stall. The angle of attack at the stall, is known as the stalling angle of attack and is the greatest angle of attack at which the aircraft can be maintained in steady, 1g flight. Any further increase in angle of attack will produce a decrease in lift coefficient and the lift force is then less than the weight of the aircraft. In this state, the aircraft will sink and, usually, pitch nose-down in the stall. The stall denotes the boundary of controlled flight and defines the low speed limit of the performance envelope of the aircraft. The stall is normally preceded by aerodynamic buffeting caused by the separation of the flow. This acts as a natural stall warning and the stall buffet boundary is sometimes used as the low speed limit to performance; the airworthiness requirements contain a number of definitions of the

Source from Yechout, T.R. "Introduction to Aircraft Flight Mechanics", AIAA education Series, 2003

stall and stall boundaries. Since the stall is an uncontrollable state of flight, all speeds scheduled for operational maneuvers will have a margin of safety over the stall speed.

The lift characteristic can be modified by leading edge and trailing edge flaps (and other devices), so that the aerodynamic properties of the wing are better suited to the different performance regimes. Figure 1.14 shows the general effects of leading and trailing edge flaps.

- The basic plain aerofoil is optimized for cruising flight; it has low drag and cruising flight takes place at a low angle of attack and hence a low lift coefficient. However, the stalling lift coefficient of the plain aerofoil would be too low for the take-off and landing maneuvers and would result in speeds for these maneuvers that would be too high. Assuming a safety margin of speed over the stall, the minimum speed in a maneuver will be typically 1.2Vs and the speed scheduled for take-off or landing will be based on a lift coefficient of $0.7C_{lmax}$(Fig.1.13).

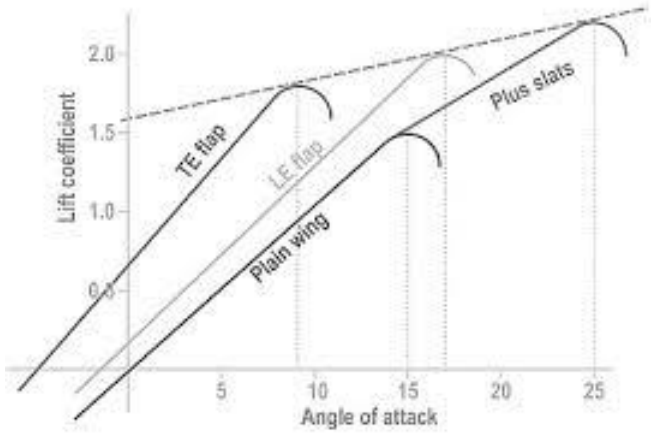

Figure:1.15 The effect of flaps on the lift characteristic

- Leading edge flap deflection has the effect of extending the lift curve to a higher stalling angle of attack, and hence lift coefficient. This would enable the take-off and landing speeds to be reduced, but it would result in a high nose-up attitude because of the large stalling angle of attack. The leading edge flap will also increase the drag, particularly at a low angle ofattack.
- The deflection of the trailing edge flaps has the effect of increasing the camber of the aerofoil section and thus shifting the lift characteristic upwards as the zero lift angle of attack becomes more negative. There is also a tendency to decrease the stalling angle of

Source from Yechout, T.R. "Introduction to Aircraft Flight Mechanics", AIAA education Series, 2003

attack slightly. The trailing edge flap allows higher lift coefficients to be achieved at lower angle of attack and, thus, at lower pitch attitudes. The deployment of the trailing edge flap is often made in several stages. First, a rearward translation of the flap without significant deflection extends the wing area. Effectively, this decreases the wing loading and permits increases in lift coefficient. Secondly, deflection of the extended flap increases the aerofoil camber. Effectively, this shifts the lift curve upwards and increases the lift coefficient for a given angle of attack. There may be a number of stages of deflection optimized for take-off, climb, descent, approach and landing.

Flap systems are often combined with slats and slots, and a flap extension may open a slot between the flap and wing, or expose a slat, to assist the flow over the aerofoil. A combination of leading edge and trailing edge flap can be found that permits the take-off and landing maneuvers, and other maneuvers, to be carried out at reasonable speeds and safe pitch attitudes. Fig 1.16 shows typical flap and angle of attack combinations for the principal states of flight.

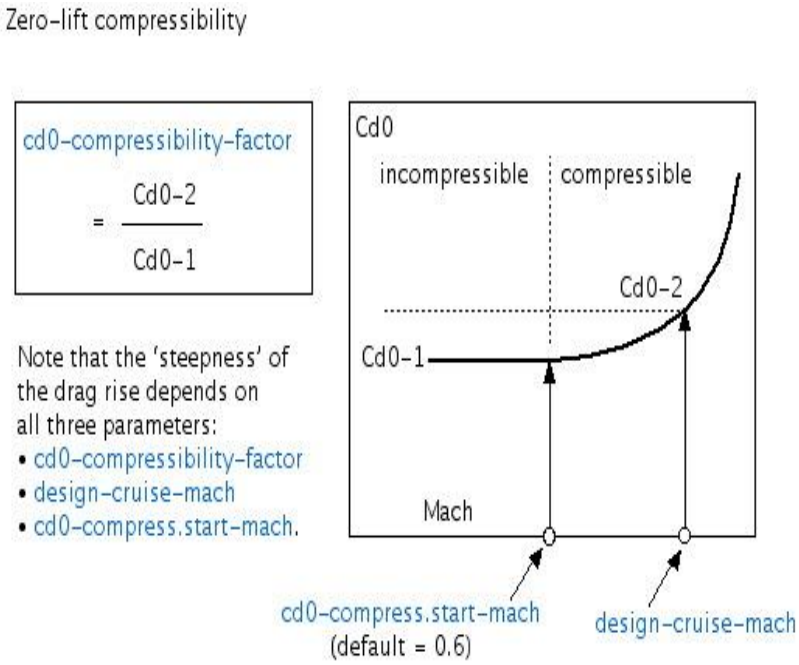

Figure:1.16The compressible lift coefficient

1.3 The effect of Mach number on lift:

The main flight variable that affects the characteristic of the lift force is the Match number. As the Mach number of the airflow increases, so the characteristics of the flow change from those of an incompressible fluid to those of a compressible fluid.

Source from Yechout, T.R. "Introduction to Aircraft Flight Mechanics", AIAA education Series, 2003

This modifies the pressure coefficients, and hence the force coefficients, generated by the aircraft. The compressible flow coefficients are related to the incompressible flow coefficients by the Prandtl-Glauert factor, So that the compressible lift coefficient is given by,

$$C_{Lc} = C_{Li}/\beta$$

Where

$$\beta = \sqrt{(1 - M^2)} \text{ for } M < 1.$$

The ratio between the compressible and in compressible lift coefficients is shown in Fig 1.15

Whilst this effect appears to be very significant when seen in terms of the lift coefficient, its real effect is felt on the angle of attack of the aircraft. Since the aircraft flies at (almost A) constant weight, the lift coefficient decreases with Mach number on the angle of squared and, at high subsonic Mach numbers, the angle of attack of the aircraft will be small.

Figure 1.16 shows the typical effect ofMach number on the angle of attack required for steady, legal, flight at constant aircraft of Mach number on the angle of attack required for steady, level, flight at constant aircraft weight in compressible flow when compared within compressible flow. It can be seen that the effect of Mach number on the angle of attack is relatively small.

Therefore, it is not likely to produce very significant effects on angle of attack dependent variables in the normal, subsonic, range of the operating Mach number.

1.4 The side force, Y

The aerodynamic side force generated by the aircraft arises from side slipping flight. If can be regarded as a lateral lift‘ due to the sided slip angle, which acts as a lateral

Source from Yechout, T.R. “Introduction to Aircraft Flight Mechanics”, AIAA education Series, 2003

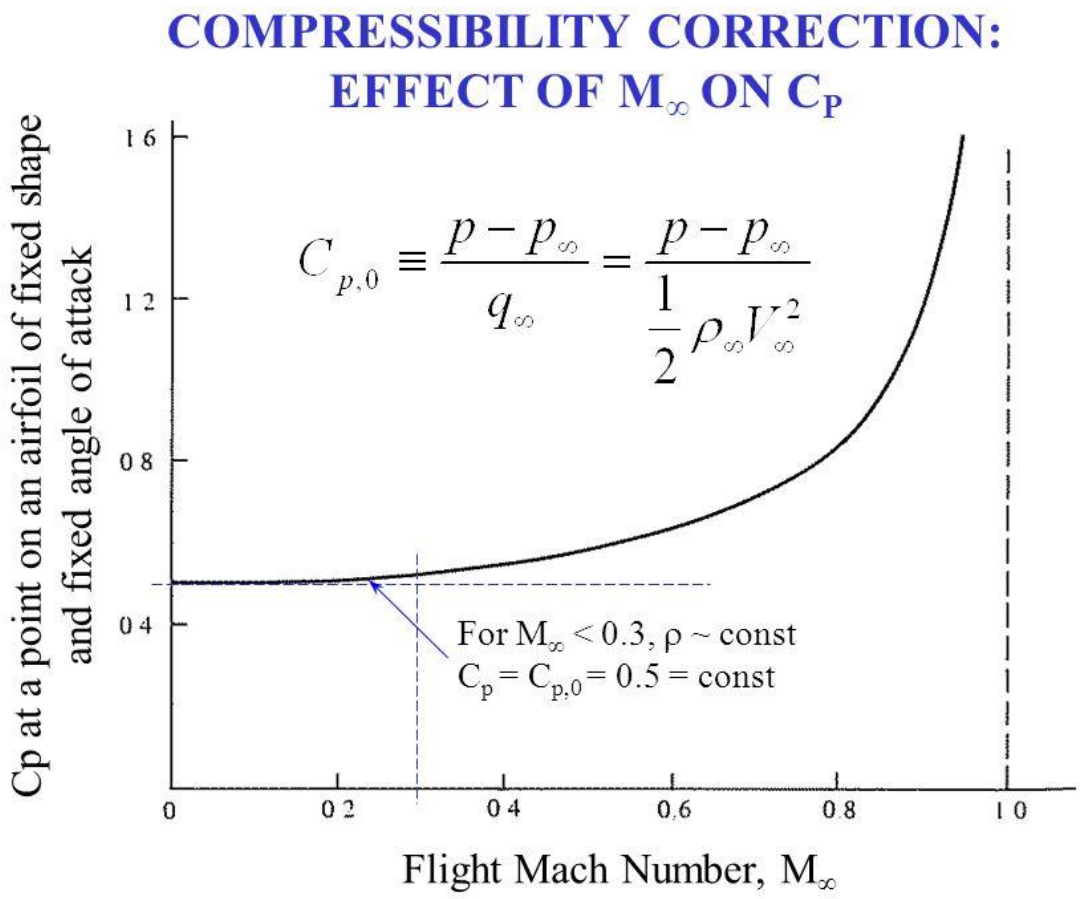

Figure:1.17 The effect of Mach number on Angle of Attack

Angle of attack; the comments on the lift force can be generally applied to the side force. In symmetric flight there is no sideslip and the aerodynamic side force will be zero. Except in special cases in which the aircraft is in asymmetric flight, for example – flight with asymmetric thrust following an engine failure – the side force has little significance on performance.

1.5 The drag force, D

The drag force is the most important aero dynamic force in aircraft performance. In subsonic flight, it is made up of several components, each of which has its own characteristics. The components are the lift independent drag, D_z, the lift dependent drag, D_i, and, at high subsonic Mach numbers, a volume dependent wave drag, D_{wv}. The sum of the drag components makes up the total drag of the aircraft.

Source from Yechout, T.R. "Introduction to Aircraft Flight Mechanics", AIAA education Series, 2003

It is usually assumed in the analysis of subsonic performance that the drag polar of the aircraft is parabolic and represented by the lift dependent and lift independent terms only, the drag coefficient being given by,

$$C_D = C_{Dz} + KC_L^2$$

Where z and K are constants.

Whilst this approximation is used to develop the basic functions of aircraft performance it should be remembered that the real drag characteristic will not be purely parabolic but will contain terms dependent on Mach number. Moreover, particularly at the higher subsonic Mach numbers, the drag characteristic of the aircraft may deviate considerably from the parabolic approximation. In the following subsections, each element of the drag force will be considered separately and the effect of the flight variables, Mach number, weight and altitude, will be assessed on each element.

DRAG POLAR

- $C_{D,0}$ is parasite drag coefficient at zero lift (α_L=0)
- $C_{D,i}$ drag coefficient due to lift (induced drag)
- Oswald efficiency factor, e, includes all effects from airplane
- $C_{D,0}$ and e are known aerodynamics quantities of airplane

$$C_D = C_{D,0} + \frac{C_L^2}{\pi e AR} = C_{D,0} + C_{D,i}$$

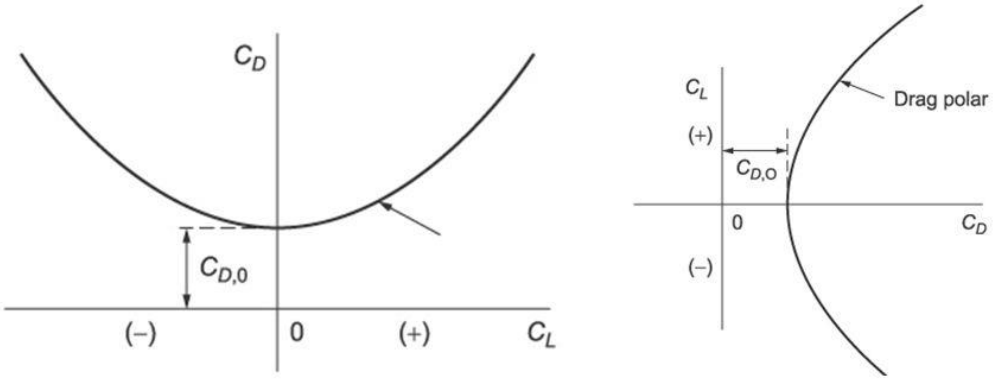

Example of Drag Polar for complete airplane

4

Figure:1.18 The zero-lift drag coefficient

1.5.1 The lift independent drag, D_z

Source from Yechout, T.R. "Introduction to Aircraft Flight Mechanics", AIAA education Series, 2003

The lift independent drag coefficient can be broken down into two parts, the surface friction drag and the profile drag. The surface friction drag coefficient, usually accounts for about 75 of the lift independent drag and tends to decrease slightly as the Mach number increases, as the result of a Reynolds number effect.

The profile drag coefficient, which accounts for the other 25% of the lift independent drag, is a pressure dependent drag. This is affected by the Prandt–Glauert factor in the same manner as the lift coefficient, increasing rapidly as the Mach number approaches unity, see Fig 1.17.

Here, it can be seen that the value of remains almost constant up to a Mach number of about 0.7; this is typical for a conventional subsonic aircraft.

When the compressible, zero-lift, drag coefficient is multiplied by the dynamic pressure, to turn to into a force, the effect of the Mach number can be seen when compared with the assumption of the constant from the parabolic drag polar, see Fig 1.18. There is good agreement between the predicted drag forces up to a Mach number of about 0.8, above which the compressible flow drag force increases significantly.

The forces are expressed here as Drag Area, D/S, which is a convenient way of expressing the drag without involving the scale of the aircraft:

The zero-lift drag force is directly proportional to the atmospheric pressure, p, since the drag force is proportional to the dynamic pressure, q, and above equation. Thus, for flight a given Mach number, the zero-lift drag force will decrease as altitude increases since the atmospheric pressure decreases as a function of altitude.

Zero–lift compressibility

cd0–compressibility–factor = Cd0–2 / Cd0–1

Note that the 'steepness' of the drag rise depends on all three parameters:
- cd0–compressibility–factor
- design–cruise–mach
- cd0–compress.start–mach.

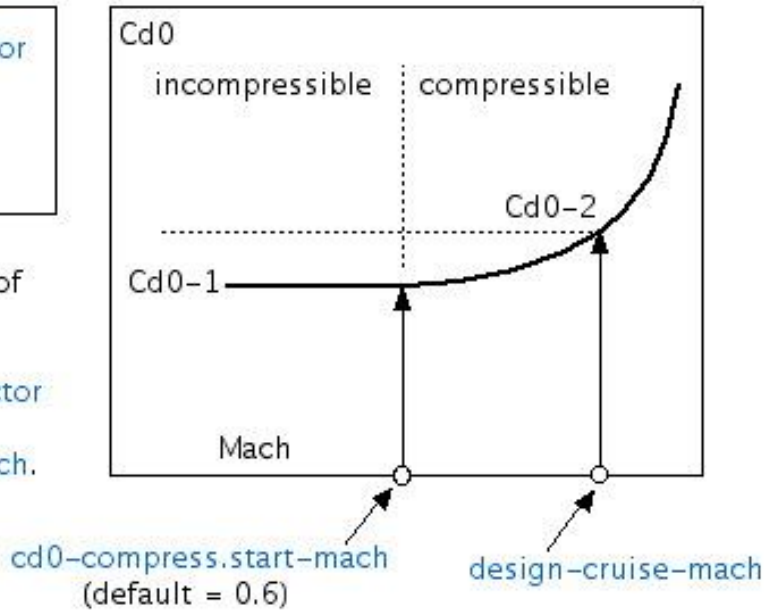

Figure:1.19 Effect of Mach number on the zero-lift drags force

Aircraft weight has no effect on the zero-lift drag force.

1.5.2 The lift dependent drag D_1

The lift dependent, or vortex drag coefficient, is a function of the angle of attack, and is usually taken to be

$C_{Di} = k C_L^2$

Where K is generally assumed to be$1/ \Pi A_e$ in compressible flow.

His approximation is based on the aspect ratio of the wing, A, and the span efficiency factor, e, which is a function of the span wise wing load distribution. However, there may be contributions to the lift force from partsof the aircraft other than the wing, notably the tail plane, and basing the lift dependent drag factor, K, on the wing alone is likely to be optimistic.

Flow separation at low airspeeds may also contribute to the effective value of the lift dependent drag factor; although it may not be strictly dependent on the lift force itself. In addition, the vortex drag is a function of angle of attack, and the Mach number effect on shown in Fig 1.16, will produce a further contribution to the value of K.

Source from Yechout, T.R. "Introduction to Aircraft Flight Mechanics", AIAA education Series, 2003

The value of the lift dependent drag factor, K, will usually have to be determined experimentally but it can be generally accepted as being reasonably constant over the working range of the lift coefficient.

The lift dependent drag force, D_i, is given, as a drag area, by

$$D_i/S = qKC_L^2 = \frac{K(W/S)^2}{\frac{1}{2}\gamma p M^2}$$

And is shown in Fig 1.19, for a given weight and altitude combination;

Since the lift dependent drag force is inversely proportional to the dynamic pressure q, it will decrease with Mach number squared and increase with increasing altitude. Increasing aircraft weight will also increase the lift dependent drag force.

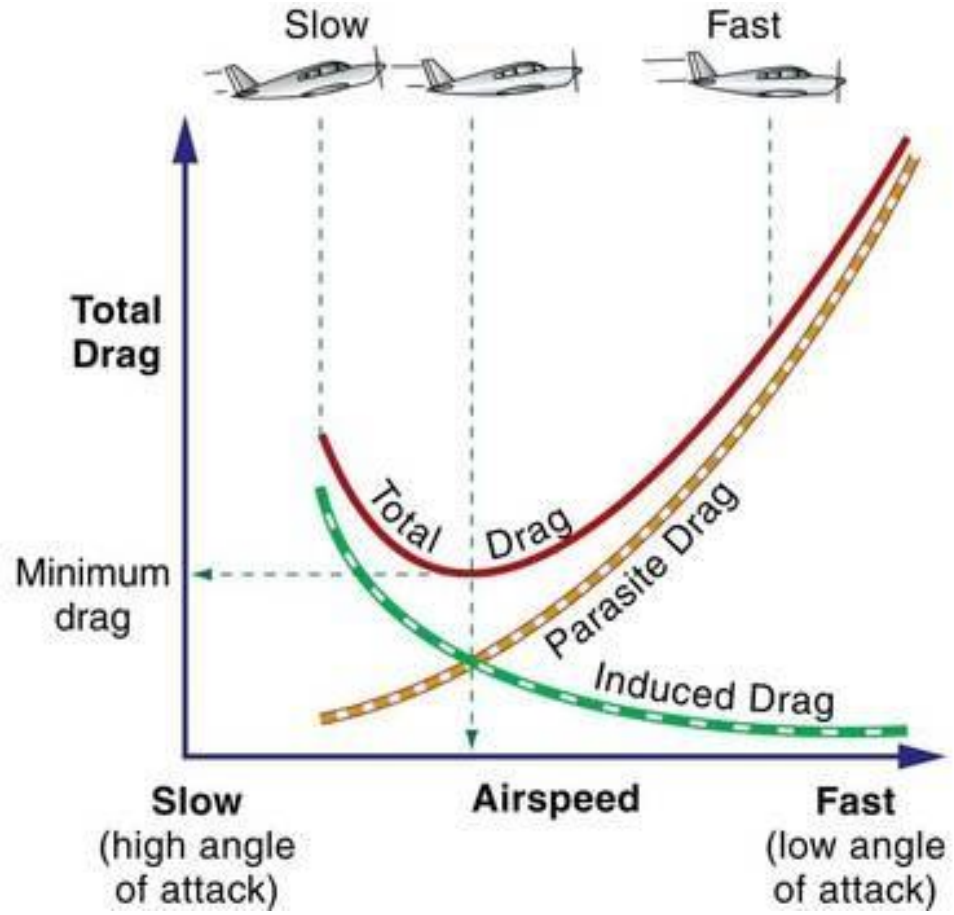

Figure:1.20 The lift dependent drag

Source from Yechout, T.R. "Introduction to Aircraft Flight Mechanics", AIAA education Series, 2003

1.5.3 The volume dependent wave drag, D_{wv}

As the aircraft passes through the air mass its volume displaces the flow and produces local disturbances in flow velocity. At the critical flight Mach number, M_{crit}, the local flow at points on the aircraft becomes supersonic and shock waves begin to form, growing in strength as the flight Mach number increases. The energy required to sustain these shock waves manifests itself as a drag force that increases rapidly as the flight Mach number exceeds its critical value.

There is no simple expression for the volume dependent wave drag. However, experimental results indicate that, above the critical Mach number, the volume dependent wave drag coefficient is related to the volume, and other dimensions, of the aircraft by a relationship – based on the slender body theory of the form,

$$C_{Dwv} \propto K_0 \mathrm{Vol}^2$$

Where K_o is a shaping factor, which is a function of Mach number. A first-order approximation to K_o is that K_o increases as Mach number squared above M_{crit} in the transonic region. In supersonic flight beyond the transonic region, KJ_o tends to decrease. On this assumption, the volume dependent wave drag can be expectedto increase as the fourth power of Mach number in the transonic region. This indicates the significance of the wave drag term in the drag characteristic of the aircraft above the critical Mach number, as shown in Fig1.20.

As in the case of the zero-lift drag, the volume dependent wave drag will decrease as altitude increases for a given Mach number and is independent of aircraft weight.

1.5.4 The overall drag force, D

The overall drag force is the sum of the components of the drag force, the zero-lift drag, the lift dependent drag and the volume dependent wave drag. Each component has been shown to be a function of Mach number, altitude (or pressure) and, in the case of the lift dependent drag, aircraft. The drag characteristic is shown in Fig 1.21. For a given weight and altitude combination.

Source from Yechout, T.R. "Introduction to Aircraft Flight Mechanics", AIAA education Series, 2003

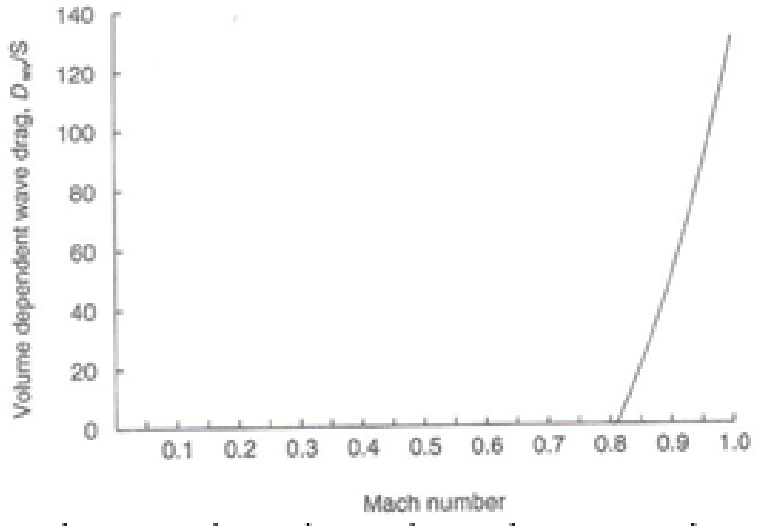

Figure:1.21 2The volume dependent wave drag

Figure 1.21 shows that, below the critical Mach number, there is a reasonable comparison between the compressible flow drag characteristic and the incompressible approximation. This justifies the use of the simple, incompressible, parabolic drag polar in the development of the basic expression of performance. However, it should be remembered that the parabolic drag polar is an approximation and that any performance characteristics estimated on the assumption of a parabolic drag polar will not be exact. In practice, it will be necessary to measure the performance of the aircraft in flight to define the actual performance achieved. At Mach numbers above are critical value, the drag force increases rapidly and the approximation becomes invalid; any estimation of the aircraft performance above M_{crit} will need consideration of the full drag characteristic of the aircraft.

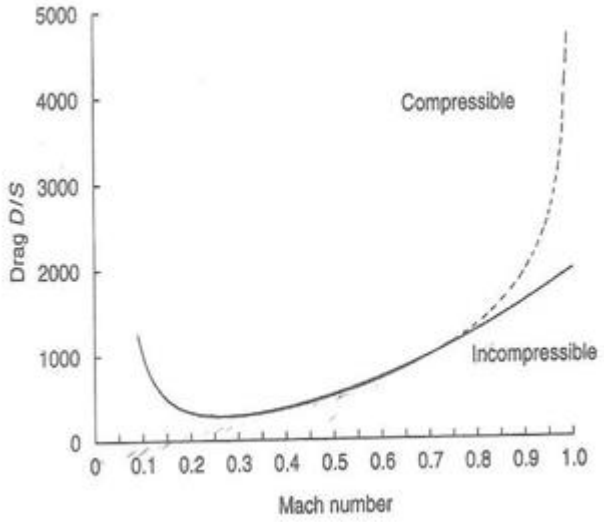

Figure:1.22 The aircraft drag polar

Source from Yechout, T.R. "Introduction to Aircraft Flight Mechanics", AIAA education Series, 2003

Source from Yechout, T.R. "Introduction to Aircraft Flight Mechanics", AIAA education Series, 2003

Introduction to lateral-direction stability- aerodynamic forces and moments, aircraft side force due to side slip, aircraft rolling moment due to side slip, and aircraft yawing moment due to side slip. Aircraft component contribution, directional static stability, Aircraft component contribution for lateral-directional stability, rudder requirements

Source from Yechout, T.R. "Introduction to Aircraft Flight Mechanics", AIAA education Series, 2003

UNIT II
LATERAL-DIRECTIONAL STATIC STABILITY

Aims of study

Suppose we have an aircraft in some state of steady flight. If it is disturbed, by a gust say, or by the pilot, it is regarded as stable if it returns to a sensibly steady state within a finite time. The final state, however, does not have to be identical to the initial state, although it often will be. Depending on circumstances we may be able to tolerate a small degree of instability or even deliberately design an aircraft to be quite unstable; in the latter case, however, a reliable automatic stabilization system will be required. We normally require more than mere stability; the response to gusts must not make the pilot's task difficult, produce an uncomfortable ride for passengers, impose excessive loads on the aircraft, or make the aircraft unsuitable as an aiming platform. The pilot must be able to control the aircraft accurately without having to perform excessive feats of skill or strength. Our first aim then is to study the dynamics of the aircraft and its interaction with the aerodynamics in order to be able to assess and possibly improve the dynamic characteristics. A further aim is to understand the physics of the processes involved. If necessary we make approximations as, while better numerical results can generally be found using a computer, little real understanding follows its use alone. With a good understanding of the physics involved, solutions to design problems can be put forward.

One of the reasons that the Wright brothers were successful in designing and constructing the first man-carrying aircraft was their realization that it was necessary to provide control about all three axes. It is all too evident from cine film of many of the early attempts to fly that control in roll was desperately needed, not least to react the propeller torque. The Wrights used wing warping and, for good measure, used coupled contra-rotating propellers. Shortly after their first flight, ailerons were invented and are almost universally used today. In this chapter we consider control and stability about the roll and yaw axes. We also introduce a notation which will be made much use of in later chapters.

2.1 Introduction to lateral stability

Lateral stability is the stability displayed around the longitudinal axis of the airplane. An airplane that tends to return to a wings-level attitude after being displaced from a level attitude by some force such as turbulent air is considered to be laterally stable.

Three factors that affect lateral stability are:

- Dihedral
- Sweepback
- Keel Effect

Source from Yechout, T.R. "Introduction to Aircraft Flight Mechanics", AIAA education Series, 2003

Dihedral

Dihedral is the angle at which the wings are slanted upward from the root to the tip. [Figure 2.1] The stabilizing effect of dihedral occurs when the airplane sideslips slightly as one wing is forced down in turbulent air. This sideslip results in a difference in the angle of attack between the higher and lower wing with the greatest angle of attack on the lower wing. The increased angle of attack produces increased lift on the lower wing with a tendency to return the airplane to wings-level flight. Note the direction of the relative wind during a slip by the arrows in figure 2.1

Fig. 2.1. Effect of dihedral

Sweepback

Sweepback is the angle at which the wings are slanted rearward from the root to the tip. The effect of sweepback in producing lateral stability is similar to that of dihedral, but not as pronounced. If one wing lowers in a slip, the angle of attack on the low wing increases, producing greater lift. This results in a tendency for the lower wing to rise, and return the airplane to level flight. Sweepback augments dihedral to achieve lateral stability. Another reason for sweepback is to place the center of lift farther rearward, which affects longitudinal stability more than it does lateral stability. [Figure 2.2]

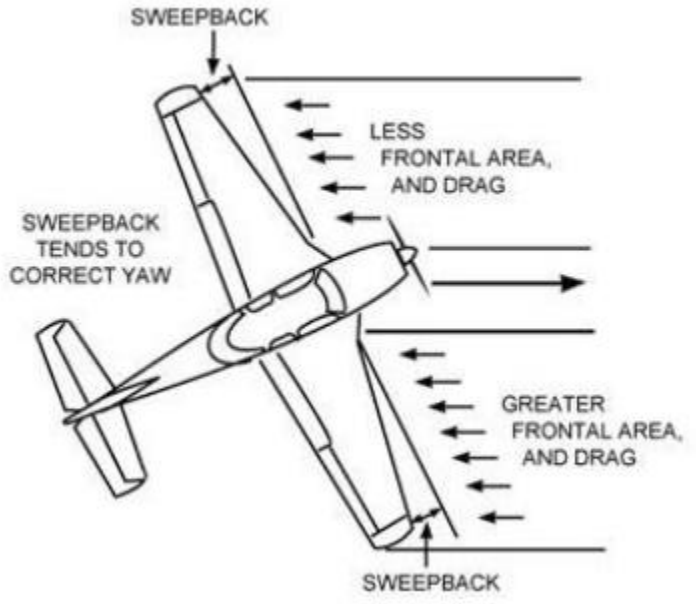

Fig 2.2 Effect of sweepback

Keel Effect

Keel effect depends upon the action of the relative wind on the side area of the airplane fuselage. In a slight slip, the fuselage provides a broad area upon which the relative wind will strike, forcing he fuselage to parallel the relative wind. This aids in producing lateral stability. [Figure 2.3]

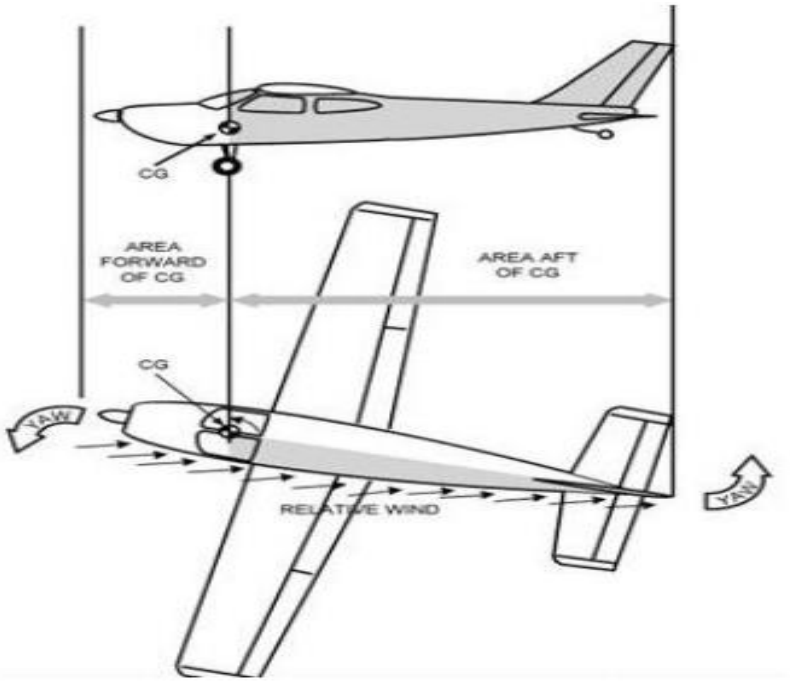

Fig 2.3 Effect of keel

Source from Yechout, T.R. "Introduction to Aircraft Flight Mechanics", AIAA education Series, 2003

Simple lateral aerodynamics

We first consider some of the simple background aerodynamics, assuming that the aircraft has conventional flap type controls and a conventional layout.

Aileron and rudder controls

To start our discussion we look at the relation between the rudder angle and the resulting yawing moment. Consider the aircraft shown in figure 6.1, where ~' is the rudder deflection angle from the neutral position, positive as shown. The sideways lift on the fin will be Y~, = *{pV~SFa~* where SF is the fin area and a~ is the rudder lift curve slope. Assuming that the centre of pressure of the lift on the fin due to rudder deflection is a distance IR aft of the cg, the yawing moment produced will be negative (see figure 2.4) and can be written

$$N_R = \mathring{N}_\zeta \cdot \zeta$$

$$\mathring{N}_\zeta = \frac{\partial N_R}{\partial \zeta} = -\tfrac{1}{2}\rho V_e^2 S_F l_R a_2^F$$

------2.1

In this expression we have used (a s a suffix to indicate differentiation with respect to rudder angle, a practice we often use. The superscript is to emphasize that the quantity is dimensional; it can be pronounced as 'ord'. The side force will also produce a rolling moment as shown in figure 2.4 and we introduce a derivative L~. to represent this effect.The ai.lerons are designed to produce a rolling moment which we write in a similar manner as L^ = L, .~j. Here L; also will be a negative quantity as positive aileron angle is defined as

Source from Yechout, T.R. "Introduction to Aircraft Flight Mechanics", AIAA education Series, 2003

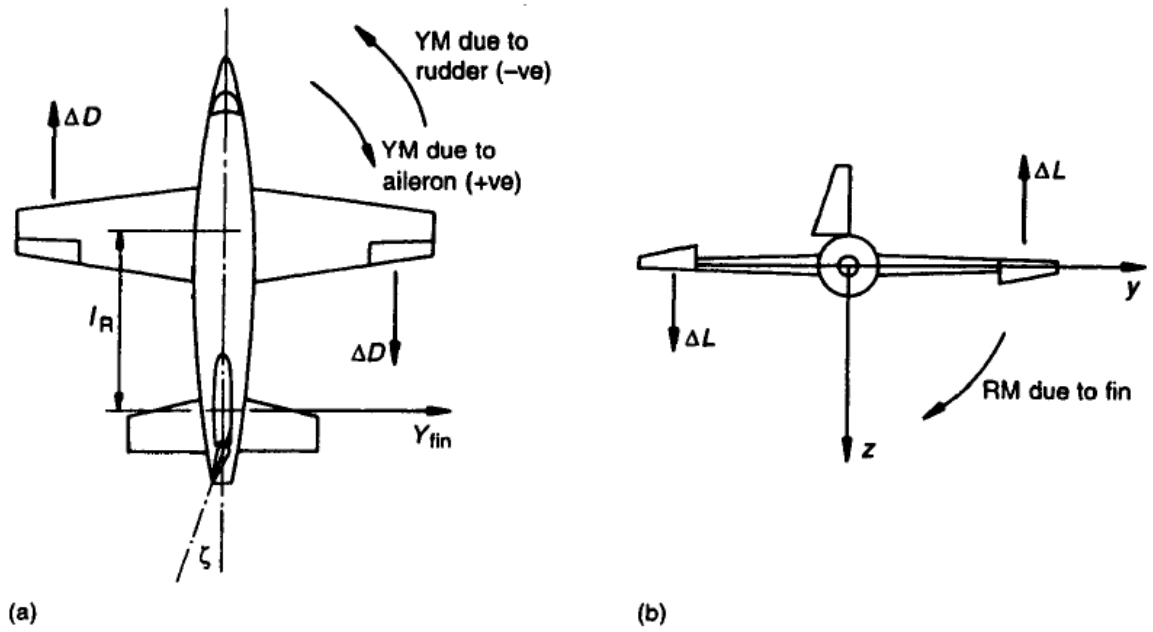

Fig 2.4 Effects of aileron and rudder deflection: (a) plan view, (b) rear view

starboard aileron down, giving a positive lift on that wing and hence a negative rolling moment. The increase of lift on the starboard wing increases the trailing vortex drag, giving a yawing moment in the positive sense. Similarly the drag on the port wing is decreased adding to the positive yawing moment. From figure 6.1 it can be seen that the yawing moment due to aileron opposes the turn. This effect is known as the 'adverse yawing moment due to aileron', and particular measures may be taken to reduce it. The rolling moment from the rudder is adverse at low incidence, but helpful at high incidence, depending on whether the centre of pressure is above or below the x-axis. However, the moment arm of the fin side force is generally small and this is therefore usually a much less serious effect. It should be noted that both the aileron and the rudder produce rolling and yawing moments,in different amounts, and so usually have to be used in a coordinated manner.

Sideslip

A pilot, by suitable adjustment of the controls, can fly an aircraft steadily in a straight line but with its longitudinal axis at an angle to the direction of flight. This manoeuvre is a 'straight sideslip', the drag is increased and so it is occasionally used to lose height. Normally the aircraft will be at a small roll angle so that there is a component of the weight to balance aerodynamic sideforces. Consider the aircraft shown in figure 6.2(a) which is in a steady sideslip, but with the wings level. The aircraft has velocity components V¢ along its X-axis and v along its Y-axis, resulting in a sideslip angle, fl, between its longitudinal axis and the direction of flight. If we neglect any interference effects from the wing or fuselage, the fin incidence angle will be fl, as shown, given by

Source from Yechout, T.R. "Introduction to Aircraft Flight Mechanics", AIAA education Series, 2003

$$\tan\beta = \frac{v}{V_e} \simeq \beta$$

----------2.2

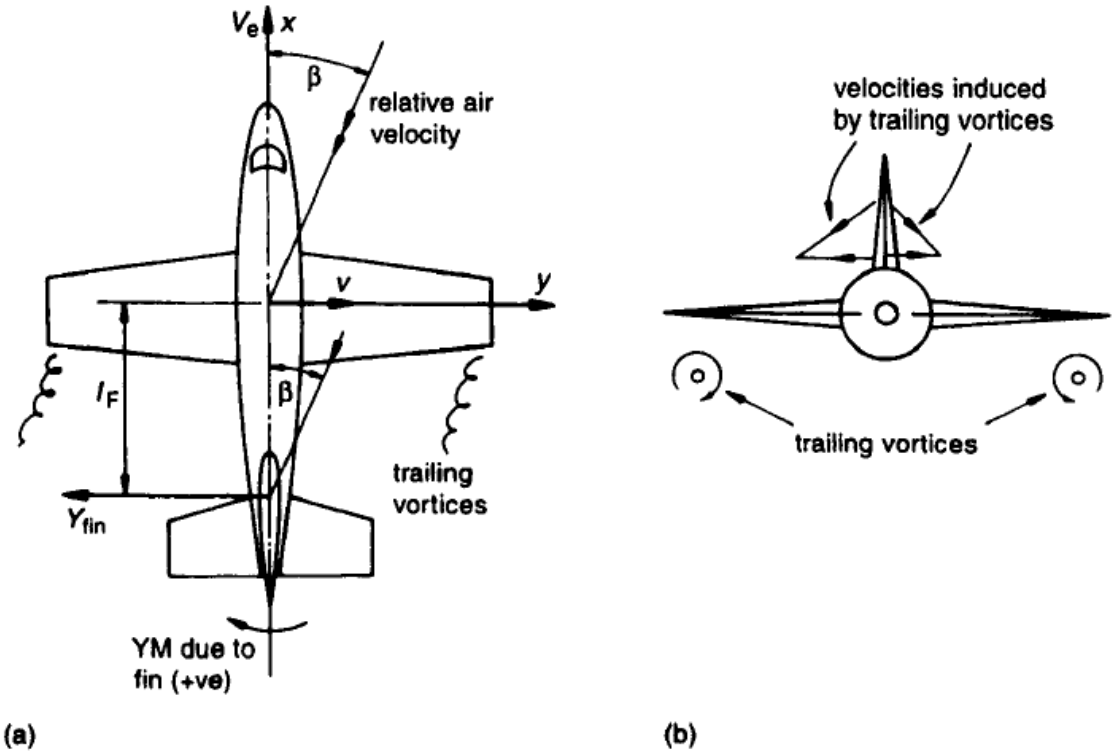

Fig 2.5 Velocities and angles in a sideslip: (a) plan view, (b) rear view

assuming that beta is a small angle. This will give a sideways lift on the fin of

$$Y_{fin} = \tfrac{1}{2}\rho V_e^2 S_F a_1^F \cdot \beta = \tfrac{1}{2}\rho V_e S_F a_1^F \cdot v$$

---------2.3

where a F is the fin lift curve slope. Assuming that the fin lift acts at a distance IF aft of the cg, there is a positive yawing moment which we write

$$N_{fin} = \dot{N}_{v,fin} \cdot v$$

$$\dot{N}_{v,fin} = \tfrac{1}{2}\rho V_e S_F l_F a_1^F$$

------2.4

Source from Yechout, T.R. "Introduction to Aircraft Flight Mechanics", AIAA education Series, 2003

Other components of the aircraft produce yawing moments; in particular the fuselage produces a moment of the opposite sign. The latter is the result of a sideways lift on it which has a centre of pressure near the nose, similar to that produced in the pitching case. The result is that the yawing moment due to sideslip derivative for the aircraft as a whole is rather less than the fin contribution.

We now consider some further effects of sideslip, namely those due to dihedral and sweepback on the wings. Figure 2.5(a) shows the rear view of an aircraft having dihedral in a sideslip. Resolving the relative air velocity into the normal to the starboard wing mean plane gives an upward velocity component of vF, where 1" is the dihedral angle, positive as shown and assumed small. The result is an increase in incidence of amount *vFIVc,* which increases the lift on the wing and gives a negative rolling moment. The opposite effect occurs on the other wing, which again produces a negative rolling moment.

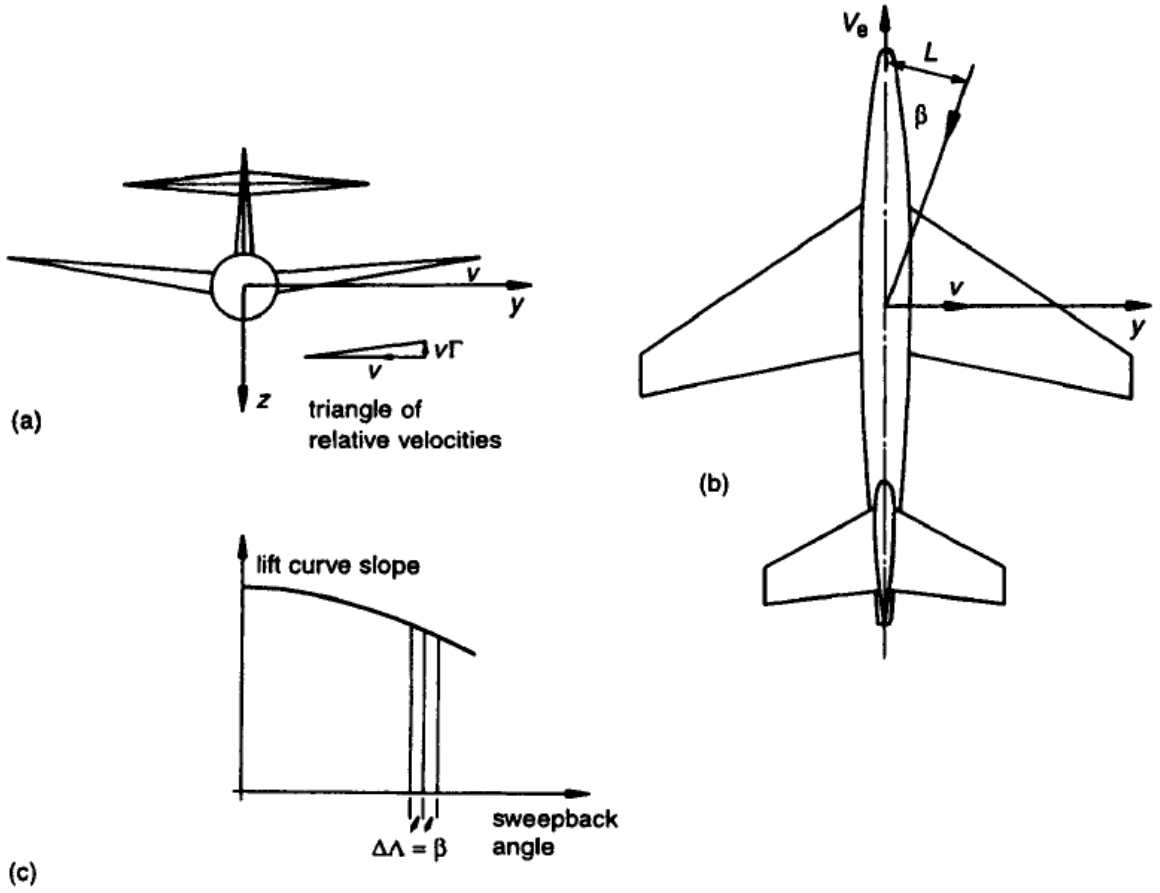

Fig.2.6 Determination of dihedral effect: (a) velocities in rear view, (b) velocities in plan view, (c) variation of lift curve slope with sweepback angle

Figure 6.7(b) shows an aircraft with sweptback wings in a sideslip. We see that the sweepback angle is decreased by ~ on the starboard wing and increased by ~ on the port wing. Now the lift curve slope of wings decreases as the sweep is increased. Assuming that this wing is at some incidence, the lift on the

Source from Yechout, T.R. "Introduction to Aircraft Flight Mechanics", AIAA education Series, 2003

starboard side therefore increases with sideslip giving a negative rolling moment. The opposite occurs on the port side, adding to the magnitude of the rolling moment.

There are still more mechanisms for producing rolling moment on an aircraft in a sideslip; we will discuss only one more, that due to wing position on the fuselage. In a sideslip the airflow past the fuselage can be thought of as composed of two flows, the flow in un side slipped flight an a flow from one side of the fuselage to the other, the 'cross flow'. Figure 2.8(a) shows the ideal flow past a circular cylinder, which resembles the cross flow expected past a circular fuselage. Figure 2.8(b) shows the cross-section of a high wing aircraft in the region of the wing. Near the point A the air is deflected upwards relative to the wing, increasing the incidence locally; similarly the incidence is decreased near B. The resulting local changes to the wing lift gives a negative rolling moment from both wings. We shall see later that the rolling moment due to sideslip effect is a stabilizing one provided that it is not too large. The effects on aircraft layout can be seen in actual designs. With unswept wings, low wing layouts usually have noticeable dihedral whilst high wing ones little or none. Highly swept, low wing aircraft have little dihedral whilst high wing ones often have negative dihedral angle, known as anhedral'. The three effects discussed above all depend on changes of lift distribution over the span of the wing, and so are accompanied by spanwise changes in the trailing vortex drag. The result in cases of dihedral and sweep is a contribution to yawing moment due to sideslip in the same sense as the fin contribution. In the case of dihedral the effect is usually small, but for sweep the effect is proportional to C~, and so can become important at high incidence. We write the sideforce, rolling and yawing moments due to sideslip for the whole aircraft using derivatives thus:

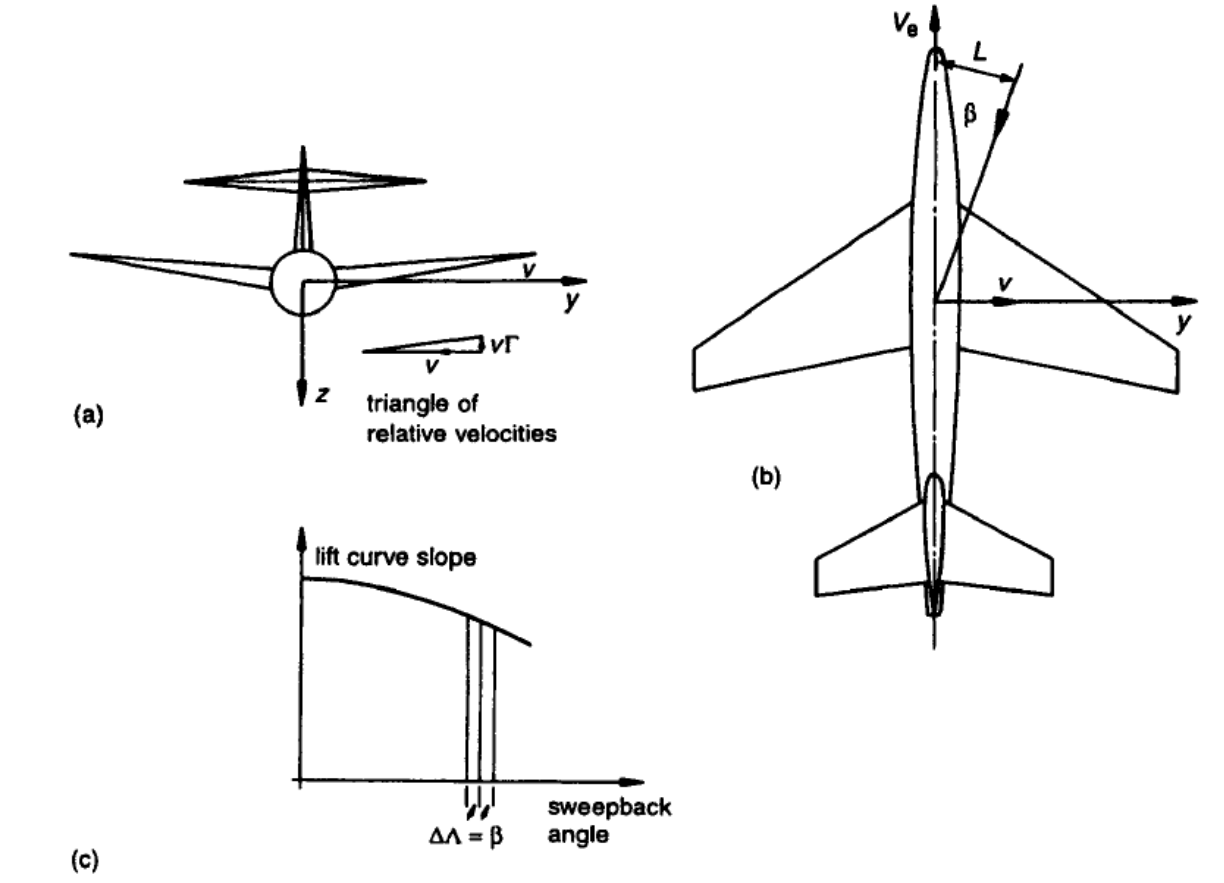

Fig 2.7 Determination of dihedral effect: (a) velocities in rear view, (b) velocities in plan view, (c) variation of lift curve slope with sweepback angle

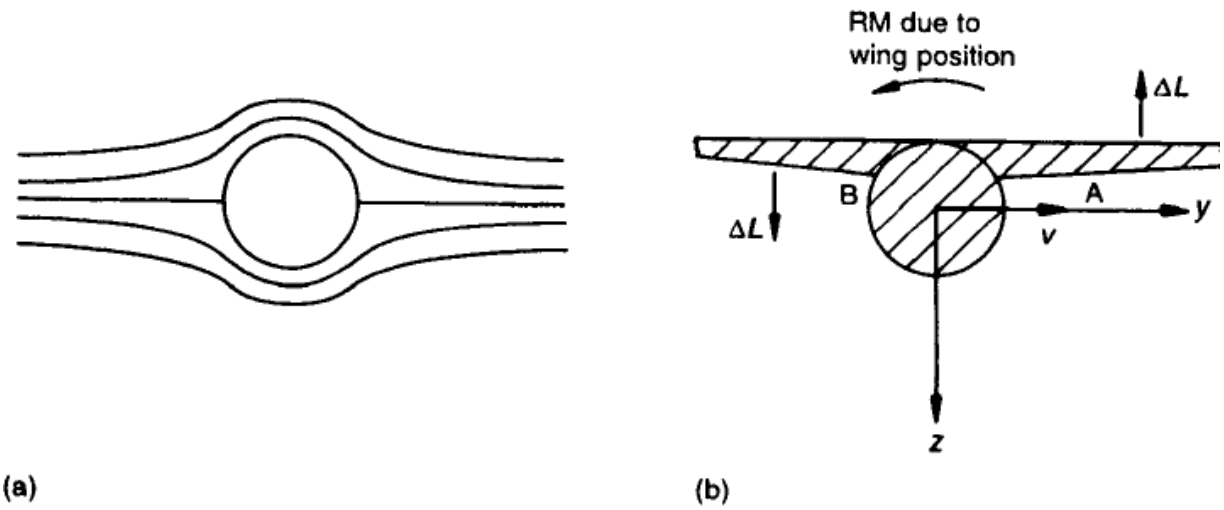

Fig.2.8. Effect of wing position on Lv: (a) ideal flow past a circular cylinder, (b) forces produced by crossflow

Effect of rate of yaw

Source from Yechout, T.R. "Introduction to Aircraft Flight Mechanics", AIAA education Series, 2003

In any turn, in order for the aircraft axis to be continually tangential to the path of the cg, the aircraft must have an angular velocity in yaw, and there are other cases in which the aircraft is yawing. Let us consider the effect of a small rate of yaw on an aircraft flying in a straight line and wings level, ,i.e. without the extra complications of a turn, as shown in figure 6.5. As a consequence of the yaw rate r, the fin has a sideways velocity of *rl*~. Then considering the triangle of relative air velocities, the fin has an incidence of o~ = *rlFIVc*, which gives rise to a sideforce of

$$Y_{\text{fin}} = \tfrac{1}{2}\rho V_e^2 S_F a_1^F \cdot \alpha_F = \tfrac{1}{2}\rho V_e S_F l_F a_1^F \cdot r$$

This in turn gives a yawing moment which opposes the yawing motion and which we write in the form

$$N_{\text{fin}} = \dot{N}_{r,\text{fin}} \cdot r$$

$$\dot{N}_{r,\text{fin}} = -\tfrac{1}{2}\rho V_e S_F l_F^2 a_1^F$$

may happen consider again the aircraft of figure 2.9. The starboard wing tip is moving backwards relative to the cg and so its nett velocity is reduced, and hence also is the lift. This gives rise to a positive rolling moment; the reverse effect appears on the port wing and so this contributes to the rolling moment in the same sense. Other parts of the aircraft also contribute to this effect. We write the sideforce, rolling and yawing moments due to rate of yaw using derivatives thus:

$$\left.\begin{aligned} Y &= \dot{Y}_r \cdot r \\ L &= \dot{L}_r \cdot r \\ N &= \dot{N}_r \cdot r \end{aligned}\right\}$$

In fact the sideforce due to yaw rate is very small and we frequently neglect it

Source from Yechout, T.R. "Introduction to Aircraft Flight Mechanics", AIAA education Series, 2003

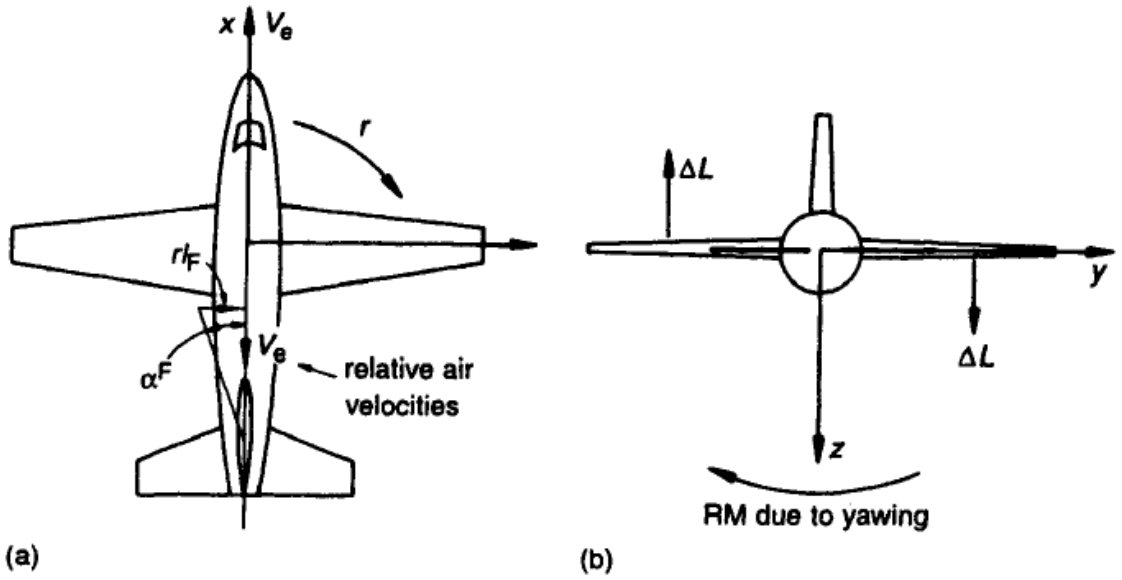

Fig. 2.9. Effect of rate of yaw: (a) velocities in plan view, (b) lift forces

Trimmed lateral manoeuvres

In this section we consider the aileron and rudder angles required to perform two simple manoeuvres, the correctly banked turn and the straight sideslip. Strictly speaking the angles found are the changes from straight and level flight, since even in that condition an aircraft may need aileron or rudder angles to counter power effects or other asymmetries. It is cumbersome and unnecessary to use the superscript in this section since it is evident that all the terms in the equations are dimensional.

-The correctly banked turn

Consider again the aircraft shown in figure 2.10, which is performing a turn at bank angle phi to the vertical.

$$L \sin \phi = m \frac{V_e^2}{R}$$

$$L \sin \phi = m V_e \omega$$

where to is the angular velocity of the aircraft about the vertical; we have again neglected the side force generated by rate of yaw. We need to resolve this velocity along the z-axis to find the rate of yaw and hence express the aerodynamic effects of yaw rate. Considering the triangle of angular velocities shown in figure 2.10 we find

Source from Yechout, T.R. "Introduction to Aircraft Flight Mechanics", AIAA education Series, 2003

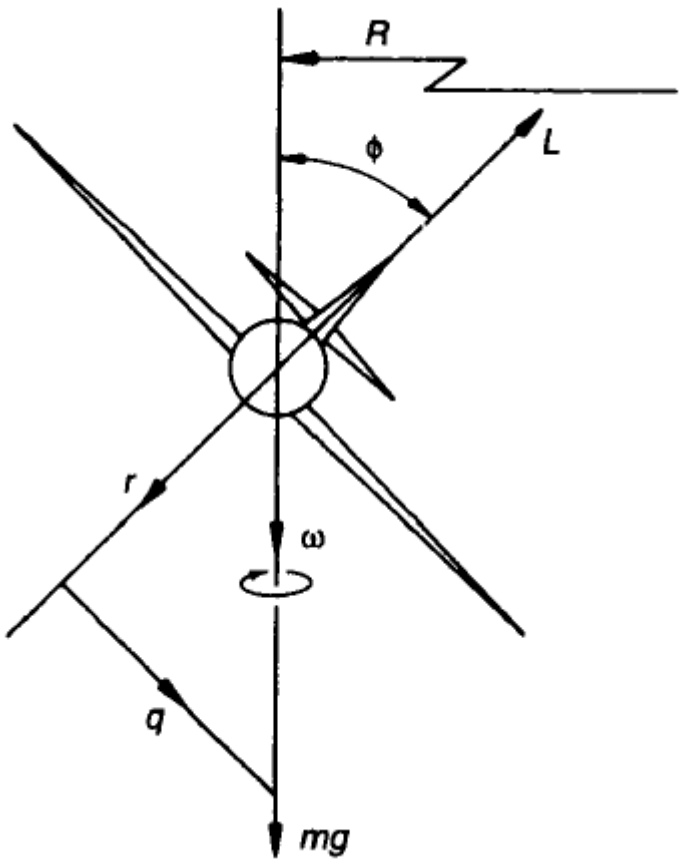

Fig 2.10 illustration of bank angle

$$r = \omega \cos \phi \tag{6.9}$$

We also find a rate of pitch, $q = r \sin \phi$. This means that there will be a change in the trim in pitch: see Section 5.5. From (3.46) we have $L \cos \phi = mg$, then using (6.9) to eliminate $\cos \phi$ in this we have

$$Lr/\omega = \text{mg}$$

and using this to eliminate ω from (6.8) gives

$$r = (g \sin \phi)/V_e \tag{6.10}$$

Since the flight condition is a steady one the total moments about the roll and yaw axes must be zero (see for comparison Section 5.2). Then adding the moments due to yaw rate and control action we have

Source from Yechout, T.R. "Introduction to Aircraft Flight Mechanics", AIAA education Series, 2003

$$\left.\begin{aligned} L_r r + L_\xi \xi + L_\zeta \zeta = 0 \\ N_r r + N_\xi \xi + N_\zeta \zeta = 0 \end{aligned}\right\} \tag{6.11}$$

Solving these simultaneous equations for ξ and ζ in terms of r and then substituting r from (6.10) gives

$$\xi = \frac{r}{\Delta}\left(L_r N_\zeta - L_\zeta N_r\right) = \frac{g \sin\phi}{V_e \Delta}\left(L_r N_\zeta - L_\zeta N_r\right) \tag{6.12}$$

$$\zeta = \frac{r}{\Delta}\left(L_\xi N_r - L_r N_\xi\right) = \frac{g \sin\phi}{V_e \Delta}\left(L_\xi N_r - L_r N_\xi\right) \tag{6.13}$$

where

$$\Delta = L_\zeta N_\xi - L_\xi N_\zeta \tag{6.14}$$

These expressions are dominated by the direct effects of the controls and the rate of yaw derivatives and can be approximated as

$$\xi \simeq -\frac{L_r \cdot r}{L_\xi} \text{ and } \zeta \simeq -\frac{N_r r}{N_\zeta} \tag{6.15}$$

This shows that the aileron is primarily used to balance the rolling moment due to yaw rate and the rudder to balance the yawing moment, as would be expected. Once the aircraft has achieved a steady turn the aileron and rudder angles required are usually quite small. Having found these angles it is possible to find the stick forces from equations of the form (4.17) and (5.54).

-Steady straight sideslip

Consider the aircraft shown in figure 2.11, which is performing a steady straight sideslip, with sideslip velocity v. Resolving forces along the Y direction and neglecting any sideforces generated by the control surfaces w.

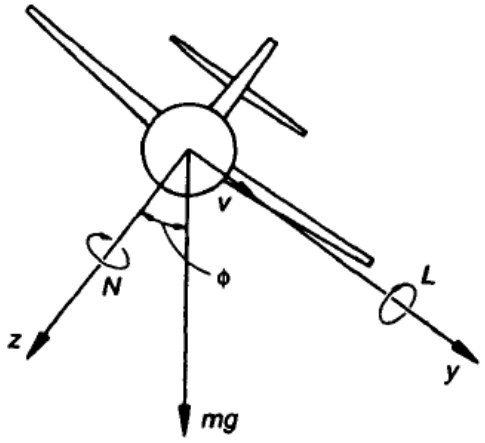

Fig 2.11 Forces in steady state slip

Source from Yechout, T.R. "Introduction to Aircraft Flight Mechanics", AIAA education Series, 2003

$$Y_v.v + mg \sin \phi = 0 \tag{6.16}$$

The rolling and yawing moments due to sideslip and from the controls must be in balance giving

$$\left.\begin{aligned} L_v \cdot v + L_\xi \cdot \xi + L_\zeta \cdot \zeta = 0 \\ N_v \cdot v + N_\xi \cdot \xi + N_\zeta \cdot \zeta = 0 \end{aligned}\right\} \tag{6.17}$$

Solving these simultaneously for ξ and ζ in terms of v gives

$$\xi = \frac{v}{\Delta}\left(L_v N_\zeta - L_\zeta N_v\right) \tag{6.18}$$

$$\zeta = \frac{v}{\Delta}\left(L_\xi N_v - L_v N_\xi\right) \tag{6.19}$$

where Δ is given by (6.14) and the roll angle can be found from (6.16). Again these expressions are dominated by the direct effects of the control angles and the effects of sideslip and can be approximated as

$$\xi \simeq -\frac{L_v \cdot v}{L_\xi} \text{ and } \zeta \simeq -\frac{N_v \cdot v}{N_\zeta} \tag{6.20}$$

This shows that in this case the aileron is primarily used to balance the rolling moment due to sideslip and the rudder to balance the yawing moment, as would be expected. The aileron and rudder angles increase rapidly with sideslip angle, whilst the roll angle increases less rapidly. Figure 6.7 shows a sketch of typical roll, aileron and rudder angles as a function of sideslip angle.

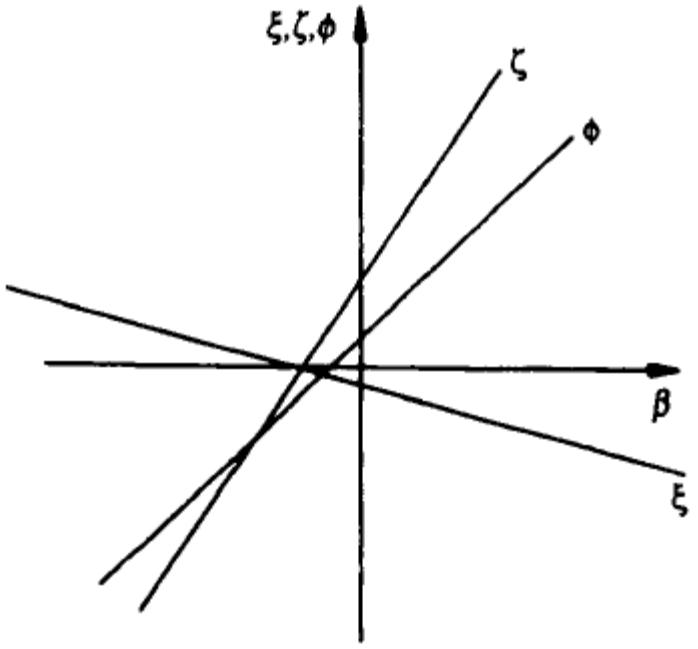

Fig. 2.12 variation of roll angle, aileron angle and rudder angle with side slip angle

Source from Yechout, T.R. "Introduction to Aircraft Flight Mechanics", AIAA education Series, 2003

-Minimum control speeds

If an engine fails on'a multi-engined aircraft then the pilot must be able to manoeuvre the aircraft. At low speeds the dynamic pressure may not be sufficient to produce sufficient yawing moment from the rudder. There is therefore a minimum speed at which the pilot can maintain straight flight. The minimum control speed in the air, VMc,, is defined in the airworthiness requirements roughly as the airspeed at which, when the critical engine is made inoperative, it is possible to maintain control of the aircraft in straight flight with a bank angle of not more than 5 ° . This has to be demonstrated by flight test when the aircraft is built. The rudder pedal force may not exceed 150 lb (= 667 N) and the change in heading may not be more than 20 °. Also VMca may not exceed 1.2Vs~. In designing an aircraft the designer will choose a value for VMc, with reference to the desired take-off performance and use it as one factor in the design of the fin and rudder. At an assumed value for VMca in the calculations, the yawing moment from the remaining engines will balance that from the fully deflected rudder. The minimum control speed on the ground, VMcg, is similarly defined; no use of a steerable nose-wheel may be assumed.

Static Stability

In this section we consider what preliminary insights we may obtain from applying the ideas of static stability. Consider an aircraft disturbed in sideslip as in figure 6.2. The yawing moment produced by the fin tends to turn the aircraft into the direction of the resultant velocity, i.e. it tends to reduce the sideslip. Therefore this is a stable response and is known as '**directional' or 'weathercock**' stability. The condition for this is then

$$N_v > 0$$

propellers ahead of the cg are destabilizing. We note that a rolling moment will also be generated through the derivative Lv so that the aircraft will be given both roll and yaw accelerations. Now let us consider an aircraft which has been given a small angle of rotation in roll around its velocity vector. No restoring moment in roll will appear because no surface of the aircraft has changed its incidence to the flow. However, there is a component of the weight along the Y-axis which will produce a sideslip; this in turn will produce a rolling moment through the derivative Lv. Positive roll angle, as shown in figure 3.9, will produce a positive sideslip velocity, and so a negative rolling moment is required for static stability. This effect is known as 'static lateral stability' and the condition for it to be positive is therefore

$$L_v < 0$$

Source from Yechout, T.R. "Introduction to Aircraft Flight Mechanics", AIAA education Series, 2003

stability into play. We see therefore that these static stability conditions are coupled and, although necessary, are not sufficient and only analysis of the dynamic stability gives the complete picture.

As in the case of static stability in pitch the measurement of the trim curves indicates the static stability. The procedure is to fly the aircraft in a series of straight sideslips, and measure the sideslip, roll, aileron and rudder angles. Then, assuming that the direct effects of the aileron and rudder are in the usual senses, (6.20) shows that for positive static lateral stability aileron angle decreases with sideslip. For positive directional stability rudder angle increases with sideslip. Figure 6.7 shows the aileron, rudder and roll angles in a sideslip for an aircraft with positive directional and lateral static stability. If stick and rudder forces are also measured then these can be used to infer the static stabilities, stick free. These are positive when the forces are in the direction to produce these stick and rudder movements. The airworthiness requirements ask that an aircraft is laterally stable as discussed above and require the trim curves and the rudder pedal force curve not to have any reversal of slope up to the maximum angles available or up to a pedal force of 180 lb (= 800 N).

Problem

A twin-engine aircraft is flying at low altitude when one engine fails. Find the slowest speed at which it can fly steadily without sideslip. Assume that the thrust of the remaining engine just balances the drag and that engine thrust is independent of speed. The maximum rudder angle is 30°, the rudder lift curve slope is 0.55 and the rudder moment arm about the cg is 16 m. Other information is as follows: mass = 200 000 kg, wing area = 300 m^2, fin area = 42 m^2, the engines are 5 m from the centreline, $C_D = 0.036 + 0.062C_L^2$. (A)

Aircraft component contribution to lateral and directional stability

-Lateral stability

An airplane is said to possess lateral static stability if after undergoing a disturbance that rolls it to some bank angle ø [Greek letter theta], it generates forces and moments that tend to reduce the bank angle and restore the equilibrium flight condition.

Dihedral is often used as a means to improve lateral stability. Figure 144(a) shows a headon view of an airplane that has dihedral where the wings are turned up at some dihedral angle to the

Source from Yechout, T.R. "Introduction to Aircraft Flight Mechanics", AIAA education Series, 2003

horizontal. Under the condition shown, in straight and level flight, the lift produced by both wings just equals the weight. Now, assume that a disturbance causes one wing to drop relative to the other as shown in figure 144(b). The lift vector rotates and there is a component of the weight acting inward which causes the airplane to move sideways in this direction. The airplane is said to sideslip and...

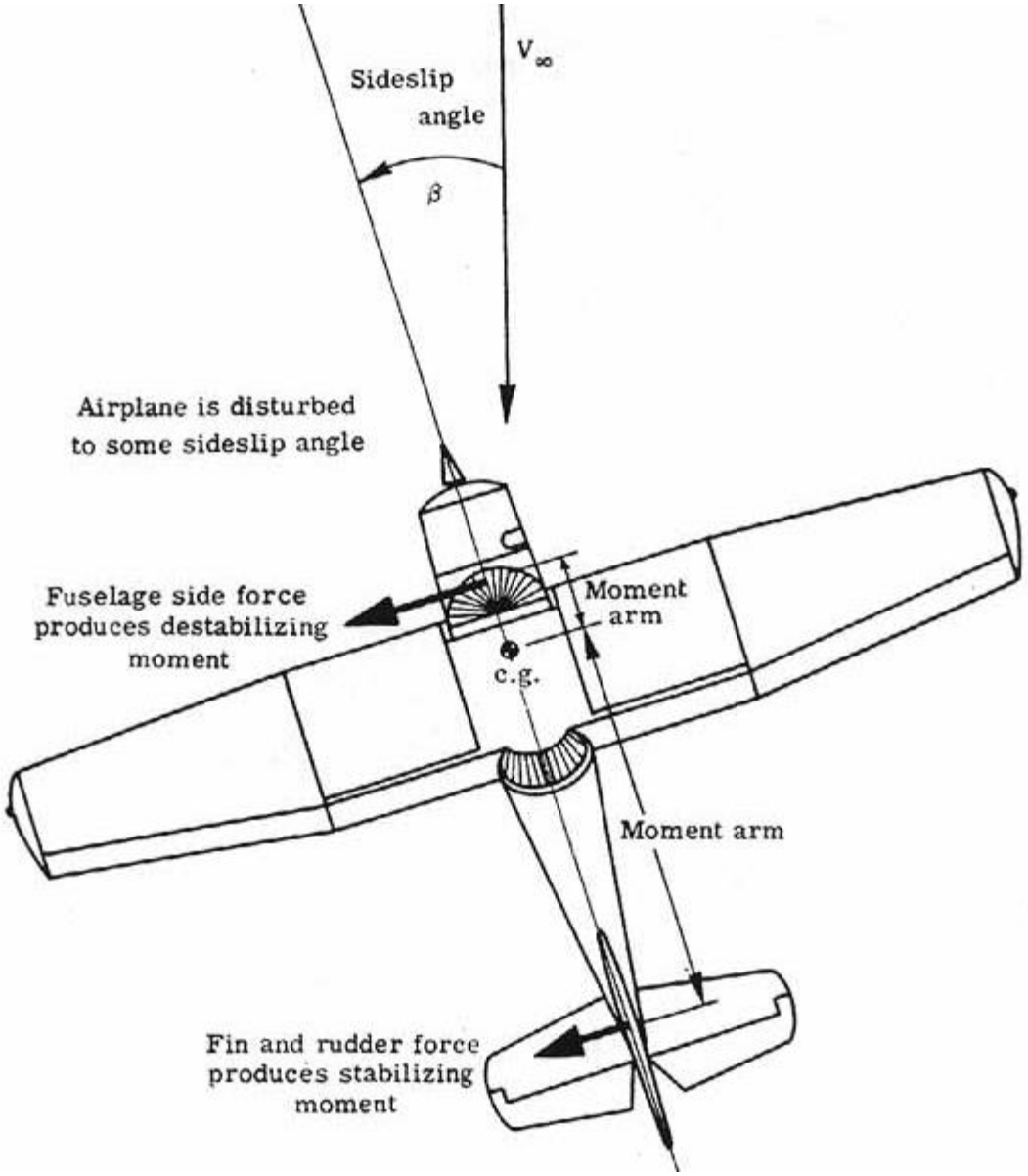

Fig.2.13 Directional stability moments.

Source from Yechout, T.R. "Introduction to Aircraft Flight Mechanics", AIAA education Series, 2003

UNIT III

Axes and notation

We have already introduced some of the notation needed in previous chapters; however, a complete statement of the basic notation will be made at this point and is shown in figure 3.1.

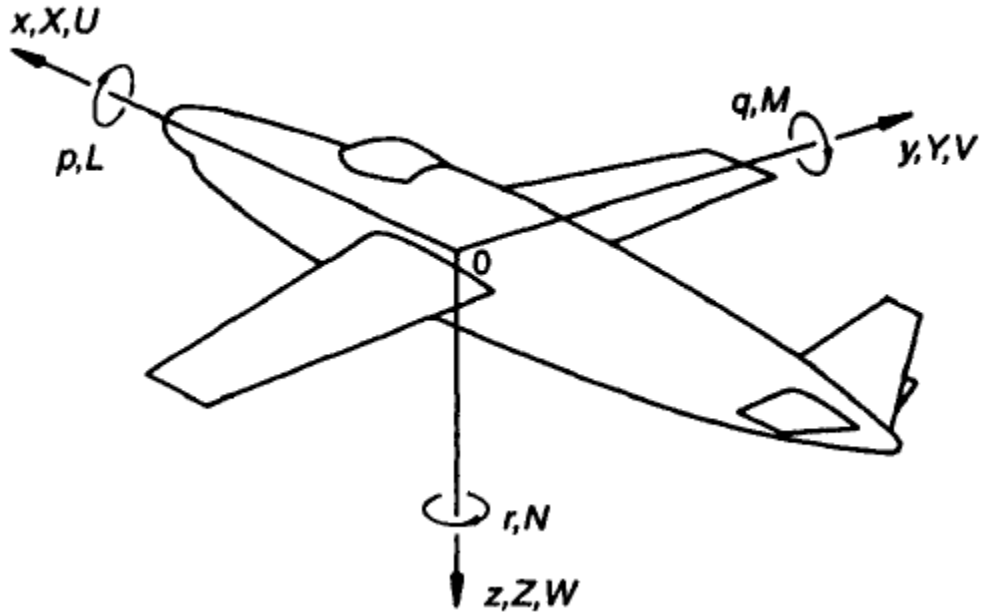

Fig.3.1 Stability axes and velocities and forces along them, angular velocities and moments around Them

We place a set of right-handed orthogonal axes with the origin at the cg. The *Ox* axis points roughly in the forward direction, *Oy* at fight angles to the plane of symmetry and towards the starboard wing tip. The z-axis points roughly downwards and completes a right-handed set. For the time being the freedom to choose the precise direction of the x-axis is left to be decided to suit the problem in hand. There are at least two natural choices: • to have the x-axis fixed initially in the direction of undisturbed flight - such axes are known as 'wind axes'; • aircraft normally have a principal axis of inertia lying roughly in the flight direction – this is sometimes a convenient direction to take as the x-axis.

Now let

• V be the velocity of the aircraft cg, with components U, V and W along *Ox, Oy* and *Oz;*

• A be the angular velocity of the aircraft, with components p, q and r about *Ox, Oy* and *Oz;*

• F be the force on the aircraft, with components X, Y and Z along *Ox, Oy* and *Oz;*

• Q be the moment on the aircraft about the cg, with components L, M and N along *Ox, Oy* and *Oz.*

The positive sense of the velocities and forces is in the direction of the axes and that of the angular velocities and moments is that of a right-hand screw advancing along the direction of the axes.

Source from Yechout, T.R. "Introduction to Aircraft Flight Mechanics", AIAA education Series, 2003

Orientation

Three rotations about non-parallel axes will move one set of axes so as to be parallel with another set; however, there are many possible choices of combinations of rotations about the axes and the order to take them in. We choose one attributed to Euler as follows: take clockwise rotations gt, 0 and ~ about the *Oz, Oy* and *Ox* axes *where rotation takes place about that position of the axis to which previous rotations have brought it.* We will rotate a set of axes parallel to the axes in the undisturbed state into parallelism with the position of the axes at some time t after the start of the disturbance. The angles of rotation required then define the orientation of the aircraft. Figure 3.2 shows the procedure.

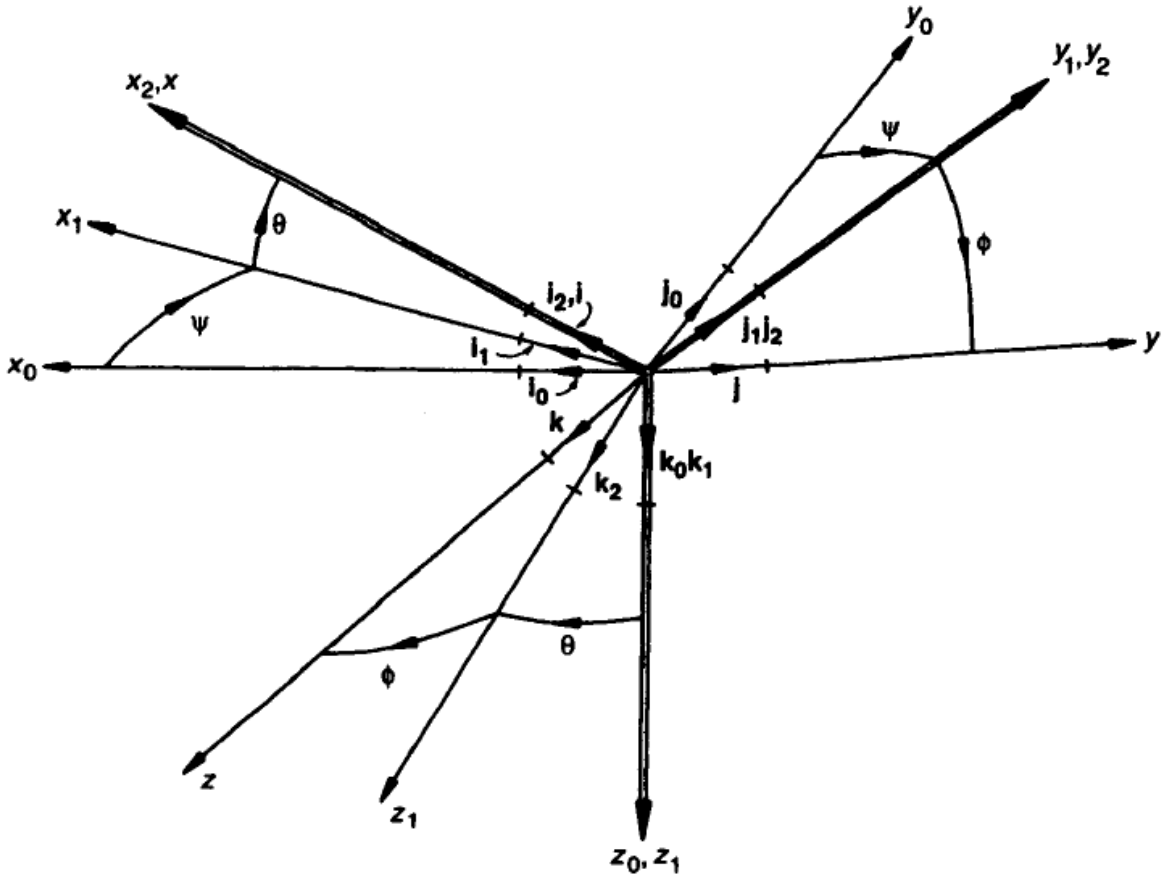

Fig:2.2 Definition of Euler angles and unit vectors along various axes

Oxyz. To keep track of the directions of the axes choose unit vectors io, Jo, ko; il, j~, kl; i2, J2, k2 and i, j, k along the axes, respectively. We now need the relations between these unit vectors. Consider the first rotation gt about the Ozo axis; figure 8.3 shows the view looking along that axis. In the figure we have dropped perpendiculars PN and QT from the ends of the unit vectors io, Jo onto the *Ox~* and O),1 axes. Then from the triangles formed we see

Source from Yechout, T.R. "Introduction to Aircraft Flight Mechanics", AIAA education Series, 2003

$$\left.\begin{aligned} \mathbf{i}_0 = \overrightarrow{OP} = \overrightarrow{ON} + \overrightarrow{NP} &= \mathbf{i}_1 \cos\psi - \mathbf{j}_1 \sin\psi \\ \mathbf{j}_0 = \overrightarrow{OQ} = \overrightarrow{OT} + \overrightarrow{TQ} &= \mathbf{j}_1 \cos\psi + \mathbf{i}_1 \sin\psi \\ \mathbf{k}_0 &= \mathbf{k}_1 \end{aligned}\right\}$$

since the perpendiculars PN and QT are parallel to -Oy~ and *Ox*~.Each rotation looks like any other when viewed along its axis of rotation, allowing for the change of labels on the axes. Hence for the rotation 0 about the Oy~ axis,

$$\left.\begin{aligned} \mathbf{i}_1 &= \mathbf{k}_2 \sin\theta + \mathbf{i}_2 \cos\theta \\ \mathbf{j}_1 &= \mathbf{j}_2 \\ \mathbf{k}_1 &= \mathbf{k}_2 \cos\theta - \mathbf{i}_2 \sin\theta \end{aligned}\right\}$$

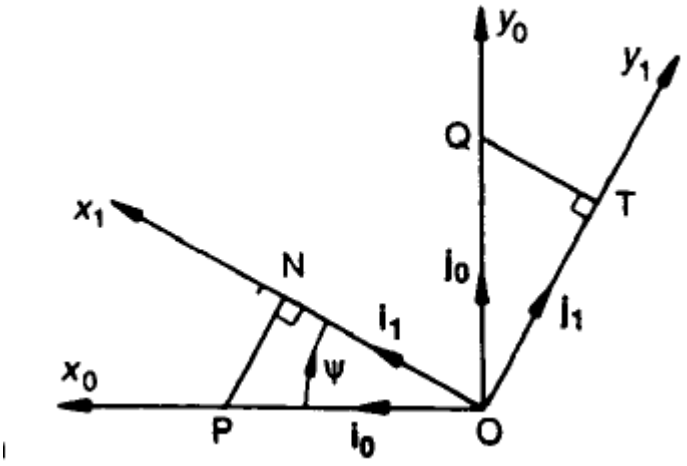

Fig 3.3 Relation for one rotation

Source from Yechout, T.R. "Introduction to Aircraft Flight Mechanics", AIAA education Series, 2003

and for the rotation ϕ about the Ox_2 axis,

$$\left.\begin{aligned} \mathbf{i}_2 &= \mathbf{i} \\ \mathbf{j}_2 &= \mathbf{j}\cos\phi - \mathbf{k}\sin\phi \\ \mathbf{k}_2 &= \mathbf{j}\sin\phi + \mathbf{k}\cos\phi \end{aligned}\right\}$$

Then on substituting back we find

$$\left.\begin{aligned} \mathbf{i}_0 &= \mathbf{i}\cos\psi\cdot\cos\theta + \mathbf{j}(\cos\psi\cdot\sin\theta\cdot\sin\phi - \sin\psi\cdot\cos\phi) \\ &\quad + \mathbf{k}(\cos\psi\cdot\sin\theta\cdot\cos\phi + \sin\psi\cdot\sin\phi) \\ \mathbf{j}_0 &= \mathbf{i}\sin\psi\cdot\cos\theta + \mathbf{j}(\sin\psi\cdot\sin\theta\cdot\sin\phi + \cos\psi\cdot\cos\phi) \\ &\quad + \mathbf{k}(\sin\psi\cdot\sin\theta\cdot\cos\phi - \cos\psi\cdot\sin\phi) \\ \mathbf{k}_0 &= -\mathbf{i}\sin\theta + \mathbf{j}\cos\theta\cdot\sin\phi + \mathbf{k}\cos\theta\cdot\cos\phi \end{aligned}\right\}$$

which are the required relationships. The inverse relations are also needed; they are a similar manner and are

$$\left.\begin{aligned} \mathbf{i} &= \mathbf{i}_0\cos\psi\cdot\cos\theta + \mathbf{j}_0\sin\psi\cdot\cos\theta - \mathbf{k}_0\sin\theta \\ \mathbf{j} &= \mathbf{i}_0(\cos\psi\cdot\sin\theta\cdot\sin\phi - \sin\psi\cdot\cos\phi) \\ &\quad + \mathbf{j}_0(\sin\psi\cdot\sin\theta\cdot\sin\phi + \cos\psi\cdot\cos\phi) + \mathbf{k}_0\cos\theta\cdot\sin\phi \\ \mathbf{k} &= \mathbf{i}_0(\sin\psi\cdot\sin\phi + \cos\psi\cdot\sin\theta\cdot\cos\phi) \\ &\quad + \mathbf{j}_0(\sin\psi\cdot\sin\theta\cdot\cos\phi - \cos\psi\cdot\sin\phi) + \mathbf{k}_0\cos\theta\cdot\cos\phi \end{aligned}\right\}$$

Relations between the rates of change of angles

Suppose we find the orientation, or Euler, angles at time t and at time t + &. Then by the usual process of taking differences, dividing by *6t* and proceeding to the limit we can define V, 0 and ¢~. The vector sum of these must be the angular velocity vector of the aircraft, A. They. are, however, measured about non-orthogonal axes; because ~ is a rotation about *Ox2,* then ~ is a vector along that axis. Similarly 0 is along *Oy*~ and ~,along Ozo. Hence we can express A as

$$\mathbf{A} = \dot{\phi}\mathbf{i}_2 + \dot{\theta}\mathbf{j}_1 + \dot{\psi}\mathbf{k}_0$$

then the appropriate substitutions from the previous section give

$$\mathbf{A} = \dot{\phi}\mathbf{i} + \dot{\theta}(\mathbf{j}\cos\phi - \mathbf{k}\sin\phi) + \dot{\psi}(-\mathbf{i}\sin\theta + \mathbf{j}\cos\theta.\sin\phi + \mathbf{k}\cos\theta.\cos\phi)$$

These then are the relations between the rates of change of the orientation angles and the components of angular velocity and, as they are linear, they can be solved for ~ 0 and ~ in terms of p, q and r. When we have solved a problem these may be integrated to find the orientation of the aircraft during the disturbance.

Source from Yechout, T.R. "Introduction to Aircraft Flight Mechanics", AIAA education Series, 2003

The aircraft angular velocity can also be expressed as

$$\mathbf{A} = p\mathbf{i} + q\mathbf{j} + r\mathbf{k}$$

Then equating the components of **A** we find

$$\left.\begin{aligned} p &= \dot{\phi} - \dot{\psi}\sin\theta \\ q &= \dot{\theta}\cos\phi + \dot{\psi}\cos\theta\cdot\sin\phi \\ r &= -\dot{\theta}\sin\phi + \dot{\phi}\cos\theta\cdot\cos\phi \end{aligned}\right\}$$

Development of the equations

At this stage we need to define the initial condition of flight as different initial conditions lead to slightly different forms of the final equations. The standard choice is that of a straight steady unsideslipped climb at speed V_e with the x-axis at an angle Θ_e to the horizontal. In straight steady flight we have

$$\mathbf{A} = \dot{\mathbf{A}} = \dot{\bar{\mathbf{v}}} = V = 0 \tag{8.9}$$

with the result that the equations of motion reduce to

$$\mathbf{F} = \mathbf{F}_{a_e} + \mathbf{F}_{g_e} = 0 \tag{8.10}$$

and

$$\mathbf{Q}_{a_e} = 0 \tag{8.11}$$

This flight condition will be referred to as the 'datum flight condition' and the values of quantities in this condition are indicated by the suffix 'e'.

-Components of the weight

We now consider the components of the weight along the various axes. Figure 8.4 shows the aircraft in the datum condition, with the x-axis at an angle α_e to the direction of flight. From the figure we see that the weight vector is initially

$$\mathbf{F}_{g_e} = mg\left[-\mathbf{i}_0\sin\Theta_e + \mathbf{k}_0\cos\Theta_e\right] \tag{8.12}$$

We substitute for $\mathbf{i}_0$ and $\mathbf{k}_0$ from (8.6) to obtain the weight vector in terms of **i**, **j** and **k**, that is we find its components along the disturbed aircraft axes. Then

$$\begin{aligned} \mathbf{F}_g = mg\Big[&-\{\mathbf{i}\cos\psi\cdot\cos\theta + \mathbf{j}(\cos\psi\cdot\sin\theta\cdot\sin\phi - \sin\psi\cdot\cos\phi) \\ &+ \mathbf{k}(\cos\psi\cdot\sin\theta\cdot\cos\phi + \sin\psi\cdot\sin\phi)\}\sin\Theta_e \\ &+ \{-\mathbf{i}\sin\theta + \mathbf{j}\cos\theta\cdot\sin\phi + \mathbf{k}\cos\theta\cdot\cos\phi\}\cos\Theta_e\Big] \\ = X_g\mathbf{i} + Y_g\mathbf{j} + Z_g\mathbf{k} \end{aligned}$$

Source from Yechout, T.R. "Introduction to Aircraft Flight Mechanics", AIAA education Series, 2003

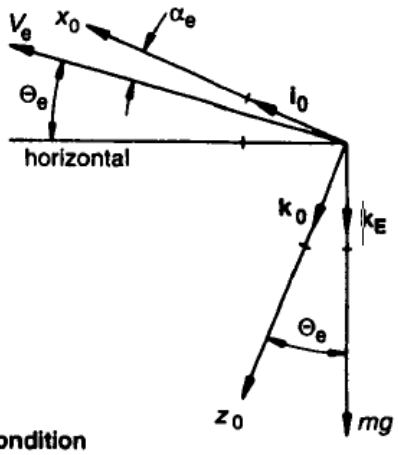

Fig. 8.4 Datum flight condition

Then equating components we have

$$\left.\begin{aligned} X_g &= -mg\left[\cos\psi\cdot\cos\theta\cdot\sin\Theta_e + \sin\theta\cdot\cos\Theta_e\right] \\ Y_g &= mg\left[\left\{\sin\psi\cdot\cos\phi - \cos\psi\cdot\sin\theta.\sin\phi\right\}\sin\Theta_e + \cos\theta\cdot\sin\phi\cdot\cos\Theta_e\right] \\ Z_g &= mg\left[-\left\{\cos\psi\cdot\sin\theta\cdot\cos\phi + \sin\psi\cdot\sin\phi\right\}\sin\Theta_e + \cos\theta\cdot\cos\phi.\cos\Theta_e\right] \end{aligned}\right\} \quad (8.13)$$

We write the aerodynamic forces in the datum condition as X_{a_e}, Y_{a_e} and Z_{a_e}. Then the equations of linear motion are

$$\left.\begin{aligned} -mg\sin\Theta_e + X_{a_e} &= 0 \\ Y_{a_e} &= 0 \\ mg\cos\Theta_e + Z_{a_e} &= 0 \end{aligned}\right\} \quad (8.14)$$

Small Perturbation

We come now to the first and most far-reaching of the simplifying assumptions; it is that the aircraft is only disturbed by small amounts from the initial steady state. From figure 8.4 we see that the initial flight velocity, V_e, can be resolved along the initial aircraft axes into U_e and W_e where

$$U_e = V_e \cos\alpha_e \text{ and } W_e = V_e \sin\alpha_e \quad (8.15)$$

We then write

$$\left.\begin{aligned} U &= U_e + u \\ V &= v \\ W &= W_e + w \end{aligned}\right\} \quad (8.16)$$

The assumption is then specifically that

- u, v and w are much less than the speed V_e;
- p, q and r are much less than V_e/l where l is a characteristic length of the aircraft. This implies, for instance, that the helix angle of the rolling wing discussed in Section 7.2.1 is small;
- ψ, θ and ϕ are small.

Source from Yechout, T.R. "Introduction to Aircraft Flight Mechanics", AIAA education Series, 2003

We come now to the first and most far-reaching of the simplifying assumptions; it is that the aircraft is only disturbed by small amounts from the initial steady state. From figure 8.4 we see that the initial flight velocity, V_e, can be resolved along the initial aircraft axes into U_e and W_e where

$$U_e = V_e \cos \alpha_e \text{ and } W_e = V_e \sin \alpha_e \tag{8.15}$$

We then write

$$\left.\begin{aligned} U &= U_e + u \\ V &= v \\ W &= W_e + w \end{aligned}\right\} \tag{8.16}$$

The assumption is then specifically that

- u, v and w are much less than the speed V_e;
- p, q and r are much less than V_e/l where l is a characteristic length of the aircraft. This implies, for instance, that the helix angle of the rolling wing discussed in Section 7.2.1 is small;
- ψ, θ and ϕ are small.

These quantities are known as 'stability derivatives'. The derivatives used in Chapters 6 and 7 are quasi-static versions of these stability derivatives; as before the superscript ord, '°', is to indicate that it is a dimensional, or 'ordinary', quantity.

To improve the correlation between theory and experiment, it has been found necessary to add derivatives with respect to linear accelerations, in particular the vertical acceleration $\dot{w}$. We will add only the two derivatives, $Z_{\dot{w}}$ and $M_{\dot{w}}$, but it is a simple matter to add more if required. If the aircraft were in a flight condition such that displacements from the datum flight path generated forces or moments then derivatives due to this source would be required. Determining these displacements is dealt with in Section 8.6.2.1. Examples of such cases are flight near the ground or in the flow field of another aircraft.

Source from Yechout, T.R. "Introduction to Aircraft Flight Mechanics", AIAA education Series, 2003

--Linearized equations of motion

$$\left.\begin{aligned} X_g + X_a &= m(\dot{u} + qW_e) \\ Y_g + Y_a &= m(\dot{v} + rU_e - pW_e) \\ Z_g + Z_a &= m(\dot{w} - qU_e) \\ L_a &= \dot{h}_1 \\ M_a &= \dot{h}_2 \\ N_a &= \dot{h}_3 \end{aligned}\right\} \qquad (8.20)$$

$$\left.\begin{aligned} X_g + X_a &= m(\dot{u} + qW_e) \\ Y_g + Y_a &= m(\dot{v} + rU_e - pW_e) \\ Z_g + Z_a &= m(\dot{w} - qU_e) \\ L_a &= \dot{h}_1 \\ M_a &= \dot{h}_2 \\ N_a &= \dot{h}_3 \end{aligned}\right\}$$

ght become

(8.20) (8.21)

$$g_1 = g \cos \Theta_e \text{ and } g_2 = g \sin \Theta_e \qquad (8.22)$$

Another drastic simplification takes place with the relation between the rates of change of orientation angles and the components of angular velocity (8.8). These become

$$\left.\begin{aligned} p &= \dot{\phi} \\ q &= \dot{\theta} \\ r &= \dot{\phi} \end{aligned}\right\} \qquad (8.23)$$

Dimensional stability equations

We can now assemble the equations for the stability. Starting from (8.20) we substitute for the components of momentum from (8.24), the components of weight from (8.21) and the aerodynamic terms from (8.17) and similar expressions with (8.25) substituted. We finally subtract the equations of motion in the datum case, (8.14). The results are

$$m(\dot{u} + qW_e) = -mg_1\theta + \overset{\circ}{X}_u u + \overset{\circ}{X}_w w + \overset{\circ}{X}_q q + \overset{\circ}{X}(t) \qquad (8.26)$$

$$m(\dot{v} + rU_e - pW_e) = m(g_1\phi + g_2\psi) + \overset{\circ}{Y}_v v + \overset{\circ}{Y}_p p + \overset{\circ}{Y}_r r + \overset{\circ}{Y}(t) \qquad (8.27)$$

Source from Yechout, T.R. "Introduction to Aircraft Flight Mechanics", AIAA education Series, 2003

$$m(\dot{w} - qU_e) = -mg_2\theta + \mathring{Z}_u u + \mathring{Z}_w w + \mathring{Z}_{\dot{w}}\dot{w} + \mathring{Z}_q q + \mathring{Z}(t \qquad (8.28)$$

$$I_x\dot{p} - I_{xz}\dot{r} = \mathring{L}_v v + \mathring{L}_p p + \mathring{L}_r r + \mathring{L}(t) \qquad (8.29)$$

$$I_y\dot{q} = \mathring{M}_u u + \mathring{M}_w w + \mathring{M}_{\dot{w}}\dot{w} + \mathring{M}_q q + \mathring{M}(t) \qquad (8.30)$$

$$I_z\dot{r} - I_{xz}\dot{p} = \mathring{N}_v v + \mathring{N}_p p + \mathring{N}_r r + \mathring{N}(t) \qquad (8.31)$$

In these equations p, q and r are related to $\dot{\psi}$, $\dot{\theta}$ and $\dot{\phi}$ by (8.23).

There are a number of observations to be made about these equations. First, we note that (8.26), (8.28) and (8.30) are independent of (8.27), (8.29) and (8.31); this is a result of the assumptions of small perturbations and of symmetry. The first three involving u, w and q comprise motion entirely in the plane of symmetry, and are known as the 'longitudinal stability equations'. The second set involving v, p and r comprise motions out of the plane and are known as the 'lateral stability equations'. They are sets of three simultaneous linear differential equations with time as the independent variable. Whilst normally a mechanical system with three degrees of freedom would be expected to result in three second-order equations, some of these equations are only of first order.

These equations cannot be regarded as sufficient to deal with all possible circumstances. In special cases additional stability derivatives, dynamic terms or terms expressing the effects of unconventional controls may be needed. In some cases it may not be justified to assume that changes in height are small and changes in density may have to be allowed for. This will require a further equation to accommodate the extra freedom and corresponding stability derivatives. Such changes can usually be made on an *ad hoc* basis.

Source from Yechout, T.R. "Introduction to Aircraft Flight Mechanics", AIAA education Series, 2003

Concise stability equations

In this case we simply divide through by the mass or inertia. We need to define concise derivatives and terms such as

$$\dot{x}_u = -\frac{\dot{X}_u}{m},\ \dot{n}_v = -\frac{\dot{N}_v}{m},\ \dot{m}_q = -\frac{\dot{M}_q}{I_y},\ \dot{l}(t) = -\frac{\dot{L}(t)}{I_x} \tag{8.41}$$

The definitions of all the concise derivatives include a change of sign as almost all derivatives are negative. We also need to define other quantities such as $x(t) = X(t)/m$ and so on for the other derivatives, also $e_x = -I_{xz}/I_x$ and $e_z = -I_{xz}/I_z$. Our equations (8.26)–(8.31) then become

$$\dot{u} + g_1\theta + \dot{x}_u u + x_w w + (x_q + W_e)q = -\dot{x}(t) \tag{8.42}$$

$$\dot{v} - g_1\phi - g_2\psi + y_v v + (y_p - W_e)p + (y_r + U_e)r = -\dot{y}(t) \tag{8.43}$$

$$\dot{w} + g_2\theta + z_u u + z_w w + z_{\dot{w}}\dot{w} + (z_q - U_e)q = -\dot{z}(t) \tag{8.44}$$

$$\dot{p} + e_x\dot{r} + l_v v + l_p p + l_r r = -\dot{l}(t) \tag{8.45}$$

$$\dot{q} + m_u u + m_w w + m_{\dot{w}}\dot{w} + m_q q = -\dot{m}(t) \tag{8.46}$$

$$\dot{r} + e_z\dot{p} + n_v v + n_p p + n_r r = -\dot{n}(t) \tag{8.47}$$

In some investigations it is necessary to work in terms of ordinary time, for instance if a real pilot is involved such as as in a flight simulator. No further manipulation of the equations then appears possible.

Source from Yechout, T.R. "Introduction to Aircraft Flight Mechanics", AIAA education Series, 2003

3.3 Aircraft Axis Systems

In this chapter we will concern ourselves with three axis systems. These include the body axis system fixed to the aircraft, the Earth axis system, which we will assume to be an inertial axis system fixed to the Earth, and the stability axis system, which is defined with respect to the relative wind. Each of these systems is useful in that they provide a convenient system for defining a particular vector, such as, the aerodynamic forces, the weight vector, or the thrust vector.

3.3.1 Body Axis System

The body axis system is fixed to the aircraft with its origin at the aircraft's center of gravity. The x axis is defined out the nose of the aircraft along some reference line. The reference line may be chosen to be the chord line of the aircraft or may be along the floor of the aircraft, as is often the case in large transports. The y axis is defined out the right wing of the aircraft, and the z axis is defined as down through the bottom of the aircraft in accordance with the right-hand rule, as shown in Fig. 3.1. The pilot sits in the body axis system, making it a very useful reference frame. Additionally, it is relatively easy to determine the moments and products of inertia in the body axis system because it is fixed to the aircraft.

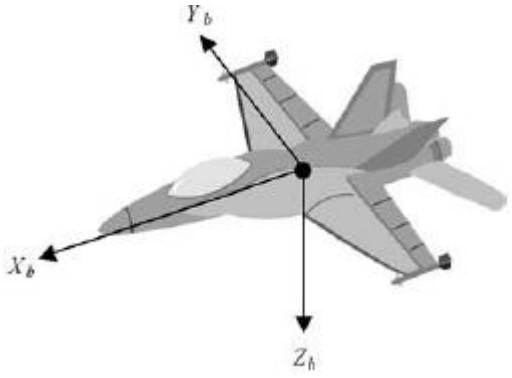

Fig 3.1 Body axis system

Earth Axis System

The Earth axis system is fixed to the Earth with its z axis pointing to the center of the Earth. The x axis and y axis are orthogonal and lie in the local horizontal plane with the origin at the aircraft center of gravity. Often, the x axis is defined as North and the y axis defined as East. The Earth axis system is assumed to be an inertial axis system for aircraft problems. This is important because Newton's 2nd law is valid only in an inertial system. While this assumption is not totally accurate, it works well for aircraft problems where the aircraft rotation rates are large compared to the rotation rate of the Earth.

Stability Axis System

The stability axis system is rotated relative to the body axis system through the angle of attack. This means that the stability x axis points in the direction of the projection of the relative wind onto the xz plane of the aircraft. The origin of the stability axis system is also at the aircraft center of gravity. The y axis is out the right wing and coincident with the y axis of the body axis system. The z axis is

orthogonal and points downward in accordance with the right-hand rule. This is illustrated in Fig. 3.2. The stability axis system is particularly useful in defining the aerodynamic forces of lift and drag.

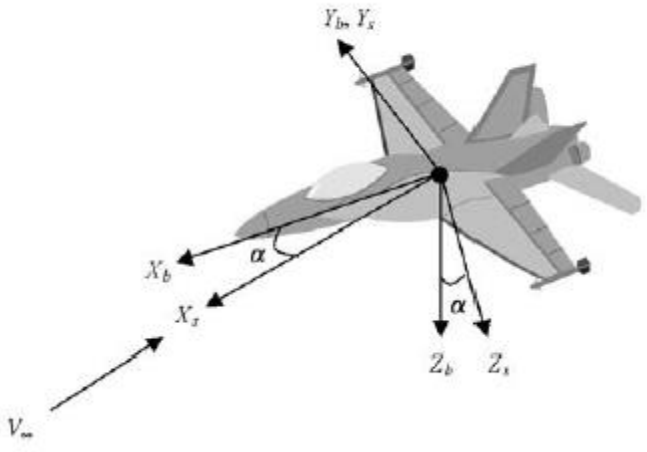

Fig. 3.2 Stability axis system

Coordinate Transformations

As stated previously, it is convenient to express certain vectors in a particular coordinate system. For example, the weight vector of the aircraft is conveniently represented in the Earth axis system where there is only a component in the positive z direction because the vector acts toward the center of the Earth, that is,

$$\bar{F}_{\text{Weight}_{\text{Earth}}} = \bar{F}_{\text{Gravity}_{\text{Earth}}} = \bar{F}_{G_E} = \begin{bmatrix} 0 \\ 0 \\ W \end{bmatrix}_{\text{Earth}} = \begin{bmatrix} 0 \\ 0 \\ mg \end{bmatrix}_{\text{Earth}} \quad 3.1$$

The aerodynamic forces are conveniently displayed in the stability axis, where drag acts in the negative x direction and lift acts in the negative z axis, that is,

$$\bar{F}_{\text{Aero}} = \bar{F}_A = \begin{bmatrix} -D \\ F_{A_y} \\ -L \end{bmatrix}_{\text{Stability}} \quad 3.2$$

Likewise, the thrust vector can easily be expressed in the body axis as

$$\bar{F}_{\text{Thrust}} = \bar{F}_T = \begin{bmatrix} T\cos(\phi_T) \\ 0 \\ -T\sin(\phi_T) \end{bmatrix}_{\text{Body}} \quad 3.3$$

where fT is the angle between the x-body axis and the thrust vector, T. While these equations are conveniently displayed in a particular axis system, they must be all transformed into the same axis system before they can be summed in the equations of motion. As a result, it is very important to understand how to transform a vector from one axis system to another.

Source from Yechout, T.R. "Introduction to Aircraft Flight Mechanics", AIAA education Series, 2003

Earth Axis to Body Axis Transformation

Transforming a vector from the Earth axis system to the body axis system requires three consecutive rotations about the z axis, y axis, and x axis, respectively. In flight mechanics, the Euler angles are used to rotate the ‘‘vehicle carried’’ Earth axis system into coincidence with the body axis system. The Euler angles are expressed as yaw (C), pitch (Y), and roll (F). Euler angles are very useful in describing the orientation of the aircraft with respect to inertial space. The proper order or rotation is illustrated in Fig. 4.3. The yaw angle, C, is defined as the angle between the projection of the x body axis onto the horizontal plane and the x axis of the Earth axis system With the Earth x axis defined as North, the yaw angle is the same as the vehicle heading angle. The pitch angle, Y, is the angle measured in a vertical plane between the x-body axis and the horizontal plane. The roll angle, F, is the angle measured in the yz plane of the vehicle body axis system, between the y-body axis and the horizontal plane. This is the same as the bank angle.

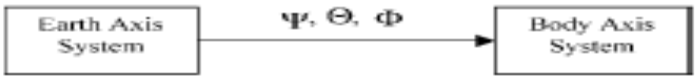

Fig. 4.3 Earth to body transformation.

for a given ψ and θ, and is a measure of the rotation about the x axis to put the aircraft in the desired position from a wing's horizontal condition. The accepted limits on the Euler angles are

$$\begin{aligned} 0 \le \Psi &\le 360 \text{ deg} \\ -90 \text{ deg} \le \Theta &\le 90 \text{ deg} \\ -180 \text{ deg} \le \Phi &\le 180 \text{ deg} \end{aligned}$$

The importance of the sequence of the Euler angle rotations cannot be overemphasized. If the sequence is performed in a different order than ψ, θ, and ϕ, the final result will be incorrect. The following illustrates the transformation of a vector, $\bar{F}_E$, in the Earth axis system into the body axis system, where

$$\bar{F}_E = X_E \hat{i}_E + Y_E \hat{j}_E + Z_E \hat{k}_E \tag{4.4}$$

and $\hat{i}_E$, $\hat{j}_E$, and $\hat{k}_E$ are the unit vectors in the Earth axis system. Therefore,

$$\bar{F}_E = \begin{bmatrix} X_E \\ Y_E \\ Z_E \end{bmatrix}_{\text{Earth}} \tag{4.5}$$

If we rotate through the yaw angle, ψ, about the z-Earth axis, $\hat{k}_E$, we end up in some intermediate axis system $\hat{i}'$, $\hat{j}'$, and $\hat{k}'$. (See Fig. 4.4.)

The vector in the intermediate axis system ($\hat{i}'$, $\hat{j}'$, and $\hat{k}'$) is:

$$\bar{F}' = X'\hat{i}' + Y'\hat{j}' + Z'\hat{k}' \tag{4.6}$$

where

$$\begin{aligned} X' &= X_E \cos\Psi + Y_E \sin\Psi \\ Y' &= -X_E \sin\Psi + Y_E \cos\Psi \\ Z' &= Z_E \end{aligned} \tag{4.7}$$

Source from Yechout, T.R. “Introduction to Aircraft Flight Mechanics”, AIAA education Series, 2003

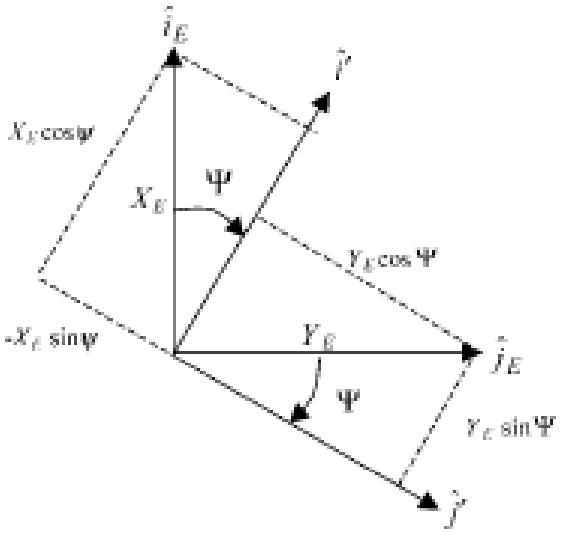

Fig. 4.4 Rotation through Ψ.

so

$$\begin{bmatrix} X' \\ Y' \\ Z' \end{bmatrix} = \underbrace{\begin{bmatrix} \cos\Psi & \sin\Psi & 0 \\ -\sin\Psi & \cos\Psi & 0 \\ 0 & 0 & 1 \end{bmatrix}}_{R_3(\Psi)} \begin{bmatrix} X_E \\ Y_E \\ Z_E \end{bmatrix} \tag{4.8}$$

$$\bar{F}' = R_3(\Psi)\bar{F}_E \tag{4.9}$$

We will now rotate this intermediate vector, $\bar{F}'$, through some pitch angle, Θ, to some other intermediate axis system, $\hat{i}''$, $\hat{j}''$, and $\hat{k}''$ as shown in Fig. 4.5.

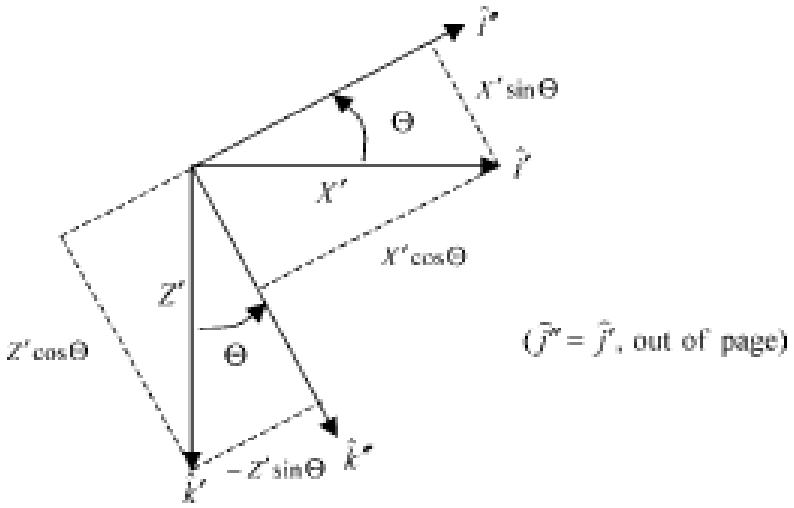

Fig. 4.5 Rotation through Θ.

Source from Yechout, T.R. "Introduction to Aircraft Flight Mechanics", AIAA education Series, 2003

The vector in the intermediate axis is

$$\bar{F}'' = X''i'' + Y''j'' + Z''k'' \tag{4.10}$$

where

$$\begin{aligned} X'' &= X' \cos\Theta - Z' \sin\Theta \\ Y'' &= Y' \\ Z'' &= X' \sin\Theta + Z' \cos\Theta \end{aligned} \tag{4.11}$$

$$\begin{bmatrix} X'' \\ Y'' \\ Z'' \end{bmatrix} = \underbrace{\begin{bmatrix} \cos\Theta & 0 & -\sin\Theta \\ 0 & 1 & 0 \\ \sin\Theta & 0 & \cos\Theta \end{bmatrix}}_{R_2(\Theta)} \begin{bmatrix} X' \\ Y' \\ Z' \end{bmatrix} \tag{4.12}$$

so,

$$\bar{F}' = R_2(\Theta)\bar{F}' = R_2(\Theta)R_3(\Psi)\bar{F}_e \tag{4.13}$$

Finally we will rotate the vector, $\bar{F}''$, through some roll angle, Φ, into the body axis system, $\hat{i}$, $\hat{j}$, and $\hat{k}$ as shown in Fig. 4.6.

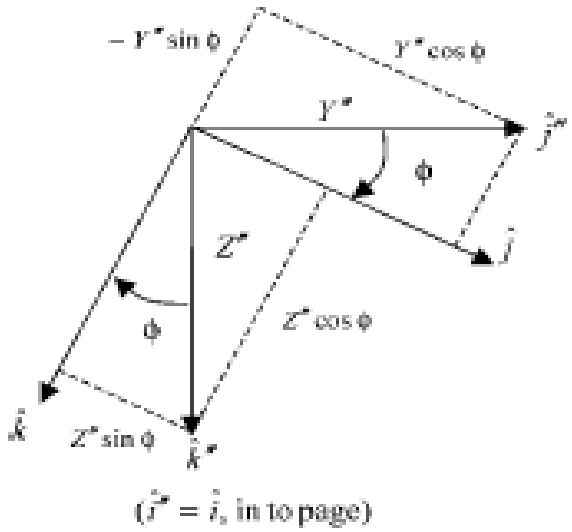

Fig. 4.6 Rotation through Φ.

Source from Yechout, T.R. "Introduction to Aircraft Flight Mechanics", AIAA education Series, 2003

The vector in the body axis system is

$$\bar{F}_B = X_B\hat{i} + Y_B\hat{j} + Z_B\hat{k} \tag{4.14}$$

where

$$\begin{aligned} X_B &= X'' && (\hat{i}\text{ direction}) \\ Y_B &= Y''\cos\Phi + Z''\sin\Phi && (\hat{j}\text{ direction}) \\ Z_B &= -Y''\sin\Phi + Z''\cos\Phi && (\hat{k}\text{ direction}) \end{aligned} \tag{4.15}$$

$$\begin{bmatrix} X_B \\ Y_B \\ Z_B \end{bmatrix} = \underbrace{\begin{bmatrix} 1 & 0 & 0 \\ 0 & \cos\Phi & \sin\Phi \\ 0 & -\sin\Phi & \cos\Phi \end{bmatrix}}_{R_1(\Phi)} \begin{bmatrix} X'' \\ Y'' \\ Z'' \end{bmatrix} \tag{4.16}$$

so,

$$\bar{F}_B = R_1(\Phi)\bar{F}' = R_1(\Phi)R_2(\Theta)R_3(\Psi)\bar{F}_E \tag{4.17}$$

Therefore, any vector in the Earth axis system can be transformed into the body axis system using the following transformation.

$$\bar{F}_B = R_1(\Phi)R_2(\Theta)R_3(\Psi)\bar{F}_E \tag{4.18}$$

This transformation is very useful in transforming the weight vector of an aircraft expressed in the Earth axis into the body axis system. As shown earlier in Eq. (4.1), the aircraft's weight vector in the Earth axis system is

$$\bar{F}_{\text{Gravity}_{\text{Earth}}} = \bar{F}_{G_E} = \begin{bmatrix} 0 \\ 0 \\ W \end{bmatrix}_{\text{Earth}} = \begin{bmatrix} 0 \\ 0 \\ mg \end{bmatrix}_{\text{Earth}} \tag{4.19}$$

The vector in the body axis system is easily found using the transformation from Eq. (4.18) as shown in Eq. (4.20).

$$\bar{F}_{\text{Gravity}_B} = \begin{bmatrix} 1 & 0 & 0 \\ 0 & \cos\Phi & \sin\Phi \\ 0 & -\sin\Phi & \cos\Phi \end{bmatrix} \begin{bmatrix} \cos\Theta & 0 & -\sin\Theta \\ 0 & 1 & 0 \\ \sin\Theta & 0 & \cos\Theta \end{bmatrix} \begin{bmatrix} \cos\Psi & \sin\Psi & 0 \\ -\sin\Psi & \cos\Psi & 0 \\ 0 & 0 & 1 \end{bmatrix} \begin{bmatrix} 0 \\ 0 \\ mg \end{bmatrix}_E \tag{4.20}$$

Source from Yechout, T.R. "Introduction to Aircraft Flight Mechanics", AIAA education Series, 2003

This yields the following weight vector in the body axis system:

$$\bar{F}_{\text{Gravity}_B} = \begin{bmatrix} -mg\sin\Theta \\ mg\sin\Phi\cos\Theta \\ mg\cos\Phi\cos\Theta \end{bmatrix}_B \tag{4.21}$$

In going from the body axis system to the Earth axis system, we go through $-\Phi$, then $-\Theta$, and then $-\Psi$. So the transformation is

$$\bar{F}_E = R_3(-\Psi)R_2(-\Theta)R_1(-\Phi)\bar{F}_B \tag{4.22}$$

For these orthonormal transformation matrices

$$\begin{aligned} R_1(-\Phi) &= R_1^T(\Phi) \\ R_2(-\Theta) &= R_2^T(\Theta) \\ R_3(-\Psi) &= R_3^T(\Psi) \end{aligned} \tag{4.23}$$

where the superscript T indicates the transposition of the matrix.

Therefore,

$$\bar{F}_E = R_3^T(\Psi)R_2^T(\Theta)R_1^T(\Phi)\bar{F}_B \tag{4.24}$$

This is convenient for transforming the acceleration or velocity vector in the body axis system into a vector in the Earth axis system, as might be measured by a radar site tracking the aircraft.

4.2.2 Stability Axis to Body Axis Transformation

It is also important to transform a vector in the stability axis system into the body axis system. This is useful in transforming the aerodynamic forces from their convenient axis system, Eq. (4.7), into the body axis system. This is accomplished by rotating the stability axis system through a positive angle of attack, as shown in Fig. 4.7.

Fig. 4.7 Stability to body axis transformation.

Source from Yechout, T.R. "Introduction to Aircraft Flight Mechanics", AIAA education Series, 2003

The transformation from stability to body is simply a rotation about the y axis through the angle α, or an $R_2(\alpha)$ transformation, namely,

$$\bar{F}_{\text{Aero}_{\text{Body}}} = R_2(\alpha)\bar{F}_{\text{Aero}_{\text{Stability}}} \tag{4.25}$$

$$\begin{bmatrix} F_{A_x} \\ F_{A_y} \\ F_{A_z} \end{bmatrix}_{\text{Body}} = \underbrace{\begin{bmatrix} \cos\alpha & 0 & -\sin\alpha \\ 0 & 1 & 0 \\ \sin\alpha & 0 & \cos\alpha \end{bmatrix}}_{R_2(\alpha)} \begin{bmatrix} -D \\ F_{A_y} \\ -L \end{bmatrix}_{\text{Stability}} \tag{4.26}$$

Therefore,

$$\begin{aligned} F_{A_{x_B}} &= -D\cos\alpha + L\sin\alpha \\ F_{A_{y_B}} &= F_{A_{y_S}} \\ F_{A_{z_B}} &= -D\sin\alpha - L\cos\alpha \end{aligned} \tag{4.27}$$

4.2.3 Summary of Axes Transformation

Figure 4.8 provides a block diagram showing the complete set of transformations from the Earth axis system to the stability axis system. As already stated, the arrow shows a positive transformation from one axis system to another.

4.3 Aircraft Force Equations

This section develops the three aircraft force equations. The force equations consist of aircraft response (in terms of accelerations) on the left-hand side of the equations, and the applied forces on the right-hand side of the equations. Newton's 2nd law states that the time rate of change of linear momentum is equal to the summation of the applied forces acting on the aircraft's center of gravity:

$$\left[\frac{\mathrm{d}(m\bar{V})}{\mathrm{d}t}\right]_{\text{Inertial}} = \bar{F} \tag{4.28}$$

It is extremely important to understand that Newton's 2nd law is only valid in an inertial reference frame. An inertial reference frame is an axis system that is

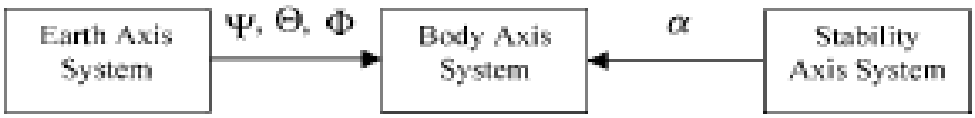

Fig. 4.8 Earth axis system to stability axis system transformation.

Source from Yechout, T.R. "Introduction to Aircraft Flight Mechanics", AIAA education Series, 2003

fixed in space with no relative motion. For the purposes of analyzing aircraft, it will be assumed that the Earth axis system is an inertial reference frame, even though it does have rotation. It is assumed that the rotation rate of the Earth is small compared to the rotation rates of the aircraft.

4.3.1 Aircraft Response

In developing the response side of the aircraft force equations, several additional assumptions will be made. First, it is assumed that the aircraft is a rigid body. This assumes that the different parts of the aircraft are not moving with respect to each other. The mass of the aircraft is also assumed to be constant, which is reasonable over a relatively short duration of time. This assumption allows Newton's 2nd law to be rewritten as

$$m\left[\frac{\mathrm{d}(\bar{V})}{\mathrm{d}t}\right]_{\text{Inertial}} = m\bar{a}_{\text{Inertial}} = \bar{F} \tag{4.29}$$

While Newton's 2nd law is only valid with respect to an inertial reference frame, the equations can be expressed in the vehicle body axis system. If the equations are expressed in the body axis system, the fact that the system is rotating with respect to an inertial reference frame must be taken into account. This is accomplished using

$$(\bar{a}_{\text{Inertial}})_{Body} = \dot{\bar{V}}_{\text{Body}} + \bar{\omega}_{\text{Body}} \times \bar{V}_{\text{Body}} \tag{4.30}$$

The velocity vector in the body axis system, $\bar{V}_{\text{Body}}$, is defined as

$$\bar{V}_{\text{Body}} = U\hat{i} + V\hat{j} + W\hat{k} \tag{4.31}$$

where U, V, and W are the velocities in the x, y, and z body axes, respectively. The aircraft angular rate in the body axis system, $\bar{\omega}_{\text{Body}}$, is defined as

$$\bar{\omega}_{\text{Body}} = P\hat{i} + Q\hat{j} + R\hat{k} \tag{4.32}$$

where P, Q, and R are the roll, pitch, and yaw rates, respectively, expressed in the body axis. Therefore,

$$(\bar{a}_{\text{Inertial}})_{Body} = \begin{bmatrix} \dot{U} \\ \dot{V} \\ \dot{W} \end{bmatrix}_{\text{Body}} + \begin{vmatrix} \hat{i} & \hat{j} & \hat{k} \\ P & Q & R \\ U & V & W \end{vmatrix}_{\text{Body}} \tag{4.33}$$

This results in

$$(\bar{a}_{\text{Inertial}})_{Body} = \begin{bmatrix} \dot{U} + QW - RV \\ \dot{V} + RU - PW \\ \dot{W} + PV - QU \end{bmatrix}_{\text{Body}} \tag{4.34}$$

Source from Yechout, T.R. "Introduction to Aircraft Flight Mechanics", AIAA education Series, 2003

Multiplying the inertial acceleration in the body axis system by the mass of the aircraft yields the three force equations

$$m\begin{bmatrix} \dot{U} + QW - RV \\ \dot{V} + RU - PW \\ \dot{W} + PV - QU \end{bmatrix}_{\text{Body}} = \begin{bmatrix} F_x \\ F_y \\ F_z \end{bmatrix}_{\text{Body}} = \bar{F}_{\text{Body}} \tag{4.35}$$

Therefore,

$$\begin{aligned} m(\dot{U} + QW - RV) &= F_x \\ m(\dot{V} + RU - PW) &= F_y \\ m(\dot{W} + PV - QU) &= F_z \end{aligned} \tag{4.36}$$

4.3.2 Applied Forces

The previous section developed the left-hand side, or response side, of the force equations. The right-hand side of each equation consists of the applied forces that act on the aircraft. They consist of the gravity forces, the aerodynamic forces, and the thrust forces.

$$\begin{aligned} m(\dot{U} + QW - RV) &= F_{G_x} + F_{A_x} + F_{T_x} \\ m(\dot{V} + RU - PW) &= F_{G_y} + F_{A_y} + F_{T_y} \\ m(\dot{W} + PV - QU) &= F_{G_z} + F_{A_z} + F_{T_z} \end{aligned} \tag{4.37}$$

Because the left-hand sides of the equations were developed in the body axis system, the right-hand side must also be in the body axis system. Therefore, each of the forces must be represented in the body axis system for the previous equations to be valid. The gravity forces, aerodynamic forces, and thrust forces were previously determined in the body axis system in Secs. 4.2.2, 4.3.2, and 4.2, respectively. Therefore, the three force equations in the body axis system are

$$\begin{aligned} m(\dot{U} + QW - RV) &= -mg\sin\Theta + (-D\cos\mathrm{A} + L\sin\mathrm{A}) + T\cos\Phi_T \\ m(\dot{V} + RU - PW) &= mg\sin\Phi\cos\Theta + F_{A_y} + F_{T_y} \\ m(\dot{W} + PV - QU) &= mg\cos\Phi\cos\Theta + (-D\sin\mathrm{A} - L\cos\mathrm{A}) - T\sin\Phi_T \end{aligned} \tag{4.38}$$

4.4 Moment Equations

The three moment equations are determined by applying Newton's 2nd law in a manner similar to the three force equations. Newton's 2nd law states that

Source from Yechout, T.R. "Introduction to Aircraft Flight Mechanics", AIAA education Series, 2003

the time rate of change in the angular momentum of the aircraft is equal to the applied moments acting on the aircraft, namely,

$$\left[\frac{d\bar{H}}{dt}\right]_{\text{Inertial}} = \bar{M} \tag{4.39}$$

$\bar{H}$ is the angular momentum of the aircraft and is defined as

$$\bar{H} = \bar{r} \times (m\bar{V}) \tag{4.40}$$

Equation (4.39) will be used, along with some simplifying assumptions, to develop the three rotational equations of motion.

4.4.1 Response Side of Moment Equations

A six-step procedure will be used to methodically build up the response side of the three moment equations. This provides both a mathematical and physical insight into the equations.

4.4.1.1 Step 1. The first step is to examine a small elemental mass, dm, of the aircraft that is located at some distance from the aircraft's center of gravity. It will be assumed that the elemental mass is rotating about the aircraft center of gravity with a positive roll rate, pitch rate, and yaw rate (P, Q, and R, respectively). The distance from the center of gravity to the small mass is defined as

$$\bar{r}_{dm} = x\hat{i} + y\hat{j} + z\hat{k} \tag{4.41}$$

where x, y, and z are the distances in the x, y, and z axes of the body axis system, respectively. This is shown in Fig. 4.9.

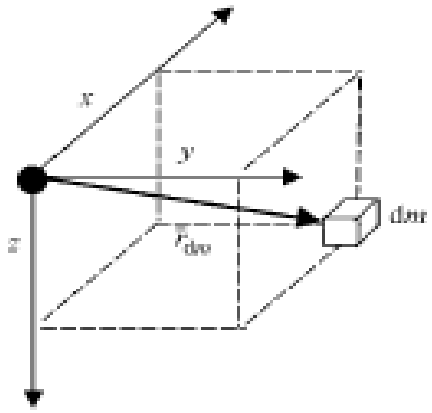

Fig. 4.9 Differential mass in body axis system.

Source from Yechout, T.R. "Introduction to Aircraft Flight Mechanics", AIAA education Series, 2003

4.4.1.2 Step 2. Next an expression is developed for the velocity of the small mass, dm, solely because of its rotation about the center of gravity. The velocity for the movement of the center of gravity of the aircraft was taken into account in the development of the three force equations. The velocity, $\bar{V}_{dm}$, of the mass relative to the center of gravity is determined using the expression

$$\bar{V}_{dm} = \left[\frac{d\bar{r}_{dm}}{dt}\right]_{Body} + \bar{\omega}_{Body} \times \bar{r}_{dm} \tag{4.42}$$

Because the aircraft was previously assumed to be a rigid body, $\bar{r}_{dm}$ is constant, so

$$\left[\frac{d\bar{r}_{dm}}{dt}\right]_{Body} = 0 \tag{4.43}$$

and therefore,

$$\bar{V}_{dm} = \bar{\omega}_{Body} \times \bar{r}_{dm} \tag{4.44}$$

Mathematically this yields

$$\bar{V}_{dm} = \begin{vmatrix} \hat{i} & \hat{j} & \hat{k} \\ P & Q & R \\ x & y & z \end{vmatrix} \tag{4.45}$$

$$\bar{V}_{dm} = (Qz - Ry)\hat{i} + (Rx - Pz)\hat{j} + (Py - Qx)\hat{k} \tag{4.46}$$

4.4.1.3 Step 3. Next an expression is developed for the linear momentum of dm solely because of its rotation about the center of gravity. The linear momentum is found simply by multiplying the mass times the velocity, namely,

$$\begin{aligned} \text{linear momentum} &= dm\bar{V} \\ &= dm[(Qz - Ry)\hat{i} + (Rx - Pz)\hat{j} + (Py - Qx)\hat{k}] \end{aligned} \tag{4.47}$$

4.4.1.4 Step 4. An expression for the angular momentum of the differential mass, dm, is developed using

$$d\bar{H}_{dm} = \bar{r}_{dm} \times (dm\bar{V}_{dm}) \tag{4.48}$$

Therefore,

$$d\bar{H}_{dm} = \begin{vmatrix} \hat{i} & \hat{j} & \hat{k} \\ x & y & z \\ dm(Qz - Ry) & dm(Rx - Pz) & dm(Py - Qx) \end{vmatrix} \tag{4.49}$$

Source from Yechout, T.R. "Introduction to Aircraft Flight Mechanics", AIAA education Series, 2003

After carrying out the cross product and regrouping the terms, the three components of the angular momentum are:

$$\begin{aligned} dH_x &= P(y^2 + z^2)dm - Qxy\ dm - Rxz\ dm \\ dH_y &= Q(x^2 + z^2)dm - Ryz\ dm - Pxy\ dm \\ dH_z &= R(x^2 + y^2)dm - Pxz\ dm - Qyz\ dm \end{aligned} \tag{4.50}$$

4.4.1.5 Step 5. The next step is to integrate the expressions for the angular momentum of dm over the entire aircraft. Because P, Q, and R are not functions of the mass, they can be taken outside of the integration. Therefore, the three components for the angular momentum of the entire aircraft are

$$\begin{aligned} H_x &= \int dH_x = P\int(y^2 + z^2)dm - Q\int xy\ dm - R\int xz\ dm \\ H_y &= \int dH_y = Q\int(x^2 + z^2)dm - R\int yz\ dm - P\int xy\ dm \\ H_z &= \int dH_z = R\int(x^2 + y^2)dm - P\int xz\ dm - Q\int yz\ dm \end{aligned} \tag{4.51}$$

The **moments of inertia** are defined as

$$\begin{aligned} I_{xx} &= \int(y^2 + z^2)dm \\ I_{yy} &= \int(x^2 + z^2)dm \\ I_{zz} &= \int(x^2 + y^2)dm \end{aligned} \tag{4.52}$$

The moments of inertia are indications of the resistance to rotation about that axis (that is, I_{xx} indicates the resistance to rotation about the x axis of the aircraft). The **products of inertia** are

$$\begin{aligned} I_{xy} &= \int xy\ dm \\ I_{xz} &= \int xz\ dm \\ I_{yz} &= \int yz\ dm \end{aligned} \tag{4.53}$$

The products of inertia are an indication of the symmetry of the aircraft. Substituting the moments and products of inertia into Eq. (4.51) yields

$$\begin{aligned} H_x &= PI_{xx} - QI_{xy} - RI_{xz} \\ H_y &= QI_{yy} - RI_{yz} - PI_{xy} \\ H_z &= RI_{zz} - PI_{xz} - QI_{yz} \end{aligned} \tag{4.54}$$

Source from Yechout, T.R. "Introduction to Aircraft Flight Mechanics", AIAA education Series, 2003

$$\bar{H} = H_x\hat{i} + H_y\hat{j} + H_z\hat{k} \tag{4.55}$$

This can also be easily found by applying an expression for angular momentum usually developed in basic physics courses, which is

$$\bar{H} = \bar{I}\bar{\omega} \tag{4.56}$$

where $\bar{I}$ is the aircraft's inertia tensor and $\bar{\omega}$ is the aircraft's angular rate. The inertia tensor for an aircraft is

$$\bar{I} = \begin{bmatrix} I_{xx} & -I_{xy} & -I_{xz} \\ -I_{xy} & I_{yy} & -I_{yz} \\ -I_{xz} & -I_{yz} & I_{zz} \end{bmatrix}_{\text{Body}} \tag{4.57}$$

Therefore,

$$H_B = \begin{bmatrix} I_{xx} & -I_{xy} & -I_{xz} \\ -I_{xy} & I_{yy} & -I_{yz} \\ -I_{xz} & -I_{yz} & I_{zz} \end{bmatrix} \begin{bmatrix} P \\ Q \\ R \end{bmatrix} \tag{4.58}$$

so,

$$\begin{aligned} H_x &= PI_{xx} - QI_{xy} - RI_{xz} \\ H_y &= QI_{yy} - RI_{yz} - PI_{xy} \\ H_z &= RI_{zz} - PI_{xz} - QI_{yz} \end{aligned} \tag{4.59}$$

Note this is the exact same result as Eq. (4.54) that resulted from applying Steps 1–5.

If the aircraft is assumed to have an xz plane of symmetry, the I_{xy} and I_{yz} products of inertia are zero. An aircraft has an xz plane of symmetry when the left side of the aircraft is a mirror image of the right side about the xz plane. The I_{xz} is not necessarily zero because the aircraft is not symmetrical from top to bottom about the xy plane and not symmetrical from front to rear about the yz plane. These concepts are illustrated in Fig. 4.10. Notice for I_{xy} and I_{yz} the reflection plane symmetry between quadrants I and IV, and II and III. This leads to a zero value for both these products of inertia. Also notice that we do not have reflection plane symmetry for the case of I_{xz}; therefore, it has a non-zero value.

Source from Yechout, T.R. "Introduction to Aircraft Flight Mechanics", AIAA education Series, 2003

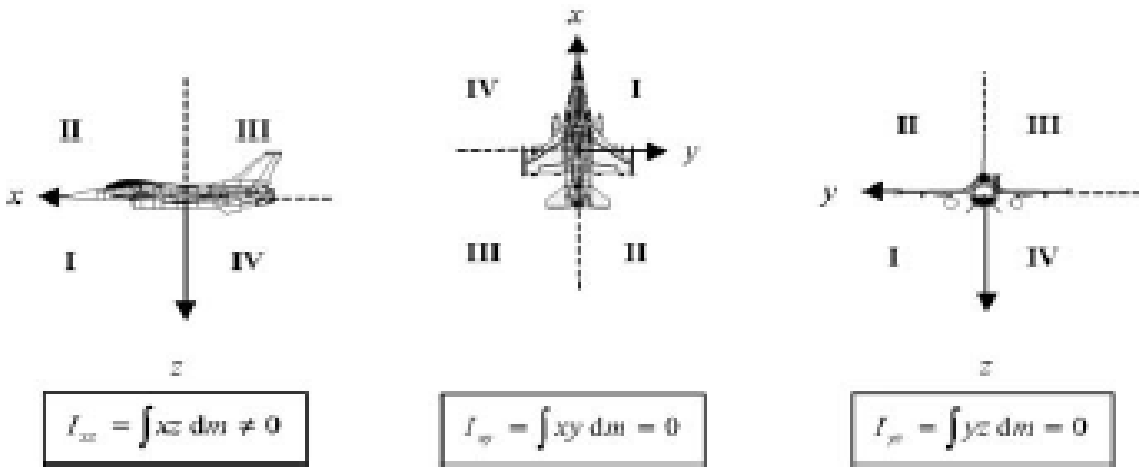

Fig. 4.10 Aircraft products of inertia.

The angular momentum components for the aircraft become

$$\begin{aligned} H_x &= PI_{xx} - RI_{xz} \\ H_y &= QI_{yy} \\ H_z &= RI_{zz} - PI_{xz} \end{aligned} \tag{4.60}$$

or

$$\bar{H} = (PI_{xx} - RI_{xz})\hat{i} + (QI_{yy})\hat{j} + (RI_{zz} - PI_{xz})\hat{k} \tag{4.61}$$

4.4.1.6 Step 6. After the angular momentum vector of the aircraft has been determined, the final step is to take the time rate of change of the angular momentum vector with respect to inertial space but represented in the aircraft body axis system. The same relationship used in developing the acceleration with respect to an inertial reference frame from the force equations can be used, namely,

$$\left[\frac{d\bar{H}}{dt}\right]_{\text{Inertial}} = \left[\frac{d\bar{H}}{dt}\right]_{\text{Body}} + \omega_{\text{Body}} \times \bar{H}_{\text{Body}} \tag{4.62}$$

$$\left[\frac{d\bar{H}}{dt}\right]_{\text{Body}} = \begin{bmatrix} \dot{P}I_{xx} - \dot{R}I_{xz} + P\dot{I}_{xx} - R\dot{I}_{xz} \\ \dot{Q}I_{yy} + Q\dot{I}_{yy} \\ \dot{R}I_{zz} - \dot{P}I_{xz} + R\dot{I}_{zz} - P\dot{I}_{xz} \end{bmatrix}_{\text{Body}} \tag{4.63}$$

Source from Yechout, T.R. "Introduction to Aircraft Flight Mechanics", AIAA education Series, 2003

Assuming that the mass distribution of the aircraft is constant, such as neglecting fuel slosh, the moments and products of inertia do not change with time, that is, $\dot{I}_{xx}$, $\dot{I}_{yy}$, $\dot{I}_{zz}$, and $\dot{I}_{xz}$ are all zero. Therefore,

$$\left[\frac{d\bar{H}}{dt}\right]_{Body} = \begin{bmatrix} \dot{P}I_{xx} - \dot{R}I_{xz} \\ \dot{Q}I_{yy} \\ \dot{R}I_{zz} - \dot{P}I_{xz} \end{bmatrix}_{Body} \tag{4.64}$$

Finally,

$$\omega \times \bar{H}_{Body} = \begin{vmatrix} i & j & k \\ P & Q & R \\ (PI_{xx} - RI_{xz}) & (QI_{yy}) & (RI_{zz} - PI_{xz}) \end{vmatrix}_{Body} \tag{4.65}$$

$$= \begin{bmatrix} Q(RI_{zz} - PI_{xz}) - RQI_{yy} \\ R(PI_{xx} - RI_{xz}) - P(RI_{zz} - PI_{xz}) \\ PQI_{yy} - Q(PI_{xx} - RI_{xz}) \end{bmatrix}_{Body} \tag{4.66}$$

Grouping terms yields

$$\left[\frac{d\bar{H}}{dt}\right]_{Inertial_{Body}} = \begin{bmatrix} \dot{P}I_{xx} + QR(I_{zz} - I_{yy}) - (\dot{R} + PQ)I_{xz} \\ \dot{Q}I_{yy} - PR(I_{zz} - I_{xx}) + (P^2 - R^2)I_{xz} \\ \dot{R}I_{zz} + PQ(I_{yy} - I_{xx}) + (QR - \dot{P})I_{xz} \end{bmatrix}_{Body} \tag{4.67}$$

Therefore, Eq. (4.68) yields the three moment equations of motion in the body axis system, where the left-hand side represents the response of the aircraft and the right-hand side consists of the applied moments.

$$\begin{aligned} &\dot{P}I_{xx} + QR(I_{zz} - I_{yy}) - (\dot{R} + PQ)I_{xz} = L \\ &\dot{Q}I_{yy} - PR(I_{zz} - I_{xx}) + (P^2 - R^2)I_{xz} = M \\ &\underbrace{\dot{R}I_{zz}}_{\text{angular acceleration terms}} + \underbrace{PQ(I_{yy} - I_{xx})}_{\text{gyro precession terms}} + \underbrace{(QR - \dot{P})I_{xz}}_{\text{coupling terms}} = N \end{aligned} \tag{4.68}$$

L, M, and N are the rolling moment, pitching moment, and yawing moment, respectively. Unfortunately, the letter L is used to also represent lift. This can be confusing and the reader is advised to carefully check the context of its use in any aeronautical engineering text. Recall that the assumptions made in developing the equations of motion were: the mass of the aircraft is constant, the aircraft is a rigid airframe, the Earth axis system is an inertial reference frame, the mass distribution of the aircraft is constant, and the aircraft has an xz plane of symmetry. It is, therefore, extremely important to realize that these

Source from Yechout, T.R. "Introduction to Aircraft Flight Mechanics", AIAA education Series, 2003

equations are valid for flight conditions where these assumptions are reasonable.

The aircraft response side of Eq. (4.68) can be divided into three types of terms: angular acceleration, gyro precession, and coupling. The angular acceleration terms are the easiest to understand. For example, if we take the rolling moment EOM and assume the gyro precession and coupling terms are negligible, we have

$$\dot{P}I_{xx} = L$$

If a rolling moment (L) is applied to the aircraft (such as with an aileron deflection), this equation predicts that an angular acceleration in roll ($\dot{P}$) will result. If a positive rolling moment is applied, a positive roll angular acceleration will result. For a given applied rolling moment, the larger the moment of inertia, I_{xx}, the smaller the roll angular acceleration. The angular acceleration terms can be thought of as describing the motion that results from the application of torque (the applied moment) to a rotating body with a moment of inertia. For example, if we apply a torque to a flywheel, it experiences an angular acceleration as it spins up.

The gyroscopic precession terms describe precession of the aircraft because of the combination of angular momentum about an axis and an applied moment. For example, consider the rolling moment EOM for the case of a rolling pull-up. We will, for the moment, assume the angular acceleration and coupling terms are negligible along with I_{xz}. This leaves us with

$$-I_{yy}QR = L$$

We next identify the angular momentum term for an aircraft in a pull-up (with positive pitch rate Q) as $I_{yy}Q$. Notice that I_{yy} is the moment of inertia (always positive) about the y axis and Q is the angular velocity about the y axis (positive for a pull-up). Multiplied together, we have angular momentum. We will rewrite this as

$$-R\underbrace{(I_{yy}Q)}_{\text{angular momentum in pitch}} = L$$

If the pilot now applies a positive rolling moment to the aircraft by deflecting the ailerons, this equation predicts that a negative yawing moment (R) must result. The precession terms describe the same type of precession that is experienced by a gyroscope when a torque is applied. We will look at a second example of a gyro precession term for the case of tail dragger propeller aircraft. Consider the pitching moment EOM. We will assume the angular acceleration and coupling terms are negligible along with I_{xz}.

$$R\underbrace{(I_{xx}P)}_{\text{angular momentum in roll}} = M$$

Source from Yechout, T.R. "Introduction to Aircraft Flight Mechanics", AIAA education Series, 2003

A propeller aircraft, such as a P-51, has a significant amount of angular momentum in roll because of the rotation of the propeller. Because the propeller usually rotates clockwise as seen from the cockpit, the roll angular momentum is positive. With the aircraft on takeoff roll, the pilot will apply a small nose down stick input (negative M) to raise the tail. Our abbreviated equation predicts that a negative yaw rate (R) must result. Skillful pilots are ready for this precession and will apply right rudder to counteract the negative yaw rate.

The coupling terms describe inertial coupling tendency of the aircraft. They can be easily identified by the I_{xz} product of inertia. A nonzero value of I_{xz} indicates inertial nonsymmetry of the aircraft. Many modern high-performance aircraft have a negative I_{xz}, which indicates a larger concentration of mass in the two negative quadrants formed by xz plane of the aircraft. Consider the pitching moment EOM with the gyro precession and applied pitching moment terms assumed negligible and zero yaw rate (R).

$$P^2 I_{xz} = -I_{yy}\dot{Q}$$

We will assume the aircraft is doing a high-speed fly-by and has a negative I_{xz}. If the pilot does a snap roll to either direction, this equation predicts that a positive angular acceleration ($\dot{Q}$) will result. This will cause the aircraft to pitch up and could lead to serious effects if the pilot does not anticipate the pitch up. It can, of course, be counteracted with a nose down stick input. This particular case is referred to as roll coupling, which resulted in the crash of several aircraft in the 1940s and 1950s, before a full understanding of coupling.

4.4.2 Applied Moments

The applied moments consist of the aerodynamic rolling, pitching, and yawing moments, L_A, M_A, and N_A, respectively, and the rolling, pitching, and yawing moments because of thrust, L_T, M_T, and N_T, respectively. There are no moments because of gravity because the weight vector acts through the center of gravity and the moment arms are zero. Also, any moments because of rotating masses (such as jet engines) on or within the aircraft have been neglected. Therefore,

$$\begin{aligned}
\dot{P}I_{xx} + QR(I_{zz} - I_{yy}) - (\dot{R} + PQ)I_{xz} &= L_A + L_T \\
\dot{Q}I_{yy} - PR(I_{zz} - I_{xx}) + (P^2 - R^2)I_{xz} &= M_A + M_T \\
\dot{R}I_{zz} + PQ(I_{yy} - I_{xx}) + (QR - \dot{P})I_{xz} &= N_A + N_T
\end{aligned} \tag{4.69}$$

The makeup of each of these moments will be discussed in detail in subsequent chapters.

Source from Yechout, T.R. "Introduction to Aircraft Flight Mechanics", AIAA education Series, 2003

4.5 Longitudinal and Lateral-Directional Equations of Motion

The six aircraft equations of motion (EOM) can be decoupled into two sets of three equations. These are the three longitudinal EOM and the three lateral-directional EOM. This is convenient in that it requires only three equations to be solved simultaneously for many flight conditions. For example, an aircraft in wings-level flight with no sideslip and a pitching motion can be analyzed using only the longitudinal EOM because the aircraft does not have any lateral-directional motion.

4.5.1 Longitudinal Equations of Motion

The three longitudinal EOM consist of the x force, z force, and y moment equations, namely,

$$\begin{aligned} m(\dot{U} + QW - RV) &= -mg\sin\Theta + (-D\cos\alpha + L\sin\alpha) + T\cos\Phi_T \\ \dot{Q}I_{yy} - PR(I_{zz} - I_{xx}) + (P^2 - R^2)I_{xz} &= M_A + M_T \\ m(\dot{W} + PV - QU) &= mg\cos\Phi\cos\Theta + (-D\sin\alpha - L\cos\alpha) - T\sin\Phi_T \end{aligned} \tag{4.70}$$

One way of thinking of the longitudinal EOM is to picture an aircraft with its xz plane coincident with an xz plane fixed in space. Longitudinal motion consists of those movements where the aircraft would only move within that xz plane, that is, translation in the x direction, translation in the z direction, and rotation about the y axis. In each of these cases, the xz plane of the aircraft would be moving within a xz plane fixed in space. It should be noted that the L in Eq. (4.70) refers to lift and not rolling moment.

4.5.2 Lateral-Directional Equations of Motion

The lateral-directional EOM consist of the y force, x moment, and z moment equations, namely,

$$\begin{aligned} \dot{P}I_{xx} + QR(I_{zz} - I_{yy}) - (\dot{R} + PQ)I_{xz} &= L_A + L_T \\ m(\dot{V} + RU - PW) &= mg\sin\Phi\cos\Theta + F_{A_y} + F_{T_y} \\ \dot{R}I_{zz} + PQ(I_{yy} - I_{xx}) + (QR - \dot{P})I_{xz} &= N_A + N_T \end{aligned} \tag{4.71}$$

For any lateral-directional motion the xz plane would move out of some xz plane fixed in space. Translation in the y direction, roll about the x axis, and yaw about the z axis would all cause the xz plane of the aircraft to move out of that arbitrarily fixed xz plane in space.

4.6 Kinematic Equations

In addition to the six force and moment EOM, additional equations are required in order to completely solve the aircraft problem. These additional equations are necessary because there are more than six unknowns due to the presence of the Euler angles in the force equations. Three equations are

Source from Yechout, T.R. "Introduction to Aircraft Flight Mechanics", AIAA education Series, 2003

obtained by relating the three body axis system rates, P, Q, and R to the three Euler rates, $\dot{\Psi}$, $\dot{\Theta}$, and $\dot{\Phi}$. Note that the Euler rates are just the time rate of change of the Euler angles.

To develop the relationship between the body rates and the Euler rates, the following equality must be satisfied because the magnitude of the three body rates must equal the magnitude of three Euler rates. Note that these are vector equations.

$$\bar{\omega}_{\text{Body}} = P\hat{i} + Q\hat{j} + R\hat{k} = \dot{\Psi} + \dot{\Theta} + \dot{\Phi} \tag{4.72}$$

In other words,

$$\sqrt{P^2 + Q^2 + R^2} = \sqrt{\dot{\Psi}^2 + \dot{\Theta}^2 + \dot{\Phi}^2}$$

Each of the three Euler rates can be conveniently displayed in one of the axis systems used in transforming a vector from the Earth axis system to the body axis system. Because $\dot{\Psi}$ represents an angular rate about the Z_E or Z' axis

$$\dot{\Psi} = \dot{\Psi}\hat{k}_E = \dot{\Psi}\hat{k}' \tag{4.73}$$

This Earth axis heading angular rate is illustrated in Fig. 4.11.

The earth axis system is first rotated about the Z_E (Z') axis through the heading angle (Ψ) into the X'-Y'-Z' axis system as shown in Fig. 4.12. The new X' axis lies directly beneath the x-body axis but is offset by the pitch angle (Θ).

This first interim coordinate system is then rotated about the Y' axis through the pitch angle (Θ) into the X''-Y''-Z'' axis system as shown in Fig. 4.13. Note that because the Y' axis is the axis of rotation, the new Y'' axis is the same as

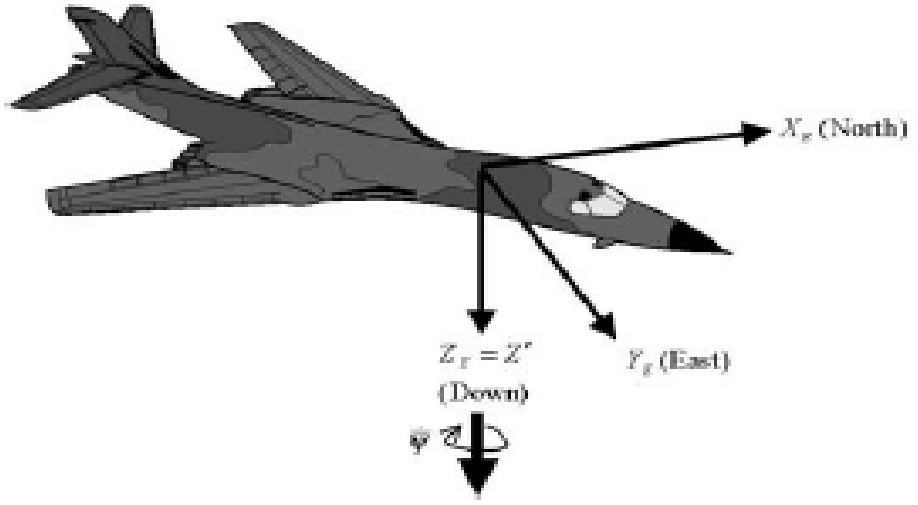

Fig. 4.11 Illustration of heading angular rate in Earth axis system.

Source from Yechout, T.R. "Introduction to Aircraft Flight Mechanics", AIAA education Series, 2003

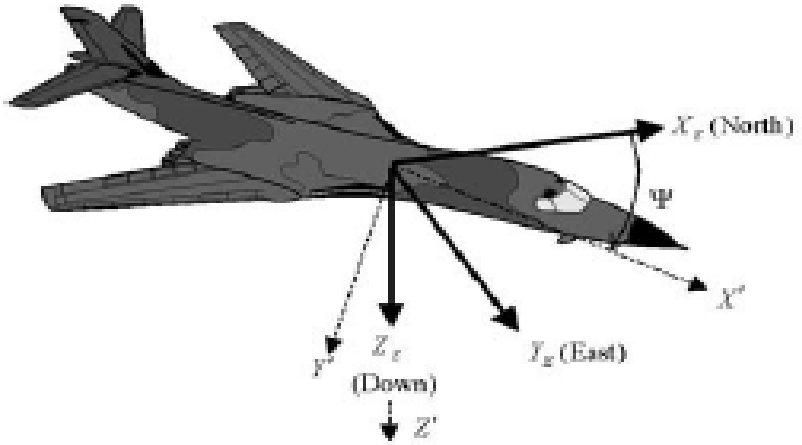

Fig. 4.12 X'-Y'-Z' interim coordinate system.

Y'. $\dot{\bar{\Theta}}$ then represents an angular rate about the Y' or Y'' axis. Mathematically, this can be summarized as

$$\dot{\bar{\Theta}} = \dot{\Theta}\hat{j}' = \dot{\Theta}\hat{j}'' \tag{4.74}$$

This second interim coordinate system aligns the X'' axis with the body x-axis as shown in Fig. 4.14.

This second interim coordinate system is then rotated about the X'' axis through the roll angle (Φ) into the body axis system as shown in Fig. 4.15. $\dot{\bar{\Phi}}$ then represents an angular rate about the X'' or X_B axis. Mathematically, this can be summarized as

$$\dot{\bar{\Phi}} = \dot{\Phi}\hat{i}'' = \dot{\Phi}\hat{i} \tag{4.75}$$

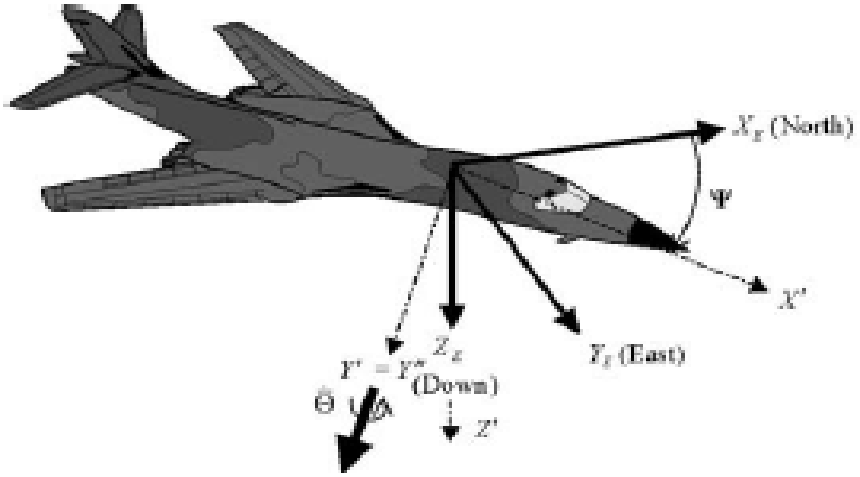

Fig. 4.13 Illustration of pitch attitude angular rate.

Source from Yechout, T.R. "Introduction to Aircraft Flight Mechanics", AIAA education Series, 2003

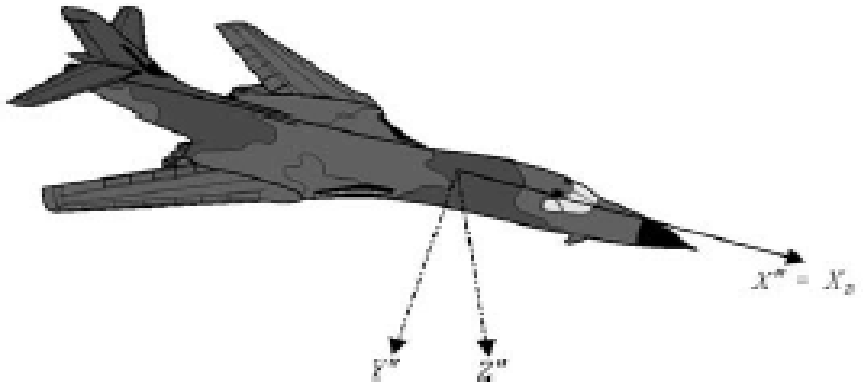

Fig. 4.14 X'-Y'-Z'' interim coordinate system.

By using the transformations discussed in Sec. 4.2.1, each of these angular rate vectors can be transformed into the body axis system. Therefore,

$$\bar{\omega}_{\text{Body}} = P\hat{i} + Q\hat{j} + R\hat{k} = R_1(\Phi)R_2(\Theta)\dot{\bar{\Psi}} + R_1(\Phi)\dot{\bar{\Theta}} + \dot{\bar{\Phi}} \tag{4.76}$$

The previous relationship is true for the following reasons. To transform $\dot{\bar{\Psi}}$ from the $\hat{k}'$ axis to the body axis system requires a positive rotation through Θ, followed by a positive rotation through Φ. To transform $\dot{\bar{\Theta}}$ from the $\hat{j}''$ axis to the body axis system requires a positive rotation through Φ only. Finally, $\dot{\bar{\Phi}}$ is already represented in the body axis system, so no transformation is necessary. Mathematically, Eq. (4.76) is carried out as shown in Eqs. (4.77–4.79).

$$\begin{bmatrix} P \\ Q \\ R \end{bmatrix} = \begin{bmatrix} 1 & 0 & 0 \\ 0 & \cos\Phi & \sin\Phi \\ 0 & -\sin\Phi & \cos\Phi \end{bmatrix} \begin{bmatrix} \cos\Theta & 0 & -\sin\Theta \\ 0 & 1 & 0 \\ \sin\Theta & 0 & \cos\Theta \end{bmatrix} \begin{bmatrix} 0 \\ 0 \\ \dot{\Psi} \end{bmatrix} + \begin{bmatrix} 1 & 0 & 0 \\ 0 & \cos\Phi & \sin\Phi \\ 0 & -\sin\Phi & \cos\Phi \end{bmatrix} \begin{bmatrix} 0 \\ \dot{\Theta} \\ 0 \end{bmatrix} + \begin{bmatrix} \dot{\Phi} \\ 0 \\ 0 \end{bmatrix} \tag{4.77}$$

$$\begin{bmatrix} P \\ Q \\ R \end{bmatrix} = \begin{bmatrix} 1 & 0 & 0 \\ 0 & \cos\Phi & \sin\Phi \\ 0 & -\sin\Phi & \cos\Phi \end{bmatrix} \begin{bmatrix} -\sin\Theta\dot{\Psi} \\ 0 \\ \cos\Theta\dot{\Psi} \end{bmatrix} + \begin{bmatrix} 0 \\ \cos\Phi\dot{\Theta} \\ -\sin\Phi\dot{\Theta} \end{bmatrix} + \begin{bmatrix} \dot{\Phi} \\ 0 \\ 0 \end{bmatrix} \tag{4.78}$$

$$\begin{bmatrix} P \\ Q \\ R \end{bmatrix} = \begin{bmatrix} -\sin\Theta\dot{\Psi} + \dot{\Phi} \\ \sin\Phi\cos\Theta\dot{\Psi} + \cos\Phi\dot{\Theta} \\ \cos\Phi\cos\Theta\dot{\Psi} - \sin\Phi\dot{\Theta} \end{bmatrix} \tag{4.79}$$

Source from Yechout, T.R. "Introduction to Aircraft Flight Mechanics", AIAA education Series, 2003

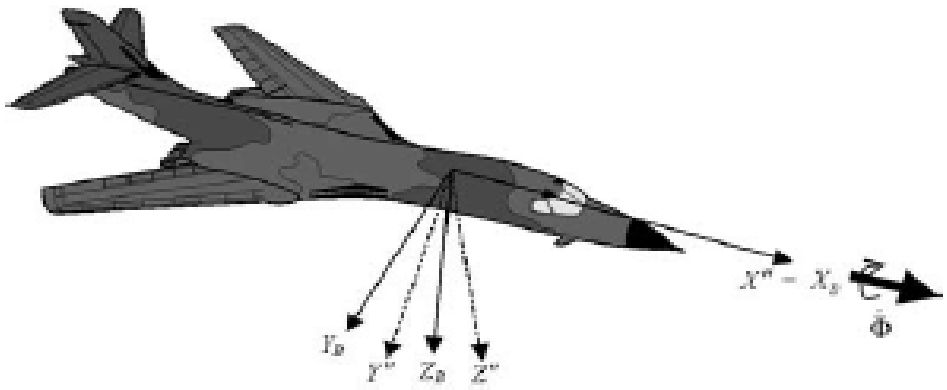

Fig. 4.15 Illustration of roll attitude angular rate.

Therefore, the three kinematic equations are

$$\begin{aligned} P &= -\sin\Theta\dot{\Psi} + \dot{\Phi} \\ Q &= \sin\Phi\cos\Theta\dot{\Psi} + \cos\Phi\dot{\Theta} \\ R &= \cos\Phi\cos\Theta\dot{\Psi} - \sin\Phi\dot{\Theta} \end{aligned} \tag{4.80}$$

Examples are provided to clearly illustrate results from the kinematic equations.

Example 4.1

An aircraft has the following Euler angles and Euler rates:

$$\begin{aligned} \Psi &= 0 \text{ deg} & \dot{\Psi} &= 10 \text{ deg/s} \\ \Theta &= 0 \text{ deg} & \dot{\Theta} &= 0 \text{ deg/s} \\ \Phi &= 90 \text{ deg} & \dot{\Phi} &= 0 \text{ deg/s} \end{aligned}$$

Applying Eq. (4.80) yields:

$$\begin{aligned} P &= 0 \text{ deg/s} \\ Q &= 10 \text{ deg/s} \\ R &= 0 \text{ deg/s} \end{aligned}$$

Note that for this flight condition, a 10 deg/s Euler yaw rate, $\dot{\Psi}$, is felt by the pilot as a 10 deg/s pitch rate, Q.

Source from Yechout, T.R. "Introduction to Aircraft Flight Mechanics", AIAA education Series, 2003

Example 4.2

An aircraft has the following Euler angles and Euler rates:

$$\Psi = 0 \text{ deg} \quad \dot{\Psi} = 0 \text{ deg/s}$$
$$\Theta = 0 \text{ deg} \quad \dot{\Theta} = 20 \text{ deg/s}$$
$$\Phi = 90 \text{ deg} \quad \dot{\Phi} = 0 \text{ deg/s}$$

Applying Eq. (4.80) yields

$$P = 0 \text{ deg/s}$$
$$Q = 0 \text{ deg/s}$$
$$R = -20 \text{ deg/s}$$

Note that for this flight condition, a 20 deg/s Euler pitch rate, $\dot{\Theta}$, is felt by the pilot as a -20 deg/s yaw rate, R.

4.7 Historical Snapshot—Genesis 2000 Flight Simulator

In the late 1980s, Veda, Incorporated, of Lexington Park, Maryland, and the U.S. Air Force Academy Department of Aeronautics developed an engineering flight simulator specifically tailored to support educational requirements.[1] The simulator was named the Genesis 2000 and solved the full six degree-of-freedom EOM Eqs. (4.38) and (4.69) in nearly real time to continuously represent almost any mission. The delay time between a pilot input and representation of aircraft motion was less than 0.12 s based on available computer speed at that

Fig. 4.16 Genesis 2000 flight station.

Source from Yechout, T.R. "Introduction to Aircraft Flight Mechanics", AIAA education Series, 2003

time. The fixed base flight station included an outside visual display complete with heads-up display (HUD), a display for flight instruments, and standard cockpit controls including a sidestick. Figure 4.16 shows the flight station.

A typical expansion of the applied force and moment side of each EOM included the influences of angle of attack, sideslip, elevator deflection, aileron deflection, rudder deflection, differential tail, speedbrakes, flaps, and spoilers through the use of appropriate derivatives, as will be discussed in Chapter 5. A key aspect of the Genesis 2000 was easy and quick access to each individual derivative. This allowed flight evaluation of the derivative's contribution to the overall handling qualities (discussed in Chapter 7) of an aircraft. To do this, another key feature of the Genesis 2000 was incorporation of specific mission tasks such as approach and landing, air-to-ground tracking, and air-to-air tracking. The system was also used by the Air Force Test Pilot School, the U.S. Naval Academy, and the British Empire Test Pilot School throughout the 1990s. At the Air Force Academy, the system was upgraded in 2000 to incorporate current computer technology.

Reference

[1] Russell, J. H., Mouch, T. N., and Yechout, T. R., "Integration of Flight Simulation Into the Undergraduate Design Experience," AIAA TP 90-3263, *AIAA/AHS/ASEE Aircraft Design Systems and Operations Conference*, Dayton, OH, Sept. 1990.

Problems

4.1 Consider the T-37 at the following Euler angles:

$$\Psi = 90 \text{ deg} \qquad \Theta = +10 \text{ deg} \qquad \Phi = +10 \text{ deg}$$

Describe the aircraft attitude and transform the weight force through these angles to the body axis system. The gross weight is 6600 lb_f.

4.2 A T-37 is executing a loop at the following conditions:

$$\text{Euler angles: } \Psi = 0 \text{ deg}, \Theta = 30 \text{ deg}, \Phi = 0 \text{ deg}$$

The pilot observes a pure pitch rate at a constant velocity in the body axis system:

$$\bar{\omega}_B = \begin{Bmatrix} 0 \\ 0.1 \\ 0 \end{Bmatrix}_B \text{rad/s} \qquad \bar{V}_B = \begin{Bmatrix} 200 \\ 0 \\ 0 \end{Bmatrix}_B \text{ft/s}$$

What is the acceleration in the Earth-fixed reference system?

UNIT IV

LINEARIZATION OF EQUATIONS OF MOTION AND AERODYNAMIC FORCES AND MOMENTS DERIVATIVES

The six aircraft equations of motion developed in Chapter 4 [see Eqs. (4.70) and (4.71)] are nonlinear differential equations. They can be solved with a variety of numerical integration techniques to obtain time histories of motion variables, but it is nearly impossible to obtain closed solutions (equations for each variable). Because valuable insight can be obtained from closed solutions regarding the dynamic response of the aircraft, this chapter will use the small perturbation approach to linearize the equations of motion and facilitate the definition of closed solutions. In addition, the dynamic derivatives associated with definition of applied forces and moments on the aircraft will be discussed.

Small Perturbation Approach

Linearization of the aircraft equations of motion begins with consideration of perturbed flight. Perturbed flight is defined relative to a steady-state (trimmed) flight condition using a combination of steady-state and perturbed variables for aircraft motion parameters and for forces and moments. Simply stated, each motion variable, Euler angle, force, and moment in the equations of motion (EOM) are redefined as the summation of a steady-state value (designated with the subscript ‘‘1’’) and a perturbed value (designated with lower case symbols) as summarized in Eq. (6.1).

$$
\begin{array}{lll}
U = U_1 + u & V = V_1 + v & W = W_1 + w \\
P = P_1 + p & Q = Q_1 + q & R = R_1 + r \\
\Psi = \Psi_1 + \psi & \Theta = \Theta_1 + \theta & \Phi = \Phi_1 + \phi \\
F_A = F_{A_1} + f_A & F_T = F_{T_1} + f_T & \\
L_A = L_{A_1} + l_A & M_A = M_{A_1} + m_A & N_A = N_{A_1} + n_A \\
L_T = L_{T_1} + l_T & M_T = M_{T_1} + m_T & N_T = N_{T_1} + n_T
\end{array}
\qquad (6.1)
$$

For example, if an aircraft has a steady-state trimmed value for U of 400 ft=s and then encounters turbulence which increases U to 402 ft=s, U at that instant would be

$$U = U_1 + u = 400 + 2$$

The ‘‘perturbed’’ x-axis velocity, u, would be 2 ft=s in this case. The assumption of small perturbations (small values for u, v, w, p, etc.), allows linearization of the aircraft EOM. The following four-step approach summarizes the linearization technique:

Step 1: Recast each variable in terms of a steady-state value and a perturbed value ($A = A_1 + a$). Assume small perturbations (a is small). Multiply out and use trig identities.

Step 2: Apply the small-angle assumption to trig functions of perturbed angles [$\cos\theta \approx 1$; $\sin\theta \approx \theta$ (in radians)]

Step 3: Assume products of small perturbations are negligible ($ab \approx 0$).

Step 4: Remove the steady-state equation from the perturbed equation. The remaining perturbed equation is a linearized differential equation with the perturbed variables as the unknowns.

This approach is illustrated in Example 6.1.

Example 6.1

Linearize the following nonlinear differential equation.

$$\dot{C} = AB\sin\Omega$$

Step 1: $A = A_1 + a$, $B = B_1 + b$, $C = C_1 + c$, $\Omega = \Omega_1 + \omega$; substitute these variables into the original equation and multiply out.

$$\dot{C}_1 + \dot{c} = (A_1 + a)(B_1 + b)\sin(\Omega_1 + \omega)$$
$$\dot{C}_1 + \dot{c} = [A_1B_1 + A_1b + aB_1 + ab]\sin(\Omega_1 + \omega)$$
$$\dot{C}_1 + \dot{c} = [A_1B_1 + A_1b + aB_1 + ab][\sin\Omega_1\cos\omega + \cos\Omega_1\sin\omega]$$

Step 2: $\cos\omega \approx 1$; $\sin\omega \approx \omega$ (in radians)

$$\dot{C}_1 + \dot{c} = [A_1B_1 + A_1b + aB_1 + ab][\sin\Omega_1 + \omega\cos\Omega_1]$$

Step 3: $ab \approx 0$

$$\dot{C}_1 + \dot{c} = [A_1B_1 + A_1b + aB_1][\sin\Omega_1 + \omega\cos\Omega_1]$$

and $a\omega$ and $b\omega \approx 0$,

$$\dot{C}_1 + \dot{c} = A_1B_1\sin\Omega_1 + A_1b\sin\Omega_1 + aB_1\sin\Omega_1 + A_1B_1\omega\cos\Omega_1$$

Step 4: The steady-state equation can be easily identified by going back to the original differential equation and inserting subscripts of "1" on each variable.

$$\dot{C}_1 = A_1B_1\sin\Omega_1$$

Subtracting the previous equation from the differential equation at the end of Step 3, we have:

$$\dot{c} = A_1b\sin\Omega_1 + aB_1\sin\Omega_1 + A_1B_1\omega\cos\Omega_1$$

Source from Yechout, T.R. "Introduction to Aircraft Flight Mechanics", AIAA education Series, 2003

which is the linearized form of the differential equation in terms of the perturbation variables a, b, c, and ω.

6.2 Developing the Linearized Aircraft Equations of Motion

The nonlinear longitudinal EOM presented in Eq. (4.70) can be rewritten as

$$\begin{aligned} m(\dot{U} + QW - RV) &= -mg\sin\Theta + F_{A_x} + F_{T_x} \\ \dot{Q}I_{yy} - PR(I_{zz} - I_{xx}) + (P^2 - R^2)I_{xz} &= M_A + M_T \\ m(\dot{W} + PV - QU) &= mg\cos\Phi\cos\Theta + F_{A_z} + F_{T_z} \end{aligned} \tag{6.2}$$

where F_{A_x} and F_{A_z} are the aero forces acting along the respective x and z axis directions. Likewise, F_{T_x} and F_{T_z} represent the thrust forces acting along their respective directions. Notice also that the Euler angles have been designated with capital letters to conform with the approach defined by Eq. (6.1).

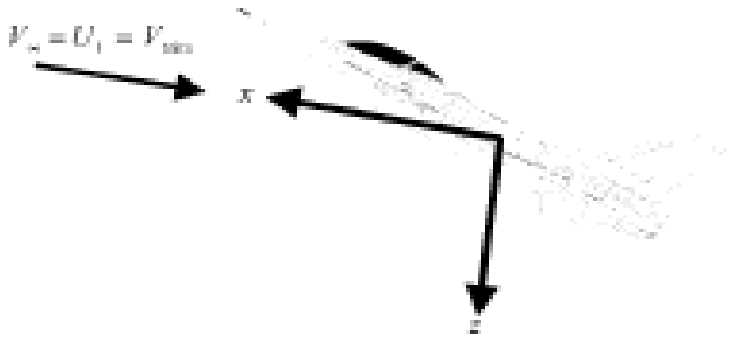

a) Body-Fixed Stability Axis During Trimmed Flight

b) Body-Fixed Stability Axis During Perturbed Flight

Fig. 6.1 Illustration of body-fixed stability axis.

Source from Yechout, T.R. "Introduction to Aircraft Flight Mechanics", AIAA education Series, 2003

The nonlinear lateral-directional equations of motion presented in Eq. (4.71) are presented again here for convenient reference.

$$\begin{aligned}
&\dot{P}I_{xx} + QR(I_{zz} - I_{yy}) - (\dot{R} + PQ)I_{xz} = L_A + L_T \\
&m(\dot{V} + RU - PW) = mg\sin\Phi\cos\Theta + F_{A_Y} + F_{T_Y} \\
&\dot{R}I_{zz} + PQ(I_{yy} - I_{xx}) + (QR - \dot{P})I_{xz} = N_A + N_T
\end{aligned} \tag{6.3}$$

As discussed in Sec. 5.3, we will use a body-fixed stability axis system where the x-stability axis is oriented directly with the steady-state relative wind. Thus, U_1 will be equal to V_{trim} while V_1 and W_1 are equal to zero. This approach simplifies representation of the aero forces and moments. However, the reader is reminded that, to be perfectly correct, the moments and products of inertia in Eqs. (6.2) and (6.3) must be defined relative to this body-fixed stability axis. Figure 6.1 illustrates the body-fixed stability axis.

6.2.1 Longitudinal Linearized EOMs

To linearize the nonlinear longitudinal EOM of Eq. (6.2), the small perturbation approach discussed in Sec. 6.1 will be used. The substitutions of Eq. (6.1) are made in Eq. (6.2) to yield

$$\begin{aligned}
&m[\dot{U}_1 + \dot{u} + (Q_1 + q)(W_1 + w) - (R_1 + r)(V_1 + v)] \\
&\quad = -mg\sin(\Theta_1 + \theta) + F_{A_{X_1}} + f_{A_x} + F_{T_{X_1}} + f_{T_x} \\
&I_{yy}(\dot{Q}_1 + \dot{q}) - (P_1 + p)(R_1 + r)(I_{zz} - I_{xx}) + [(P_1 + p)^2 - (R_1 + r)^2]I_{xz} \\
&\quad = M_{A_1} + m_A + M_{T_1} + m_T \\
&m[\dot{W}_1 + \dot{w} + (P_1 + p)(V_1 + v) - (Q_1 + q)(U_1 + u)] \\
&\quad = mg\cos(\Phi_1 + \phi)\cos(\Theta_1 + \theta) + F_{A_{Z_1}} + f_{A_z} + F_{T_{Z_1}} + f_{T_z}
\end{aligned}$$

Applying Steps 2–4 of Sec. 6.1, these reduce to

$$\begin{aligned}
&m(\dot{u} - V_1 r - R_1 v + W_1 q + Q_1 w) = -mg\theta\cos\Theta_1 + f_{A_x} + f_{T_x} \\
&I_{yy}\dot{q} + (I_{xx} - I_{zz})(P_1 r + R_1 p) + I_{xz}(2P_1 p - 2R_1 r) = m_A + m_T \\
&m(\dot{w} - U_1 q - Q_1 u + V_1 p + P_1 v) = -mg\theta\cos\Phi_1\sin\Theta_1 \\
&\qquad\qquad - mg\phi\sin\Phi_1\cos\Theta_1 + f_{A_z} + f_{T_z}
\end{aligned} \tag{6.4}$$

Equation (6.4) represents the linearized longitudinal EOM as a function of the variables u, v, w, p, q, r, θ and ϕ.

Source from Yechout, T.R. "Introduction to Aircraft Flight Mechanics", AIAA education Series, 2003

6.2.2 Lateral-Directional Linearized EOMs

Linearization of the nonlinear lateral-directional EOM presented in Eq. (6.3) also use the small perturbation approach of Sec. 6.1. The small perturbation substitutions result in:

$$
\begin{aligned}
&(\dot{P}_1 + \dot{p})I_{xx} + (Q_1 + q)(R_1 + r)(I_{zz} - I_{yy}) - [\dot{R}_1 + \dot{r} + (P_1 + p)(Q_1 + q)]I_{xz} \\
&\qquad = L_A + l_A + L_T + l_T \\
&m[\dot{V}_1 + v + (R_1 + r)(U_1 + u) - (P_1 + p)(W_1 + w)] \\
&\qquad = mg\sin(\Phi_1 + \phi)\cos(\Theta_1 + \theta) + F_{A_{x_1}} + f_{A_x} + F_{T_{x_1}} + f_{T_x} \\
&(\dot{R}_1 + \dot{r})I_{zz} + (P_1 + p)(Q_1 + q)(I_{yy} - I_{xx}) + [(Q_1 + q)(R_1 + r) - (\dot{P}_1 + \dot{p})]I_{xz} \\
&\qquad = N_{A_1} + n_A + N_{T_1} + n_T
\end{aligned}
$$

Applying Steps 2–4 of Sec. 6.1, these reduce to

$$
\begin{aligned}
&I_{xx}\dot{p} - I_{xz}\dot{r} - I_{xz}(P_1 q + Q_1 p) + (I_{zz} - I_{yy})(R_1 q + Q_1 r) = l_A + l_T \\
&m(\dot{v} + U_1 r + R_1 u - W_1 p - P_1 w) = -mg\theta\sin\Phi_1\sin\Theta_1 \\
&\qquad + mg\phi\cos\Phi_1\cos\Theta_1 + f_{A_y} + f_{T_y} \\
&I_{zz}\dot{r} - I_{xz}\dot{p} + (I_{yy} - I_{xx})(P_1 q + Q_1 p) + I_{xz}(Q_1 r + R_1 q) = n_A + n_T
\end{aligned}
\tag{6.5}
$$

Equation (6.5) represents the linearized lateral-directional EOM as a function of the variables u, v, w, p, q, r, θ and ϕ, the same variables in the linearized longitudinal EOM. We thus have a situation with six equations and eight unknowns. The kinematic equations [Eq. (4.80)] may be linearized using a similar approach[1] to yield three additional equations and one additional unknown (ψ)—a solvable nine-equation/nine-unknown problem for the perturbed aircraft EOM.

6.2.3 Simplifying the Linearized EOMs for Wings Level, Straight Flight

Equations (6.4) and (6.5) may be simplified with the assumption of wings level, straight line flight for the initial trim, or steady state, condition. With this constraint,

$$\Phi_1 = P_1 = Q_1 = R_1 = \beta = 0$$

In addition, our choice of the body-fixed stability axis, as discussed in Sec. 6.2, leads to the additional simplification of:

$$V_1 = W_1 = 0$$

Source from Yechout, T.R. "Introduction to Aircraft Flight Mechanics", AIAA education Series, 2003

With these assumptions, the linearized longitudinal EOM of Eq. (6.4) become

$$\begin{aligned} m\dot{u} &= -mg\theta\cos\Theta_1 + f_{A_x} + f_{T_x} \\ I_{yy}\dot{q} &= m_A + m_T \\ m(\dot{w} - U_1 q) &= -mg\theta\sin\Theta_1 + f_{A_z} + f_{T_z} \end{aligned} \tag{6.6}$$

and the linearized lateral-directional EOM of Eq. (6.5) become

$$\begin{aligned} I_{xx}\dot{p} - I_{xz}\dot{r} &= l_A + l_T \\ m(\dot{v} + U_1 r) &= mg\phi\cos\Theta_1 + f_{A_y} + f_{T_y} \\ I_{zz}\dot{r} - I_{xz}\dot{p} &= n_A + n_T \end{aligned} \tag{6.7}$$

At this point, it is reasonable to ask if the restrictive assumptions of wings-level, straight flight will restrict our study of aircraft dynamic stability characteristics. Fortunately, the answer is no, because the fundamental dynamic modes of the aircraft are still present with these assumptions and dynamic stability characteristics observed about a wings-level, straight-line, trimmed flight condition are representative of those experienced during maneuvering flight. In short, these assumptions and choice of the body-fixed stability axis system have allowed simplification of the EOM to a manageable form so that understanding of dynamic stability concepts can be maximized.

6.3 First-Order Approximation of Applied Aero Forces and Moments

We will now focus on the applied aerodynamic force and moment terms (include f_{A_x} and m_A) in Eqs. (6.6) and (6.7). These represent the perturbed change in an aerodynamic force or moment that results from a nonzero value of a perturbed motion variable like u. We begin with the observation that the longitudinal perturbed forces and moment are a function primarily of five parameters:

$$f_{A_x}, m_A, f_{A_z} = f(u, \hat{\alpha}, \dot{\alpha}, q, \hat{\delta}_e) \tag{6.8}$$

As a reminder, the parameters u, $\hat{\alpha}$, $\dot{\alpha}$, q, and $\hat{\delta}_e$ are perturbation variables. $\hat{\alpha}$, $\dot{\alpha}$, and $\hat{\delta}_e$ deserve explanation because we have not discussed them before. The angle of attack is defined using the perturbation variable $\hat{\alpha}$ with the same approach as in Eq. (6.1).

$$\alpha = \alpha_1 + \hat{\alpha}$$

$\dot{\alpha}$ could be thought about in the same manner:

$$\dot{\alpha} = \dot{\alpha}_1 + \dot{\hat{\alpha}}$$

Source from Yechout, T.R. "Introduction to Aircraft Flight Mechanics", AIAA education Series, 2003

Because $\dot{\alpha}_1$ is equal to zero (the derivative of a constant), we have $\dot{\alpha} = \dot{\hat{\alpha}}$, and we will dispense with the hat for simplicity. The perturbed elevator deflection, $\hat{\delta}_e$, is defined in a similar manner as used with Eq. (6.1):

$$\delta_e = \delta_{e_1} + \hat{\delta}_e$$

Recall that the subscript "1" indicates the steady-state or trimmed value of the parameter.

We will use a first-order Taylor series to approximate how the longitudinal perturbed forces and moment vary as a function of the five perturbed variables presented in Eq. (6.8).

$$\begin{aligned} f_{A_x} &= \frac{\partial F_{A_x}}{\partial u}u + \frac{\partial F_{A_x}}{\partial \hat{\alpha}}\hat{\alpha} + \frac{\partial F_{A_x}}{\partial \dot{\alpha}}\dot{\alpha} + \frac{\partial F_{A_x}}{\partial q}q + \frac{\partial F_{A_x}}{\partial \hat{\delta}_e}\hat{\delta}_e \\ m_A &= \frac{\partial M_A}{\partial u}u + \frac{\partial M_A}{\partial \hat{\alpha}}\hat{\alpha} + \frac{\partial M_A}{\partial \dot{\alpha}}\dot{\alpha} + \frac{\partial M_A}{\partial q}q + \frac{\partial M_A}{\partial \hat{\delta}_e}\hat{\delta}_e \\ f_{A_z} &= \frac{\partial F_{A_z}}{\partial u}u + \frac{\partial F_{A_z}}{\partial \hat{\alpha}}\hat{\alpha} + \frac{\partial F_{A_z}}{\partial \dot{\alpha}}\dot{\alpha} + \frac{\partial F_{A_z}}{\partial q}q + \frac{\partial F_{A_z}}{\partial \hat{\delta}_e}\hat{\delta}_e \end{aligned} \tag{6.9}$$

Next, we will use the same approach to define the perturbed lateral-directional force and moments. We begin with the observation that six parameters primarily influence the lateral-directional perturbed force and moments:

$$l_A, f_{A_y}, n_A = f(\hat{\beta}, \dot{\hat{\beta}}, p, r, \hat{\delta}_a, \hat{\delta}_r) \tag{6.10}$$

Again, $\hat{\beta}$, $\dot{\hat{\beta}}$, p, r, $\hat{\delta}_a$, and $\hat{\delta}_r$ are perturbation variables. The perturbed sideslip, $\hat{\beta}$, is defined using the same approach as in Eq. (6.1).

$$\beta = \beta_1 + \hat{\beta}$$

For wings-level, trimmed, straight-line flight, β_1 equals zero and we have $\beta = \hat{\beta}$. We will dispense, at this point, with the hat for simplicity. $\dot{\hat{\beta}}$ should be considered in the same manner.

$$\dot{\beta} = \dot{\beta}_1 + \dot{\hat{\beta}}$$

Source from Yechout, T.R. "Introduction to Aircraft Flight Mechanics", AIAA education Series, 2003

Because $\dot{\beta}_1$ is equal to zero (the derivative of a constant), we have $\dot{\beta} = \hat{\dot{\beta}}$, and we will again dispense with the hat. The perturbed aileron and rudder deflections, $\hat{\delta}_a$ and $\hat{\delta}_r$, are also defined as perturbations to the steady-state value:

$$\delta_a = \delta_{a_1} + \hat{\delta}_a$$
$$\delta_r = \delta_{r_1} + \hat{\delta}_r$$

We will again use a first-order Taylor series to approximate how the lateral-directional perturbed force and moments vary as a function of the six perturbed variables presented in Eq. (6.10).

$$\begin{aligned} l_A &= \frac{\partial L_A}{\partial \beta}\beta + \frac{\partial L_A}{\partial \dot{\beta}}\dot{\beta} + \frac{\partial L_A}{\partial p}p + \frac{\partial L_A}{\partial r}r + \frac{\partial L_A}{\partial \hat{\delta}_a}\hat{\delta}_a + \frac{\partial L_A}{\partial \hat{\delta}_r}\hat{\delta}_r \\ f_{A_y} &= \frac{\partial F_{A_y}}{\partial \beta}\beta + \frac{\partial F_{A_y}}{\partial \dot{\beta}}\dot{\beta} + \frac{\partial F_{A_y}}{\partial p}p + \frac{\partial F_{A_y}}{\partial r}r + \frac{\partial F_{A_y}}{\partial \hat{\delta}_a}\hat{\delta}_a + \frac{\partial F_{A_y}}{\partial \hat{\delta}_r}\hat{\delta}_r \\ n_A &= \frac{\partial N_A}{\partial \beta}\beta + \frac{\partial N_A}{\partial \dot{\beta}}\dot{\beta} + \frac{\partial N_A}{\partial p}p + \frac{\partial N_A}{\partial r}r + \frac{\partial N_A}{\partial \hat{\delta}_a}\hat{\delta}_a + \frac{\partial N_A}{\partial \hat{\delta}_r}\hat{\delta}_r \end{aligned} \qquad (6.11)$$

The Taylor series representation of Eqs. (6.9) and (6.11) makes the quasi-steady assumption that the perturbed forces and moment are only a function of the instantaneous values of the perturbed motion variables. For the majority of rigid airplane dynamic stability analysis (at frequencies below 10 rad/s), this assumption provides accurate results.

6.3.1 Nondimensionalizing the First-Order Approximations

At this point, it is customary to nondimensionalize the perturbed variables in Eqs. (6.9) and (6.11). This is typically done to facilitate comparisons. It is accomplished in a straightforward manner. First, all angles (α, $\hat{\delta}_e$, β, $\hat{\delta}_a$, and $\hat{\delta}_r$) are represented in radians, which are dimensionless. Second, the perturbed x-axis velocity u is divided by the steady-state velocity U_1 to yield u/U_1, which is a dimensionless ratio. Third, the perturbed longitudinal angular rates ($\dot{\alpha}$ and q) are multiplied by $\bar{c}/2U_1$ to yield $\dot{\alpha}\bar{c}/2U_1$ and $q\bar{c}/2U_1$, both nondimensional ratios when $\dot{\alpha}$ and q have units of radians/second. Fourth, the perturbed lateral-directional angular rates (β, p, and r) are multiplied by $b/2U_1$ to form $\beta b/2U_1$, $pb/2U_1$, and $rb/2U_1$. Again, β, p, and r must have units of radians/second to make the ratios dimensionless. This is the conventional approach to nondimensionalizing the perturbation variables. The "2" in the denominator of the nondimensional angular rate terms comes from the roll helix angle (the angle that a wing tip makes with the forward velocity vector during a rolling maneuver). It is maintained in the other angular rate terms for

Source from Yechout, T.R. "Introduction to Aircraft Flight Mechanics", AIAA education Series, 2003

consistency. With the nondimensional perturbation variables incorporated, Eqs. (6.9) and (6.11) become

$$
\begin{aligned}
f_{A_x} &= \frac{\partial F_{A_x}}{\partial \frac{u}{U_1}}\left(\frac{u}{U_1}\right) + \frac{\partial F_{A_x}}{\partial \hat{\alpha}}\hat{\alpha} + \frac{\partial F_{A_x}}{\partial \frac{\dot{\alpha}\bar{c}}{2U_1}}\left(\frac{\dot{\alpha}\bar{c}}{2U_1}\right) + \frac{\partial F_{A_x}}{\partial \frac{q\bar{c}}{2U_1}}\left(\frac{q\bar{c}}{2U_1}\right) + \frac{\partial F_{A_x}}{\partial \hat{\delta}_e}\hat{\delta}_e \\
m_A &= \frac{\partial M_A}{\partial \frac{u}{U_1}}\left(\frac{u}{U_1}\right) + \frac{\partial M_A}{\partial \hat{\alpha}}\hat{\alpha} + \frac{\partial M_A}{\partial \frac{\dot{\alpha}\bar{c}}{2U_1}}\left(\frac{\dot{\alpha}\bar{c}}{2U_1}\right) + \frac{\partial M_A}{\partial \frac{q\bar{c}}{2U_1}}\left(\frac{q\bar{c}}{2U_1}\right) + \frac{\partial M_A}{\partial \hat{\delta}_e}\hat{\delta}_e \qquad (6.12) \\
f_{A_z} &= \frac{\partial F_{A_z}}{\partial \frac{u}{U_1}}\left(\frac{u}{U_1}\right) + \frac{\partial F_{A_z}}{\partial \hat{\alpha}}\hat{\alpha} + \frac{\partial F_{A_z}}{\partial \frac{\dot{\alpha}\bar{c}}{2U_1}}\left(\frac{\dot{\alpha}\bar{c}}{2U_1}\right) + \frac{\partial F_{A_z}}{\partial \frac{q\bar{c}}{2U_1}}\left(\frac{q\bar{c}}{2U_1}\right) + \frac{\partial F_{A_z}}{\partial \hat{\delta}_e}\hat{\delta}_e
\end{aligned}
$$

$$
\begin{aligned}
l_A &= \frac{\partial L_A}{\partial \beta}\beta + \frac{\partial L_A}{\partial \frac{\dot{\beta}b}{2U_1}}\left(\frac{\dot{\beta}b}{2U_1}\right) + \frac{\partial L_A}{\partial \frac{pb}{2U_1}}\left(\frac{pb}{2U_1}\right) + \frac{\partial L_A}{\partial \frac{rb}{2U_1}}\left(\frac{rb}{2U_1}\right) \\
&\quad + \frac{\partial L_A}{\partial \delta_a}\hat{\delta}_a + \frac{\partial L_A}{\partial \delta_r}\hat{\delta}_r \\
f_{A_y} &= \frac{\partial F_{A_y}}{\partial \beta}\beta + \frac{\partial F_{A_y}}{\partial \frac{\dot{\beta}b}{2U_1}}\left(\frac{\dot{\beta}b}{2U_1}\right) + \frac{\partial F_{A_y}}{\partial \frac{pb}{2U_1}}\left(\frac{pb}{2U_1}\right) + \frac{\partial F_{A_y}}{\partial \frac{rb}{2U_1}}\left(\frac{rb}{2U_1}\right) \\
&\quad + \frac{\partial F_{A_y}}{\partial \delta_a}\hat{\delta}_a + \frac{\partial F_{A_y}}{\partial \delta_r}\hat{\delta}_r \qquad (6.13) \\
n_A &= \frac{\partial N_A}{\partial \beta}\beta + \frac{\partial N_A}{\partial \frac{\dot{\beta}b}{2U_1}}\left(\frac{\dot{\beta}b}{2U_1}\right) + \frac{\partial N_A}{\partial \frac{pb}{2U_1}}\left(\frac{pb}{2U_1}\right) + \frac{\partial N_A}{\partial \frac{rb}{2U_1}}\left(\frac{rb}{2U_1}\right) \\
&\quad + \frac{\partial N_A}{\partial \delta_a}\hat{\delta}_a + \frac{\partial N_A}{\partial \delta_r}\hat{\delta}_r
\end{aligned}
$$

Equation (6.12) is the nondimensionalized, longitudinal equation for perturbed forces and moment, and Eq. (6.13) is the nondimensionalized, lateral-directional, perturbed force and moments equation.

6.3.2 Longitudinal Perturbed Force and Moment Derivatives

We will next analyze each of the partial derivative terms in Eq. (6.12) so that they may be expressed with common longitudinal aerodynamic coefficients such as C_L, C_D, and C_m. To do this, we will analyze a perturbation in angle of attack ($\hat{\alpha}$) about the body-fixed stability axis. Figure 6.2 presents the axis systems associated with an exaggerated $\hat{\alpha}$ perturbation. Notice that the instantaneous velocity, V_∞, defines the direction of the lift and drag coefficients (C_L

Source from Yechout, T.R. "Introduction to Aircraft Flight Mechanics", AIAA education Series, 2003

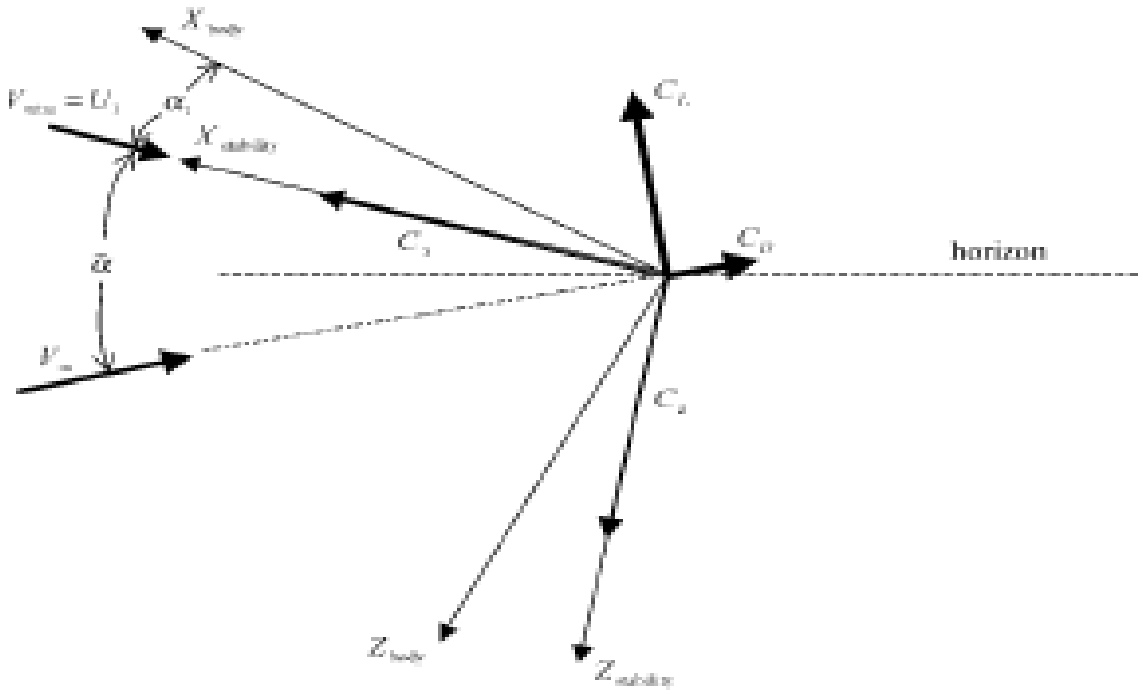

Fig. 6.2 Axis systems associated with an angle of attack perturbation.

and C_D). The coefficients C_x and C_z are defined relative to the body-fixed stability axis, which has its x axis aligned with V_{trim}.

6.3.2.1 u/U_1 derivatives. The u/U_1 derivatives consist of $\partial F_{A_x}/\partial(u/U_1)$, $\partial M_A/\partial(u/U_1)$, and $\partial F_{A_z}/\partial(u/U_1)$ in Eq. (6.12). We will begin with $\partial F_{A_x}/\partial(u/U_1)$. F_{A_x} is defined along $X_{stability}$, the body-fixed stability x axis. Figure 6.3 presents the vectors associated with the analysis. Notice that the vectors U_1 and V_∞ are now shown relative to fixed space.

F_{A_x} may be defined in terms of the coefficient C_x, which is shorthand for $C_{F_{A_x}}$, as

$$F_{A_x} = C_x \bar{q} S$$

We then have

$$\frac{\partial F_{A_x}}{\partial \dfrac{u}{U_1}} = \left.\frac{\partial (C_x \bar{q} S)}{\partial \dfrac{u}{U_1}}\right|_1$$

where the $|_1$ indicates that the partial derivative must be evaluated at the steady-state condition where the perturbation variables such as $\hat{\alpha}$ and u are zero. We must do this because the partial derivatives in the Taylor series expansions of Eqs. (6.12) and (6.13) are simply slopes used for a linear projec-

Source from Yechout, T.R. "Introduction to Aircraft Flight Mechanics", AIAA education Series, 2003

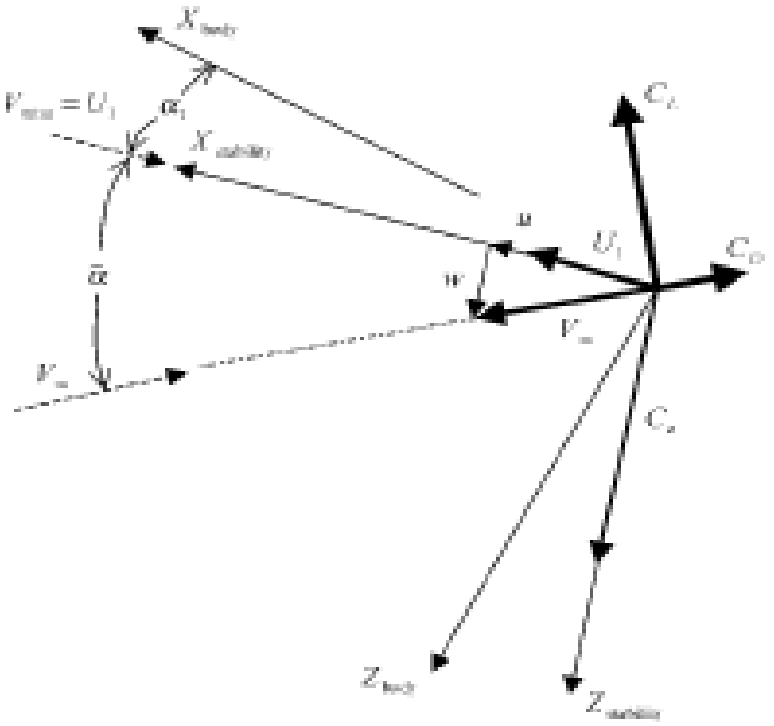

Fig. 6.3 Illustration of a u perturbation.

tion of perturbation values about the steady-state trimmed condition. Because both C_x and $\bar{q}$ may vary with u, we take the derivative in two parts:

$$\frac{\partial F_{A_x}}{\partial \frac{u}{U_1}} = \frac{\partial (C_x \bar{q} S)}{\partial \frac{u}{U_1}}\bigg|_1 = \underbrace{\frac{\partial C_x}{\partial \frac{u}{U_1}} \bar{q} S\bigg|_1}_{A} + \underbrace{C_x S \frac{\partial \bar{q}}{\partial \frac{u}{U_1}}\bigg|_1}_{B} \tag{6.14}$$

We will address part A of Eq. (6.14) first.

From Fig. 6.4, we have

$$C_x = -C_D \cos\hat{\alpha} + C_L \sin\hat{\alpha}$$

and with the small perturbation assumption, this becomes

$$C_x \approx -C_D + C_L \hat{\alpha} \tag{6.15}$$

Using Eq. (6.15),

$$\frac{\partial C_x}{\partial \frac{u}{U_1}} \approx -\frac{\partial C_D}{\partial \frac{u}{U_1}}\bigg|_1 + \frac{\partial C_L}{\partial \frac{u}{U_1}} \hat{\alpha}\bigg|_1 \tag{6.16}$$

Source from Yechout, T.R. "Introduction to Aircraft Flight Mechanics", AIAA education Series, 2003

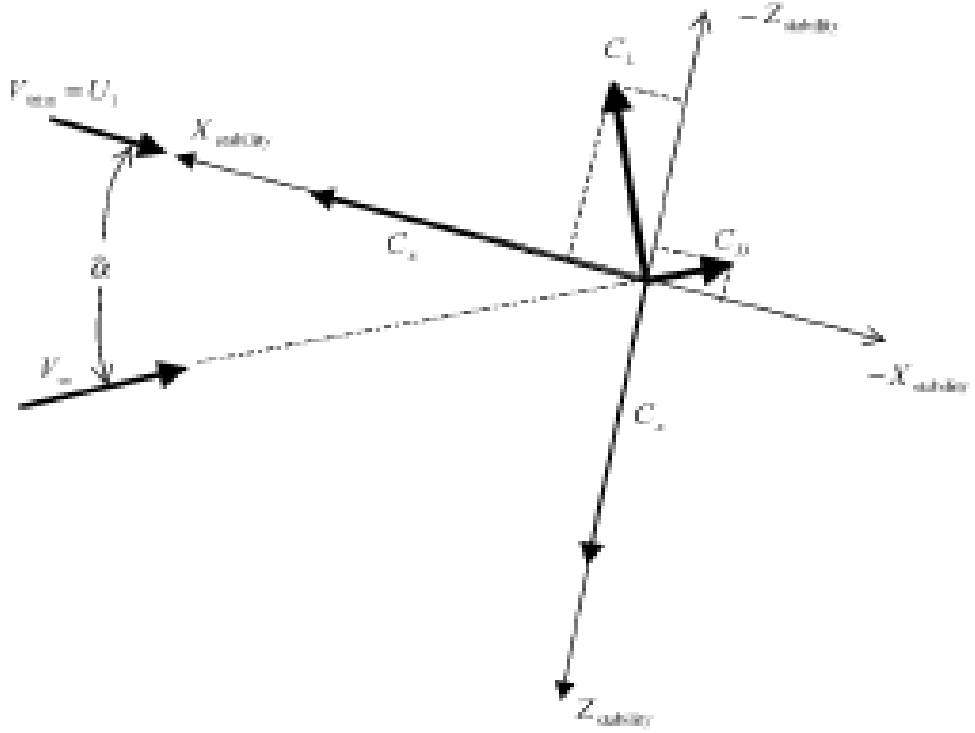

Fig. 6.4 Illustration of resolution of lift and drag coefficient.

Evaluating Eq. (6.16) at the steady-state condition, $\dot{\alpha} = 0$, and, for part A we have

$$\frac{\partial C_x}{\partial \frac{u}{U_1}} \approx -\frac{\partial C_D}{\partial \frac{u}{U_1}} = -C_{D_u} \tag{6.17}$$

C_{D_u} is called the **speed damping derivative**. It represents the change in drag coefficient with respect to u/U_1 and its value is dependent on Mach number. The value of C_{D_u} is generally zero or very small for pretransonic, subsonic Mach numbers. In the subsonic, transonic regime approaching Mach 1, C_{D_u} is generally positive indicating the significant drag rise as sonic flight is approached. Above Mach 1, C_{D_u} is generally negative.

Returning to Eq. (6.14), we now look at part B.

$$\frac{\partial \bar{q}}{\partial \frac{u}{U_1}} = U_1 \frac{\partial \bar{q}}{\partial u} = U_1 \frac{\partial [\frac{1}{2}\rho\{(U_1+u)^2 + v^2 + w^2\}]}{\partial u}\bigg|_1 = U_1 \left(\frac{1}{2}\right)\rho(2\{U_1+u\})|_1$$

Evaluation at the steady state condition were $u = 0$ yields

$$\frac{\partial \bar{q}}{\partial \frac{u}{U_1}} = \rho U_1^2 = 2\bar{q}_1 \tag{6.18}$$

Source from Yechout, T.R. "Introduction to Aircraft Flight Mechanics", AIAA education Series, 2003

where $\bar{q}_1$ is the steady-state dynamic pressure. We now are able to incorporate Eqs. (6.17) and (6.18) into Eq. (6.14).

$$\frac{\partial F_{A_x}}{\partial \frac{u}{U_1}} = -C_{D_u}\bar{q}S|_1 + C_x S(2\bar{q}_1)|_1$$

When evaluated at the steady-state condition, $C_x = -C_{D_1}$ and $\bar{q} = \bar{q}_1$. These substitutions result in

$$\frac{\partial F_{A_x}}{\partial \frac{u}{U_1}} = -(C_{D_u} + 2C_{D_1})\bar{q}_1 S \tag{6.19}$$

The beauty of Eq. (6.19) is that the derivative is now expressed in terms of aerodynamic characteristics such as C_{D_u} and C_{D_1}, which can be estimated analytically, determined from wind tunnel testing, or computed with computational fluid dynamics (CFD) techniques.

The next u/U_1 derivative to be considered is $\partial M_A/\partial(u/U_1)$. Because $M_A = C_m \bar{q} S\bar{c}$ and both C_m and $\bar{q}$ may vary with u, we have

$$\frac{\partial M_A}{\partial \frac{u}{U_1}} = \frac{\partial C_m}{\partial\left(\frac{u}{U_1}\right)}\bar{q}S\bar{c}\,\Bigg|_1 + C_m S\bar{c}\,\frac{\partial \bar{q}}{\partial\left(\frac{u}{U_1}\right)}\,\Bigg|_1 \tag{6.20}$$

We will define

$$\frac{\partial C_m}{\partial\left(\frac{u}{U_1}\right)} = C_{m_u} \tag{6.21}$$

Note again that the subscript u in C_{m_u} really implies partial differentiation of C_m with respect to "u/U_1". With the substitutions of Eqs. (6.18) and (6.21), along with evaluation at the steady-state condition, Eq. (6.20) becomes

$$\frac{\partial M_A}{\partial \frac{u}{U_1}} = C_{m_u}\bar{q}_1 S\bar{c} + C_{m_1} S\bar{c}(2\bar{q}_1)$$

and, in combined form

$$\frac{\partial M_A}{\partial \frac{u}{U_1}} = (C_{m_u} + 2C_{m_1})\bar{q}_1 S\bar{c} \tag{6.22}$$

The derivative C_{m_u} results from changes in C_{m_0} and the aerodynamic center location with changes with forward speed. Probably the most notable effect on

Source from Yechout, T.R. "Introduction to Aircraft Flight Mechanics", AIAA education Series, 2003

C_{m_u} is the aft shift in aerodynamic center that occurs in the subsonic, transonic speed range. As the aerodynamic center moves aft, a negative pitching moment results that typically results in a negative C_{m_u}. Thus, in this range, the aircraft tends to experience a nose-down pitching moment with increasing speed. This phenomena is commonly referred to as "Mach Tuck," a characteristic that caused the crash of several high-speed subsonic aircraft that were not able to pull out of steep dives as the speed increased and C_{m_u} became more negative. As a result, C_{m_u} is commonly called the **Mach tuck derivative.** C_{m_1} is the steady-state aerodynamic pitching moment. It will be nonzero for cases where a thrust pitching moment must be counteracted by an aerodynamic pitching moment to trim the aircraft to a total pitch moment of zero. For all other cases such as gliders and power-off flight, C_{m_1} will be equal to zero.

The last u/U_1 derivative is $\partial F_{A_x}/\partial(u/U_1)$. We begin by referring to Fig. 6.2 and defining

$$F_{A_x} = C_x \bar{q} S$$

Using the same approach as with Eq. (6.14), we have

$$\frac{\partial F_{A_x}}{\partial \frac{u}{U_1}} = \left.\frac{\partial (C_x \bar{q} S)}{\partial \frac{u}{U_1}}\right|_1 = \left.\frac{\partial C_x}{\partial \frac{u}{U_1}} \bar{q} S\right|_1 + C_x S \left.\frac{\partial \bar{q}}{\partial \frac{u}{U_1}}\right|_1$$

where (referring to Fig. 6.4)

$$C_x = -C_L \cos\hat{\alpha} - C_D \sin\hat{\alpha}$$

With the assumption of small perturbations, this becomes

$$C_x \approx -C_L - C_D \hat{\alpha} \tag{6.23}$$

and

$$\frac{\partial C_x}{\partial \frac{u}{U_1}} \approx -\left.\frac{\partial C_L}{\partial \frac{u}{U_1}}\right|_1 - \left.\frac{\partial C_L}{\partial \frac{u}{U_1}} \hat{\alpha}\right|_1 \tag{6.24}$$

Evaluating Eq. (6.24) at the steady-state condition, $\hat{\alpha} = 0$, we have

$$\frac{\partial C_x}{\partial \frac{u}{U_1}} \approx -\frac{\partial C_L}{\partial \frac{u}{U_1}} = -C_{L_u} \tag{6.25}$$

C_{L_u} represents the change in lift coefficient with respect to velocity. The $\partial \bar{q}/\partial(u/U_1)$ derivative in Eq. (6.23) follows the same development as found

Source from Yechout, T.R. "Introduction to Aircraft Flight Mechanics", AIAA education Series, 2003

with Eq. (6.18), $\partial\bar{q}/\partial(u/U_1) = 2\bar{q}_1$. Incorporating Eqs. (6.18) and (6.25) into the original expression for $\partial F_{A_x}/\partial(u/U_1)$ and realizing that $C_x = C_{L_1}$ at steady state, we have

$$\frac{\partial F_{A_x}}{\partial \dfrac{u}{U_1}} = -(C_{L_u} + 2C_{L_1})\bar{q}_1 S \tag{6.26}$$

Example 6.2

Find the u/U_1 derivative $\partial F_{A_x}/\partial(u/U_1)$ for the F-4C aircraft at 35,000 ft and Mach 0.9 ($U_1 = 876$ ft/s, $\bar{q} = 283.2$ lb/ft^2, $S = 530$ ft^2) if $C_{D_1} = 0.03$ and $C_{D_u} = 0.027$. If U is perturbed to 880 ft/s, find the perturbed applied aero force along the x stability axis (f_{A_x}).

Starting with Eq. (6.19),

$$\frac{\partial F_{A_x}}{\partial \dfrac{u}{U_1}} = -(C_{D_u} + 2C_{D_1})\bar{q}_1 S = -(0.027 + 2[0.03])283.2(530)$$

$$\frac{\partial F_{A_x}}{\partial \dfrac{u}{U_1}} = -13{,}058.4 \text{ lb}$$

To find f_{A_x}, we first find the perturbed velocity u.

$$u = U - U_1 = 880 - 876 = 4 \text{ ft/s}$$

and, from Eq. (6.12) for only a u perturbation

$$f_{A_x} = \frac{\partial F_{A_x}}{\partial \dfrac{u}{U_1}}\left(\frac{u}{U_1}\right) = -13{,}058.4\left(\frac{4}{876}\right) = -59.6 \text{ lb}$$

Because f_{A_x} is positive along the positive x stability axis, we have predicted a 59.6-lb increase in the drag of the aircraft if the velocity perturbs by 4 ft/s.

6.3.2.2 $\hat{\alpha}$ derivatives. The $\hat{\alpha}$, or perturbed angle of attack derivatives, consist of $\partial F_{A_x}/\partial\hat{\alpha}$, $\partial M_A/\partial\hat{\alpha}$, and $\partial F_{A_z}/\partial\hat{\alpha}$ in Eq. (6.12). We begin with $\partial F_{A_x}/\partial\hat{\alpha}$ and Eq. (6.15) for C_x.

$$\frac{\partial F_{A_x}}{\partial\hat{\alpha}} = \frac{\partial C_x}{\partial\hat{\alpha}}\bar{q}S$$

Source from Yechout, T.R. "Introduction to Aircraft Flight Mechanics", AIAA education Series, 2003

and

$$\frac{\partial C_x}{\partial \hat{\alpha}} = -\frac{\partial C_D}{\partial \hat{\alpha}} + \frac{\partial C_L}{\partial \hat{\alpha}}\hat{\alpha} + C_L \tag{6.27}$$

Evaluating Eq. (6.27) at the steady-state flight condition ($\hat{\alpha} = 0$),

$$\frac{\partial C_x}{\partial \hat{\alpha}} = -C_{D_\alpha} + C_{L_1}$$

and

$$\frac{\partial F_{A_x}}{\partial \hat{\alpha}} = (-C_{D_\alpha} + C_{L_1})\bar{q}_1 S \tag{6.28}$$

C_{D_α} is the same as the C_{D_α} discussed in Sec. 5.3.1 and Eq. (5.16). It is basically the slope of the C_D vs α plot at the trim condition, α_1 (see Fig. 5.4).

The next $\hat{\alpha}$ derivative to be considered is $\partial M_A/\partial\hat{\alpha}$. This becomes

$$\frac{\partial M_A}{\partial \hat{\alpha}} = \frac{\partial C_m}{\partial \hat{\alpha}}\bar{q}S\bar{c}\bigg|_1 = C_{m_\alpha}\bar{q}_1 S\bar{c} \tag{6.29}$$

C_{m_α} is the same as the C_{m_α} discussed in Sec. 5.3.3.1 and Eq. (5.43). It is the **longitudinal static stability** derivative, which must be negative in value for longitudinal static stability.

The last $\hat{\alpha}$ derivative is $\partial F_{A_z}/\partial\hat{\alpha}$. We begin by referring to Fig. 6.4 and Eq. (6.23).

$$\frac{\partial F_{A_z}}{\partial \hat{\alpha}} = \frac{\partial C_z}{\partial \hat{\alpha}}\bar{q}S = \left(-\frac{\partial C_L}{\partial \hat{\alpha}} - \frac{\partial C_D}{\partial \hat{\alpha}}\hat{\alpha} - C_D\right)\bar{q}S\bigg|_1 \tag{6.30}$$

Evaluating Eq. (6.30) at the steady state flight condition, $\hat{\alpha} = 0$, we have

$$\frac{\partial F_{A_z}}{\partial \hat{\alpha}} = -(C_{L_\alpha} + C_{D_1})\bar{q}_1 S \tag{6.31}$$

C_{L_α} is the same as the C_{L_α} discussed in Sec. 5.3.2 and Eq. (5.30). It is commonly referred to as the **lift curve slope**.

Example 6.3

Find the $\hat{\alpha}$ derivative $\partial F_{A_z}/\partial\hat{\alpha}$ for the F-4C aircraft at the same flight conditions as those of Example 6.2. C_{L_α} is equal to 3.75/rad. If the F-4C is trimmed at an angle of attack of 2.6deg and then is perturbed to 3.1 deg, find the perturbed aero force along the z stability axis (f_{A_z}).

Source from Yechout, T.R. "Introduction to Aircraft Flight Mechanics", AIAA education Series, 2003

Starting with Eq. (6.31),

$$\frac{\partial F_{A_s}}{\partial \hat{\alpha}} = -(C_{L_\alpha} + C_{D_1})\bar{q}_1 S = -(3.75 + 0.03)(283.2)(530)$$

$$\frac{\partial F_{A_s}}{\partial \hat{\alpha}} = -567,363 \text{ lb/rad}$$

To find f_{A_s}, we first find the perturbed angle of attack $\hat{\alpha}$

$$\hat{\alpha} = \alpha - \alpha_1 = 3.1 \text{ deg} - 2.6 \text{ deg} = 0.5 \text{ deg} = 0.00873 \text{ rad}$$

and from Eq. (6.12) for only an $\hat{\alpha}$ perturbation

$$f_{A_s} = \frac{\partial F_{A_s}}{\partial \hat{\alpha}}\hat{\alpha} = -567,363(0.00873) = -4951 \text{ lb}$$

Because f_{A_s} is positive along the positive z stability axis, we have predicted a 4951 lb increase in the lift of the aircraft if the angle of attack perturbs by one-half degree. This may seem very large, but remember the aircraft is at Mach 0.9.

6.3.2.3 Quasi-steady $\dot{\alpha}\bar{c}/2U_1$ derivatives. If a rate of change in angle of attack ($\dot{\alpha}$) is present, a lag in the development of downwash at the horizontal tail occurs. Because the α derivatives assume that the downwash is fully developed, the "$\dot{\alpha}\bar{c}/2U_1$" derivatives provide a correction to the α derivatives when the aircraft is undergoing a rate of change in angle of attack.

The first $\dot{\alpha}\bar{c}/2U_1$ derivative in Eq. (6.12) to be considered is $\partial F_{A_s}/\partial(\dot{\alpha}\bar{c}/2U_1)$. Using a similar approach to the u/U_1 and α derivatives, we have

$$\frac{\partial F_{A_s}}{\partial \frac{\dot{\alpha}\bar{c}}{2U_1}} = \frac{\partial (C_x \bar{q} S)}{\partial \frac{\dot{\alpha}\bar{c}}{2U_1}} = C_{x_{\dot{\alpha}}} \bar{q} S = -C_{D_{\dot{\alpha}}} \bar{q}_1 S \tag{6.32}$$

The derivative $C_{D_{\dot{\alpha}}}$ represents the change in drag coefficient with respect to nondimensional $\dot{\alpha}$. For most applications, the lag in downwash because of $\dot{\alpha}$ has little effect on the drag coefficient, therefore, it is typically assumed that $C_{D_{\dot{\alpha}}} = 0$.

The next $\dot{\alpha}\bar{c}/2U_1$ derivative that we will consider is $\partial F_{A_s}/\partial(\dot{\alpha}\bar{c}/2U_1)$. Again, we have

$$\frac{\partial F_{A_s}}{\partial \frac{\dot{\alpha}\bar{c}}{2U_1}} = \frac{\partial (C_z \bar{q} S)}{\partial \frac{\dot{\alpha}\bar{c}}{2U_1}} = C_{z_{\dot{\alpha}}} \bar{q} S = -C_{L_{\dot{\alpha}}} \bar{q}_1 S \tag{6.33}$$

The derivative $C_{L_{\dot{\alpha}}}$ is significant, and we will develop an approach to estimate it. Remember that $C_{L_{\dot{\alpha}}}$ should be considered a correction to C_{L_α} for nonsteady-

Source from Yechout, T.R. "Introduction to Aircraft Flight Mechanics", AIAA education Series, 2003

state conditions. Figure 6.5 presents an aircraft experiencing an $\dot{\alpha}$ as it transitions from $\alpha_{initial}$ to α_{final}. If this change in α takes place in Δt seconds, we have

$$\dot{\alpha} = \frac{\alpha_{final} - \alpha_{initial}}{\Delta t}$$

This figure also shows the change in downwash angle that occurs at the horizontal tail. The change in downwash angle will be defined as

$$\Delta\varepsilon = \varepsilon_{initial} - \varepsilon_{final}$$

$\Delta\varepsilon$ can also be viewed as the correction needed to the steady-state downwash angle to compensate for the downwash lag. It can also be estimated with

$$\Delta\varepsilon = -\frac{d\varepsilon}{d\alpha}\frac{d\alpha}{dt}\Delta t = -\frac{d\varepsilon}{d\alpha}\dot{\alpha}\Delta t \tag{6.34}$$

$d\varepsilon/d\alpha$ is the rate of change of downwash angle with angle of attack as discussed in Sec. 5.3.2. Δt is the time it takes for the final downwash to travel back to the horizontal tail. Referring to Fig. 6.5, Δt is normally estimated as

$$\Delta t = \frac{X_h}{U_1} = \frac{x_{AC_h} - x_{cg}}{U_1} \tag{6.35}$$

Thus, Eq. (6.34) becomes

$$\Delta\varepsilon = -\frac{d\varepsilon}{d\alpha}\dot{\alpha}\frac{X_h}{U_1} \tag{6.36}$$

Because the estimate of the lift coefficient at the horizontal tail is based on the steady-state angle of attack (by using $C_{L_{\alpha_h}}$), we next estimate the correction ($\Delta C_{L_{\alpha_h}}$) needed to the lift coefficient because of the lag in downwash (resulting from $\dot{\alpha}$). This becomes

$$\Delta C_{L_{\alpha_h}} = -C_{L_{\alpha_h}}(\Delta\varepsilon) = (C_{L_{\alpha_h}})\frac{d\varepsilon}{d\alpha}\dot{\alpha}\frac{X_h}{U_1} \tag{6.37}$$

The correction to lift coefficient is positive because the steady-state lift coefficient assumes a fully developed downwash angle that reduces the lift. Downwash lag results in the original downwash angle being maintained, resulting in additional lift over that predicted for the steady-state angle of attack during this interim period. We next use the techniques of Sec. 5.3.2 and Eq. (6.37) to predict the increase in lift coefficient for the entire aircraft.

$$\Delta C_L = \Delta C_{L_{\alpha_h}}\eta_h\frac{S_h}{S} = (C_{L_{\alpha_h}})\frac{d\varepsilon}{d\alpha}\dot{\alpha}\frac{X_h}{U_1}\eta_h\frac{S_h}{S} \tag{6.38}$$

Source from Yechout, T.R. "Introduction to Aircraft Flight Mechanics", AIAA education Series, 2003

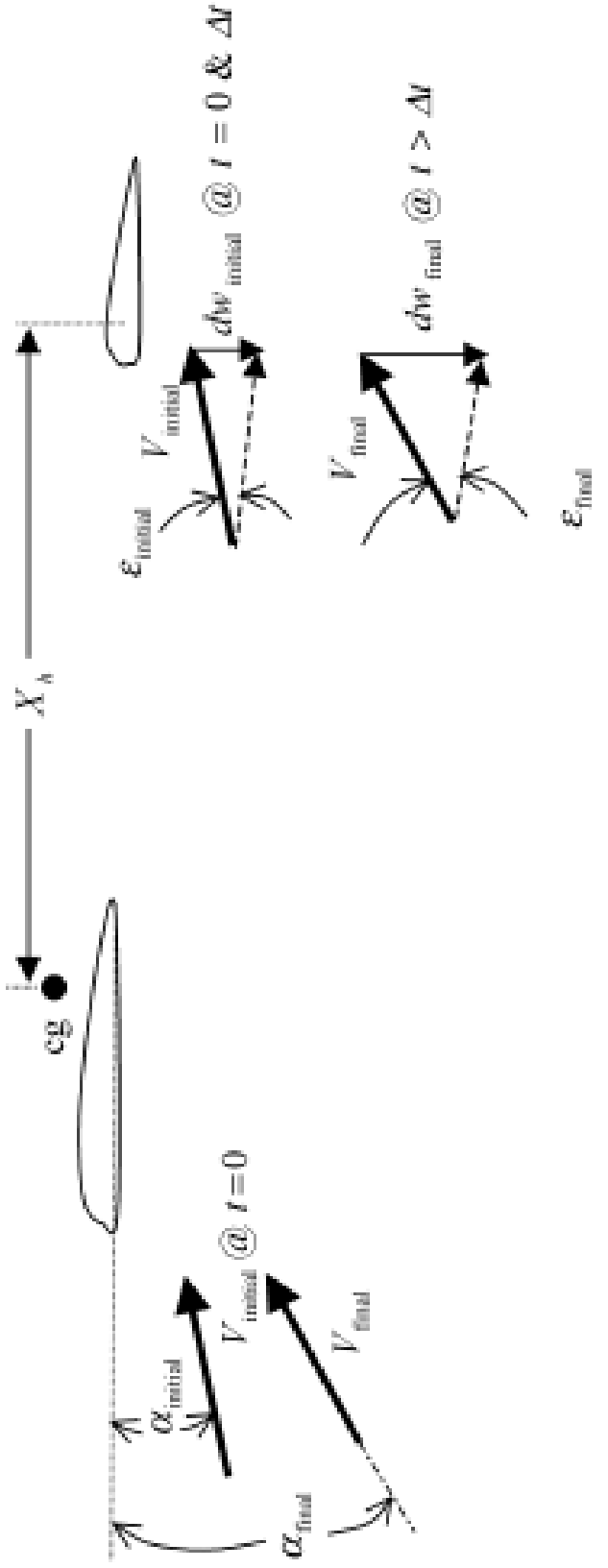

Fig. 6.5 Illustration of downwash lag.

Source from Yechout, T.R. "Introduction to Aircraft Flight Mechanics", AIAA education Series, 2003

Recalling from Eq. (6.33) that we wanted to develop an expression for $C_{L_{\dot{\alpha}}}$, we have

$$C_{L_{\dot{\alpha}}} = \frac{\partial C_L}{\partial \frac{\dot{\alpha}\bar{c}}{2U_1}} = \frac{2U_1}{\bar{c}} \frac{\partial C_L}{\partial \dot{\alpha}} \tag{6.39}$$

Finally, we can take the partial derivative of Eq. (6.38) with respect to $\dot{\alpha}$ and substitute the result into Eq. (6.39)

$$C_{L_{\dot{\alpha}}} = \frac{2U_1}{\bar{c}}(C_{L_{\alpha_h}}) \frac{d\varepsilon}{d\alpha} \frac{X_h}{U_1} \eta_h \frac{S_h}{S} \tag{6.40}$$

Recalling from Eq. (5.44) that the tail volume ratio, $\bar{V}_h$, is equal to $\frac{X_h}{\bar{c}} \frac{S_h}{S}$, Eq. (6.40) becomes

$$C_{L_{\dot{\alpha}}} = 2(C_{L_{\alpha_h}}) \frac{d\varepsilon}{d\alpha} \eta_h \bar{V}_h \tag{6.41}$$

The last $\dot{\alpha}\bar{c}/2U_1$ derivative to be considered is $\partial M_A/\partial(\dot{\alpha}\bar{c}/2U_1)$. Again, we have

$$\frac{\partial M_A}{\partial \frac{\dot{\alpha}\bar{c}}{2U_1}} = \frac{\partial C_m \bar{q} S \bar{c}}{\partial \frac{\dot{\alpha}\bar{c}}{2U_1}} = C_{m_{\dot{\alpha}}} \bar{q}_1 S \bar{c} \tag{6.42}$$

$C_{m_{\dot{\alpha}}}$ results from the same downwash lag phenomena that was analyzed to obtain the estimate of $C_{L_{\dot{\alpha}}}$. Thus, Eq. (6.41) is multiplied by the nondimensional moment arm $X_h/\bar{c}$ along with a negative sign indicating that positive lift on the horizontal tail produces a nose-down (negative) pitching moment to obtain $C_{m_{\dot{\alpha}}}$.

$$C_{m_{\dot{\alpha}}} = -2(C_{L_{\alpha_h}}) \frac{d\varepsilon}{d\alpha} \eta_h \bar{V}_h \frac{X_h}{\bar{c}} \tag{6.43}$$

As a rule of thumb, for many airplanes $C_{m_{\dot{\alpha}}}$ is approximately equal to one third the value of C_{m_q} [Eq. (6.49)].

Example 6.4

Find the $\dot{\alpha}\bar{c}/2U_1$ derivative $\partial M_A/\partial(\dot{\alpha}\bar{c}/2U_1)$ for the F-4C at the same conditions as presented in Example 6.2. $\bar{c}$ for the F-4C is 16 ft and $C_{m_{\dot{\alpha}}}$ is -1.3 per rad. If $\dot{\alpha}$ is 0.5 deg/s, find the perturbed pitching moment m_A.

Starting with Eq. (6.42),

$$\frac{\partial M_A}{\partial \frac{\dot{\alpha}\bar{c}}{2U_1}} = C_{m_{\dot{\alpha}}} \bar{q}_1 S \bar{c} = -1.3(283.2)530(16) = -3{,}121{,}997 \text{ ft} \cdot \text{lb/rad}$$

Source from Yechout, T.R. "Introduction to Aircraft Flight Mechanics", AIAA education Series, 2003

To find $m_{\dot{\alpha}}$, we use Eq. (6.12) for only an $\dot{\alpha}$ perturbation

$$m_{\dot{\alpha}} = \frac{\partial M_A}{\partial \dfrac{\dot{\alpha}\bar{c}}{2U_1}}\left(\frac{\dot{\alpha}\bar{c}}{2U_1}\right) = -3{,}121{,}997\left(\frac{(0.5/57.3)(16)}{2(876)}\right) = -248.8 \text{ ft} \cdot \text{lb}$$

Notice that degrees/second are converted to radians/second to maintain consistent units. We have predicted a nose-down pitching moment of 248.8 ft/lb resulting from a positive 0.5 deg/s $\dot{\alpha}$.

6.3.2.4 Pitch rate $q\bar{c}/2U_1$ derivatives. The $q\bar{c}/2U_1$ derivatives consist of $\partial F_{A_x}/\partial(q\bar{c}/2U_1)$, $\partial M_A/\partial(q\bar{c}/2U_1)$ and $\partial F_{A_z}/\partial(q\bar{c}/2U_1)$ in Eq. (6.12). We begin with $\partial F_{A_x}/\partial(q\bar{c}/2U_1)$.

$$\frac{\partial F_{A_x}}{\partial \dfrac{q\bar{c}}{2U_1}} = \frac{\partial(C_x \bar{q} S)}{\partial \dfrac{q\bar{c}}{2U_1}} = C_{x_q}\bar{q}S = -C_{D_q}\bar{q}_1 S \tag{6.44}$$

The derivative C_{D_q} represents the change in drag coefficient with respect to nondimensional pitch rate. For most applications, this derivative is very small and assumed to be equal to zero ($C_{D_q} \approx 0$).

The next "$q\bar{c}/2U_1$" derivative to be considered is $\partial F_{A_z}/\partial(q\bar{c}/2U_1)$.

$$\frac{\partial F_{A_z}}{\partial \dfrac{q\bar{c}}{2U_1}} = \frac{\partial(C_z \bar{q} S)}{\partial \dfrac{q\bar{c}}{2U_1}} = C_{z_q}\bar{q}S = -C_{L_q}\bar{q}_1 S \tag{6.45}$$

C_{L_q} should be thought of as the change in lift coefficient because of pitch rate. Referring to Fig. 6.6, it can be seen that a positive pitch rate, q, results in a downward velocity, qX_h, at the horizontal tail.

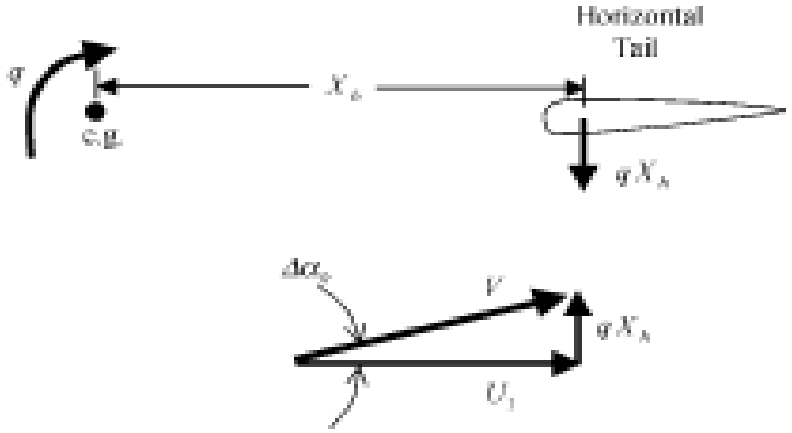

Fig. 6.6 Illustration of change in angle of attack at the horizontal tail because of pitch rate.

Source from Yechout, T.R. "Introduction to Aircraft Flight Mechanics", AIAA education Series, 2003

This downward velocity induces an increase in the angle of attack for the horizontal tail, $\Delta\alpha_h$, which can be defined as

$$\Delta\alpha_h = \tan^{-1}\frac{qX_h}{U_1} \approx \frac{qX_h}{U_1}$$

This increase in angle of attack results in an increase in horizontal tail lift, which can be quantified in terms of an increase in lift coefficient because of pitch rate

$$\Delta C_{L_h} = C_{L_{\alpha_h}}(\Delta\alpha_h) = C_{L_{\alpha_h}}\left(\frac{qX_h}{U_1}\right)$$

The change in lift coefficient for the entire aircraft then becomes (using the techniques of Sec. 5.3.2)

$$\Delta C_L = C_{L_{\alpha_h}}\left(\frac{qX_h}{U_1}\right)\eta_h\frac{S_h}{S} \tag{6.46}$$

C_{L_q} may be determined using Eq. (6.47)

$$C_{L_q} = \frac{\partial C_L}{\partial\dfrac{q\bar{c}}{2U_1}} = \frac{\Delta C_L}{\Delta\dfrac{q\bar{c}}{2U_1}} = 2C_{L_{\alpha_h}}\frac{X_h}{\bar{c}}\eta_h\frac{S_h}{S} = 2C_{L_{\alpha_h}}\eta_h\bar{V}_h \tag{6.47}$$

The derivative C_{L_q} will typically have a positive value and vary with Mach number.

The final $q\bar{c}/2U_1$ derivative to be considered is $\partial M_A/\partial(q\bar{c}/2U_1)$. Again, we have

$$\frac{\partial M_A}{\partial\dfrac{q\bar{c}}{2U_1}} = \frac{\partial C_m\bar{q}S\bar{c}}{\partial\dfrac{q\bar{c}}{2U_1}} = C_{m_q}\bar{q}_1 S\bar{c} \tag{6.48}$$

C_{m_q} results from the same increase in horizontal tail lift because of pitch rate as was discussed for C_{L_q}. Thus, Eq. (6.47) is simply multiplied by the nondimensional moment arm $X_h/\bar{c}$ and a negative sign is added to indicate that a positive pitch rate results in a nose-down (negative) pitching moment.

$$C_{m_q} = \frac{\partial C_m}{\partial\dfrac{q\bar{c}}{2U_1}} = -2C_{L_{\alpha_h}}\eta_h\bar{V}_h\frac{X_h}{\bar{c}} \tag{6.49}$$

C_{m_q} is called the **pitch damping derivative**. It is a very important factor for longitudinal dynamic stability characteristics. It is negative (providing a moment that opposes the direction of the pitch rate) and will be the primary factor (along with C_{m_α}) for damping out pitch oscillations. For most aircraft,

Source from Yechout, T.R. "Introduction to Aircraft Flight Mechanics", AIAA education Series, 2003

the wing and fuselage also contribute to pitch damping; to account for this effect, the value of C_{m_q} predicted by Eq. (6.49) is typically increased by approximately 10%. Of course, for tailless aircraft the wing body contribution becomes the primary contributor to C_{m_q}. An analysis of Eq. (6.49) reveals that C_{m_q} is proportional to the square of X_h ($\bar{V}_h$ contains an X_h term). Thus, X_h becomes an important design parameter when considering longitudinal dynamic stability.

Example 6.5

Find the $q\bar{c}/2U_1$ derivative $\partial F_{A_z}/\partial(q\bar{c}/2U_1)$ for the F-4C aircraft at the same flight conditions as those of Example 6.2. C_{L_α} is equal to 1.80. If q is 2.5 deg/s, find the perturbed aero force along the z stability axis (f_{A_z}).

Starting with Eq. (6.45),

$$\frac{\partial F_{A_z}}{\partial \dfrac{q\bar{c}}{2U_1}} = -C_{L_\alpha}\bar{q}_1 S = -1.8(283.2)(530)$$

$$\frac{\partial F_{A_z}}{\partial \dfrac{q\bar{c}}{2U_1}} = -270{,}172.8 \text{ lb/rad}$$

To find f_{A_z}, we use Eq. (6.12) for only a q perturbation

$$f_{A_z} = \frac{\partial F_{A_z}}{\partial \dfrac{q\bar{c}}{2U_1}}\left(\frac{q\bar{c}}{2U_1}\right) = -270{,}172.8\left(\frac{(2.5/57.3)(16)}{2(876)}\right) = -107.7 \text{ lb}$$

Notice that degrees/second are converted to radians/second to maintain consistent units. Because f_{A_z} is positive along the positive z stability axis, we have predicted 107.7 lb increase in lift if pitch rate perturbs by 2.5 deg/s.

Example 6.6

Estimate the pitch damping derivative, C_{m_q}, for an aircraft with the following characteristics: $C_{L_{\alpha_h}} = 0.075/\text{deg}$, $\eta_h = 0.98$, $\bar{V}_h = 0.375$, $(X_h/\bar{c}) = 3.0$.

Starting with Eq. (6.49),

$$C_{m_q} = -2C_{L_{\alpha_h}}\eta_h \bar{V}_h \frac{X_h}{\bar{c}} = -2(0.075)(57.3)0.98(0.375)3.0$$

$$C_{m_q} = -9.48/\text{rad}$$

Notice that $C_{L_{\alpha_h}}$ has been converted to per radian.

Source from Yechout, T.R. "Introduction to Aircraft Flight Mechanics", AIAA education Series, 2003

6.3.2.5 $\dot{\delta}_e$ derivatives. The $\dot{\delta}_e$ derivatives consist of $\partial F_{A_z}/\partial \dot{\delta}_e$, $\partial M_A/\partial \dot{\delta}_e$, and $\partial F_{A_x}/\partial \dot{\delta}_e$ in Eq. (6.12). Using a similar development to that for the previous derivatives, we have

$$\frac{\partial F_{A_z}}{\partial \dot{\delta}_e} = \frac{\partial (C_z \bar{q} S)}{\partial \dot{\delta}_e} = C_{z_{\dot{\delta}_e}} \bar{q} S = -C_{D_{\dot{\delta}_e}} \bar{q}_1 S \tag{6.50}$$

$C_{D_{\dot{\delta}_e}}$ is the change in drag coefficient because of elevator deflection. As discussed in Sec. 5.3.1, it is typically very small and usually assumed to be equal to zero.

$\partial M_A/\partial \dot{\delta}_e$ becomes

$$\frac{\partial M_A}{\partial \dot{\delta}_e} = \frac{\partial C_m \bar{q} S \bar{c}}{\partial \dot{\delta}_e} = C_{m_{\dot{\delta}_e}} \bar{q}_1 S \bar{c} \tag{6.51}$$

$C_{m_{\dot{\delta}_e}}$ is the change in pitching moment coefficient because of elevator deflection and is a **primary control derivative**, as discussed in Sec. 5.2. It is also referred to as the **elevator control power** derivative. It was previously defined with Eq. (5.46).

Finally, $\partial F_{A_x}/\partial \dot{\delta}_e$ becomes

$$\frac{\partial F_{A_x}}{\partial \dot{\delta}_e} = \frac{\partial (C_x \bar{q} S)}{\partial \dot{\delta}_e} = C_{x_{\dot{\delta}_e}} \bar{q} S = -C_{L_{\dot{\delta}_e}} \bar{q}_1 S \tag{6.52}$$

$C_{L_{\dot{\delta}_e}}$ is the change in lift coefficient because of elevator deflection. This derivative was discussed in Sec. 5.3.2 and was defined with Eq. (5.32).

The $\dot{\delta}_e$ derivatives were developed assuming a conventional (tail aft) aircraft with a horizontal tail and elevator configuration. Of course, a variety of other longitudinal control configurations may be used with modern aircraft. These include stabilators, canards, and flaps. For these cases, appropriate control derivatives must be developed using the same approach presented here for the $\dot{\delta}_e$ derivatives.

Example 6.7

Find the $\dot{\delta}_e$ derivative $\partial M_A/\partial \dot{\delta}_e$ for the F-4C aircraft at the same flight conditions as those of Example 6.2. $C_{m_{\dot{\delta}_e}}$ is equal to -0.058/rad. If $\dot{\delta}_e$ is 1 deg, find the perturbed pitching moment, m_A.

Starting with Eq. (6.51),

$$\frac{\partial M_A}{\partial \dot{\delta}_e} = C_{m_{\dot{\delta}_e}} \bar{q}_1 S \bar{c} = -0.058(283.2)530(16) = -139{,}289 \text{ ft} \cdot \text{lb/rad}$$

Source from Yechout, T.R. "Introduction to Aircraft Flight Mechanics", AIAA education Series, 2003

Table 6.1 Summary of longitudinal derivatives

Derivative	Name	Normal sign
C_{D_u}	Speed damping derivative	+ or −
C_{m_u}	Mach tuck derivative	+ or −
C_{L_u}	None	+ or −
C_{D_α}	None	+
C_{m_α}	Longitudinal static stability derivative	−
C_{L_α}	Lift curve slope	+
$C_{D_{\dot{\alpha}}}$	Quasi-steady derivative	≈ 0
$C_{m_{\dot{\alpha}}}$	Quasi-steady derivative	−
$C_{L_{\dot{\alpha}}}$	Quasi-steady derivative	+
C_{D_q}	None	≈ 0
C_{m_q}	Pitch damping derivative	−
C_{L_q}	None	+
$C_{D_{\delta_e}}$	None	≈ 0
$C_{m_{\delta_e}}$	Elevator control power	−
$C_{L_{\delta_e}}$	None	+

right of the aircraft nose or, from the pilot's perspective, "wind in the right ear." A review of the lateral-directional control deflection sign convention from Sec. 5.2 is also helpful. Trailing edge up right aileron deflection and trailing edge down left aileron deflection is defined as a positive δ_a. Trailing edge left rudder deflection is defined as a positive δ_r.

6.3.3.1 Sideslip "β" derivatives. The β derivatives consist of $\partial L_A/\partial\beta$, $\partial F_{A_z}/\partial\beta$, and $\partial N_A/\partial\beta$ in Eq. (6.13). We will begin with $\partial L_A/\partial\beta$. L_A is the aerodynamic rolling moment and may be defined in terms of the rolling moment coefficient C_l with Eq. (5.87).

$$L_A = C_l \bar{q}_1 Sb$$

We then have

$$\frac{\partial L_A}{\partial \beta} = \frac{\partial C_l}{\partial \beta}\bar{q}_1 Sb = C_{l_\beta}\bar{q}_1 Sb \tag{6.54}$$

C_{l_β} is the **lateral** (roll) **static stability** derivative as discussed in Sec. 5.5.2.1. It must be negative if an aircraft has roll static stability. An estimate of C_{l_β} can be obtained through analysis of the four aircraft design aspects that have the greatest influence on C_{l_β}, namely, geometric dihedral, wing position, wing sweep angle, and the vertical tail. Reference 1 presents such an approach. However, because of the complex interaction of each design feature, wind tunnel and/or computational fluid dynamic analysis is also suggested.

Source from Yechout, T.R. "Introduction to Aircraft Flight Mechanics", AIAA education Series, 2003

In a similar manner, development of $\partial F_{A_y}/\partial\beta$ begins with a restatement of Eq. (5.85):

$$F_{A_y} = C_y \bar{q}_1 S$$

and

$$\frac{\partial F_{A_y}}{\partial \beta} = \frac{\partial C_y}{\partial \beta} \bar{q}_1 S = C_{y_\beta} \bar{q}_1 S \tag{6.55}$$

The derivative C_{y_β} is normally negative and was discussed in Sec. 5.5.1.

Finally, $\partial N_A/\partial\beta$ is developed in the same manner starting with Eq. (5.94).

$$N_A = C_n \bar{q}_1 S b$$

We then have

$$\frac{\partial N_A}{\partial \beta} = \frac{\partial C_n}{\partial \beta} \bar{q}_1 S b = C_{n_\beta} \bar{q}_1 S b \tag{6.56}$$

The derivative C_{n_β} is the **directional** (yaw) **static stability** as discussed in Sec. 5.5.3.1. It must be positive for the aircraft to have directional static stability.

Example 6.8

Find the β derivative $\partial L_A/\partial\beta$ for the F-4C aircraft at 35,000 ft and Mach 0.9 ($U_1 = 876$ ft/s, $\bar{q} = 283.2$ lb/ft^2, $S = 530$ ft^2, $b = 38.7$ ft) if $C_{l_\beta} = -0.08$. If β is perturbed to 1 deg, find the perturbed rolling moment l_A.

Starting with Eq. (6.54),

$$\frac{\partial L_A}{\partial \beta} = C_{l_\beta} \bar{q}_1 S b = -0.08(283.2)530(38.7) = -464,697 \text{ ft} \cdot \text{lb/rad}$$

To find l_A, we use Eq. (6.13) for only a β perturbation

$$l_A = \frac{\partial L_A}{\partial \beta} \beta = -464,697(1/57.3) = -8,109.9 \text{ ft/lb}$$

Notice that degrees are converted to radians to maintain consistent units.

6.3.3.2 Quasi-steady $\dot{\beta}b/2U_1$ derivatives. Similar to the discussion of Sec. 6.3.2.3, if a rate of change in sideslip ($\dot{\beta}$) is present, a lag in the development of sidewash at the vertical tail occurs. Because the β derivatives assume that the sidewash is fully developed, the $\dot{\beta}b/2U_1$ derivatives provide a correction to the β derivatives when the aircraft is undergoing a rate of change in sideslip. These derivatives are generally considered negligible because of the relatively

Source from Yechout, T.R. "Introduction to Aircraft Flight Mechanics", AIAA education Series, 2003

unobstructed flow that is present at most vertical tails. However, they may be significant in the high subsonic speed region.

The first $\dot{\beta}b/2U_1$ derivative in Eq. (6.13) to be considered is $\partial L_A/\partial(\dot{\beta}b/2U_1)$. Using a similar approach as with the β derivatives, we have:

$$\frac{\partial L_A}{\partial \frac{\dot{\beta}b}{2U_1}} = \frac{\partial C_l \bar{q}_1 Sb}{\partial \frac{\dot{\beta}b}{2U_1}} = C_{l_{\dot{\beta}}} \bar{q}_1 Sb \tag{6.57}$$

The next two $\dot{\beta}b/2U_1$ derivatives follow the same pattern.

$$\frac{\partial F_{A_y}}{\partial \frac{\dot{\beta}b}{2U_1}} = \frac{\partial C_y \bar{q}_1 S}{\partial \frac{\dot{\beta}b}{2U_1}} = C_{y_{\dot{\beta}}} \bar{q}_1 S \tag{6.58}$$

$$\frac{\partial N_A}{\partial \frac{\dot{\beta}b}{2U_1}} = \frac{\partial C_n \bar{q}_1 Sb}{\partial \frac{\dot{\beta}b}{2U_1}} = C_{n_{\dot{\beta}}} \bar{q}_1 Sb \tag{6.59}$$

Methods for estimating the $\dot{\beta}b/2U_1$ derivatives are presented in several flight mechanics and aircraft design texts.

6.3.3.3 Roll rate $pb/2U_1$ derivatives. The $pb/2U_1$ derivatives consist of $\partial L_A/\partial(pb/2U_1)$, $\partial F_A/\partial(pb/2U_1)$, and $\partial N_A/\partial(pb/2U_1)$ in Eq. (6.13). We begin with $\partial L_A/\partial(pb/2U_1)$.

$$\frac{\partial L_A}{\partial \frac{pb}{2U_1}} = \frac{\partial C_l}{\partial \frac{pb}{2U_1}} \bar{q}_1 Sb = C_{l_p} \bar{q}_1 Sb \tag{6.60}$$

The derivative C_{l_p} is called the **roll damping derivative**. It represents the change in rolling moment coefficient with respect to nondimensional roll rate and is usually negative (providing a moment that opposes the direction of the roll rate). C_{l_p} is a very important factor for lateral-directional dynamic stability characteristics. Three aircraft components have a primary influence on the value of C_{l_p}: the wing, the horizontal tail, and the vertical tail.

As illustrated in Fig. 6.7, roll rate induces a vertical velocity contribution on the wing and horizontal tail. At the wing tips, this vertical velocity because of roll rate has a magnitude of $pb/2$. Of course, the vertical velocity because of roll rate decreases as the distance from the fuselage decreases.

Figure 6.8 illustrates how this vertical velocity because of roll rate changes the angle of attack at the left and right wing tip.

Thus, with this illustration for a positive roll rate, an increase in angle of attack is experienced on the right wing and a decrease in angle of attack is experienced on the left wing. This change in angle of attack on the wings and horizontal tail because of roll rate results in an increase in lift on the right

Source from Yechout, T.R. "Introduction to Aircraft Flight Mechanics", AIAA education Series, 2003

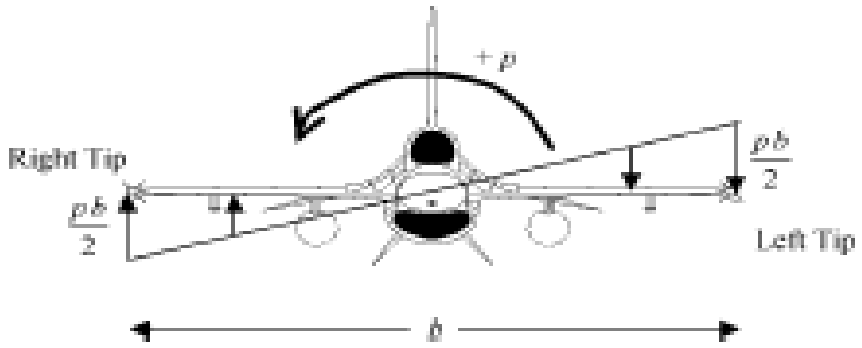

Fig. 6.7 Wing velocity distribution because of roll rate.

wing and a decrease in lift on the left wing. Thus, a roll damping moment is created that is in the opposite direction of the roll rate and C_{l_p} is negative. Of course, this analysis assumes that the angle of attack remains below the stall angle of attack on both wings. Methods for estimating the wing and horizontal tail contribution to C_{l_p} are presented in several flight mechanics and aircraft design texts. In general terms, increases in the span and/or area of the wing and horizontal tail will result in an increase in C_{l_p}.

The absolute value of this change in angle of attack at the wing tips due to roll rate ($pb/2U_1$) is called the **roll helix angle**. It provides the basis for the form of the nondimensionalization approach used for angular rates in Sec. 6.3.1. The roll helix angle has physical meaning as well. It can be thought of generally as the angle that the wing tip light would make with the horizon for an aircraft undergoing a roll rate (if observed as the aircraft passes through wings level).

The contribution of the vertical tail to C_{l_r} may be estimated by first finding the force on the vertical tail because of roll rate. Looking at the aircraft from the rear using Fig. 6.9, we see that a positive roll rate creates a force on the tail in the negative y direction. We call this sideforce F_s, where $F_{A_{y_{\text{vertical tail}}}} = -F_s$.

Figure 6.10 analyzes the velocity components at the center of pressure for the aircraft shown in Fig. 6.9. There is a velocity component in the x direction because of the forward velocity and a velocity component in the y direction because of the roll rate, p.

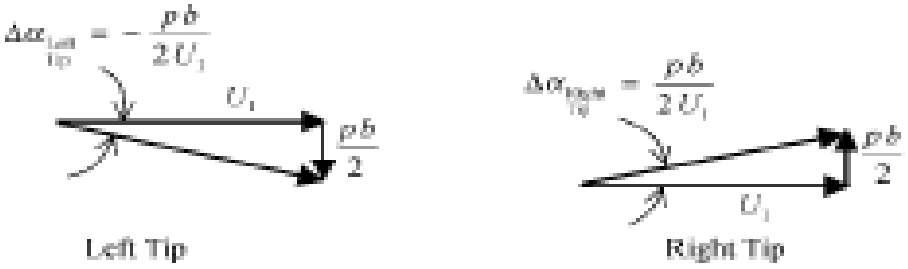

Source from Yechout, T.R. "Introduction to Aircraft Flight Mechanics", AIAA education Series, 2003

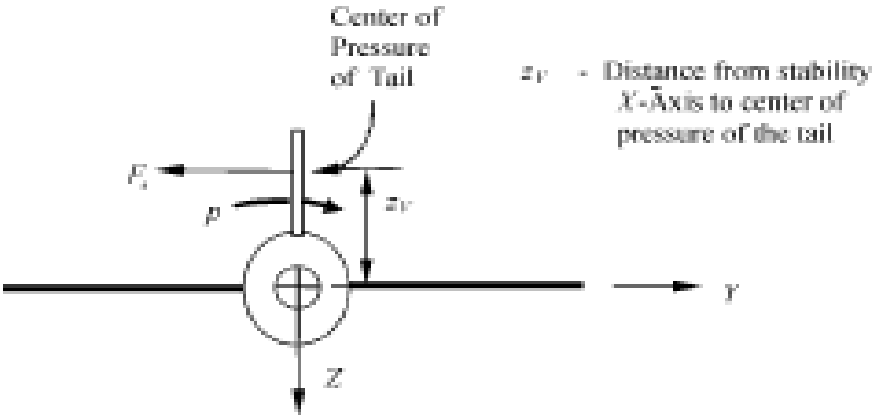

Fig. 6.9 Rear view of aircraft undergoing positive roll rate.

The angle $\Delta\alpha_v$ is the same as an effective sideslip on the vertical tail and may be approximated with the following equation:

$$\Delta\alpha_v \approx \frac{pz_v}{U_1} \tag{6.61}$$

$\Delta\alpha_v$ results in generation of the sideforce, F_z, based on the lift curve slope of the vertical tail, $C_{L_{\alpha_v}}$. F_z therefore becomes

$$F_z = C_{L_{\alpha_v}} \Delta\alpha_v \bar{q}_v S_v = C_{L_{\alpha_v}} \left(\frac{pz_v}{U_1}\right) \bar{q}_v S_v \tag{6.62}$$

This sideforce on the vertical tail because of roll rate also produces a negative rolling moment (L_{A_v}) about the center of gravity because it acts at z_v above the c.g. Recalling that, $F_{A_{v_{\text{vertical tail}}}} = -F_z$,

$$L_{A_v} = F_{A_{v_v}} z_v = -F_z z_v = C_{l_v} \bar{q} S b \tag{6.63}$$

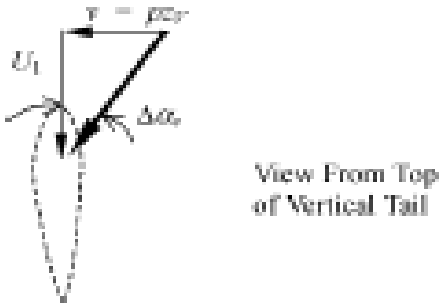

Fig. 6.10 Velocity components at the vertical tail resulting from positive roll rate.

Source from Yechout, T.R. "Introduction to Aircraft Flight Mechanics", AIAA education Series, 2003

Combining Eqs. (6.62) and (6.63), and solving for C_{l_v}, we have

$$C_{l_v} = -C_{L_{\alpha_v}}\left(\frac{pz_v}{U_1}\right)\eta_v\frac{S_v}{S}\left(\frac{z_v}{b}\right) \tag{6.64}$$

Taking the partial derivative of Eq. (6.64) with respect to p,

$$\frac{\partial C_{l_v}}{\partial p} = -C_{L_{\alpha_v}}\left(\frac{z_v}{U_1}\right)\eta_v\frac{S_v}{S}\left(\frac{z_v}{b}\right)$$

Finally, we obtain an estimate for the vertical tail contribution to the roll damping derivative in nondimensional form

$$C_{l_{p_v}} = \frac{\partial C_l}{\partial\left(\frac{pb}{2U_1}\right)} = \frac{2U_1}{b}\frac{\partial C_{l_v}}{\partial p} = -2C_{L_{\alpha_v}}\left(\frac{z_v}{b}\right)^2\eta_v\frac{S_v}{S} \tag{6.65}$$

Because $C_{L_{\alpha_v}}$, $(z_v/b)^2$, η_v, and S_v/S are all positive, $C_{l_{p_v}}$ must be negative.

The next $pb/2U_1$ derivative to be considered is $\partial F_{A_y}/\partial(pb/2U_1)$. We begin with

$$\frac{\partial F_{A_y}}{\partial\frac{pb}{2U_1}} = \frac{\partial C_y\bar{q}S}{\partial\frac{pb}{2U_1}} = C_{y_p}\bar{q}_1 S \tag{6.66}$$

The vertical tail is the major contributor to C_{y_p} and the preceding analysis to estimate C_{l_p} is appropriate. Recalling that $F_{A_{y_{wing}}} = -F_{z_{wing}}$, we express F_z (the side force because of roll rate) in terms of the side force coefficient of the entire aircraft:

$$F_z = -F_{A_y} = -C_{y_p}\bar{q}_1 S \tag{6.67}$$

Equation (6.62) is then substituted into Eq. (6.67) and solved for C_{y_v}

$$C_{y_v} = -C_{L_{\alpha_v}}\left(\frac{pz_v}{U_1}\right)\frac{\bar{q}_v}{\bar{q}_1}\frac{S_v}{S}$$

Taking the partial derivative with respect to p, we have

$$\frac{\partial C_{y_v}}{\partial p} = -C_{L_{\alpha_v}}\left(\frac{z_v}{U_1}\right)\eta_v\frac{S_v}{S} \tag{6.68}$$

Source from Yechout, T.R. "Introduction to Aircraft Flight Mechanics", AIAA education Series, 2003

Finally, we obtain an estimate for the vertical tail contribution to the side force with respect to roll rate derivative in nondimensional form

$$\frac{\partial C_{y_v}}{\partial\left(\frac{pb}{2U_1}\right)} = \frac{2U_1}{b}\frac{\partial C_{y_v}}{\partial p} = C_{y_{p_v}} \approx C_{y_p} \tag{6.69}$$

Combining Eqs. (6.68) and (6.69), we have

$$C_{y_p} \approx \frac{2U_1}{b}(-C_{L_{\alpha_v}})\left(\frac{z_v}{U_1}\right)\eta_v\frac{S_v}{S}$$

Simplifying and rearranging, we have

$$C_{y_p} \approx -2C_{L_{\alpha_v}}\left(\frac{z_v}{b}\right)\eta_v\frac{S_v}{S} \tag{6.70}$$

C_{y_p} is generally negative; however, at high angles of attack, z_v may become negative as the center of pressure of the vertical tail drops below the x stability axis. For that case, C_{y_p} will be positive.

The final $pb/2U_1$ derivative to be considered is $\partial N_A/\partial(pb/2U_1)$. In a similar manner, we have

$$\frac{\partial N_A}{\partial\frac{pb}{2U_1}} = \frac{\partial C_n \bar{q} S b}{\partial\frac{pb}{2U_1}} = C_{n_p}\bar{q}_1 S b \tag{6.71}$$

C_{n_p} is called a **cross derivative** because it represents the change in yawing moment coefficient (a moment about the z axis) because of a nondimensional roll rate (an angular rate about the x axis). The wing and vertical tail are the primary components that contribute to C_{n_p}. The contribution of the horizontal tail is typically small compared to the wing because of its smaller area.

The wing contributes to C_{n_p} in three ways that will be addressed qualitatively. The first contribution comes from the 1) increase in drag that results from the increase in angle of attack on the wing being rolled into, and 2) decrease on drag that results from the decrease in angle of attack on the wing being rolled away from. For example, a positive right wing down roll rate will increase the angle of attack on the right wing and decrease the angle of attack on the left wing. The increased drag on that results on the right wing and decreased drag that results on the left wing will provide a positive yawing moment to the aircraft, resulting in a positive contribution to C_{n_p}. The second contribution to C_{n_p} results from tilting of the lift vector on each wing because of the change in angle of attack. Recall that lift is defined in a direction perpendicular to the relative wind. For our example, the increase in angle of attack on the right wing results in tilting of the lift vector forward, while the decrease in angle of attack on the left wing provides an aft tilting of the lift vector. The net result is a negative contribution to yawing moment; thus, a

Source from Yechout, T.R. "Introduction to Aircraft Flight Mechanics", AIAA education Series, 2003

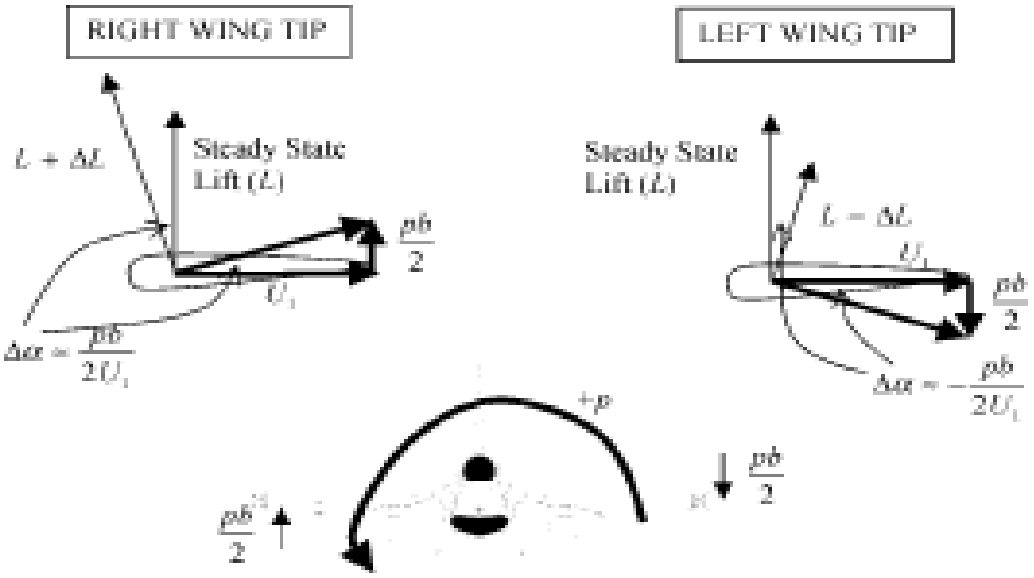

Fig. 6.11 Illustration of lift vector tilting because of roll rate.

negative contribution to C_{n_p}. The lift vector tilting effect is illustrated in Fig. 6.11.

The final contribution may result from an asymmetrical sideforce generated at each wing tip. Again returning to our example with positive roll rate, the right wing experiences higher lift (and lower upper surface pressure) because of the increased angle of attack. Conversely, the left wing experiences a decrease in lift (and higher upper surface pressure) because of the decreased angle of attack. As a result, there is a greater tendency for a positive sideforce to develop at the right wing tip as the flow migrates from the lower surface to the low-pressure upper surface. At the left wing tip, a lower magnitude negative sideforce develops because the pressure on the left wing upper surface is higher (a smaller differential pressure than on the right wing). The net result should be a positive sideforce acting through the right wing tip. If this sideforce acts behind the c.g., a negative yawing moment results and the wing tip sideforce effect makes a negative contribution to C_{n_p} as illustrated in Fig. 6.12. If this sideforce acts in front of the c.g. (unusual), a positive yawing moment results and the wing tip sideforce effect makes a positive contribution to C_{n_p}. The wing tip sideforce effect is most pronounced on low aspect ratio wings (strong wing tip vorticies) with relatively thick wing tips.

The contribution of the vertical tail to C_{n_p} results from the sideforce because of roll rate (F_y) illustrated in Fig. 6.9 and defined by Eq. (6.62). As discussed for a positive roll rate, a negative sideforce at the vertical tail results. This negative sideforce produces a positive yawing moment provided the distance z_v is positive (the case for low to moderate angles of attack). Thus, the contribution of the vertical tail to C_{n_p} is generally positive but may be negative at high angles of attack. If we define x_v as the distance from the c.g. to the aerody-

Source from Yechout, T.R. "Introduction to Aircraft Flight Mechanics", AIAA education Series, 2003

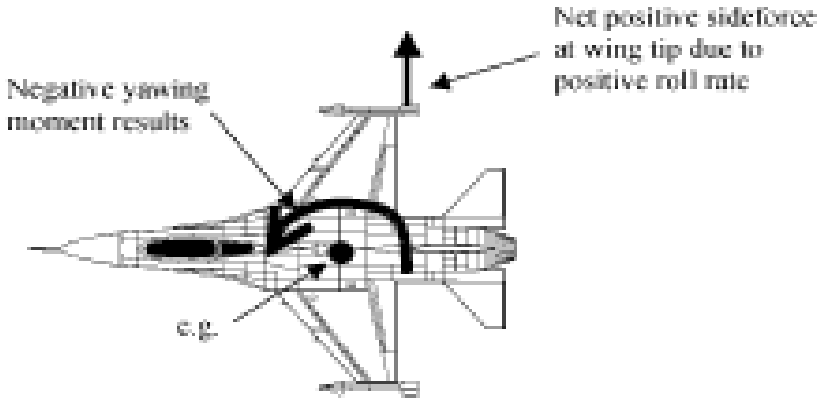

Fig. 6.12 Illustration of wing tip sideforce effect because of positive roll rate.

namic center of the vertical tail, then a similar analysis to that which led to Eq. (6.65) yields an estimate for the vertical contribution to C_{n_p}.

$$C_{n_{p_v}} = 2C_{L_{\alpha_v}}\left(\frac{z_v}{b}\right)\left(\frac{x_v}{b}\right)\eta_v\frac{S_v}{S} \tag{6.72}$$

An estimate for the wing contribution to C_{n_p}, $C_{n_{p_w}}$, developed in some texts[1] using wing strip theory, follows:

$$C_{n_{p_w}} = -\frac{C_L}{8}$$

Two observations may be made regarding this estimate. First, $C_{n_{p_w}}$ is directly proportional to the overall aircraft lift coefficient; second, the estimate assumes that lift vector tilting is the dominant contribution based on the negative sign.

C_{n_p} is one of the more difficult derivatives to estimate because some aircraft components make positive contributions, others make negative contributions, and in some cases the sign of the contribution depends on angle of attack. Fortunately, in most applications C_{n_p} has a relatively small influence on dynamic stability characteristics.

Example 6.9

Find the $pb/2U_1$ derivative $\partial N_A/\partial(pb/2U_1)$ for the F-4C at the same conditions as presented in Example 6.7. C_{n_p} for the F-4C is -0.036. If p is 5 deg/s, find the perturbed yawing moment, n_A.

Starting with Eq. (6.71),

$$\frac{\partial N_A}{\partial\dfrac{pb}{2U_1}} = C_{n_p}\bar{q}_1 Sb = -0.036(283.2)530(38.7) = -209{,}114 \text{ ft} \cdot \text{lb/rad}$$

Source from Yechout, T.R. "Introduction to Aircraft Flight Mechanics", AIAA education Series, 2003

To find n_A, we use Eq. (6.13) for only a roll rate perturbation:

$$n_A = \frac{\partial N_A}{\partial \dfrac{pb}{2U_1}}\left(\frac{pb}{2U_1}\right) = -209.114\left(\frac{(5/57.3)(38.7)}{2(876)}\right) = -403.1 \text{ ft} \cdot \text{lb}$$

Notice that degrees/second are converted to radians/second to maintain consistent units.

6.3.3.4 Yaw rate $rb/2U_1$ derivatives. The $rb/2U_1$ derivatives consist of $\partial L_A/\partial(rb/2U_1)$, $\partial F_{A_y}/\partial(rb/2U_1)$, and $\partial N_A/\partial(rb/2U_1)$ in Eq. (6.13). We begin with $\partial L_A/\partial(rb/2U_1)$.

$$\frac{\partial L_A}{\partial \dfrac{rb}{2U_1}} = \frac{\partial C_l}{\partial \dfrac{rb}{2U_1}}\bar{q}_1 Sb = C_{l_r}\bar{q}_1 Sb \tag{6.73}$$

The derivative C_{l_r} is called a **cross derivative**. It represents the change in rolling moment coefficient (a moment about the x axis) due to nondimensional yaw rate (an angular rate about the z axis). The wing and vertical tail are the primary aircraft components that contribute to C_{l_r}.

The wing contribution to C_{l_r} results from the yaw rate increasing the effective velocity on one wing and decreasing the effective velocity on the opposite wing. For example, a positive nose right yaw rate will provide an angular rate that increases the effective velocity on the left wing and that decreases the effective velocity on the right wing. The increase in velocity results in increased lift on the left wing, and the decrease in velocity results in decreased lift on the right wing. The net result is a positive rolling moment (right wing down). Thus, the wings make a positive contribution to C_{l_r}.

The vertical tail contribution to C_{l_r} results from the change in angle of attack (actually a sideslip angle) experienced by the vertical tail because of yaw rate. For example, for a positive yaw rate, the vertical tail will experience an increase in angle of attack—actually sideslip—($\Delta\alpha_v$) on the left side of the vertical tail, which produces a side force (F_z) in the positive y direction. This is illustrated in Fig. 6.13.

The angle $\Delta\alpha_v$ is the effective sideslip on the vertical tail and may be approximated with the following equation:

$$\Delta\alpha_v \approx \frac{rx_v}{U_1} \tag{6.74}$$

where x_v is the distance from the c.g. to the a.c. of the vertical tail. F_z therefore becomes

$$F_z = C_{L_{\alpha_v}}\Delta\alpha_v \bar{q}_v S_v = C_{L_{\alpha_v}}\left(\frac{rx_v}{U_1}\right)\bar{q}_v S_v \tag{6.75}$$

Source from Yechout, T.R. "Introduction to Aircraft Flight Mechanics", AIAA education Series, 2003

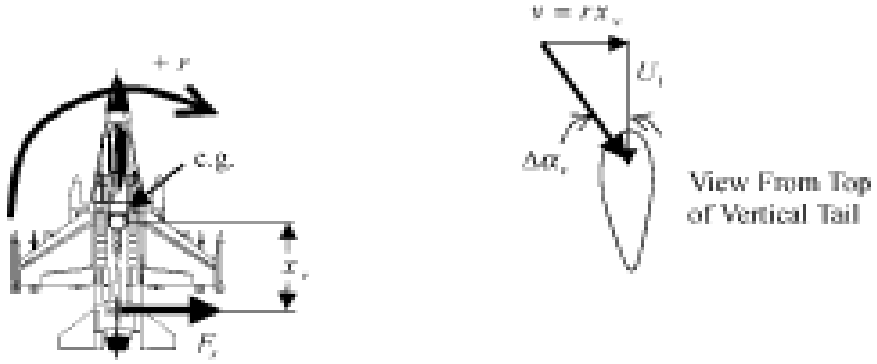

Fig. 6.13 Illustration of sideforce and change in angle of attack at the vertical tail resulting from positive yaw rate.

This sideforce on the vertical tail because of yaw rate also produces a positive rolling moment (L_{A_v}) about the center of gravity because it acts at z_v (see Fig. 6.9) above the c.g. Thus,

$$L_{A_v} = F_v z_v = C_{l_v} \bar{q} S b \tag{6.76}$$

Combining Eqs. (6.75) and (6.76), and solving for C_{l_v}, we have

$$C_{l_v} = C_{L_{\alpha_v}} \left(\frac{r x_v}{U_1}\right) \eta_v \frac{S_v}{S} \left(\frac{z_v}{b}\right) \tag{6.77}$$

Taking the partial derivative of Eq. (6.77) with respect to r,

$$\frac{\partial C_{l_v}}{\partial r} = C_{L_{\alpha_v}} \left(\frac{x_v}{U_1}\right) \eta_v \frac{S_v}{S} \left(\frac{z_v}{b}\right)$$

Finally, we obtain an estimate for the vertical tail contribution to C_{l_r}. In non-dimensional form

$$C_{l_{r_v}} = \frac{\partial C_{l_v}}{\partial\left(\frac{rb}{2U_1}\right)} = \frac{2U_1}{b} \frac{\partial C_{l_v}}{\partial r} = 2C_{L_{\alpha_v}} \left(\frac{x_v z_v}{b^2}\right) \eta_v \frac{S_v}{S} \tag{6.78}$$

As seen from Eq. (6.78), the vertical tail makes a positive contribution to C_{l_r} at low to moderate values of angle of attack where z_v is positive. However, at high angles of attack, z_v may be negative and then the vertical tail contribution to C_{l_r} will be negative. Because the wing contribution normally outweighs the vertical tail contribution to C_{l_r}, C_{l_r} is usually positive for most flight conditions.

Source from Yechout, T.R. "Introduction to Aircraft Flight Mechanics", AIAA education Series, 2003

The next $rb/2U_1$ derivative to be considered is $\partial F_{A_y}/\partial(rb/2U_1)$. We begin with

$$\frac{\partial F_{A_y}}{\partial \dfrac{rb}{2U_1}} = \frac{\partial C_y \bar{q} S}{\partial \dfrac{rb}{2U_1}} = C_{y_r} \bar{q}_1 S \tag{6.79}$$

The vertical tail is the major contributor to C_{y_r} and the preceding analysis to estimate C_{l_r} is appropriate. We begin with the estimate of sideforce on the vertical tail because of roll rate (F_z) defined by Eq. (6.75).

$$F_z = C_{L_{\alpha_v}} \left(\frac{r x_v}{U_1}\right) \bar{q}_v S_v = C_{y_r} \bar{q}_1 S \tag{6.80}$$

Solving for C_{y_r},

$$C_{y_r} = C_{L_{\alpha_v}} \left(\frac{x_v}{U_1}\right) \eta_v \frac{S_v}{S}$$

Taking the partial derivative with respect to r, we have

$$\frac{\partial C_{y_v}}{\partial r} = C_{L_{\alpha_v}} \left(\frac{x_v}{U_1}\right) \eta_v \frac{S_v}{S} \tag{6.81}$$

Finally, C_{y_r} may be obtained in nondimensional form

$$\frac{\partial C_{y_v}}{\partial \left(\dfrac{rb}{2U_1}\right)} = \frac{2U_1}{b} \frac{\partial C_{y_v}}{\partial r} = C_{y_{r_v}} \approx C_{y_r} \tag{6.82}$$

Combining Eqs. (6.81) and (6.82), we have

$$C_{y_r} \approx 2 C_{L_{\alpha_v}} \left(\frac{x_v}{b}\right) \eta_v \frac{S_v}{S} \tag{6.83}$$

C_{y_r} is a positive derivative because a positive yaw rate results in a positive sideforce on the vertical tail.

The final $rb/2U_1$ derivative to be considered is $\partial N_A/\partial(rb/2U_1)$. In a similar manner, we have

$$\frac{\partial N_A}{\partial \dfrac{rb}{2U_1}} = \frac{\partial C_n \bar{q} S b}{\partial \dfrac{rb}{2U_1}} = C_{n_r} \bar{q}_1 S b \tag{6.84}$$

The derivative C_{n_r} is called the **yaw damping derivative**. It represents the change in yawing moment coefficient with respect to nondimensional yaw rate and will always be **negative** (providing a moment which opposes the direction

Source from Yechout, T.R. "Introduction to Aircraft Flight Mechanics", AIAA education Series, 2003

of the yaw rate). C_{n_r} is also an important factor in lateral-directional stability characteristics. The wing and vertical tail are the primary components that contribute to C_{n_r}.

The wing contribution to C_{n_r} results from the yaw rate, increasing the effective velocity on one wing and decreasing the effective velocity on the opposite wing as discussed previously. A positive "nose right" yaw rate will provide an angular rate that increases the effective velocity on the left wing and decreases the effective velocity on the right wing. The increase in velocity results in increased lift and induced drag on the left wing, and the decrease in velocity results in decreased lift and decreased induced drag on the right wing. The net result is a negative yawing moment (nose left). Thus, the wings make a negative contribution to C_{n_r}.

The vertical tail contribution to C_{n_r} results from the sideforce (F_y) on the vertical tail resulting from yaw rate as presented in Eq. (6.75). Referring also to Fig. 6.13, the yawing moment resulting from a positive yaw rate on the aircraft is

$$N_{A_v} = -F_y x_v = C_{n_v} \bar{q} S b \tag{6.85}$$

Combining Eqs. (6.75) and (6.85) and solving for C_{n_v}, we have

$$C_{n_v} = -C_{L_v} \left(\frac{r x_v}{U_1}\right) \eta_v \frac{S_v}{S} \left(\frac{x_v}{b}\right) \tag{6.86}$$

Taking the partial derivative of Eq. (6.86) with respect to r,

$$\frac{\partial C_{n_v}}{\partial r} = -C_{L_v} \left(\frac{x_v}{U_1}\right) \eta_v \frac{S_v}{S} \left(\frac{x_v}{b}\right) \tag{6.87}$$

Finally, C_{n_r} may be obtained in nondimensional form

$$\frac{\partial C_{n_v}}{\partial \left(\frac{rb}{2U_1}\right)} = \frac{2U_1}{b} \frac{\partial C_{n_v}}{\partial r} = C_{n_{r_v}} \tag{6.88}$$

Combining Eqs. (6.87) and (6.88), we have

$$C_{n_{r_v}} = -C_{L_v} \left(\frac{2x_v^2}{b^2}\right) \eta_v \frac{S_v}{S} \tag{6.89}$$

Equation (6.89) provides an estimate of the vertical tail contribution to C_{n_r}, which can also be seen to be negative. For a complete estimate of C_{n_r}, the wing contribution must be added to this estimate.

Example 6.10

Estimate the yaw damping derivative, C_{n_r}, for an aircraft based on the contribution of the vertical tail. The aircraft has the following characteristics

$$C_{L_{\alpha_v}} = 0.08/\text{deg}, \quad \frac{x_v}{b} = 0.6, \quad \eta_v = 0.95, \quad \frac{S_v}{S} = 0.125$$

Starting with Eq. (6.89),

$$C_{n_{r_v}} = -C_{L_{\alpha_v}} \left(\frac{2x_v^2}{b^2}\right) \eta_v \frac{S_v}{S} = (-0.08)(57.3)2(0.6)^2(0.95)(0.125)$$

$$C_{n_{r_v}} = -0.392$$

Notice that $C_{L_{\alpha_v}}$ has been converted to "per radian" to keep consistent units.

6.3.3.5 δ_a derivatives. The δ_a derivatives consist of $\partial L_A/$, $\partial F_{A_y}/\partial\delta_a$, and $\partial N_A/\partial\delta_a$ in Eq. (6.13). Using a similar development to that for the previous derivatives, we have

$$\frac{\partial L_A}{\partial \delta_a} = \frac{\partial C_l}{\partial \delta_a} \bar{q}_1 Sb = C_{l_{\delta_a}} \bar{q}_1 Sb \tag{6.90}$$

$C_{l_{\delta_a}}$ is a **primary control derivative** and is also called the **aileron control power**. It was discussed in Sec. 5.5.2.2. The sign of $C_{l_{\delta_a}}$ is **positive** with our sign convention. Thus, a positive aileron deflection (normally right aileron trailing edge up/left aileron trailing edge down) will produce a positive rolling moment.

$\partial F_{A_y}/\partial\delta_a$ is developed in a similar manner.

$$\frac{\partial F_{A_y}}{\partial \delta_a} = \frac{\partial C_y}{\partial \delta_a} \bar{q}_1 S = C_{y_{\delta_a}} \bar{q}_1 S \tag{6.91}$$

$C_{y_{\delta_a}}$ is the change in sideforce coefficient resulting from an aileron deflection. It generally has a negligible value. It may have a negative value for situations where differential horizontal tail is used to generate rolling moment as discussed in Sec. 5.5.1.

Finally, the development of $\partial N_A/\partial\delta_a$ follows the same approach.

$$\frac{\partial N_A}{\partial \delta_a} = \frac{\partial C_n}{\partial \delta_a} \bar{q}_1 Sb = C_{n_{\delta_a}} \bar{q}_1 Sb \tag{6.92}$$

$C_{n_{\delta_a}}$ is a **cross-control derivative** that was discussed in Sec. 5.5.3.2. If it is positive, the aircraft exhibits proverse yaw. More typically, it is negative, indicating that adverse yaw is generated as a result of an aileron input.

Source from Yechout, T.R. "Introduction to Aircraft Flight Mechanics", AIAA education Series, 2003

6.3.3.6 δ_r derivatives. The δ_r derivatives are $\partial L_A/\partial\delta_r$, $\partial F_{A_y}/\partial\delta_r$, and $\partial N_A/\partial\delta_r$ in Eq. (6.13). Using the same approach as with the δ_a derivatives,

$$\frac{\partial L_A}{\partial \delta_r} = \frac{\partial C_l}{\partial \delta_r}\bar{q}_1 Sb = C_{l_{\delta_r}}\bar{q}_1 Sb \tag{6.93}$$

$C_{l_{\delta_r}}$ is a **cross-control derivative** that was discussed in Sec. 5.5.2.3. It is usually positive because the rudder is normally above the x-body axis.

$\partial F_{A_y}/\partial\delta_r$ is developed in a similar manner.

$$\frac{\partial F_{A_y}}{\partial \delta_r} = \frac{\partial C_y}{\partial \delta_r}\bar{q}_1 S = C_{y_{\delta_r}}\bar{q}_1 S \tag{6.94}$$

$C_{y_{\delta_r}}$ is the change in sideforce coefficient resulting from a rudder deflection. It was discussed in Sec. 5.5.1. and generally has a positive value because a positive rudder deflection will generate a sideforce along the positive y axis.

Finally, the development of $\partial N_A/\partial\delta_r$ follows the same approach.

$$\frac{\partial N_A}{\partial \delta_r} = \frac{\partial C_n}{\partial \delta_r}\bar{q}_1 Sb = C_{n_{\delta_r}}\bar{q}_1 Sb \tag{6.95}$$

$C_{n_{\delta_r}}$ is a **primary control derivative** and is also called the **rudder control power**. It was discussed in Sec. 5.5.3.3. The sign of $C_{n_{\delta_r}}$ is **negative** with our sign convention. Thus, a positive rudder deflection (trailing edge left) will produce a negative yawing moment.

6.3.3.7 Summary. We now define the lateral-directional forces and moments from Eq. (6.13) using the derivatives developed in Secs. 6.3.3.1–6.3.3.6. This recasting of the equations will use matrix format and Eqs. (6.54–6.60), (6.66), (6.71), (6.73), (6.79), (6.84), and (6.90–6.95), resulting in

$$\begin{bmatrix} \dfrac{l_A}{\bar{q}_1 Sb} \\ \dfrac{f_{A_y}}{\bar{q}_1 S} \\ \dfrac{n_A}{\bar{q}_1 Sb} \end{bmatrix} = \begin{bmatrix} C_{l_\beta} & C_{l_{\dot\beta}} & C_{l_p} & C_{l_r} & C_{l_{\delta_a}} & C_{l_{\delta_r}} \\ C_{y_\beta} & C_{y_{\dot\beta}} & C_{y_p} & C_{y_r} & C_{y_{\delta_a}} & C_{y_{\delta_r}} \\ C_{n_\beta} & C_{n_{\dot\beta}} & C_{n_p} & C_{n_r} & C_{n_{\delta_a}} & C_{n_{\delta_r}} \end{bmatrix} \begin{bmatrix} \beta \\ \dfrac{\dot\beta b}{2U_1} \\ \dfrac{pb}{2U_1} \\ \dfrac{rb}{2U_1} \\ \delta_a \\ \delta_r \end{bmatrix} \tag{6.96}$$

Source from Yechout, T.R. "Introduction to Aircraft Flight Mechanics", AIAA education Series, 2003

Table 6.2 Summary of lateral-directional derivatives

Derivative	Name	Normal sign
C_{l_β}	Lateral static stability derivative	−
C_{Y_β}	None	−
C_{n_β}	Directional static stability derivative	+
$C_{l_{\dot\beta}}$	Quasi-steady derivative	≈ 0
$C_{Y_{\dot\beta}}$	Quasi-steady derivative	≈ 0
$C_{n_{\dot\beta}}$	Quasi-steady derivative	≈ 0
C_{l_p}	Roll damping derivative	−
C_{Y_p}	None	−
C_{n_p}	Cross derivative	+ or −
C_{l_r}	Cross derivative	+
C_{Y_r}	None	+
C_{n_r}	Yaw damping derivative	−
$C_{l_{\delta_a}}$	Aileron control power	+
$C_{Y_{\delta_a}}$	None	≈ 0
$C_{n_{\delta_a}}$	Cross control derivative (proverse or adverse yaw)	+ or −
$C_{l_{\delta_r}}$	Cross control derivative	+
$C_{Y_{\delta_r}}$	None	+
$C_{n_{\delta_r}}$	Rudder control power	−

The advantage of Eq. (6.96) over Eq. (6.13) is that the lateral-directional perturbed forces and moments are now expressed in terms of common "aero" derivatives such as C_{l_β}, $C_{Y_{\delta_a}}$, and C_{n_r}. The value of these derivatives can be estimated with analytical or experimental techniques. Remember that each derivative in Eq. (6.96) is dimensionless—for example, C_{n_r} is the abbreviated form of $\partial C_n/\partial(rb/2U_1)$. Table 6.2 summarizes the derivatives discussed for the perturbed lateral-directional force and moment estimates.

6.4 First-Order Approximation of Perturbed Thrust Forces and Moments

We will now focus on the perturbed thrust force and moment terms (such as f_{T_x} and m_T) in Eqs. (6.6) and (6.7). These represent the perturbed change in a thrust force or moment that results from a nonzero value of a perturbation variable like u. We begin with the assumption that these perturbed thrust terms are only a function of u, $\dot{\alpha}$, and β, which is generally the case but does neglect effects from p, q, r, $\dot{\alpha}$, $\dot{\beta}$, and the control deflections. The longitudinal perturbed thrust forces and moment can thus be represented using a Taylor

Source from Yechout, T.R. "Introduction to Aircraft Flight Mechanics", AIAA education Series, 2003

series and the nondimensional perturbed longitudinal variables (defined along the x, y, and z stability axis) as

$$f_{T_x} = \frac{\partial F_{T_x}}{\partial\left(\frac{u}{U_1}\right)}\left(\frac{u}{U_1}\right) + \frac{\partial F_{T_x}}{\partial \hat{\alpha}}\hat{\alpha} \tag{6.97}$$

$$m_T = \frac{\partial M_T}{\partial\left(\frac{u}{U_1}\right)}\left(\frac{u}{U_1}\right) + \frac{\partial M_T}{\partial \hat{\alpha}}\hat{\alpha} \tag{6.98}$$

$$f_{T_z} = \frac{\partial F_{T_z}}{\partial\left(\frac{u}{U_1}\right)}\left(\frac{u}{U_1}\right) + \frac{\partial F_{T_z}}{\partial \hat{\alpha}}\hat{\alpha} \tag{6.99}$$

The longitudinal thrust forces and moment can be expressed in coefficient form as

$$F_{T_x} = C_{T_x}\bar{q}_1 S \tag{6.100}$$

$$M_T = C_{m_T}\bar{q}_1 S\bar{c} \tag{6.101}$$

$$F_{T_z} = C_{T_z}\bar{q}_1 S \tag{6.102}$$

The lateral-directional perturbed thrust force and moments can be represented in a similar manner as a function of β

$$l_T = \frac{\partial L_T}{\partial \beta}\beta \tag{6.103}$$

$$f_{T_y} = \frac{\partial F_{T_y}}{\partial \beta}\beta \tag{6.104}$$

$$n_T = \frac{\partial N_T}{\partial \beta}\beta \tag{6.105}$$

The lateral-directional thrust force and moments can be expressed in coefficient form as

$$L_T = C_{l_T}\bar{q}_1 Sb \tag{6.106}$$

$$F_{T_y} = C_{T_y}\bar{q}_1 S \tag{6.107}$$

$$N_T = C_{n_T}\bar{q}_1 Sb \tag{6.108}$$

6.4.1 Longitudinal Perturbed Thrust Force and Moment Derivatives

We will next analyze each of the partial derivative terms in Eqs. (6.97–6.99) so that they may be expressed with common thrust coefficient derivatives.

Source from Yechout, T.R. "Introduction to Aircraft Flight Mechanics", AIAA education Series, 2003

6.4.1.1 u/U_1 derivatives. The u/U_1 derivatives consist of $\partial F_{T_x}/\partial(u/U_1)$, $\partial M_T/\partial(u/U_1)$, and $\partial F_{T_z}/\partial(u/U_1)$ in Eqs. (6.97–6.99). We will begin with $\partial F_{T_x}/\partial(u/U_1)$. F_{T_x} is defined along the body-fixed stability x axis as discussed in Secs. 6.3.2. and 6.3.2.1. Using a similar approach as that for $\partial F_{A_x}/\partial(u/U_1)$ in Sec. 6.3.2.1, we have

$$\frac{\partial F_{T_x}}{\partial \dfrac{u}{U_1}} = \frac{\partial C_{T_x}}{\partial \dfrac{u}{U_1}} \bar{q} S + C_{T_x} S \left(\frac{\partial \bar{q}}{\partial \dfrac{u}{U_1}} \right) = C_{T_{x_u}} \bar{q}_1 S + 2 C_{T_{x_1}} \bar{q}_1 S \tag{6.109}$$

In comparing Eq. (6.109) to Eq. (6.19), notice the similarities with the exception of the negative sign in Eq. (6.19). This results because drag is defined as positive in the negative x direction while thrust is defined as positive in the positive x direction. For gliders or power-off flight, $C_{T_{x_u}}$ and $C_{T_{x_1}}$ are equal to zero and thus $\partial F_{T_x}/\partial(u/U_1)$ becomes zero. Estimates of $C_{T_{x_u}}$ and $C_{T_{x_1}}$ for powered cases are dependent of the type of propulsion system used in the aircraft.

The next u/U_1 derivative to be considered is $\partial M_T/\partial(u/U_1)$. Using a similar approach as that for $\partial M_A/\partial(u/U_1)$ in Sec. 6.3.2.1, we have

$$\frac{\partial M_T}{\partial \dfrac{u}{U_1}} = C_{m_{T_u}} \bar{q}_1 S \bar{c} + C_{m_{T_1}} S \bar{c} (2 \bar{q}_1) \tag{6.110}$$

and, in combined form

$$\frac{\partial M_T}{\partial \dfrac{u}{U_1}} = (C_{m_{T_u}} + 2 C_{m_{T_1}}) \bar{q}_1 S \bar{c} \tag{6.111}$$

For steady-state trimmed flight, the total pitching moment acting on the aircraft should be zero. Thus, the sum of the steady-state thrust pitching moment and steady-state aerodynamic pitching moment [referring to Eq. (6.22)] should be

$$C_{m_{T_1}} + C_{m_1} = 0 \qquad @ \text{ trim} \tag{6.112}$$

Combining Eqs. (6.22), (6.111), and (6.112), we have

$$\frac{\partial (M_A + M_T)}{\partial \dfrac{u}{U_1}} = (C_{m_u} + C_{m_{T_u}}) \bar{q}_1 S \bar{c} \tag{6.113}$$

The derivative $C_{m_{T_u}}$ has a negligible value for situations where the thrust vector passes through the center of gravity.

Source from Yechout, T.R. "Introduction to Aircraft Flight Mechanics", AIAA education Series, 2003

UNIT –V

AIRCRAFT DYNAMIC STABILITY

Introduction

Aircraft dynamic stability focuses on the time history of aircraft motion after the aircraft is disturbed from an equilibrium or trim condition. This motion may be first order (exponential response) or second order (oscillatory response), and will have either positive dynamic stability (aircraft returns to the trim condition as time goes to infinity), neutral dynamic stability (aircraft neither returns to trim nor diverges further from the disturbed condition), or dynamic instability (aircraft diverges from the trim condition and the disturbed condition as time goes to infinity). The study of dynamic stability is important to understanding aircraft handling qualities and the design features that make an airplane fly well or not as well while performing specific mission tasks. The differential equations that define the aircraft equations of motion (EOM) form the starting point for the study of dynamic stability.

Mass–Spring–Damper System and Classical Solutions of Ordinary Differential Equations

The mass–spring–damper system illustrated in Fig. 5.1 provides a starting point for analysis of system dynamics and aircraft dynamic stability. This is an excellent model to begin the understanding of dynamic response.

We will first develop an expression for the sum of forces in the vertical direction. Notice that xðtÞ is defined as positive for an upward displacement and that the zero position is chosen as the point where the system is initially at rest or at equilibrium. We know that

$$\sum F_x = m\frac{d^2x}{dt^2} \quad \text{----------5.1}$$

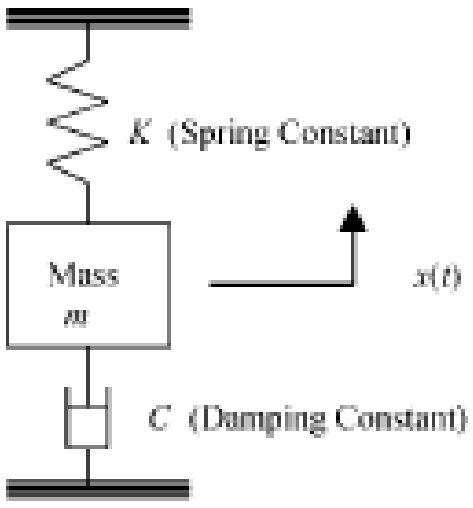

Fig 5.1 Mass–spring–damper system

Source from Yechout, T.R. "Introduction to Aircraft Flight Mechanics", AIAA education Series, 2003

There are two forces acting on the mass, the damping force, and the spring force. For the damping or frictional force (Ff), this can be approximated by a linear relationship of damping force as a function of velocity or dx=dt (see Fig. 5.2). A damper can be thought of as a ‘‘shock absorber’’ with a piston moving up and down inside a cylinder. The piston is immersed in a fluid and the fluid is displaced through a small orifice to provide a resistance force directly proportional to the velocity of the piston. This resistance force (Ff) can be expressed as

$$F_f = CV$$

where C is the slope in Fig. 5.2. The spring force (F_s) is directly proportional to the displacement (x) of the mass and can be represented as

$$F_s = Kx$$

where K is the spring constant. If the mass is displaced in the positive x direction, both the damping and spring forces act in a direction opposite to this displacement and can be represented by

$$F_f + F_s = -CV - Kx \qquad \text{----5.2}$$

$$V = \frac{dx}{dt} \qquad \text{-------5.3}$$

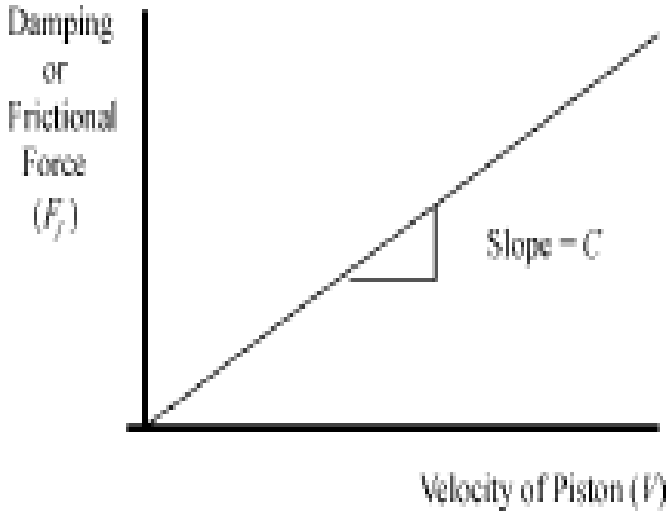

Fig. 5.2 Damper relationship

Source from Yechout, T.R. “Introduction to Aircraft Flight Mechanics”, AIAA education Series, 2003

$$m\left(\frac{d^2x}{dt^2}\right) = -C\left(\frac{dx}{dt}\right) - Kx$$

$$m\left(\frac{d^2x}{dt^2}\right) + C\left(\frac{dx}{dt}\right) + Kx = 0 \qquad \text{---5.4}$$

which is the differential equation for the mass–spring–damper system with zero initial displacement (x = 0). If we initially stretch the spring from its original position by a distance y as shown in Fig. 5.3, we build in a forcing function that must be added to Eq. (5.4). Because the upper ‘‘tie down’’ point is moved up by a distance y to achieve this stretch or preload, the preload has a positive sign and a magnitude of Ky. It can be conveniently added to the right side of Eq. (5.4) to obtain

$$m\left(\frac{d^2x}{dt^2}\right) + C\left(\frac{dx}{dt}\right) + Kx = Ky \qquad \text{---5.5}$$

This is the differential equation for the spring–mass–damper system with a preload as shown. At this point, we should observe that if the mass is free to move, it will obtain a steady-state condition (a new equilibrium location) when d2x=dt2 and dx=dt equal zero; and the new equilibrium position will be x = y. Now that the differential equation for the spring–mass–damper system has been defined, we will review classical approaches to solving ordinary differential equations of this type. Keep in mind that Eq. (5.5) is also representative of aircraft motion and that is why we are investigating it in depth.

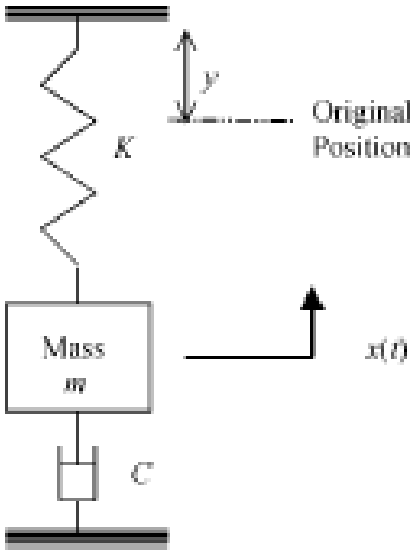

Fig.5.3. Adding a forcing function to the spring–mass–damper system

First-Order Systems

Source from Yechout, T.R. “Introduction to Aircraft Flight Mechanics”, AIAA education Series, 2003

A special case of Eq. (5.5), which we will consider first, addresses a spring–mass–damper system where the mass is very small or negligible compared to the size of the spring and damper. We will call such a system a massless or first-order (referring to the order of the highest derivative) system. The following differential equation results when the mass is set equal to zero.

$$C\left(\frac{dx}{dt}\right) + Kx = Ky \qquad \text{-----5.6}$$

To solve this differential equation, we will first describe the method of differential operators where P is defined as the differential operator, d/dt, so that

$$Px = \frac{dx}{dt} \qquad P^2x = \frac{d^2x}{dt^2} \qquad \frac{x}{P} = \int x\,dt$$

We will first attack the homogeneous form (forcing function equal to zero) of Eq. (5.6),

$$C\left(\frac{dx}{dt}\right) + Kx = 0 \qquad \text{-----5.7}$$

Substituting in the differential operator, P, Eq. (5.7) becomes

$$CPx + Kx = 0$$

We then solve for P, which now becomes a root of the equation,

$$(CP + K)x = 0$$
$$P = -(K/C)$$

The homogeneous solution is then of the form

$$x(t) = C_1 e^{Pt} = C_1 e^{(-K/C)t} \qquad \text{----7.8}$$

where C1 is determined from initial conditions. The homogeneous solution will also be called the transient solution when we are dealing with aircraft response.

Example 5.1

Source from Yechout, T.R. "Introduction to Aircraft Flight Mechanics", AIAA education Series, 2003

Solve the following first-order differential equation

$$\frac{dx}{dt} + 2x = 0$$

subjected to the following initial condition: x(0) = 1

Solution:

$$Px + 2x = 0$$
$$(P + 2)x = 0$$
$$P = -2$$
$$x(t) = C_1 e^{-2t}$$

Using the initial condition $x(0) = 1$ to evaluate C_1

$$1 = C_1$$

and

$$x(t) = e^{-2t}$$

is the solution, or time response.

The solution is graphed in Fig. 5.4. Notice that it starts off at a value of one at time equal to zero and exponentially decays to zero. It is also important to note that a first-order system has a first order or exponential transient response (no oscillations). Next, we will look at solving a first-order nonhomogeneous differential equation like Eq. (5.6). A forcing function is included with a nonhomogeneous differential equation and the solution is called the nonhomogeneous or particular solution. It is also called the steady-state solution when we are dealing with aircraft response. To achieve a solution using differential operators, we must assume a form of the solution based on the form of the forcing function as outlined in Table 5.1. The first step in solving a nonhomogeneous differential equation involves setting the forcing function to zero and obtaining the homogeneous solution. Next, the appropriate assumed solution is input into the nonhomogeneous
differential equation so that the constants A, B, C, (as appropriate) can be determined and the nonhomogeneous solution defined. Finally, the homogeneous and nonhomogeneous are added together to obtain the total solution. Example 5.2 will help clarify these steps.

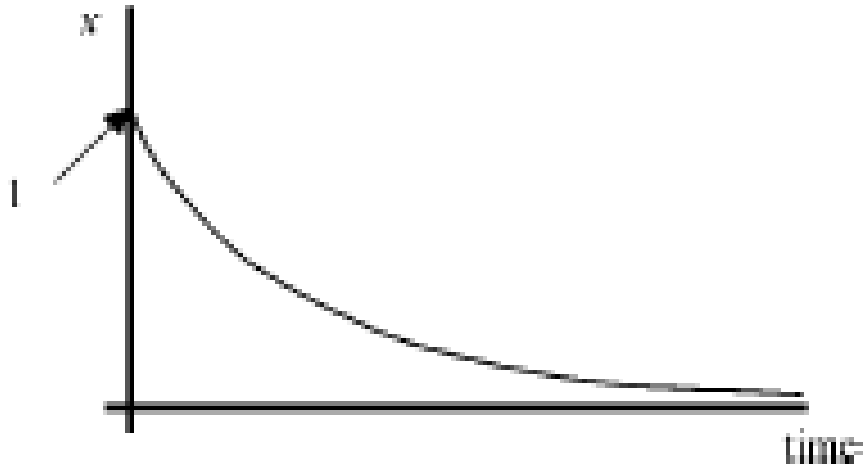

Fig. 5.4 Transient time response of a first-order differential equation

Table 5.1 Assumed solutions for nonhomogeneous differential equations

Forcing function	Assumed solution
K	A
Kt	$At + B$
Kt^2	$At^2 + Bt + C$
$K \sin wt$	$A \sin wt + B \cos wt$

EXAMPLE 5.2

Source from Yechout, T.R. "Introduction to Aircraft Flight Mechanics", AIAA education Series, 2003

Solve the following first-order differential equation:

$$2\frac{dx}{dt} + 3x = 6$$

subject to the following initial condition: $x(0) = 0$

Homogeneous (Transient) Solution:

$$2Px + 3x = 0$$
$$(2P + 3)x = 0$$
$$P = -3/2$$
$$x_h(t) = C_1 e^{(-3/2)t}$$

(Homogeneous Solution)

Nonhomogeneous (Steady-State) Solution:

Assume a steady-state solution of the form $x(t) = A$ because the forcing function is a constant.

Substitute $x_{nh}(t) = A$ into the original differential equation:

$$2(0) + 3A = 6$$
$$A = 2$$

And the nonhomogeneous solution is:

$$x_{nh}(t) = 2$$

The forcing function should be thought of as a constant equal to 2 with the 6 on the right-hand side of the differential equation being equal to the spring constant ($K = 3$) times the forcing function.

The total solution is the combination of the homogeneous and nonhomogeneous solutions:

$$x(t) = x_h(t) + x_{nh}(t) = C_1 e^{(-3/2)t} + 2$$

To evaluate the constant C_1, we use the initial condition $x(0) = 0$

$$0 = C_1 + 2$$
$$C_1 = -2$$

and

$$x(t) = -2e^{(-3/2)t} + 2$$

or

$$x(t) = 2(1 - e^{(-3/2)t})$$

becomes the total solution.

Time constant

Source from Yechout, T.R. "Introduction to Aircraft Flight Mechanics", AIAA education Series, 2003

We will next introduce the important concept of Time Constant (t). If we return to Eq. (7.6) and solve it in general form for an initial condition of xð0Þ ¼ 0, we obtain

$$x(t) = y(1 - e^{(-K/C)t})$$

Figure 5.6 presents a graph of the time response. Notice that the steady-state value is y, which equates to the value of the displacement of the forcing function. We will begin referring to a constant forcing function as a step input. Notice also the exponential rise to achieve the steady-state value. The lag time associated with this rise to the steady-state value is an important consideration in determining the acceptability of the response from an aircraft handling qualities standpoint. This lag time is typically quantified with the time constant (t),

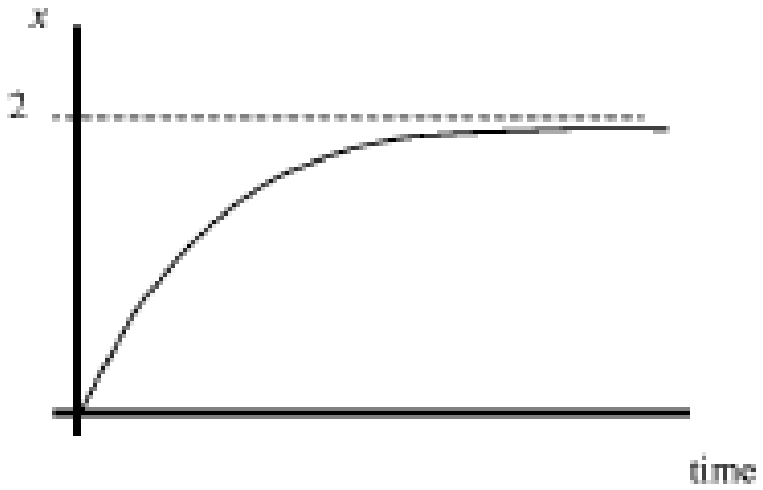

Fig.5.5. Time response for example 5.2

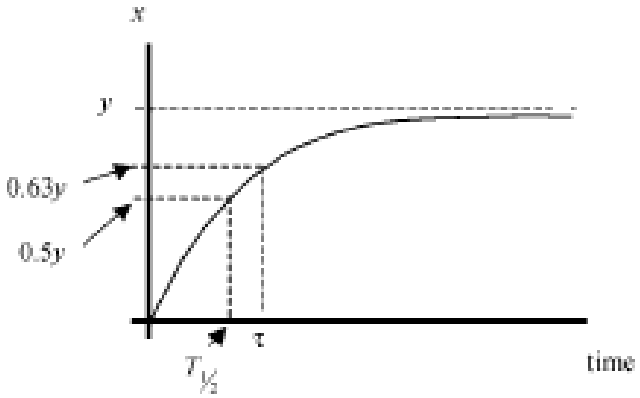

Fog 5.5 Generalized response of first order system

Time to half and double amplitude

Source from Yechout, T.R. "Introduction to Aircraft Flight Mechanics", AIAA education Series, 2003

Another measure of the lag time associated with a systems response is the time to half amplitude (T1=2). Referring to Fig. 5.6, this is simply the time it takes to achieve 50% of the steady state value. It can be easily shown that

$$T_{1/2} = \tau(\ln 2) = 0.693\tau$$

------5.10

For unstable first order systems (P > 0), a measure used as an indication of the instability is the time to double amplitude (T2). T2 is the time it takes for the response to achieve twice the amplitude of an input disturbance. It can be found using

$$T_2 = \frac{\ln 2}{P} = \frac{0.693}{P}$$

---5.11

Source from Yechout, T.R. "Introduction to Aircraft Flight Mechanics", AIAA education Series, 2003

7.1.2 Second-Order Systems

We now return to Eq. (7.5) in its entirety for a spring–mass–damper system where the mass provides significant inertial effects. Equation (7.5) is a second-order differential equation (referring to the highest-order derivative) or simply a second-order system. It becomes

$$M\ddot{x} + C\dot{x} + Kx = Ky$$

or

$$\ddot{x} + \frac{C}{M}\dot{x} + \frac{K}{M}x = \frac{K}{M}y \tag{7.12}$$

To solve Eq. (7.12), we will again use the method of differential operators on the homogeneous differential equation to obtain the transient solution or transient response.

$$(MP^2 + CP + K)x = 0$$

We can then solve for the roots (P) of this equation using the quadratic formula.

$$P_{1,2} = -\frac{C}{2M} \pm \frac{\sqrt{C^2 - 4KM}}{2M}$$

Three cases must be considered based on the sign of the expression under the radical.

Case 1: Two Real Unequal Roots or $C^2 > 4KM$

This results in an **overdamped** system (no oscillations) with a general solution of the form

$$x(t) = C_1 e^{P_1 t} + C_2 e^{P_2 t} \tag{7.13}$$

The constants C_1 and C_2 must be evaluated based on the initial conditions.

Case 2: Two Real Repeated Roots or $C^2 = 4KM$

This results in a **critically damped** system (no oscillations) with a general solution of the form

$$x(t) = C_1 e^{Pt} + C_2 t e^{Pt} \tag{7.14}$$

Again, the constants C_1 and C_2 must be evaluated based on initial conditions.

Source from Yechout, T.R. "Introduction to Aircraft Flight Mechanics", AIAA education Series, 2003

Case 3: Two Complex Conjugate Roots or $4KM > C^2$
This results in an **underdamped** (with oscillations) system. The roots are

$$P_{1,2} = -\frac{C}{2M} \pm i\frac{\sqrt{4KM - C^2}}{2M} = a \pm ib$$

and the general solution is of the form

$$x(t) = e^{at}[C_1 \sin bt + C_2 \cos bt]$$

or

$$x(t) = C_3 e^{at} \sin(bt + \phi) \tag{7.15}$$

where

$$|C_3| = \sqrt{C_1^2 + C_2^2}$$

and

$$\phi = \tan^{-1}\left(\frac{C_2}{C_1}\right)$$

Notice in Eq. (7.15) that the real part of the root (a) determines the exponential decay (damping) portion of the time response and that the imaginary part of the root (b) is the frequency of the oscillation. The **phase angle** (ϕ) can be thought of for now as a lag between an input and output. Case 3 is typical of three dynamic modes of motion for most aircraft (the short period, the phugoid, and the dutch roll modes), which we will discuss in detail later.

7.1.2.1 Damping ratio and natural frequency. We can recast Eq. (7.12) in terms of two new parameters: damping ratio (ζ) and natural frequency (ω_N). These parameters have physical meaning for Case 3 and lead directly to the time solution for common inputs such as steps and impulses.

$$\ddot{x} + 2\zeta\omega_N\dot{x} + \omega_N^2 x = \omega_N^2 y \tag{7.16}$$

The damping ratio provides an indication of the system damping and will fall between -1 and 1 for Case 3. For stable systems, the damping ratio will be between 0 and 1. For this case, the higher the damping ratio, the more damping is present in the system. Figure 7.7 presents a family of second order responses to a unit step ($y = 1$) input, which show the influence of damping ratio. Notice that the number of overshoots/undershoots varies inversely with the damping ratio.

The natural frequency is the frequency (in rad/s) that the system would oscillate at if there were no damping. It represents the highest frequency that

Source from Yechout, T.R. "Introduction to Aircraft Flight Mechanics", AIAA education Series, 2003

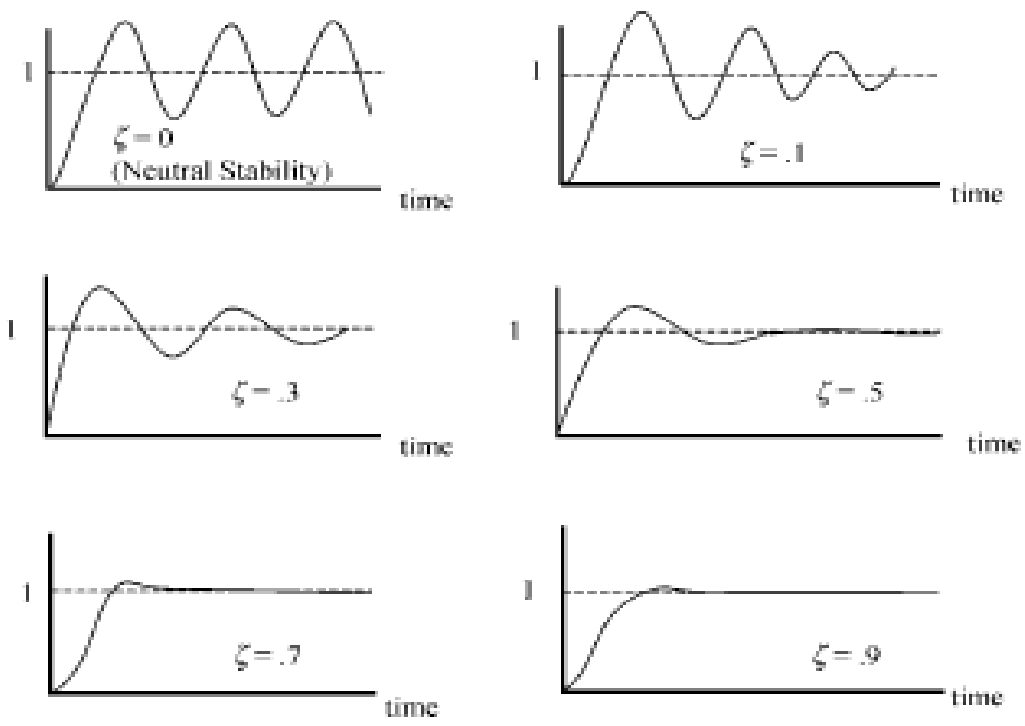

Fig. 7.7 Unit step responses for different damping ratios.

the system is capable of, but it is not the frequency that the system actually oscillates at if damping is present. For the mass–spring–damper system, $\omega_N = \sqrt{K/M}$.

7.1.2.2 Damped frequency. The damped frequency (ω_D) represents the frequency (in rad/s) that the system actually oscillates at with damping present. Returning to Eq. (7.16), we can use the quadratic formula to solve for the roots of the homogeneous form of the equation.

$$P_{1,2} = -\zeta\omega_N \pm i\omega_N\sqrt{1-\zeta^2} = -\zeta\omega_N \pm i\omega_D = a \pm ib \tag{7.17}$$

where

$$\omega_D = \omega_N\sqrt{1-\zeta^2} = \text{Damped Frequency} \tag{7.18}$$

7.1.2.3 Time constant. The time constant (τ) for a second order system can be found by examining the real part of the roots ($-\zeta\omega_n$) in Eq. (7.17) and recalling our discussion in Sec. 7.1.1.1. The time constant (τ) for the generalized

Source from Yechout, T.R. "Introduction to Aircraft Flight Mechanics", AIAA education Series, 2003

case of Eq. (7.16) becomes

$$\tau = \frac{1}{\zeta\omega_N} \tag{7.19}$$

This is similar to the way we computed the time constant for a first-order system ($\tau = -1/P$). Notice that the larger the $\zeta\omega_N$, the smaller τ and the faster the response.

7.1.2.4 Period of oscillation. The period of oscillation (T) for a second-order system is the time it takes between consecutive peaks of an oscillation. The period is inversely proportional to the damped frequency and is defined by

$$T = \frac{2\pi}{\omega_D} \tag{7.20}$$

where ω_D must be in units of radians/second.

The time response for the homogeneous case of Eq. (7.16) is

$$x(t) = C_3 e^{-\zeta\omega_N t}\sin(\omega_D t + \phi) \tag{7.21}$$

Figure 7.8 illustrates this response. The system has been initially disturbed by an impulse input (which may be thought of as a very short duration spike input that excites the system dynamics). The figure also illustrates several of the concepts just discussed.

The steady-state (nonhomogeneous) solution will be defined next for Eq. (7.16). Because the forcing function, $\omega_n^2 y$, is a constant we can assume the form of the solution as

$$x_{SS}(t) = A$$

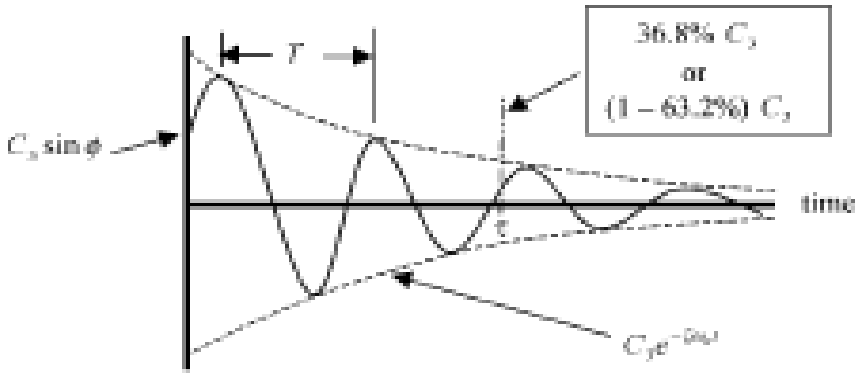

Fig. 7.8 Second-order time response.

Source from Yechout, T.R. "Introduction to Aircraft Flight Mechanics", AIAA education Series, 2003

Therefore,

$$\frac{d^2A}{dt^2} = 0, \quad \frac{dA}{dt} = 0 \Rightarrow 0 + 0 + \omega_N^2 x = \omega_N^2 y$$

and

$$A = y$$

We will assume a unit step input ($y = 1$) in most cases so the particular (steady solution) is

$$x_{SS}(t) = 1$$

The total solution then becomes

$$x(t) = x_{\text{transient}}(t) + x_{SS}(t)$$

or

$$x(t) = 1 + C_3 e^{-\zeta\omega_N t} \sin(\omega_D t + \phi) \tag{7.22}$$

Please note that the C_3 in Eq. (7.22) will typically not have the same value as the C_3 in Eq. (7.15).

Example 7.3

Find the time solution for the following differential equation:

$$\ddot{x} + 5\dot{x} + 25x = 25$$

First, we apply the generalized form for a second-order differential equation Eq. (7.16):

$$\ddot{x} + 2\zeta\omega_N\dot{x} + \omega_N^2 x = \omega_N^2 y$$

The first thing we notice is the unit step input ($y = 1$). Next, we can determine the values of natural frequency, damping ratio, and damped frequency:

$$\omega_N = \sqrt{25} = 5 \text{ rad/s} \qquad 2\zeta\omega_N = 5 \Rightarrow \zeta = 0.5$$

$$\omega_D = \omega_N\sqrt{1 - \zeta^2} = 4.33 \text{ rad/s}$$

We can then input these values into the generalized solution from Eq. (7.20) for a second-order differential equation with a unit step input:

$$x(t) = 1 + C_3 e^{-2.5t} \sin(4.33t + \phi)$$

Source from Yechout, T.R. "Introduction to Aircraft Flight Mechanics", AIAA education Series, 2003

We still need to determine C_3 and ϕ, which can be evaluated from initial conditions and a relationship that we will develop in the next section for ϕ.

7.2 Root Representation Using the Complex Plane

The roots of Eq. (7.16) were presented in Eq. (7.17) and are repeated here.

$$P_{1,2} = -\zeta\omega_N \pm i\omega_D = a \pm ib$$

These roots can be represented on a complex plane as shown in Fig. 7.9. The complex plane plots the real part of the root on the horizontal axis and the imaginary part of the root on the vertical axis.

From trigonometry

$$\cos\phi = \frac{|-\zeta\omega_N|}{r} = \frac{|-\zeta\omega_N|}{\omega_N} = \zeta$$

so

$$\zeta = \cos\phi$$

or

$$\phi = \cos^{-1}\zeta \tag{7.23}$$

It is good to keep ϕ in units of radians, as we will soon see. Also

$$\tan\phi = \frac{\omega_N\sqrt{1-\zeta^2}}{|-\zeta_N|} = \frac{\sqrt{1-\zeta^2}}{\zeta}$$

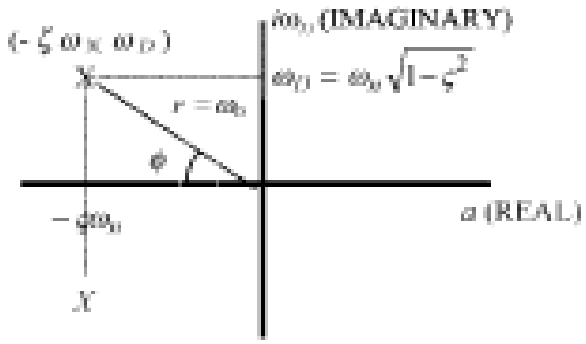

ϕ is the same ϕ used in the phase angle solution of Eq. (7.21) and (7.22).

Fig. 7.9 Root representation using the complex plane.

Source from Yechout, T.R. "Introduction to Aircraft Flight Mechanics", AIAA education Series, 2003

Therefore, if we know ζ we can find ϕ for Eqs. (7.21) and (7.22). This leaves only C_3 to be evaluated. To do this we can assume the initial conditions of $x(0) = \dot{x}(0) = 0$, and use Eq. (7.22).

$$x(0) = 1 + C_3(1)\sin\phi = 0$$

to obtain

$$C_3 = -\frac{1}{\sin\phi}$$

Also, we know that

$$\dot{x}(t) = -C_3\zeta\omega_N e^{-\zeta\omega_N t}\sin(\omega_D t + \phi) + C_3\omega_D e^{-\zeta\omega_N t}\cos(\omega_D t + \phi)$$

$$\dot{x}(0) = -C_3\zeta\omega_N \sin\phi + C_3\omega_D\cos\phi = 0$$

$$\frac{\sin\phi}{\cos\phi} = \frac{\omega_D}{\zeta\omega_N} = \frac{\omega_N\sqrt{1-\zeta^2}}{\zeta\omega_N} = \frac{\sqrt{1-\zeta^2}}{\zeta} = \tan\phi$$

This is the same result as found from the complex plane trigonometry, which proves that the ϕs are the same.

Because $C_3 = -1/\sin\phi$ and $\sin\phi = \sqrt{1-\zeta^2}$,

$$C_3 = -\frac{1}{\sqrt{1-\zeta^2}}$$

Therefore, for an underdamped second-order system with a step input of magnitude y, the time response is

$$x(t) = y\left(1 - \frac{e^{-\zeta\omega_N t}}{\sqrt{1-\zeta^2}}\sin(\omega_D t + \phi)\right) \tag{7.24}$$

This is much nicer than solving for the transient and steady-state solutions and evaluating the constants as in Example 7.2. All we need to determine from the original differential equation is ω_n, ζ, and y. Radians are compatible units for ϕ in Eq. (7.24) because $\omega_D t$ will have units of radians. Use of Eq. (7.24) is illustrated in Example 7.4.

Source from Yechout, T.R. "Introduction to Aircraft Flight Mechanics", AIAA education Series, 2003

Example 7.4

Find the time response of the following differential equation with zero initial conditions:

$$\ddot{x} + 5\dot{x} + 25x = 25,$$
$$\omega_N = 5 \text{ rad/s},$$
$$\zeta = 0.5,$$
$$y = 1$$
$$\omega_D = 4.33 \text{ rad/s from Example 7.3}$$
$$\phi = \cos^{-1}(\zeta) = \cos^{-1}(0.5) = 60 \text{ deg} = \frac{\pi}{3}$$

substituting into (Eq. 7.24) yields

$$x(t) = 1 - 1.155e^{-2.5t}\sin\left(4.33t + \frac{\pi}{3}\right)$$

Notice the difference in effort required between Example 7.2 and 7.4. Remember that the solution using Eq. (7.24) is for a system with $-1 < \zeta < 1$ and a step input of magnitude y. If $\zeta \geq 1$ or $\zeta \leq -1$, the responses are aperiodic (exponential without oscillations) as discussed in Cases I and II.

The **stability** of a system can be determined directly from looking at the roots of the differential equation. If the root is real and has a negative value, it is stable [for example, $P_1 = -2$ and $x(t) = c_1e^{-2t}$, which decays to 0 as time goes to infinity]. If the root is real and positive, the response is unstable [$P_1 = 2 \Rightarrow x(t) = C_1e^{2t}$, which grows without bounds with time]. For complex roots, it is the real part of the root that determines stability. For $P_{1,2} = a \pm ib$, if $a < 0$ the system is stable. In the form $P_{1,2} = -\zeta\omega_N \pm i\omega_D$ this occurs when $\zeta > 0$. If $a > 0$, the system is unstable, which occurs when $\zeta < 0$. Therefore, if the roots occur to the left of the imaginary axis (the left half of the complex plane) the system is stable. Similarly, if the roots are to the right of the imaginary axis ($\zeta = 0$), the system is unstable. If the roots are on the imaginary axis ($\zeta = 0$), the system is neutrally stable (undamped). Time response characteristics for an impulse input are illustrated in Fig. 7.10 for various root locations. Notice the changes in damped frequency and time constant.

Examples 7.5 and 7.6 further illustrate our simplified approach for solving second-order linear differential equations. Remember that the general form of the differential equation is

$$\ddot{x} + 2\zeta\omega_N\dot{x} + \omega_N^2x = \omega_N^2y$$

Depending on the value of ζ, the solution will be in the form of Case 1, Case 2, or Case 3.

Source from Yechout, T.R. "Introduction to Aircraft Flight Mechanics", AIAA education Series, 2003

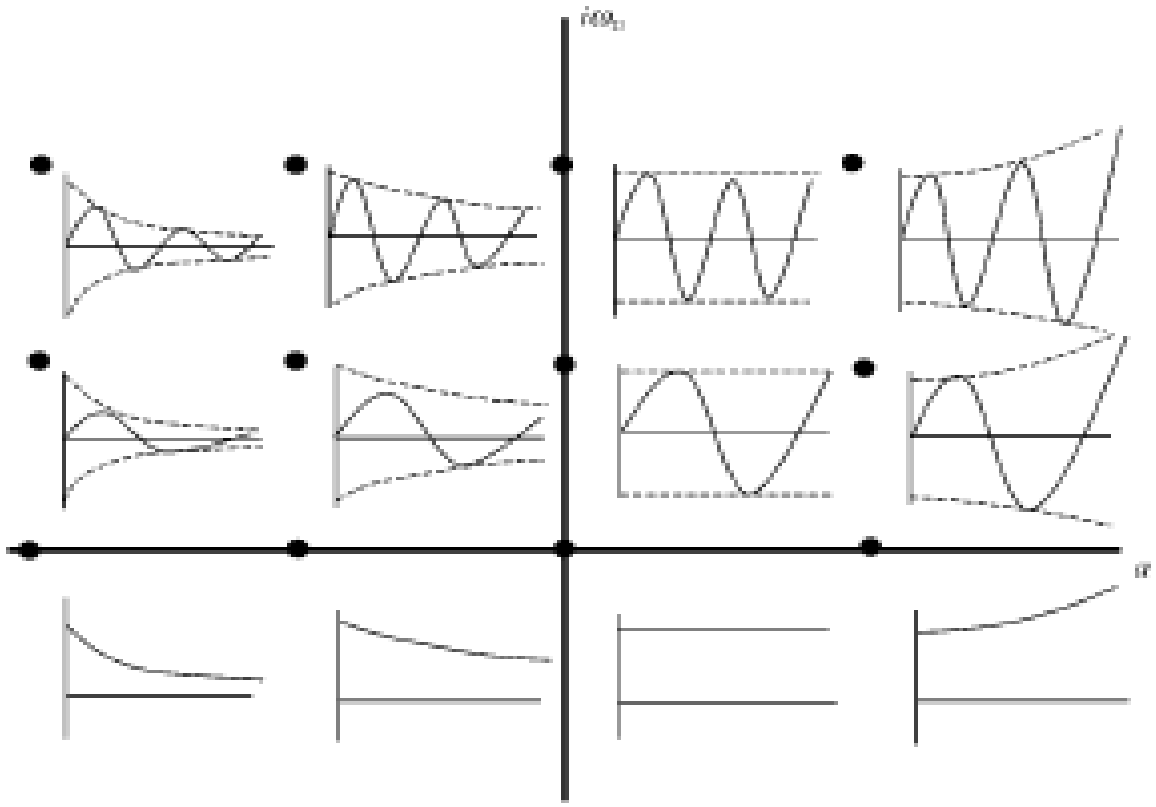

Fig. 7.10 Influence of complex plane root location on the transient response to an impulse input.

Example 7.5

Find the time response for the following system:

$$\ddot{x} + 10\dot{x} + 16x = 32; \quad x(0) = 0; \quad \dot{x}(0) = 0$$

Applying the general form of a second-order differential equation

$$\ddot{x} + 2\zeta\omega_N\dot{x} + \omega_N^2 x = \omega_N^2 y$$

we have

$$\omega_n = \sqrt{16} = 4 \text{ rad/s}$$
$$2\zeta\omega_N = 10 \Rightarrow 2\zeta(4) = 10 \Rightarrow \zeta = 1.25$$

Because $\zeta > 1$ we know that the solution is of the form of Case 1 (2 real unequal roots). Therefore, we need to solve for the roots:

$$P_{1,2} = \frac{-10 \pm \sqrt{10^2 - 4(1)(16)}}{2(1)} = -5 \pm 3 = -2, \ -8$$

Source from Yechout, T.R. "Introduction to Aircraft Flight Mechanics", AIAA education Series, 2003

The homogeneous (transient solution) is:

$$x_{trans}(t) = C_1 e^{-2t} + C_2 e^{-8t}$$

To find the steady-state solution, assume $x_{ss}(t) = A$

$$\overset{0}{\cancel{\ddot{A}}} + 10\overset{0}{\cancel{\dot{A}}} + 16A = 32 \Rightarrow A = 2$$

We then have

$$x(t) = x_{ss}(t) + x_{trans}(t) = 2 + C_1 e^{-2t} + C_2 e^{-8t}$$

and

$$\begin{aligned} x(0) &= 0 = 2 + C_1 + C_2 \\ \dot{x}(t) &= -2C_1 e^{-2t} - 8C_2 e^{-8t} \\ \dot{x}(0) &= 0 = -2C_1 - 8C_2 \Rightarrow C_1 = -4C_2 \\ 2 &- 4C_2 + C_2 = 0 \Rightarrow C_2 = \frac{2}{3} \\ C_1 &= -\frac{8}{3} \end{aligned}$$

Substituting back in, the time response becomes

$$x(t) = 2 - \frac{8}{3} e^{-2t} + \frac{2}{3} e^{-8t}$$

This response has two time constants:

$$\tau_1 = -\frac{1}{P_1} = -\frac{1}{-2} = 0.5 \text{ s}$$
$$\tau_2 = -\frac{1}{P_2} = -\frac{1}{-8} = 0.125 \text{ s}$$

Example 7.6

Find the time response for the following system:

$$\ddot{x} + 5\dot{x} + 25x = 75; \quad x(0) = 0, \quad \dot{x}(0) = 0$$

Source from Yechout, T.R. "Introduction to Aircraft Flight Mechanics", AIAA education Series, 2003

Using the general form of a second-order differential equation, we have

$$\omega_n = \sqrt{25} = 5 \text{ rad/s}; \quad y = 3 \text{ because } \omega_n^2 = 25$$
$$2\zeta\omega_N = 5 \Rightarrow 2\zeta(5) = 5 \Rightarrow \zeta = 0.5$$
$$\omega_D = \omega_n\sqrt{1-\zeta^2} = 5\sqrt{1-(0.5)^2} = 4.333 \text{ rad/s}$$
$$\phi = \cos^{-1}\zeta = \cos^{-1}(0.5) = 60 \text{ deg} = \frac{\pi}{3}$$

Because $-1 < \zeta < 1$ and the input is a step input of magnitude 3 ($y = 3$), the solution is of the form presented in Eq. (7.24)

$$x(t) = y\left[1 - \frac{e^{-\zeta\omega_N t}}{\sqrt{1-\zeta^2}}\sin(\omega_D t + \phi)\right] \qquad \text{(Case 3)}$$

Substituting in the appropriate values

$$x(t) = 3\left[1 - \frac{e^{-(0.5)(5)t}}{\sqrt{1-(0.5)^2}}\sin\left(4.333t + \frac{\pi}{3}\right)\right]$$

and the solution or time response is:

$$x(t) = 3\left[1 - 1.155e^{-2.5t}\sin\left(4.333t + \frac{\pi}{3}\right)\right]$$

Recall that the roots are

$$P_{1,2} = -\zeta\omega_N \pm i\omega_D$$
$$= -2.5 \pm i(4.333)$$

which could easily be plotted on the complex plane. The time constant is:

$$\tau = \frac{1}{\zeta\omega_N} = \frac{1}{2.5} = 0.4 \text{ s}$$

As a reminder, if $\zeta = -1$ or $\zeta = 1$, then the solution would be of the form of Case 2.

7.3 Transforming the Linearized EOM to the Laplace Domain

Another common approach used in solving differential equations is that of Laplace transforms. We will begin with a short review of Laplace transform techniques and then apply these techniques to the six linearized differential equations of motion for the aircraft. The differential operator, P, discussed in Sec. 7.1.1.1, is analogous to the Laplace variable, s. The insight gained with

Source from Yechout, T.R. "Introduction to Aircraft Flight Mechanics", AIAA education Series, 2003

the roots of transformed differential equations obtained using the differential operator will directly transfer to the roots obtained with the Laplace variable, s.

7.3.1 Laplace Transforms

It is assumed that the reader has gained familiarity with solution of differential equations using Laplace transforms from a previous course. It is the intent of this text to simply review highlights of the Laplace method. Simply stated, the Laplace method transforms a linear differential equation from the time domain (the derivatives are with respect to time) into an algebraic equation in the Laplace domain where the variable s is used. We will denote this Laplace transform operation with the symbol L. The methods of algebra are then used in a straightforward manner to solve for the parameter of interest. The resulting equation is transformed back to the time domain, referred to as an inverse Laplace transform operation and denoted with the symbol L^{-1} so that the time response can be obtained. By convention, small letters are used to represent functions of time and upper case letters are used to represent their Laplace transforms.

$$L[f(t)] = F(s)$$

and

$$L^{-1}[F(s)] = f(t)$$

The Laplace transform of the derivative of a function $f(t)$ is given by

$$L[\mathrm{d}f(t)/\mathrm{d}t] = sF(s) - f(0)$$

Where $f(0) = f(t)$ at $t = 0$. This is commonly called an initial condition. A second derivative is given by

$$L[\mathrm{d}^2 f(t)/\mathrm{d}t^2] = s^2 F(s) - sf(0) - \dot{f}(0)$$

Higher-order derivatives follow in a similar fashion.

7.3.1.1 Standardized inputs. We will be concerned with primarily two types of inputs or forcing functions: the unit impulse [$\delta(t)$] and the unit step [$1(t)$]. The unit impulse is defined as occuring at $t = 0$, and having zero duration, infinite magnitude, and a strength of unity. When considered as an input to the aircraft, test pilots refer to an impulse as a stick rap. The aircraft is trimmed and the stick is rapidly moved forward or aft from the trimmed position and then returned to the trimmed position. This input can be thought of as basically hitting or rapping the stick and allowing it to return to the trim position. A unit impulse is illustrated in Fig. 7.11.

Source from Yechout, T.R. "Introduction to Aircraft Flight Mechanics", AIAA education Series, 2003

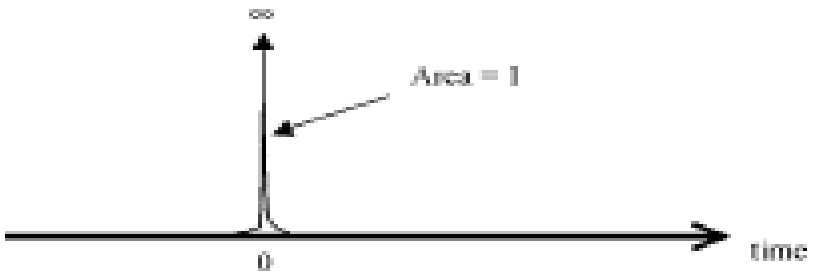

Fig. 7.11 Unit impulse.

A unit step is defined by the following:

$$0 \text{ for } t < 0; \quad 1 \text{ for } t > 0$$

A unit step is illustrated in Fig. 7.12. A test pilot will input a step input by rapidly moving the stick forward or aft from the trimmed postion and holding it. Of course, test pilot inputs only approximate the ideal unit impulse and unit step inputs. These approximations are generally sufficient to excite the dynamics and response of the aircraft, so we have a convenient way to compare the ideal world of the unit impulse and unit step to the practical world of the aircraft in flight.

The Laplace transform of a unit impulse is

$$L[\delta(t)] = 1$$

and for a unit step

$$L[1(t)] = 1/s$$

7.3.1.2 Laplace tables. To simplify transforming expressions from the time domain to the Laplace domain and the taking of the inverse transform to go from the Laplace domain back to the time domain, we will rely on a table of Laplace transforms. Such a table is presented in Appendix E, which contains most of the expressions we will need. More detailed tables are available in a variety of references.

7.3.1.3 Solving differential equations using Laplace transforms. Laplace transforms are used to solve differential equations through a three-step

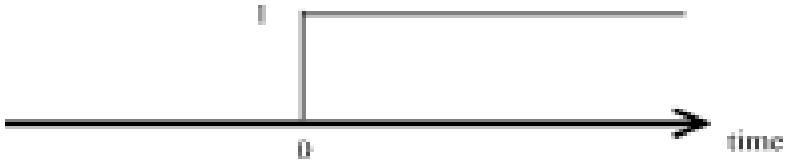

Fig. 7.12 Unit step.

Source from Yechout, T.R. "Introduction to Aircraft Flight Mechanics", AIAA education Series, 2003

process. First, the Laplace transform of the differential equation is obtained; second, the resulting equation is solved algebraically for the unknown variable/variables; and third, the inverse Laplace transform of each variable is obtained resulting in the desired time solution of the original differential equation. A simple example will illustrate this method.

Example 7.7

Find the time response for the following differential equation:

$$\ddot{x} = 6; \quad x(0) = \dot{x}(0) = 0$$

Taking the Laplace transform,

$$s^2 X(s) = 6/s$$

Solving for $X(s)$,

$$X(s) = 6/s^3$$

and taking the inverse Laplace using #8 in Appendix E,

$$x(t) = 3t^2$$

which is the time solution.

7.3.1.4 Transfer functions and the characteristic equation. A transfer function is defined as the ratio of Laplace transforms of output to input. Outputs for our applications will typically be motion variables such as u, angle of attack, and yaw rate, which describe velocities, angles, or angular rates of the aircraft. Inputs for our applications will be aircraft control surface deflections such as elevator deflection (δ_e) or aileron deflection (δ_a). In simple terms

$$\text{Transfer function} = L\left[\frac{\text{Output}}{\text{Input}}\right]$$

A transfer function will be expressed in Laplace notation and will be obtained from the Laplace form of the aircraft equations of motion. Example 7.8 illustrates how a transfer function is obtained from a differential equation and the utility it has for a variety of inputs.

Example 7.8

Find the transfer function $\phi(s)/\delta_a(s)$ for the following simplified differential equation defining roll angle response. Assume zero initial conditions.

$$\ddot{\phi} + 0.704\dot{\phi} = 0.037\delta_a$$

Source from Yechout, T.R. "Introduction to Aircraft Flight Mechanics", AIAA education Series, 2003

Taking the Laplace transform

$$s^2\phi(s) + 0.704s\phi(s) = 0.037\delta_a(s)$$

Solving for $\phi(s)$

$$\phi(s) = \frac{0.037\delta_a(s)}{s(s + 0.0704)}$$

and obtaining the transfer function

$$\frac{\phi(s)}{\delta_a(s)} = \frac{0.037}{s(s + 0.0704)}$$

For an impulse input, $\delta_a(s) = 1$

$$\phi(s) = \frac{0.037}{s(s + 0.0704)}$$

and, taking the inverse Laplace transform using the Laplace tables we have the time response

$$\phi(t) = \frac{0.037}{0.0704}(1 - e^{-0.0704t})$$

For a unit step input, $\delta_a(s) = 1/s$

$$\phi(s) = \frac{0.037}{s^2(s + 0.0704)}$$

and the time response is

$$\phi(t) = \frac{0.037}{(0.0704)}(0.0704t - 1 + e^{-0.0704t})$$

The **characteristic equation** of a transfer function is obtained by setting the polynomial in the denominator of the transfer function equal to zero. For Example 7.8, the characteristic equation is

$$s(s + 0.0704) = 0 \tag{7.25}$$

The roots of a characteristic equation will define the overall system dynamic characteristics such as time constant (for first-order systems), and damping ratio and natural frequency (for second-order systems) as discussed in Sec. 7.1.2. For Eq. (7.25), the root $s = 0$ leads to a steady state value term in the time solution, and the root $s = -0.0704$ leads to a time constant of 1/0.0704 s and a $e^{-0.0704t}$ term in the time solution.

7.3.1.5 Partial fraction expansion. A key step in using Laplace transforms to solve differential equations involves using the Laplace transform tables to find inverse transforms. It is impossible to cover every potential case in a table, but the method of partial fractions can aid in breaking up involved transfer functions into pieces, which may be included in a standard table. This text will only review the case of a transfer function with nonrepeated real roots in the characteristic equation. A more detailed coverage of partial fraction expansion techniques is included in most engineering mathematics textbooks such as *Advanced Engineering Mathematics*, by Erwin Kreyszig.

Consider the transfer function:

$$\frac{X(s)}{Y(s)} = \frac{s+2}{s^3+8s^2+19s+12} = \frac{s+2}{(s+3)(s+4)(s+1)}$$

It can be rewritten using a partial fraction expansion as

$$\frac{X(s)}{Y(s)} = \frac{A_1}{s+3} + \frac{A_2}{s+4} + \frac{A_3}{s+1}$$

To evaluate the constants A_1, A_2, and A_3, which are also called residues, we use the following approach:

$$A_1 = \left.\frac{s+2}{(s+4)(s+1)}\right|_{s=-3} = \frac{1}{2}$$

$$A_2 = \left.\frac{s+2}{(s+3)(s+1)}\right|_{s=-4} = -\frac{2}{3}$$

$$A_3 = \left.\frac{s+2}{(s+3)(s+4)}\right|_{s=-1} = \frac{1}{6}$$

The partial fraction representation of the transfer function then becomes

$$\frac{X(s)}{Y(s)} = \frac{\frac{1}{2}}{s+3} + \frac{-\frac{2}{3}}{s+4} + \frac{\frac{1}{6}}{s+1}$$

Each of the partial fraction expressions can be transformed to the time domain using the common first-order transform found in all Laplace tables.

$$L^{-1}\left(\frac{K}{s+a}\right) = Ke^{-at}$$

For this example, we then have

$$\frac{x(t)}{y(t)} = \frac{1}{2}e^{-3t} - \frac{2}{3}e^{-4t} + \frac{1}{6}e^{-t}$$

Source from Yechout, T.R. "Introduction to Aircraft Flight Mechanics", AIAA education Series, 2003

The residues (A_1, A_2, and A_3) also provide a weighting of the relative magnitude of each component of the response.

Slightly modified partial fraction approaches are defined in mathematics texts for characteristic equation roots, which are repeated real numbers, complex conjugates, and a repeated pair of complex conjugates.

7.3.1.6 Initial and final value theorems. The initial value of a function (at $t = 0$) can be found if its Laplace transform is known using the following theorem:

$$f(t)|_{t\to 0} = \lim|_{s\to\infty} sF(s)$$

For example, consider the function

$$f(t) = e^{-3t}$$

$$L(e^{-3t}) = \frac{1}{s+3}$$

Applying the initial value theorem,

$$\lim|_{t\to 0} e^{-3t} = \lim|_{s\to\infty} s\left(\frac{1}{s+3}\right) = 1 = e^{-3(0)}$$

This theorem is useful in verifying the accuracy of Laplace transforms because the initial conditions are normally known.

The steady-state ($t \to \infty$) value of a time domain function can be found if its Laplace transform is known and if it has a finite steady-state value using the following theorem:

$$\lim|_{t\to\infty} f(t) = \lim|_{s\to 0} sF(s)$$

This theorem does not apply to unstable functions or undamped sinusoidal functions. As an example of application of this theorem, consider the Laplace transform:

$$X(s) = \frac{1}{s(s+1)}$$

To find the steady-state value of x at $t = \infty$, we can apply the final value theorem:

$$\lim|_{t\to\infty} x(t) = \lim|_{s\to 0} s\left(\frac{1}{s(s+1)}\right) = 1 = x(\infty)$$

Source from Yechout, T.R. "Introduction to Aircraft Flight Mechanics", AIAA education Series, 2003

This result can be checked using

$$L^{-1}\left(\frac{1}{s(s+1)}\right) = 1 - e^{-t} = x(t)$$

and

$$x(\infty) = 1 - e^{-\infty} = 1$$

The final value value theorem provides an easy method to find the steady-state value of a Laplace expression.

7.3.2 Longitudinal Linearized EOM in Laplace Form

We will now use the power of Laplace transforms to recast the aircraft EOM developed in Sec. 6.5. The equations become somewhat long but the concepts are not complex. Equation (6.127), the longitudinal linearized differential EOM for the aircraft, are repeated for reference.

$$\begin{aligned} \dot{u} &= -g\theta\cos\Theta_1 + X_u u + X_{T_u} u + X_\alpha \alpha + X_{\delta_e}\delta_e \\ \dot{w} - U_1 q &= -g\theta\sin\Theta_1 + Z_u u + Z_\alpha \alpha + Z_{\dot{\alpha}}\dot{\alpha} + Z_q q + Z_{\delta_e}\delta_e \\ \dot{q} &= M_u u + M_{T_u} u + M_\alpha \alpha + M_{T_\alpha}\alpha + M_{\dot{\alpha}}\dot{\alpha} + M_q q + M_{\delta_e}\delta_e \end{aligned} \tag{7.26}$$

We will take the Laplace transform of these equations, but first it is important to note that these three EOM have five aircraft motion variables (u, θ, α, w, and q) and δ_e. Because we only have three defining equations, we need to reduce this down to three motion variables and δ_e becomes the input or forcing function for the system We will use the kinematic relations and the approximation for angle of attack, α, to reduce to the three motion variables of α, u, and θ.

From the kinematic equations [Eq. (4.80)] and the assumption of initial trimmed flight with the wings level condition

$$q = \dot{\theta}, \quad \dot{q} = \ddot{\theta}$$

Also, for small perturbations

$$\alpha \approx \frac{w}{U_1} \Rightarrow w = \alpha U_1 \quad \text{and} \quad \dot{w} = \dot{\alpha} U_1$$

Therefore, our aircraft motion variables are reduced to α, u, and θ. These should be thought of as the outputs for our system of differential equations.

Source from Yechout, T.R. "Introduction to Aircraft Flight Mechanics", AIAA education Series, 2003

With zero initial conditions, the Laplace transform of Eq. (7.26) yields

$$su(s) = -g\theta(s)\cos\Theta_1 + X_u u(s) + X_{T_u} u(s) + X_\alpha \alpha(s) + X_{\delta_e}\delta_e(s)$$
$$sU_1\alpha(s) - U_1 s\theta(s) = -g\theta(s)\sin\Theta_1 + Z_u u(s) + Z_\alpha \alpha(s) + Z_{\dot\alpha} s\alpha(s) + Z_q s\theta(s) + Z_{\delta_e}\delta_e(s)$$
$$s^2\theta(s) = M_u u(s) + M_{T_u} u(s) + M_\alpha \alpha(s) + M_{T_\alpha}\alpha(s) + M_{\dot\alpha} s\alpha(s) + M_q s\theta(s) + M_{\delta_e}\delta_e(s)$$

Combining terms yields

$$(s - X_u - X_{T_u})u(s) - X_\alpha\alpha(s) + g\cos\Theta_1\theta(s) = X_{\delta_e}\delta_e(s)$$
$$-Z_u u(s) + [(U_1 - Z_{\dot\alpha})s - Z_\alpha]\alpha(s) + [-(Z_q - U_1)s + g\sin\Theta_1]\theta(s) = Z_{\delta_e}\delta_e(s)$$
$$-(M_u + M_{T_u})u(s) - [M_{\dot\alpha}s + M_\alpha + M_{T_\alpha}]\alpha(s) + (s^2 - M_q s)\theta(s) = M_{\delta_e}\delta_e(s)$$

Notice at this point that we have moved the terms with δ_e (elevator deflection) to the right-hand side of the equal sign because δ_e is the forcing function (or input) for each of the three differential equations. In matrix form this yields

$$\begin{bmatrix} (s - X_u - X_{T_u}) & -X_\alpha & g\cos\Theta_1 \\ -Z_u & [s(U_1 - Z_{\dot\alpha}) - Z_\alpha] & [-(Z_q + U_1)s + g\sin\Theta_1] \\ -(M_u + M_{T_u}) & -[M_{\dot\alpha}s + M_\alpha + M_{T_\alpha}] & (s^2 - M_q s) \end{bmatrix} \begin{bmatrix} u(s) \\ \alpha(s) \\ \theta(s) \end{bmatrix} = \begin{bmatrix} X_{\delta_e} \\ Z_{\delta_e} \\ M_{\delta_e} \end{bmatrix} \delta_e(s)$$

In terms of the transfer functions $\frac{u(s)}{\delta_e(s)}$, $\frac{\alpha(s)}{\delta_e(s)}$, and $\frac{\theta(s)}{\delta_e(s)}$, we have

$$\begin{bmatrix} (s - X_u - X_{T_u}) & -X_\alpha & g\cos\Theta_1 \\ -Z_u & [s(U_1 - Z_{\dot\alpha}) - Z_\alpha] & [-(Z_q + U_1)s + g\sin\Theta_1] \\ -(M_u + M_{T_u}) & -[M_{\dot\alpha}s + M_\alpha + M_{T_\alpha}] & (s^2 - M_q s) \end{bmatrix} \begin{bmatrix} \frac{u(s)}{\delta_e(s)} \\ \frac{\alpha(s)}{\delta_e(s)} \\ \frac{\theta(s)}{\delta_e(s)} \end{bmatrix} = \begin{bmatrix} X_{\delta_e} \\ Z_{\delta_e} \\ M_{\delta_e} \end{bmatrix} \tag{7.27}$$

and each of the three longitudinal transfer functions can be determined using Cramer's rule as presented in Appendices F and G. It is important at this point

Source from Yechout, T.R. "Introduction to Aircraft Flight Mechanics", AIAA education Series, 2003

not to lose sight of what we have developed. Each of these transfer functions can be represented as the ratio of two polynomials in the Laplace variables.

$$\frac{u(s)}{\delta_e(s)} = \frac{A_u s^3 + B_u s^2 + C_u s + D_u}{Es^4 + Fs^3 + Gs^2 + Hs + I} \tag{7.28}$$

$$\frac{\alpha(s)}{\delta_e(s)} = \frac{A_\alpha s^3 + B_\alpha s^2 + C_\alpha s + D_\alpha}{Es^4 + Fs^3 + Gs^2 + Hs + I} \tag{7.29}$$

$$\frac{\theta(s)}{\delta_e(s)} = \frac{A_\theta s^2 + B_\theta s + C_\theta}{Es^4 + Fs^3 + Gs^2 + Hs + I} \tag{7.30}$$

Notice that all three longitudinal transfer functions have the same input (δ_e) and the same denominator. There is a separate transfer function for each of our three longitudinal motion variables (u, α, and θ). Also, each of these transfer functions has the same characteristic equation:

$$Es^4 + Fs^3 + Gs^2 + Hs + I = 0$$

Recall that *the characteristic equation determines the dynamic stability characteristics* of the response, and therefore all three transfer functions will have the same dynamic characteristics (parameters such as ζ, ω_n, and τ). Notice also that the numerator of each transfer function is different. Each numerator coefficient is designated by an A, B, C, or D with a subscript appropriate to its respective transfer function. The numerator affects the magnitude of the response, and therefore each motion variable will have a different magnitude of response but with the same dynamic characteristics.

7.3.2.1 Three-degree-of-freedom analysis of longitudinal modes of motion. The preceding development included the three motion variables u, α, and θ. This analysis may also be termed a three-degree-of-freedom (3 DOF) determination of the longitudinal transfer functions. Normally, with the help of root solvers such as those available in MATLAB® (a registered trademark of The MathWorks, Inc.), the fourth order characteristic equation for longitudinal motion can be written as the product of two second-order (oscillatory) polynomials.

$$(s^2 + 2\zeta_{SP}\omega_{n_{SP}}s + \omega_{n_{SP}}^2)(s^2 + 2\zeta_{PH}\omega_{n_{PH}}s + \omega_{n_{PH}}^2) = 0 \tag{7.31}$$

The subscript *SP* refers to the short period mode and the subscript *PH* refers to the phugoid mode. All airplanes have these two longitudinal dynamic modes. Each of these polynomials can be thought of as a separate characteristic equation that defines the dynamic characteristics of its respective dynamic mode.

The coefficients (and roots) of each characteristic equation change with flight condition, airplane mass, mass distribution, airplane geometry, and aerodynamic characteristics. These changes translate to changes in ω_n and ζ, but the fundamental presence of the short period and phugoid modes is maintained.

Source from Yechout, T.R. "Introduction to Aircraft Flight Mechanics", AIAA education Series, 2003

The **short period mode** is characterized by **complex conjugate roots** with a moderate to relatively high damping ratio and relatively high natural frequency and damped frequency (short period). It is easily demonstrated by first trimming the aircraft and then disturbing it from trim with a forward-aft-neutral pitch stick input (commonly called a doublet). The resulting response back to trim may be either first order (exponential decay) or second order (oscillatory). Significant variations in the angle of attack (α), and pitch attitude (θ) longitu-dinal motion variables occur while the airspeed (u) motion variable remains fairly constant. Trim is generally regained in a few seconds, thus the descriptive name short period and the small variation in airspeed. Typical time histories for the short period response of a fighter aircraft to a doublet input are presented in Fig. 7.13.

Notice that the response is second order (oscillatory) and that u remains fairly constant. Oscillations of larger magnitude are observed with α and θ. Notice also that the response is stable.

The **phugoid mode** is characterized by **complex conjugate roots** with a relatively low damping ratio and natural/damped frequency (long period). It is demonstrated by trimming the aircraft in level flight, then inputting aft stick for approximately 2–3 s, bleeding off some airspeed, and then returning the stick to the neutral (trimmed) position. The resulting response is usually oscil-latory with significant variations in pitch attitude and airspeed, while angle of attack remains relatively constant. The phugoid has been described as an up and down roller coaster oscillation in the sky that trades off kinetic and poten-tial energy. As the oscillation starts, airspeed decreases while the airplane gains altitude (pitch angle is positive). The aircraft then begins to lose altitude, and airspeed increases while the pitch angle decreases. This is followed by the aircraft pulling up gradually and returning to the climb portion of the phugoid oscillation. The period for the phugoid is typically quite long (somewhere

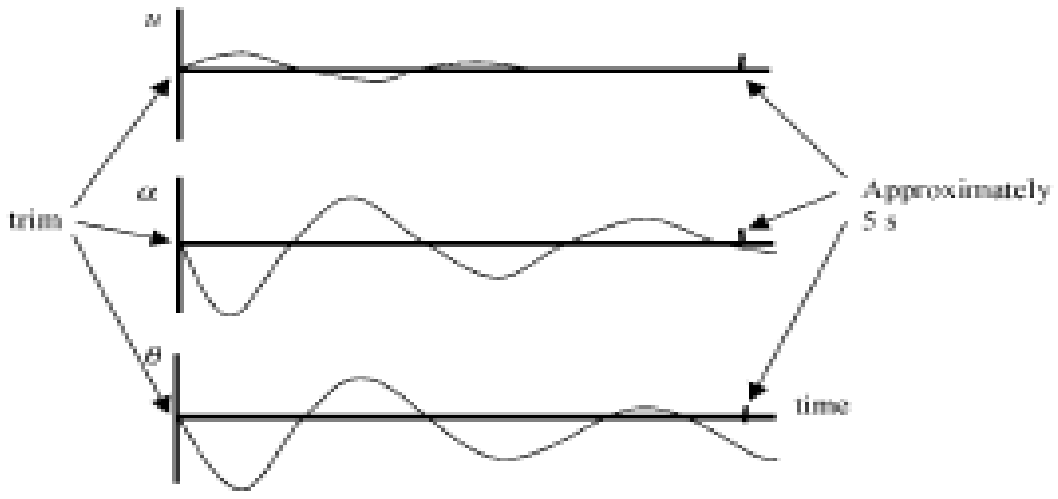

Fig. 7.13 u, α, and θ time history plots illustrating the short period mode.

Source from Yechout, T.R. "Introduction to Aircraft Flight Mechanics", AIAA education Series, 2003

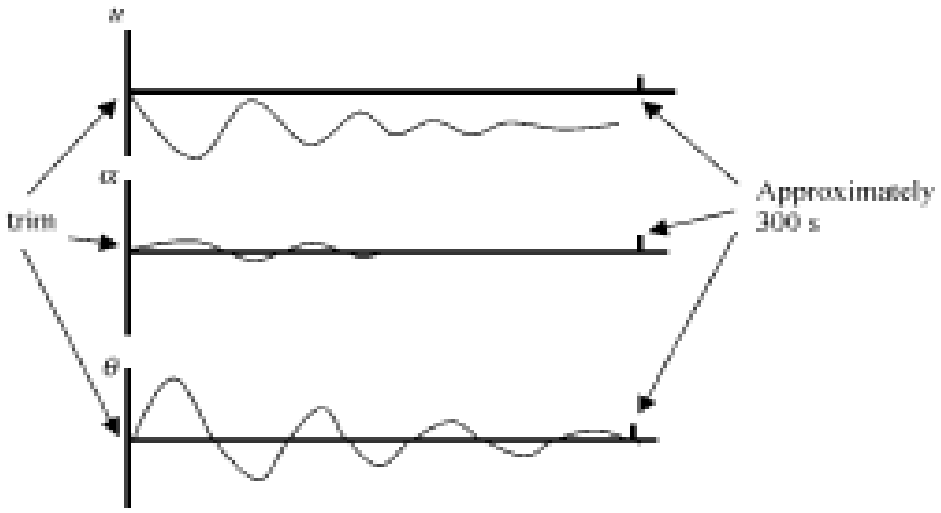

Fig. 7.14 u, α, and θ time history plots for the phugoid mode.

between 30 and 120 s). Typical time histories for the phugoid mode are presented in Fig. 7.14.

Notice that the response is also second order for the phugoid and that angle of attack remains relatively constant. The frequency of the oscillation for the phugoid is much lower than that observed for the short period mode. The phugoid as shown in Fig. 7.14 is stable, but this may not be the case for all flight conditions.

Example 7.9

The α/δ_e transfer function for a T-37 cruising at 30,000 ft and 0.46 Mach follows. Find the natural frequency, damping ratio, damped frequency, and time constant for the short period and phugoid modes.

$$\frac{\alpha}{\delta_e} = -0.0924 \frac{(s + 336.1)(s^2 + 0.0105s + 0.0097)}{(s^2 + 4.58s + 21.6)(s^2 + 0.0098s + 0.0087)}$$

We go immediately to the two characteristic equations

$$s^2 + 4.58s + 21.6 = 0$$
$$s^2 + 0.0098s + 0.0087 = 0$$

The natural frequency (ω_n) for the first characteristic equation is

$$\omega_n = \sqrt{21.6} = 4.65 \text{ rad/s}$$

Source from Yechout, T.R. "Introduction to Aircraft Flight Mechanics", AIAA education Series, 2003

and for the second equation

$$\omega_n = \sqrt{0.0087} = 0.0933 \text{ rad/s}$$

We can identify the first characteristic equation as being for the short period mode because of the higher natural frequency. The phugoid dynamics are contained in the second characteristic equation. Thus

$$\omega_{n_{sp}} = 4.65 \text{ rad/s}$$
$$\omega_{n_{ph}} = 0.0933 \text{ rad/s}$$

and

$$\zeta_{sp} = \frac{4.58}{2\omega_{n_{sp}}} = 0.493$$
$$\zeta_{ph} = \frac{0.0098}{2\omega_{n_{ph}}} = 0.0525$$

Notice that both the short period and phugoid responses will be second order because ζ is less than 1. Both responses are stable because $\zeta\omega_n$ is positive for each mode. The damped frequency is

$$\omega_D = \omega_n\sqrt{1-\zeta^2}$$
$$\omega_{D_{sp}} = \omega_{n_{sp}}\sqrt{1-\zeta_{sp}^2} = 4.65\sqrt{1-(0.493)^2} = 4.046 \text{ rad/s}$$
$$\omega_{D_{ph}} = \omega_{n_{ph}}\sqrt{1-\zeta_{ph}^2} = 0.0933\sqrt{1-(0.0525)^2} = 0.0932 \text{ rad/s}$$

and for the time constant

$$\tau_{sp} = \frac{1}{\zeta_{sp}\omega_{n_{sp}}} = \frac{1}{(0.493)(4.65)} = 0.436 \text{ s}$$
$$\tau_{ph} = \frac{1}{\zeta_{ph}\omega_{n_{ph}}} = \frac{1}{(0.0525)(0.0933)} = 204.2 \text{ s}$$

7.3.2.2 Two-degree-of-freedom short period approximation. To gain insight into the stability parameters and derivatives that influence the dynamic characteristics of the short period mode, we will look at a two-degree-of-freedom (2 DOF) approximation. This is a solution in which the motion is constrained to

Source from Yechout, T.R. "Introduction to Aircraft Flight Mechanics", AIAA education Series, 2003

two motion variables rather than three. Recalling our discussion on the short period mode, we will make the simplifying assumption that u **remains near zero** and can be removed from Eq. (7.27). With this assumption and the **elimination of the x-force equation** (which is assumed to have a negligible effect if u is approximately constant), we retain the z-force equation and the pitching moment equation along with the motion variables α and θ.

$$\begin{bmatrix} (s - X_u) & -X_\alpha & g\cos\Theta_1 \\ -Z_u & [s(U_1 - Z_{\dot\alpha}) - Z_\alpha] & [-(Z_q + U_1)s + g\sin\Theta_1] \\ -(M_u + M_{T_u}) & -[M_{\dot\alpha}s + M_\alpha + M_{T_\alpha}] & (s^2 - M_q s) \end{bmatrix} \begin{bmatrix} u(s) \\ \alpha(s) \\ \theta(s) \end{bmatrix} = \begin{bmatrix} X_{\delta_e} \\ Z_{\delta_e} \\ M_{\delta_e} \end{bmatrix} \delta_e(s)$$

Equation (7.27) becomes

$$\begin{bmatrix} [s(U_1 - Z_{\dot\alpha}) - Z_\alpha] & [-(Z_q + U_1)s + g\sin\Theta_1] \\ -[M_{\dot\alpha}s + M_\alpha + M_{T_\alpha}] & (s^2 - M_q s) \end{bmatrix} \begin{bmatrix} \alpha(s) \\ \theta(s) \end{bmatrix} = \begin{bmatrix} Z_{\delta_e} \\ M_{\delta_e} \end{bmatrix} \delta_e(s) \tag{7.32}$$

We will next focus on the dynamic characteristics and the characteristic equation (which is the determinant of the first coefficient matrix). We will look at the short period approximation assuming that $Z_{\dot\alpha} = Z_q = \Theta_1 = M_{T_\alpha} = 0$ because these terms are generally small compared to the others.

Equation (7.32) becomes

$$\begin{bmatrix} sU_1 - Z_\alpha & -U_1 s \\ -[M_{\dot\alpha}s + M_\alpha] & s^2 - M_q s \end{bmatrix} \begin{bmatrix} \alpha(s) \\ \theta(s) \end{bmatrix} = \begin{bmatrix} Z_{\delta_e} \\ M_{\delta_e} \end{bmatrix} \delta_e(s)$$

The characteristic equation is

$$(sU_1 - Z_\alpha)(s^2 - M_q s) - (-U_1 s)(-[M_{\dot\alpha}s + M_\alpha]) = 0$$

or

$$sU_1\left[s^2 - \left(M_q + \frac{Z_\alpha}{U_1} + M_{\dot\alpha}\right)s + \left(\frac{Z_\alpha M_q}{U_1} - M_\alpha\right)\right] = 0$$

and in simplified form

$$s^2 - \left(M_q + \frac{Z_\alpha}{U_1} + M_{\dot\alpha}\right)s + \left(\frac{Z_\alpha M_q}{U_1} - M_\alpha\right) = 0 \tag{7.33}$$

Source from Yechout, T.R. "Introduction to Aircraft Flight Mechanics", AIAA education Series, 2003

For this 2-DOF approximation we can find $\alpha(s)/\delta_e(s)$ and $\theta(s)/\delta_e(s)$ using Cramer's rule as before.

$$\frac{\alpha(s)}{\delta_e(s)} = \frac{Z_{\delta_e}s + (M_{\delta_e}U_1 - M_q Z_{\delta_e})}{U_1\left[s^2 - \left(M_q + \frac{Z_\alpha}{U_1} + M_{\dot{\alpha}}\right)s + \left(\frac{Z_\alpha M_q}{U_1} - M_\alpha\right)\right]}$$

$$\frac{\theta(s)}{\delta_e(s)} = \frac{(U_1 M_{\delta_e} + Z_{\delta_e}M_{\dot{\alpha}})s + (M_\alpha Z_{\delta_e} - Z_\alpha M_{\delta_e})}{sU_1\left[s^2 - (M_q + \frac{Z_\alpha}{U_1} + M_{\dot{\alpha}})s + \left(\frac{Z_\alpha M_q}{U_1} - M_\alpha\right)\right]} \quad (7.34)$$

An approximation of natural frequency and damping ratio can then be determined using Eq. (7.33).

$$\omega_{n_{SP}} \approx \sqrt{\frac{Z_\alpha M_q}{U_1} - M_\alpha} \quad (7.35)$$

$$\zeta_{SP} \approx \frac{-\left(M_q + \frac{Z_\alpha}{U_1} + M_{\dot{\alpha}}\right)}{2\omega_{n_{SP}}} \quad (7.36)$$

Typically, $-M_\alpha$ is much larger that $Z_\alpha M_q/U_1$ (as long as the c.g. is not too far aft). This results in

$$\omega_{n_{SP}} \approx \sqrt{-M_\alpha} = \sqrt{\frac{-C_{m_\alpha}\bar{q}_1 S\bar{c}}{I_{yy}}} \quad (7.37)$$

The following insights can be observed from Eq. (7.37) for the short period mode natural frequency: 1) $\omega_{n_{SP}}$ will increase as static longitudinal stability ($-C_{m_\alpha}$) increases or as the distance between the c.g. and the aircraft AC increases; 2) $\omega_{n_{SP}}$ will increase as dynamic pressure ($\bar{q}_1$) increases; and 3) $\omega_{n_{SP}}$ will decrease as the pitching moment of inertia (I_{yy}) increases.

Equation (7.36) also leads to important insights for the short period damping ratio: 1) M_q, the pitch damping derivative, is the driving term, because 2) Z_α/U_1 is generally driven by other requirements, and 3) $M_{\dot{\alpha}}$ is generally driven by the same design features (horizontal tail size and the distance from the c.g. to the AC of the tail) as M_q, and $M_{\dot{\alpha}}$ is typically about one-third the value of M_q. One of the limitations of this approximation for damping ratio is that it assumes that ζ is positive (a stable case), which is not always true. It is recommended that unstable cases be analyzed using a 3-DOF solution.

7.3.2.3 Two-degree-of-freedom phugoid approximation. As with the short period approximation, we will look at a 2-DOF approximation for the phugoid mode to gain insight into the parameters that influence dynamic characteristics. For the phugoid approximation, we will assume that α is constant

Source from Yechout, T.R. "Introduction to Aircraft Flight Mechanics", AIAA education Series, 2003

with u and θ (or q) as the motion variables. We can eliminate the $\alpha(s)$ terms and the moment equation in Eq. (7.27) to yield two equations with two motion variables.

$$\begin{bmatrix} s - X_u - X_{T_u} & -X_\alpha & g\cos\Theta_1 \\ -Z_u & [s(U_1 - Z_{\dot\alpha}) - Z_\alpha] & [-(Z_q + U_1)s + g\sin\Theta_1] \\ -(M_u + M_{T_u}) & -[M_{\dot\alpha}s + M_\alpha + M_{T_\alpha}] & (s^2 - M_q s) \end{bmatrix} \begin{bmatrix} u(s) \\ \alpha(s) \\ \theta(s) \end{bmatrix} = \begin{bmatrix} X_{\delta_e} \\ Z_{\delta_e} \\ M_{\delta_e} \end{bmatrix} \delta_e(s)$$

or

$$\begin{bmatrix} s - X_u - X_{T_u} & g\cos\Theta_1 \\ -Z_u & [-(Z_q + U_1)s + g\sin\Theta_1] \end{bmatrix} \begin{bmatrix} u(s) \\ \theta(s) \end{bmatrix} = \begin{bmatrix} X_{\delta_e} \\ Z_{\delta_e} \end{bmatrix} \delta_e(s)$$

If we assume $X_{\delta_e} = Z_q = \Theta_1 \approx 0$ we get

$$\begin{bmatrix} s - X_u - X_{T_u} & g \\ -Z_u & -U_1 s \end{bmatrix} \begin{bmatrix} u(s) \\ \theta(s) \end{bmatrix} = \begin{bmatrix} 0 \\ Z_{\delta_e} \end{bmatrix} \delta_e(s) \tag{7.38}$$

The characteristic equation becomes

$$\begin{aligned} &(s - X_u - X_{T_u})(-U_1 s) + gZ_u = 0 \\ &-U_1\left[s^2 - (X_u + X_{T_u})s - \frac{Z_u}{U_1}g\right] = 0 \end{aligned} \tag{7.39}$$

We then have

$$\omega_{n_{SP}} \approx \sqrt{\frac{-Z_u g}{U_1}} = \sqrt{\frac{-g}{U_1}\left[\frac{-(\bar{q}_1 S)(C_{L_u} + 2C_{L_1})}{mU_1}\right]}$$

or

$$\omega_{n_{SP}} \approx \sqrt{\frac{g(\bar{q}_1 S)(C_{L_u} + 2C_{L_1})}{U_1^2 m}}$$

Source from Yechout, T.R. "Introduction to Aircraft Flight Mechanics", AIAA education Series, 2003

Typically $C_{L_u} \ll 2C_{L_1}$ and $C_{L_1} = mg/\bar{q}_1 S$. With these assumptions we have

$$\omega_{n_{ph}} \approx \sqrt{\frac{g(\bar{q}_1 S)}{U_1^2 m}\left[\frac{2mg}{\bar{q}_1 S}\right]} = \sqrt{\frac{2g^2}{U_1^2}}$$

or

$$\omega_{n_{ph}} \approx \frac{g}{U_1}\sqrt{2} \tag{7.40}$$

Therefore, we can observe that the natural frequency of the phugoid mode is approximately inversely proportional to the forward velocity, U_1.

Returning to the characteristic equation [Eq. (7.39)], we can define an approximation for the phugoid damping ratio:

$$\zeta_{ph} \approx \frac{-(X_u - X_{T_u})}{2\omega_{n_{ph}}}$$

Because

$$X_u = -\frac{(C_{D_u} + 2C_{D_1})\bar{q}_1 S}{mU_1} \qquad \text{and} \qquad X_{T_u} = \frac{(C_{T_{x_u}} + 2C_{T_{x_1}})\bar{q}_1 S}{mU_1}$$

We can substitute these values into the expression for ζ_{ph}

$$\zeta_{ph} \approx \frac{(C_{D_u} + 2C_{D_1} - C_{T_{x_u}} - 2C_{T_{x_1}})\bar{q}_1 S}{2mU_1\omega_{n_{ph}}} \tag{7.41}$$

Equation (7.41) provides us with an approximation for the phugoid damping ratio. To gain a little more insight, we will look at the case of unpowered or gliding flight where

$$C_{T_{x_1}} = C_{T_{x_u}} = 0$$

With this assumption

$$\zeta_{ph} = \frac{(C_{D_u} + 2C_{D_1})\bar{q}_1 S}{2mU_1\omega_{n_{ph}}} = \frac{(C_{D_u} + 2C_{D_1})\bar{q}_1 S U_1}{2mU_1 g\sqrt{2}}$$

$$\zeta_{ph} = \frac{(C_{D_u} + 2C_{D_1})\bar{q}_1 S}{2\sqrt{2}mg} = \frac{(C_{D_u} + 2C_{D_1})}{2\sqrt{2}}\frac{1}{C_{L_1}}$$

Source from Yechout, T.R. "Introduction to Aircraft Flight Mechanics", AIAA education Series, 2003

At this point we can make one additional assumption for low-speed flight where

$$C_{D_0} \approx 0.$$

With this additional assumption, we have

$$\zeta_{ph} \approx \frac{2C_{D_1}}{2\sqrt{2}C_{L_1}} = \frac{1}{\sqrt{2}} \frac{C_{D_1}}{C_{L_1}} \tag{7.42}$$

Equation (7.42) indicates that the phugoid damping ratio is inversely proportional to the lift to drag ratio (L/D). Of course we must keep in mind all the assumptions we made to obtain this result. It does indicate that airplanes with high values of L/D may have poor phugoid damping. If this is the case, precise control of speed becomes difficult, which can be a problem during the initial phases of a landing pattern. However, after the gear and flaps have been lowered, L/D is reduced and damping of the phugoid improves.

Example 7.10

To illustrate the concepts of transfer functions, characteristic equations, and the modes of motion, we will consider a Lear Jet flying at 0.7 Mach and 40,000 ft. The 3-DOF longitudinal transfer functions are approximated by

$$\frac{u(s)}{\delta_e(s)} = \frac{(6.312)s^2 - (4927)s - 4302}{(675.9)s^4 + (1371)s^3 + (5459)s^2 + (86.31)s + 44.78}$$

$$\frac{\alpha(s)}{\delta_e(s)} = \frac{(0.746)s^3 + (208.3)s^2 + (2.665)s + 1.39}{(675.9)s^4 + (1371)s^3 + (5459)s^2 + (86.31)s + 44.78}$$

$$\frac{\theta(s)}{\delta_e(s)} = \frac{(208.1)s^2 + (136.9)s + 2.380}{(675.9)s^4 + (1371)s^3 + (5459)s^2 + (86.31)s + 44.78}$$

Find the natural frequency, damping ratio, damped frequency, time constant, and period of oscillation for the short period and phugoid modes.

The characteristic equation is found by setting the denominator of the transfer function equal to 0. The characteristic equation for the Lear Jet's longitudinal motion is

$$675.9s^4 + 1371s^3 + 5459s^2 + 86.31s + 44.78 = 0$$

or

$$s^4 + 2.0284s^3 + 8.0766s^2 + 0.1277s + 0.06625 = 0$$

Source from Yechout, T.R. "Introduction to Aircraft Flight Mechanics", AIAA education Series, 2003

Using a root solver, such as those available in MATLAB, the four roots are found to be

$$s_{1,2} = \zeta_{SP}\omega_{N_{SP}} \pm i\omega_{D_{SP}} = -1.008 \pm i(2.651)$$
$$s_{3,4} = \zeta_{PH}\omega_{N_{PH}} \pm i\omega_{D_{PH}} = -0.0069 \pm i(0.0905)$$

The roots with the largest ω_D are obviously associated with the short period mode of motion, while the other roots are associated with the phugoid mode of motion.

$$\zeta_{SP}\omega_{N_{SP}} = 1.008\omega_{D_{SP}} = 2.651 \text{ rad/s} \quad \text{(short period)}$$
$$\zeta_{PH}\omega_{N_{PH}} = 0.0069\omega_{D_{PH}} = 0.0905 \text{ rad/s} \quad \text{(phugoid)}$$
$$\omega_{N_{SP}} = \sqrt{(-\zeta\omega_N)^2_{SP} + \omega^2_{D_{SP}}} = \sqrt{(-1.008)^2 + (2.651)^2} = 2.836 \text{ rad/s}$$
$$\omega_{N_{PH}} = \sqrt{(-\zeta\omega_N)^2_{PH} + \omega^2_{D_{PH}}} = \sqrt{(-0.0069)^2 + (0.0905)^2} = 0.091 \text{ rad/s}$$
$$\zeta_{SP} = \frac{\zeta_{SP}\omega_{N_{SP}}}{\omega_{N_{SP}}} = \frac{1.008}{2.836} = 0.355$$
$$\zeta_{PH} = \frac{\zeta_{PH}\omega_{N_{PH}}}{\omega_{N_{PH}}} = \frac{0.0069}{0.091} = 0.076$$
$$\tau_{SP} = \frac{1}{\zeta_{SP}\omega_{N_{SP}}} = \frac{1}{1.008} = 0.992 \text{ s}$$
$$\tau_{PH} = \frac{1}{\zeta_{PH}\omega_{N_{PH}}} = \frac{1}{0.0069} = 144.93 \text{ s}$$

The fourth-order characteristic equation can therefore be written as two second-order (oscillatory) characteristic equations in the form

$$(s^2 + 2\zeta_{SP}\omega_{N_{SP}}s + \omega^2_{N_{SP}})(s^2 + 2\zeta_{PH}\omega_{N_{PH}}s + \omega^2_{N_{PH}}) = 0$$

For the Lear Jet example, this is

$$(s^2 + 2.016s + 8.0429)(s^2 + 0.0138s + 0.00828) = 0$$

Note that the relative magnitudes of the short period and phugoid characteristics are as expected

$$\omega_{N_{SP}} = 2.836 \text{ rad/s} > \omega_{N_{PH}} = 0.091 \text{ rad/s}$$
$$\zeta_{SP} = 0.355 > \zeta_{PH} = 0.076$$
$$\omega_{D_{SP}} = 2.651 \text{ rad/s} > \omega_{D_{PH}} = 0.905 \text{ rad/s}$$
$$\tau_{SP} = 0.992 \text{ s} < \tau_{PH} = 144.93 \text{ s}$$

Source from Yechout, T.R. "Introduction to Aircraft Flight Mechanics", AIAA education Series, 2003

The period of oscillation can be found using

$$T = \frac{2\pi}{\omega_D}$$

$$T_{sp} = \frac{2\pi}{2.651}\ \text{s} = 2.37\ \text{s}$$

$$T_{ph} = \frac{2\pi}{0.0905}\ \text{s} = 69.43\ \text{s}$$

It is also worthwhile to plot the short period and phugoid roots from Example 7.10 on the complex plane. This is accomplished in Fig. 7.15. Notice that the short period roots are further out from the origin and have a higher damping ratio than the phugoid roots. The relative location of these roots is typical for most aircraft.

Example 7.11

Use the short period and phugoid 2-DOF approximations to estimate the natural frequency, damping ratio, damped frequency, and period of oscillation for the Lear Jet. Compare the approximation results to those obtained in Example 7.10.

Using the short period approximation Eq. (7.34), we have

$$s^2 + 2.0173s + 8.0777 = 0$$

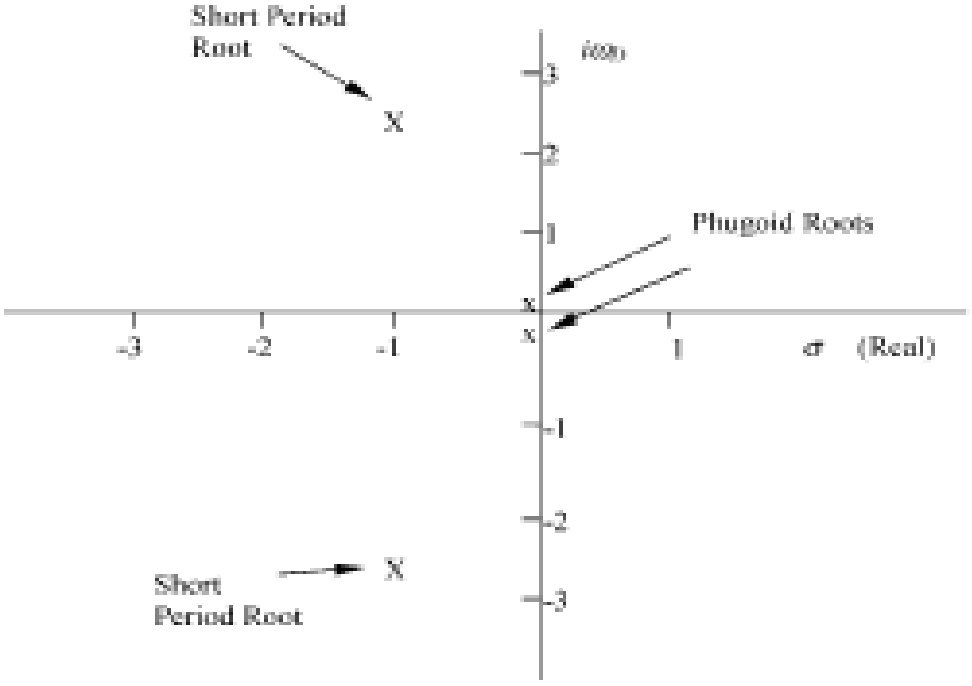

Fig. 7.15 Complex plane plot of longitudinal roots for Example 7.10.

Source from Yechout, T.R. "Introduction to Aircraft Flight Mechanics", AIAA education Series, 2003

$$\omega_{n_{sp}} = \sqrt{8.0777}\ \text{rad/s} = 2.842\ \text{rad/s} \qquad (2.836\ \text{rad/s for the 3-DOF case})$$

Because

$$2\zeta_{sp}\omega_{n_{sp}} = 2.0173 \Rightarrow \zeta_{sp} = 0.355 \qquad (0.355\ \text{for the 3-DOF case})$$

and

$$\omega_{D_{sp}} = \omega_{n_{sp}}\sqrt{1-\zeta_{sp}^2} = 2.657\ \text{rad/s} \qquad (2.651\ \text{rad/s for the 3-DOF case})$$

$$T_{sp} = \frac{2\pi}{\omega_{D_{sp}}} = 2.365\ \text{s} \qquad (2.37\ \text{s for the 3-DOF case})$$

As can be seen, the comparisons with the 3-DOF case are very good.

For the phugoid approximation, we use Eq. (7.39) to obtain the characteristic equation:

$$s^2 + 0.0075s + 0.00663 = 0$$

For natural frequency we have

$$\omega_{n_{PH}} = \sqrt{0.00663}\ \text{rad/s} = 0.0814\ \text{rad/s} \qquad (0.091\ \text{rad/s for the 3-DOF case})$$

To obtain damping ratio,

$$2\zeta_{PH}\omega_{n_{PH}} = 0.0075 \Rightarrow \zeta_{PH} = 0.0461 \qquad (0.076\ \text{for the 3-DOF case})$$

and

$$\omega_{D_{PH}} = \omega_{n_{PH}}\sqrt{1-\zeta_{PH}^2} = 0.0813\ \text{rad/s} \qquad (0.0905\ \text{rad/s for the 3-DOF case})$$

$$T_{PH} = \frac{2\pi}{\omega_{D_{PH}}} = 77.27\ \text{s} \qquad (69.43\ \text{s for the 3-DOF case})$$

In this example, the 2-DOF phugoid approximation provides estimates to approximately 10% accuracy with the exception of damping ratio, which has a 40% error.

Source from Yechout, T.R. "Introduction to Aircraft Flight Mechanics", AIAA education Series, 2003

7.3.3 Lateral-Directional Linearized EOM in Laplace Form

We next use the same approach developed in Sec. 7.3.2 to transform the linearized lateral-directional EOM developed in Sec. 6.5 to the Laplace domain. Again, the linearized EOM Eq. (6.133) are repeated for reference

$$\begin{aligned} \dot{v} + U_1 r &= g\phi\cos\Theta_1 + Y_\beta\beta + Y_p p + Y_r r + Y_{\delta_a}\delta_a + Y_{\delta_r}\delta_r \\ \dot{p} - \tilde{A}_1\dot{r} &= L_\beta\beta + L_p p + L_r r + L_{\delta_a}\delta_a + L_{\delta_r}\delta_r \\ \dot{r} - \tilde{B}_1\dot{p} &= N_\beta\beta + N_{T_\beta}\beta + N_r r + N_{\delta_a}\delta_a + N_{\delta_r}\delta_r \end{aligned} \tag{7.43}$$

where

$$\tilde{A}_1 = \frac{I_{xz}}{I_{xx}} \qquad \text{and} \qquad \tilde{B}_1 = \frac{I_{xz}}{I_{zz}}$$

Notice that the three EOM have five aircraft motion variables (v, p, r, ϕ, and β) along with δ_a and δ_r. δ_a and δ_r are the inputs or forcing functions for the lateral-directional system. Because we have only three equations, we will reduce the number of motion variables to three by using the kinematic equations [Eq. (4.80)] and the assumption of a small pitch attitude angle (Θ_1). Also recall that we previously made the assumption of $\phi = 0$ (wings level in trimmed flight) in Sec. 7.3.2. With these assumptions, we have

$$p = \dot{\phi} \qquad \text{and} \qquad r = \dot{\psi}$$

Also, for small perturbations

$$\beta \approx \frac{v}{U_1} \Rightarrow v \approx \beta U_1 \qquad \text{and} \qquad \dot{v} \approx \dot{\beta} U_1$$

Therefore, we can reduce our aircraft motion variables to β, ϕ, and ψ. These should be thought of as the outputs for our system of lateral-directional differential equations. We could have easily chosen v, p, and r for the output variables but instead chose the three angles. With zero initial conditions, the Laplace transform of Eq. (7.43) becomes

$$\begin{aligned} s\beta(s)U_1 + s\psi(s) &= g\phi(s)\cos\Theta_1 + Y_\beta\beta(s) + Y_p s\phi(s) + Y_r s\psi(s) + Y_{\delta_a}\delta_a(s) \\ &\quad + Y_{\delta_r}\delta_r(s) \\ s^2\phi(s) - \tilde{A}_1 s^2\psi(s) &= L_\beta\beta(s) + L_p s\phi(s) + L_r s\psi(s) + L_{\delta_a}\delta_a(s) + L_{\delta_r}\delta_r(s) \\ s^2\psi(s) - \tilde{B}_1 s^2\phi(s) &= N_\beta\beta(s) + N_{T_\beta}\beta(s) + N_p s\phi(s) + N_r s\psi(s) + N_{\delta_a}\delta_a(s) \\ &\quad + N_{\delta_r}\delta_r(s) \end{aligned}$$

Source from Yechout, T.R. "Introduction to Aircraft Flight Mechanics", AIAA education Series, 2003

Combining terms and moving the control inputs to the right-hand side of the equal sign, we have

$$(sU_1 - Y_\beta)\beta(s) - (sY_p + g\cos\Theta_1)\phi(s) + s(U_1 - Y_r)\psi(s) = Y_{\delta_a}\delta_a(s) + Y_{\delta_r}\delta_r(s)$$
$$-L_\beta\beta(s) + (s^2 - L_p s)\phi(s) - (s^2\bar{A}_1 + L_r s)\psi(s) = L_{\delta_a}\delta_a(s) + L_{\delta_r}\delta_r(s)$$
$$-(N_\beta + N_{T_\beta})\beta(s) - (s^2\bar{B}_1 + N_p s)\phi(s) + (s^2 - sN_r)\psi(s) = N_a\delta_a(s) + N_r\delta_r(s)$$

Regrouping in matrix form

$$\begin{bmatrix} (sU_1 - Y_\beta) & -(sY_p + g\cos\Theta_1) & s(U_1 - Y_r) \\ -L_\beta & (s^2 - L_p s) & -(s^2\bar{A}_1 + sL_r) \\ -N_\beta - N_{T_\beta} & -(s^2\bar{B}_1 + N_p s) & (s^2 - sN_r) \end{bmatrix} \begin{bmatrix} \beta(s) \\ \phi(s) \\ \psi(s) \end{bmatrix}$$
$$= \begin{bmatrix} Y_{\delta_a} & Y_{\delta_r} \\ L_{\delta_a} & L_{\delta_r} \\ N_{\delta_a} & N_{\delta_r} \end{bmatrix} \begin{bmatrix} \delta_a(s) \\ \delta_r(s) \end{bmatrix} \tag{7.44}$$

and each of the six lateral-directional transfer functions can be determined using Cramer's rule as presented in Appendices F and G. The six lateral-directional transfer functions are

$$\beta(s)/\delta_a(s), \quad \beta(s)/\delta_r(s), \quad \phi(s)/\delta_a(s), \quad \phi(s)/\delta_r(s),$$
$$\psi(s)/\delta_a(s), \quad \text{and} \quad \psi(s)/\delta_r(s).$$

Notice that there are six lateral-directional transfer functions vs the three we have for longitudinal motion. This results from the fact that we have two possible control inputs (δ_a and δ_r), each of which can cause changes in the three lateral-directional motion variables. In an attempt to minimize the number of equations needed to represent these transfer functions, we will temporarily drop the subscript on δ_a and δ_r because the transfer functions for each have the same general form (Appendix G). Each of the lateral-directional transfer functions can then be represented as the ratio of two polynominals in the Laplace variables.

$$\frac{\beta(s)}{\delta(s)} = \frac{A_\beta s^3 + B_\beta s^2 + C_\beta s + D_\beta}{E's^4 + F's^3 + G's^2 + H's + I'} \tag{7.45}$$

$$\frac{\phi(s)}{\delta(s)} = \frac{A_\phi s^2 + B_\phi s + C_\phi}{E's^4 + F's^3 + G's^2 + H's + I'} \tag{7.46}$$

$$\frac{\psi(s)}{\delta(s)} = \frac{A_\psi s^3 + B_\psi s^2 + C_\psi s + D_\psi}{s(E's^4 + F's^3 + G's^2 + H's + I')} \tag{7.47}$$

Equations (7.45), (7.46), and (7.47) represent the general form of the six lateral-directional transfer functions. For example, to obtain the $\beta(s)/\delta_a(s)$

Source from Yechout, T.R. "Introduction to Aircraft Flight Mechanics", AIAA education Series, 2003

transfer function, simply use Eq. (7.45) and use the δ_a derivatives (Y_{δ_a}, L_{δ_a}, and N_{δ_a}) in the determination of A_β, B_β, C_β, and D_β (see Appendix G). In a similar fashion, to obtain the $\beta(s)/\delta_r(s)$ transfer function, Eq. (7.45) is used, and the δ_r derivatives (Y_{δ_r}, L_{δ_r}, and N_{δ_r}) are used in the determination of A_β, B_β, C_β, and D_β. As in the case of the longitudinal transfer functions, the numerator of each lateral-directional transfer function is different. Because the numerator affects the magnitude of the response, each of the three motion variables will have a different magnitude of response.

All six lateral-directional transfer functions have essentially the same denominator, which leads to the same characteristic equation:

$$E's^4 + F's^3 + G's^2 + H's + I' = 0$$

The extra s in the denominator of the $\psi(s)/\delta(s)$ transfer function indicates that the airplane is neutrally stable in heading (that is, it will not return to a trim heading when disturbed). The associated piece of the characteristic equation ($s = 0$) leads to a constant in the time response but is not that interesting from the standpoint of dynamic stability. Notice that E', F', G', H', and I', are not the same as the value of E, F, G, H, and I in Eqs. (7.28–7.30) (the longitudinal transfer functions). Because the characteristic equation determines the dynamic stability characteristics of the response, all six transfer functions will have the same dynamic characteristics (ζ, ω_n, and τ) but a different magnitude of response.

7.3.3.1 Three-degree-of-freedom analysis of the lateral-directional modes of motion. The preceding development of transfer functions for the three lateral-directional motion variables β, ϕ, and ψ leads to a 3-DOF solution for lateral-directional motion. Normally, the fourth-order characteristic equation for lateral-directional motion is written as the product of one second-order (oscillatory) and two first-order (nonoscillatory) polynomials.

$$(s^2 + 2\zeta_{DR}\omega_{n_{DR}}s + \omega_{n_{DR}}^2)\left(s + \frac{1}{\tau_r}\right)\left(s + \frac{1}{\tau_s}\right) = 0 \qquad (7.48)$$

The subscript DR refers to the dutch roll mode, the subscript r refers to the roll mode, and the subscript s refers to the spiral mode. All airplanes have these three lateral-directional dynamic modes. Each of these polynominals can be thought of as a separate characteristic equation that defines the dynamic characteristics of its respective mode.

As with the longitudinal case, *the coefficients (and roots) of each characteristic equation change with flight condition, airplane mass, mass distribution, airplane geometry, and aerodynamic characteristics*. These changes translate to changes in $\omega_{n_{DR}}$, ζ_{DR}, τ_r, and τ_s, but the fundamental presence of the dutch roll, roll, and spiral modes is maintained.

The **dutch roll mode** is a second-order response (**complex conjugate roots**) usually characterized by concurrent oscillations in the three lateral-directional motion variables β, ϕ, and ψ. In the discussion on static stability, it was observed that sideslip generates both yawing and rolling moments that lead to a coupled motion between β, ϕ, and ψ. These oscillations may be of high or

Source from Yechout, T.R. "Introduction to Aircraft Flight Mechanics", AIAA education Series, 2003

low frequency and may be lightly or heavily damped. The dutch roll usually begins with a sideslip perturbation followed by oscillations in roll and yaw. The dutch roll motion is something like that of an ice skater's body weaving back and forth as weight shifts from one foot to the other. As the magnitude of C_{l_β} (lateral static stability) becomes larger, more roll coupling is present during dutch roll oscillations, and the dutch roll characteristics typically become more objectionable. Objectionable dutch roll characteristics adversely affect precision tasks like air-to-air and air-to-ground tracking, and formation flying.

The **roll mode** has a **real root** and a first-order (nonoscillatory) response that involves almost a pure rolling motion about the x stability axis. It is usually stable at low and moderate angles of attack but may be unstable at high angles of attack. The roll mode can be excited by a disturbance or an aileron input. It is easiest to characterize the roll mode when discussing response to an aileron input. If a step aileron input (δ_a) is made to the aircraft, there is an exponential rise in roll rate ($\approx \dot{\phi}$) until a steady state roll rate is achieved. We saw this first-order type response in Sec. 7.1.1.1. From the pilot's standpoint, the time taken during the exponential rise to steady state is interpreted as a finite delay, which we usually characterize with the time constant (τ_r). If τ_r is too large, the aircraft is considered sluggish because it may take too long for the commanded roll rate to build up. Likewise, if τ_r is too small, the aircraft may be too responsive to external disturbances such as turbulence.

The **spiral mode** is a first-order response (**real root**) that involves a relatively slow roll and yawing motion of the aircraft. It may be stable or unstable. The spiral is usually initiated by a displacement in roll angle and appears as a descending turn with increasing roll angle if unstable. If the spiral is stable, the aircraft simply returns to wings level after a roll angle displacement. The primary motion variables during the spiral are ϕ and ψ, while β remains close to zero. A high degree of lateral stability (C_{l_β}) will tend to make the spiral stable, while a high degree of directional stability (C_{n_β}) will tend to make the spiral unstable. Fortunately, spiral instability can be tolerated as long as the time to double amplitude (based on the initial roll angle displacement) is gradual (greater than approximately 4 s). Under these conditions, the pilot can return the aircraft to wings level flight with little difficulty using an aileron input. If the spiral mode is unstable, the time to double amplitude (T_2) is calculated with

$$T_2 = \frac{\ln 2}{\text{unstable root}} = \frac{0.693}{\text{unstable root}} \tag{7.49}$$

Spiral stability is usually compromised for good dutch roll characteristics that are typically achieved with relatively high directional stability and relatively low lateral stability.

Example 7.12

The β/δ_a transfer function for a T-37 cruising at 30,000 ft and 0.46 Mach is given next. Find the natural frequency, damping ratio, and damped frequency for the dutch roll mode, and the time constant for the dutch roll, roll, and

Source from Yechout, T.R. "Introduction to Aircraft Flight Mechanics", AIAA education Series, 2003

spiral modes.

$$\frac{\beta}{\delta_a} = 1.41\frac{(s+2.05)(s+0.0741)}{(s+1.27)(s+0.0037)(s^2+0.227s+5.80)}$$

We go immediately to the three characteristic equations

$$s^2 + 0.227s + 5.8 = 0$$
$$s + 1.27 = 0$$
$$s + 0.0037 = 0$$

The second-order equation is for the dutch roll mode, and we have

$$\omega_{n_{DR}} = \sqrt{5.8} = 2.41 \text{ rad/s}$$

The damping ratio for dutch roll becomes

$$\zeta_{DR} = \frac{0.227}{2\omega_{n_{DR}}} = 0.0471$$

and the damped frequency is

$$\omega_{D_{DR}} = \omega_{n_{DR}}\sqrt{1-\zeta_{DR}^2} = 2.41\sqrt{1-(0.0471)^2} = 2.407 \text{ rad/s}$$

The time constant for dutch roll is

$$\tau_{DR} = \frac{1}{\zeta_{DR}\omega_{n_{DR}}} = \frac{1}{(0.0471)(2.41)} = 8.81 \text{ s}$$

At this point, we should comment on the relatively low damping ratio and large time constant for the dutch roll mode. As we will see, these do not pass military specifications. As a result, the T-37 has a yaw damper installed to improve the basic airframe dutch roll characteristics.

The two first-order characteristic equations are for the roll and spiral modes. Referring back to Eq. (7.48) and realizing that the roll mode will have a smaller time constant than the spiral mode, we have

$$\tau_r = \frac{1}{1.27} = 0.787 \text{ s}$$
$$\tau_s = \frac{1}{0.0037} = 270 \text{ s}$$

A few observations are in order. With the roll mode time constant being less than 1 s, we can see that the T-37 roll response is fairly crisp. The spiral mode is stable for this flight condition as indicated by the negative root

Source from Yechout, T.R. "Introduction to Aircraft Flight Mechanics", AIAA education Series, 2003

($s = -0.0037$). Because it is stable, the time constant indicates the time it takes to return to 36.8% (1–0.632) of the initial displaced roll angle as the aircraft returns to a wings-level attitude. For example, if the initial displaced roll angle is 10 deg, it will take about 4.5 min (270 s) to return to a 3.68-deg roll attitude (assuming the pilot makes no aileron input).

If the characteristic equation for the spiral had been

$$s - 0.0037 = 0$$

then the spiral would be unstable (a positive root at $s = 0.0037$) and the time to double amplitude would have been [using Eq. (7.49)]

$$T_2 = \frac{0.693}{0.0037} = 187 \text{ s}$$

A summary of root and response characteristics for the two longitudinal and three lateral-directional dynamic modes of aircraft motion is presented in Table 7.2.

7.3.3.2 One-degree-of-freedom roll approximation. To gain an understanding of the stability parameters and derivatives that influence the roll mode, we can eliminate two of the three degrees of freedom or motion variables. The roll mode is the simplest of the five dynamic modes. We begin with Eq. (7.44) and retain only the ϕ motion variable, the δ_a control input, and the rolling moment equation. Thus, Eq. (7.44) simplifies to

$$(s^2 - L_p s)\phi(s) = L_{\delta_a}\delta_a(s)$$

The roll approximation transfer function becomes

$$\frac{\phi(s)}{\delta_a(s)} = \frac{L_{\delta_a}}{s(s - L_p)} \tag{7.50}$$

Table 7.2 Root and response characteristics for the aircraft dynamic modes of motion

Mode	Root type	Response
Longitudinal		
Short period	Complex conjugate	Oscillatory
Phugoid	Complex conjugate	Oscillatory
Lateral-directional		
Dutch roll	Complex conjugate	Oscillatory
Roll	Real	Nonoscillatory
Spiral	Real	Nonoscillatory

Source from Yechout, T.R. "Introduction to Aircraft Flight Mechanics", AIAA education Series, 2003

Equation (7.50) yields two roots for the characteristic equation: 0 and L_p. The root at $s = 0$ is of little interest because it leads to the steady-state value; however, the root $s = L_p$ is of more interest because it leads directly to an estimate of the time constant for the roll mode

$$\tau_r \approx -\frac{1}{L_p} \tag{7.51}$$

Recall that L_p is the roll damping stability parameter that is a direct function of C_{l_p} the roll damping derivative. L_p typically is negative, which makes the roll mode stable. Thus, we can deduce from Eq. (7.51) that the higher the roll damping, the smaller the roll mode time constant. This may seem counter-intuitive at first, but remember that the time constant is only an indicator of the time to a steady-state value. Our intuition tells us that more damping should lead to a lower steady-state value, so we will investigate roll rate response to a step aileron input using our approximation. We will define the magnitude of the step aileron input as δ_a. Thus

$$\delta_a(s) = \frac{\delta_a}{s}$$

and from Eq. (7.50)

$$\phi(s) = \frac{L_{\delta_a}\delta_a}{s^2(s - L_p)}$$

The first step in finding the time response involves partial fractions.

$$\phi(s) = \frac{A}{s^2} + \frac{B}{s} + \frac{C}{(s - L_p)}$$

where

$$A = s^2\phi(s)|_{s=0} = -\frac{L_{\delta_a}\delta_a}{L_p}$$

$$B = \frac{\mathrm{d}}{\mathrm{d}s}[s^2\phi(s)]_{s=0} = -\frac{L_{\delta_a}\delta_a}{(s - L_p)}\bigg|_{s=0} = -\frac{L_{\delta_a}}{L_p^2}\delta_a$$

$$C = (s - L_p s)\phi(s)|_{s=L_p} = \frac{L_{\delta_a}\delta_a}{s^2}\bigg|_{s=L_p} = \frac{L_{\delta_a}}{L_p^2}\delta_a$$

Combining and taking the inverse Laplace,

$$\phi(t) = -\frac{L_{\delta_a}}{L_p}\delta_a t - \frac{L_{\delta_a}}{L_p^2}\delta_a + \frac{L_{\delta_a}}{L_p^2}\delta_a e^{L_p t} = -\frac{L_{\delta_a}}{L_p}\delta_a t + \left(\frac{L_{\delta_a}}{L_p^2}\delta_a\right)(e^{L_p t} - 1)$$

Source from Yechout, T.R. "Introduction to Aircraft Flight Mechanics", AIAA education Series, 2003

Figure 7.16 plots a time response of the previous equation for roll angle to illustrate a graphical method for obtaining the time constant.

To obtain roll rate, we take the time derivative:

$$\dot{\phi}(t) = p = -\frac{L_{\delta_a}}{L_p}\delta_a + L_p\left(\frac{L_{\delta_a}}{L_p^2}\right)\delta_a e^{L_p t}$$

or

$$\dot{\phi} = -\frac{L_{\delta_a}\delta_a}{L_p}(1 - e^{L_p t}) \tag{7.52}$$

We can make several observations based on Eq. (7.52). The steady-state roll rate achieved will be $-L_{\delta_a}\delta_a/L_p$, which indicates that the larger the aileron control power stability parameter (L_{δ_a}) and/or the larger the magnitude of the aileron input (δ_a), the larger the steady-state roll rate will be. We can also see that the magnitude of the steady-state roll rate is inversly proportional to the roll damping stability parameter (L_p). In addition, the time constant predicted by Eq. (7.51) is evident in the exponential term. To illustrate this, let $t = -1/L_p$ in Eq. (7.52).

$$\dot{\phi} = -\frac{L_{\delta_a}\delta_a}{L_p}(1 - e^{L_p(-1/L_p)}) = -\frac{L_{\delta_a}\delta_a}{L_p}(1 - e^{-1}) = 0.632\left(-\frac{L_{\delta_a}\delta_a}{L_p}\right)$$

Thus, we can see that at $t = \tau_r$, the roll rate is equal to 63.2% of the steady-state value. Figure 7.17 illustrates these points.

7.3.3.3 Two-degree-of-freedom spiral approximation. Spiral motion is dominated by bank angle, ϕ, and heading angle, ψ, while β is very small. To

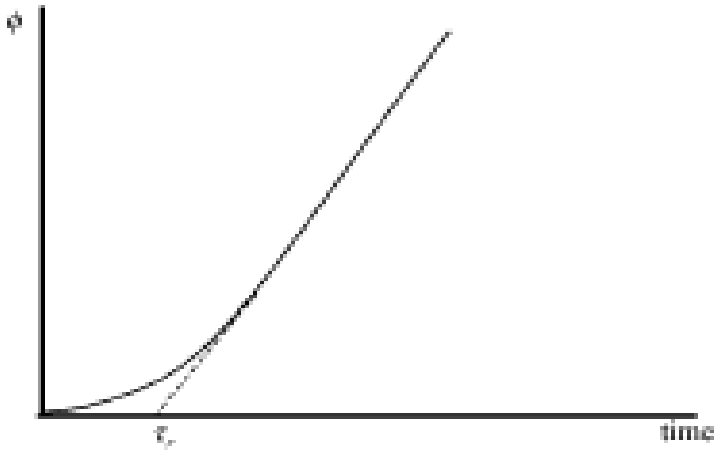

Fig. 7.16 Roll angle response to a step aileron input.

Source from Yechout, T.R. "Introduction to Aircraft Flight Mechanics", AIAA education Series, 2003

achieve a 2-DOF approximation, we will neglect the roll angle motion variable and the sideforce equation. We neglect ϕ because banking does not induce terms that cause the aircraft to roll out (there are no terms like C_{l_ϕ}). β terms do have an effect on roll out because of C_{l_β} to (lateral static stability). Thus, Eq. (7.44) can be simplified to

$$\begin{bmatrix} -L_\beta & -s(s\tilde{A}_1 + L_r) \\ -N_\beta & s(s - N_r) \end{bmatrix} \begin{bmatrix} \beta(s) \\ \psi(s) \end{bmatrix} = \begin{bmatrix} L_{\delta_a} & L_{\delta_r} \\ N_{\delta_a} & N_{\delta_r} \end{bmatrix} \begin{bmatrix} \delta_a(s) \\ \delta_r(s) \end{bmatrix}$$

The characteristic equation becomes:

$$-L_\beta s(s - N_r) - (-N_\beta)\left[-s\left(s\frac{I_{xz}}{I_{xx}} + L_r\right)\right] = 0$$

Close inspection reveals that a common factor in the characteristic equation is s, which can be cancelled. Algebraic manipulation yields the root of the spiral approximation characteristic equation as

$$s \approx \frac{L_\beta N_r - N_\beta L_r}{L_\beta + N_\beta\left(\frac{I_{xz}}{I_{xx}}\right)} \tag{7.53}$$

For the spiral to be stable, this root must be negative. The denominator of Eq. (7.53) is normally negative. Because L_β and N_r are negative, and N_β and L_r are positive, we can deduce that the magnitude of L_β (lateral static stability) should be larger than the magnitude of N_β (directional static stability) for a stable spiral mode (assuming N_r and L_r are of approximately equal magnitude). As discussed earlier, the unfavorable impact of this tradeoff on the dutch roll may drive the designers to accept an unstable spiral (more directional stability)

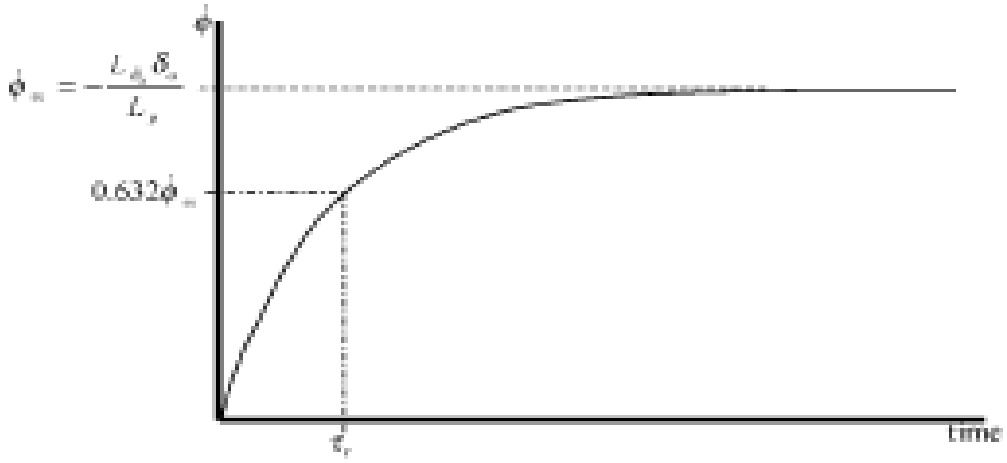

Fig. 7.17 Roll rate response to a step aileron input.

Source from Yechout, T.R. "Introduction to Aircraft Flight Mechanics", AIAA education Series, 2003

in favor of acceptable dutch roll characteristics, especially at low speeds. From Eq. (7.53), the spiral time constant can be approximated by

$$\tau_s \approx \frac{L_\beta + N_\beta\left(\frac{I_{xz}}{I_{xx}}\right)}{N_\beta L_r - L_\beta N_r} \tag{7.54}$$

Unfortunately, the 2-DOF spiral approximation tends to yield poor results. It does, however, provide insight into stability parameters and design features that affect the spiral mode.

7.3.3.4 Two-degree-of-freedom dutch roll approximations. The dutch roll mode is probably the most difficult aircraft dynamic mode to analyze. Several 2-DOF approximations are possible for the dutch roll based on which simplifying assumptions are made. In many cases, it is best to look at an estimate of the absolute value of the ratio of roll angle to sideslip $|\phi/\beta|$ present during a dutch roll oscillation to help guide dutch roll approximation assumptions. It is basically the ratio of the numerator of the $\phi(s)/\delta(s)$ transfer function to the numerator of the $\beta(s)/\delta(s)$ transfer function evaluated at the specific damping ratio and damped frequency conditions. The ϕ/β ratio tells us if the dutch roll is composed of mostly yawing motion, mostly rolling motion, or approximately equal excursions of each. ϕ/β can be visualized by thinking about the pattern a wing tip light traces as the aircraft goes through a dutch roll oscillation. If the pattern is a horizontal ellipse (major axis horizontal), ϕ/β is less than 1 and the roll angle excursions are low compared to the sideslip excursions. If the wing tip pattern is a circle, ϕ/β is approximately 1. A vertical ellipse pattern indicates ϕ/β greater than 1 and the aircraft is considered "rolly", generally because of a high degree of lateral stability. This last case is usually objectionable for precision tracking tasks. The approximation

$$\left|\frac{\phi}{\beta}\right| \approx \left[\frac{C_{l_\beta}}{C_{n_\beta}}\frac{I_{xz}}{I_{xx}}\frac{1}{\rho U_1}\right] \tag{7.55}$$

will give us an estimate of ϕ/β as a start. We will look at three different approximations for dutch roll dynamic characteristics based on this estimate.

Test Pilot School approximation. This approximation is used by the USAF Test Pilot School and assumes the dutch roll motion is mostly sideslip ($|\phi/\beta|$ very low). It is believed that the approximations for damping ratio and natural frequency are based on experience.

$$\begin{aligned}\zeta_{DR} &\approx \left(\frac{1}{8}\sqrt{2Sb^3}\right)(-C_{n_r})\left(\frac{\rho}{I_{zz}C_{n_\beta}}\right)^{1/2} \\ \omega_{n_{DR}} &\approx \left(\frac{Sb}{2}\right)^{1/2} U_1\left(\frac{C_{n_\beta}\rho}{I_{zz}}\right)^{1/2}\end{aligned} \tag{7.56}$$

Source from Yechout, T.R. "Introduction to Aircraft Flight Mechanics", AIAA education Series, 2003

Two-degree-of-freedom approximation for low ϕ/β. Here again, the assumption is made that the motion consists primarily of sideslipping and yawing. This is generally the case for aircraft with relatively low lateral stability (C_{l_β}). This approximation eliminates the ϕ motion variable and the rolling moment equation from Eq. (7.44). The result is

$$\begin{bmatrix} (sU_1 - Y_\beta) & s(U_1 - Y_r) \\ -N_\beta & s^2 - sN_r \end{bmatrix} \begin{bmatrix} \beta(s) \\ \psi(s) \end{bmatrix} = \begin{bmatrix} Y_{\delta_a} & Y_{\delta_r} \\ N_{\delta_a} & N_{\delta_r} \end{bmatrix} \begin{bmatrix} \delta_a(s) \\ \delta_r(s) \end{bmatrix}$$

The characteristic equation is obtained from the determinant of the first matrix

$$s\left[s^2 - s\left(N_r + \frac{Y_\beta}{U_1}\right) + \left(\frac{Y_\beta N_r}{U_1} + N_\beta - \frac{N_\beta Y_r}{U_1}\right)\right] = 0$$

and natural frequency and damping ratio are obtained in the usual manner

$$\omega_{n_{DR}} \approx \sqrt{\left\{N_\beta + \frac{1}{U_1}(Y_\beta N_r - N_\beta Y_r)\right\}}$$

$$\zeta_{DR} = \frac{-\left(N_r + \frac{Y_\beta}{U_1}\right)}{2\omega_{n_d}} \tag{7.57}$$

With the previous approximation equations, the strong influence of directional stability (N_β) and yaw damping (N_r) can be seen.

Two-degree-of-freedom approximation for high ϕ/β. This approximation makes the assumption that the dutch roll consists primarily of rolling motion. This may be the case for aircraft with high lateral stability. The ψ motion variable and the yawing moment equation are eliminated from Eq. (7.44).

$$\begin{bmatrix} sU_1 - Y_\beta & -s(Y_p + g) \\ -L_\beta & s^2 - L_p s \end{bmatrix} \begin{bmatrix} \beta(s) \\ \phi(s) \end{bmatrix} = \begin{bmatrix} Y_{\delta_a} & Y_{\delta_r} \\ L_{\delta_a} & L_{\delta_r} \end{bmatrix} \begin{bmatrix} \delta_a(s) \\ \delta_r(s) \end{bmatrix}$$

and, after a few simplifications (Y_p and $\ddot{\phi}$ negligible), the significant characteristic equation becomes

$$(sU_1 - Y_\beta)(-L_p s) - (-g)(-L_\beta) = 0$$

or

$$s^2 - \frac{Y_\beta}{U_1}s + \frac{g}{U_1}\frac{L_\beta}{L_p} = 0$$

Source from Yechout, T.R. "Introduction to Aircraft Flight Mechanics", AIAA education Series, 2003

We then have

$$\omega_{n_{DR}} \approx \sqrt{\frac{g}{U_1}\frac{L_\beta}{L_p}}$$
$$\zeta_{DR} \approx -\frac{Y_\beta}{U_1}\sqrt{\frac{U_1}{g}\frac{L_p}{L_\beta}} \tag{7.58}$$

Notice the strong influence of lateral stability (L_β) and roll damping (L_p) in the previous equations.

The three approximations presented for estimating dutch roll dynamic characteristics all have significant limitations because of the highly coupled motion of the dutch roll. A 3-DOF solution is generally preferred when analyzing the dutch roll.

Example 7.13

Using the same aircraft and flight condition as in Example 7.10, the six lateral-directional transfer functions for the Lear Jet are approximated by

$$\frac{\beta(s)}{\delta_a(s)} = \frac{(4.184)s^2 + (5.589)s + 0.363}{(674.9)s^4 + (421.2)s^3 + (1808)s^2 + (897.9)s + 0.903}$$
$$\frac{\phi(s)}{\delta_a(s)} = \frac{(79.59)s^2 + (14.24)s + 189.3}{(674.9)s^4 + (421.2)s^3 + (1808)s^2 + (897.9)s + 0.903}$$
$$\frac{\psi(s)}{\delta_a(s)} = \frac{-(4.189)s^3 + (2.150)s^2 - (0.150)s + 8.991}{s[(674.9)s^4 + (421.1)s^3 + (1808)s^2 + (897.9)s + 0.903]}$$
$$\frac{\beta(s)}{\delta_r(s)} = \frac{(0.185)s^3 + (18.16)s^2 + (8.285)s - 0.0933}{(674.9)s^4 + (421.2)s^3 + (1808)s^2 + (897.9)s + 0.903}$$
$$\frac{\phi(s)}{\delta_r(s)} = \frac{(8.188)s^2 - (2.045)s - 53.85}{(674.9)s^4 + (421.2)s^3 + (1808)s^2 + (897.9)s + 0.903}$$
$$\frac{\psi(s)}{\delta_r(s)} = \frac{-(18.08)s^3 - (8.921)s^2 - (0.4481)s + 2.559}{s[(674.9)s^4 + (421.2)s^3 + (1808)s^2 + (897.9)s + 0.903]}$$

Find the time constant for the roll and spiral modes and the natural frequency, damping ratio, damped frequency, time constant, and period of oscillation for the dutch roll modes.

The characteristic equation is

$$674.9s^4 + 421.2s^3 + 1808s^2 + 897.9s + 0.903 = 0$$

Source from Yechout, T.R. "Introduction to Aircraft Flight Mechanics", AIAA education Series, 2003

or, in standard form

$$s^4 + 0.6241s^3 + 2.6789s^2 + 1.3304s + 0.001338 = 0$$

Using a root solver such as that available in MATLAB, we have two real roots and one pair of complex conjugates:

$$s_1 = -0.00101 = s_{\text{SPIRAL}} \quad \text{(smaller real root)}$$
$$s_2 = -0.507 = s_{\text{ROLL}} \quad \text{(larger real root)}$$
$$s_{3,4} = -0.0580 \pm j1.617 = -\zeta_{DR}\omega_{N_{DR}} \pm j\omega_{D_{DR}}$$

With these roots, the characteristic equation can be written as

$$(s + 0.00101)(s + 0.507)(s^2 + 0.116s + 2.618) = 0$$

For the roll mode, we have:

$$\tau_{\text{ROLL}} = -\frac{1}{-0.507}\text{ s} = 1.972\text{ s}$$

For the spiral mode, the root is stable (negative) so we have

$$\tau_{\text{SPIRAL}} = -\frac{1}{-0.00101}\text{ s} = 991.8\text{ s}$$

And for the dutch roll, we have:

$$\omega_{D_{DR}} = 1.617 \text{ rad/s}$$
$$\omega_{N_{DR}} = 1.618 \text{ rad/s}$$
$$\zeta_{DR} = 0.036$$
$$\tau_{DR} = -\frac{1}{-\zeta\omega_N} = -\frac{1}{-0.058} = 17.24\text{ s}$$
$$T_{DR} = \frac{2\pi}{\omega_{D_{DR}}} = \frac{2\pi}{1.617} = 3.88\text{ s}$$

Example 7.14

Use the 1-DOF roll approximation, the 2-DOF spiral approximation, and the three dutch roll approximations to approximate the lateral-directional stability characteristics for the Lear Jet. Compare to the 3-DOF values obtained in Example 7.13.

Source from Yechout, T.R. "Introduction to Aircraft Flight Mechanics", AIAA education Series, 2003

For the roll approximation, we use Eq. (7.50) and recall that $\dot{\phi} = p = s\phi$

$$\frac{p(s)}{\delta_a(s)} = s\frac{\phi(s)}{\delta_a(s)} = s\frac{L_{\delta_a}}{s(s - L_p)}$$

Substituting in the values for the Lear Jet:

$$\frac{p(s)}{\delta_a(s)} = \frac{6.77}{s + 0.437}$$

The time constant becomes:

$$\tau_r = -\frac{1}{-0.437} = 2.29\,\text{s} \quad \text{(1-DOF approximation)}$$

Recalling that the 3-DOF roll time constant was 1.972 s, the approximation compares within approximately 16%.

For the spiral mode, Eq. (7.53) yields: $s = -0.0065$. For the time constant we have

$$\tau_s = -\frac{1}{-0.0065} = 153.8\,\text{s} \quad \text{(2-DOF approximation)}$$

The spiral approximation gives a poor prediction of spiral time constant when compared to the 3-DOF value of 991.8 s.

For the dutch roll mode, we first use Eq. (7.55) to calculate

$$\left|\frac{\phi}{\beta}\right| = 3.66$$

We next use the dutch roll approximations to obtain estimates for natural frequency and damping ratio [using Eqs. (7.56–7.58)]. These results are summarized in Table 7.3.

We can see that the Test Pilot School approximation gives reasonably good values for both damping ratio and natural frequency. The 2-DOF low ϕ/β ratio approximation gives a close value for natural frequency but a poor prediction

Table 7.3 Comparison of dutch roll 3-DOF and approximation solutions

	ω_n	ζ
Exact solution (3-DOF Case)	1.618 rad/s	0.036
1) Test Pilot School Approx.	1.69 rad/s	0.033
2) DOF Approx. Low $\lvert\phi/\beta\rvert$	1.62 rad/s	0.058
3) 2 DOF Approx. High $\lvert\phi/\beta\rvert$	0.68 rad/s	0.062

Source from Yechout, T.R. "Introduction to Aircraft Flight Mechanics", AIAA education Series, 2003

for damping ratio. The 2-DOF high ϕ/β approximation has poor predictions for both natural frequency and damping ratio (despite this being a relatively high ϕ/β case). The limitations of each approximation are, of course, directly related to the assumptions made.

7.4 Dynamic Stability Guidelines

In designing an aircraft, there are several guidelines available for natural frequency, damping ratio, and/or time constant for each of the dynamic modes. These guidelines are based on approximately the past half century of flying experience. Dynamic stability characteristics directly affect the "flyability" or handling qualities of an aircraft. The interface between the human pilot (with physical and mental limitations) and inherent aircraft response characteristics must allow for accomplishment of mission objectives throughout the flight envelope. Precision tasks such as landing approach, tracking, and formation flying can only be accomplished successfully if the aircraft's dynamic stability characteristics are within acceptable ranges. These ranges are usually presented in terms of the dynamic characteristics we have discussed. Of course, another aspect of acceptable aircraft handling qualities involves sufficient control authority (usually referred to as control power) to trim and maneuver the aircraft throughout the flight envelope. We will focus on acceptable dynamic stability characteristics as presented in a Military Specification (MIL-F-8785C).[1] Although this specification is no longer a requirement for military aircraft, it does provide a good reference for the designer and establishes the concept of flying qualities levels. Another specification is published for civilian aircraft in Federal Aviation Requirement (FAR) documents.

The advent of modern high-performance aircraft with high-authority control augmentation systems (F-15) and fly-by-wire control systems (F-16 and F-22) has resulted in dynamic stability characteristics that do not conform to classic first- and second-order responses. Military Standard 1797 is currently used to address these advances. However, for purposes of this text, MIL-F-8785C provides a good first step in the discussion of acceptable dynamic stability characteristics.

7.4.1 Aircraft Class

Acceptable flying qualities are a function of the size and mission of an aircraft. To account for this, MIL-F-8785C specifies four classes of aircraft as presented in Table 7.4. The determination of aircraft class is usually the first step in utilization of MIL-F-8785C.

7.4.2 Flight Phase Category

MIL-F-8785C dynamic stability requirements also are a function of the flight phase, or mission segment, that an aircraft is engaged in because different demands are placed on the pilot. For example, air-to-ground tracking requires a higher degree of dutch roll damping than cruising flight. The different flight phases may also be associated with different dynamic pressure conditions, which have a direct effect on dynamic stability characteristics. Table 7.5

Source from Yechout, T.R. "Introduction to Aircraft Flight Mechanics", AIAA education Series, 2003

Table 7.4 MIL-F-8785C aircraft classes

Class	General aircraft types	Specific examples
Class I small, light airplanes	Light utility	T-41
	Primary trainer	T-6
	Light observation	O-1, O-2
Class II medium weight; low-to-medium maneuverability airplanes	Heavy utility/search and rescue	C-21
	Light or medium transport/cargo/tanker	C-130
	Early warning/ECM/Command & control	E-2
	Anti-submarine	S-3A
	Assault transport	C-130
	Reconnaissance	U-2
	Tactical bomber	B-66
	Heavy attack	A-6
	Trainer for Class II	T-1A
Class III large, heavy, low-to-medium maneuverability airplanes	Heavy transport/cargo/tanker	KC-10, C-17
	Heavy bomber	B-52, B-1, B-2
	Patrol/Early warning/ECM/Command & control	P-3, SR-71
	Trainer for Class III	TC-135
Class IV high-maneuverability airplanes	Figher/Intecepter	F-22, F-15, F-16
	Attack	F-15E, A-10
	Tactical reconnaissance	RF-4
	Observation	OV-10
	Trainer for Class IV	T-38

presents the three flight phase categories into which MIL-F-8785C divides all mission segments for military aircraft. Terminal refers to the takeoff and landing phases accomplished in a terminal area. Normally, the gear and flaps down configuration is associated with the terminal flight phase (Category C), while the gear and flaps up configuration is associated with Category A and B. When no flight phase category is stated in a dynamic stability requirement, that requirement applies to all three categories.

7.4.3 Flying Quality Levels

An aircraft's compliance to the dynamic stability requirements of MIL-8785C is defined in terms of three flying quality levels. These are summarized in Table 7.6.

Level 1 is the highest level of flying qualities and is the requirement within the operational flight envelope with all aircraft systems in their normal operating state. It is important to define the term operational flight envelope. Flight envelopes are usually defined by boundaries of speed, altitude, load factor, angle of attack, and/or sideslip. The operational flight envelope is the innermost or inside envelope when compared with the boundaries of the service

Source from Yechout, T.R. "Introduction to Aircraft Flight Mechanics", AIAA education Series, 2003

Table 7.5 MIL-F-8785C flight phase categories

Category A	Those nonterminal flight phases that require rapid maneuvering, precision tracking, or precise flight-path control. Included in this category are: (a) Air-to-air combat (CO) (b) Ground attack (GA) (c) Weapon delivery/launch (WD) (d) Aerial recovery (AR) (e) Reconnaissance (RC) (f) In-flight refueling (receiver) (RR) (g) Terrain following (TF) (h) Antisubmarine search (AS) (i) Close formation flying (FF)
Category B	Those nonterminal flight phases that are normally accomplished using gradual maneuvers and without precision tracking, although accurate flight-path control may be required. Included in this category are: (a) Climb (CL) (b) Cruise (CR) (c) Loiter (LO) (d) In-flight refueling (tanker) (RT) (e) Descent (D) (f) Emergency descent (ED) (g) Emergency deceleration (DE) (h) Aerial delivery (AD)
Category C	Those terminal flight phases that are normally accomplished using gradual maneuvers and which usually require accurate flight-path control. Included in this category are: (a) Takeoff (TO) (b) Catapult takeoff (CT) (c) Approach (PA) (d) Wave-off/go-around (WO) (e) Landing (L)

flight envelope and the permissible flight envelope (to be discussed later in this section). The boundaries of the operational flight envelope are set by **mission requirements**. Expected missions are analyzed to determine what speed, altitude, load factor, angle of attack, and/or sideslip ranges will be needed to accomplish each mission, and this information is used to define the operational flight envelope.

Level 2 implies an increase in pilot workload and/or a degredation in mission effectiveness because of decreased dynamic stability (or control power) characteristics. Level 2 is considered acceptable when the cumulative probability of all failure states that could result in Level 2 flying qualities within the operational flight envelope is less than once every 100 flights. For example, an aircraft has ten failure states that result in Level 2 flying qualities in the opera-

Table 7.6 MIL-F-8785C flying quality levels

Level 1	Flying qualities clearly adequate for the mission flight phase
Level 2	Flying qualities adequate to accomplish the mission flight phase, but some increase in pilot workload or degradation in mission effectiveness, or both, exists
Level 3	Flying qualities such that the airplane can be controlled safely, but pilot workload is excessive or mission effectiveness is inadequate, or both. Category A flight phases can be terminated safely, and Category B and C flight phases can be completed

Source from Yechout, T.R. "Introduction to Aircraft Flight Mechanics", AIAA education Series, 2003

tional flight envelope, two of which each have a probability of 5×10^{-3}/flight, and the other eight each have probabilities of 1×10^{-3}/flight. Such a situation fails the MIL-F-8785C requirement because the cumulative probability is 1.8×10^{-2}/flight, nearly twice the allowable limit. The reliability of these failure states would have to be improved to meet the cumulative requirement.

Level 3 requires that control of the airplane is maintained but allows excessive pilot workload and/or inadequate mission effectiveness. It is basically a "get home" level and is considered acceptable when the cumulative probability of all failure states that result in Level 3 in the operational flight envelope is less than once every 10,000 flights, and the cumulative probability of all failure states that result in Level 3 in the service flight envelope is less than once every 100 flights. Before defining the service flight envelope, we will define the outermost flight envelope, the permissible flight envelope. The boundaries of the permissible flight envelope are set by aircraft performance and safety limits. The aircraft either is not capable of exceeding these limits, or, if it can exceed these limits, potentially catastrophic failures may occur (such as structural failure or engine failure) when beyond these limits. The boundaries of the service flight envelope are between the operational flight envelope and the permissible flight envelope (that is, its boundaries contain the operational flight envelope but it is contained within the permissible flight envelope). Outside the service flight envelope, but within the permissible flight envelope, the handling qualities with the aircraft systems in the normal state are expected to be at least recoverable. This means that controlled flight may be temporarily lost (as in a stall), but the pilot can safely return to the service flight envelope and regain control. The service flight envelope basically acts as a safety margin between the operational flight envelope and the permissible flight envelope. The handling qualities of an aircraft may degrade as it nears the limits of the permissible flight envelope, but we want the degradation to be gradual, not sudden. Level 2 handling qualities are generally the minimum requirement, with all systems in the normal state, within the service flight envelope but outside the operational flight envelope. This ensures that the pilot has handling qualities good enough to avoid entering or exceeding the permissible flight envelope inadvertently. A level better than the one specified is also considered acceptable for a given failure situation. Section 7.3.5 will discuss the Cooper-Harper rating scale for aircraft flying qualities which has a direct correlation to the MIL-F-8785C levels discussed here. A simplified decision process for using MIL-F-8785C is presented in Fig. 7.18.*

7.4.4 Short Period

Dynamic stability guidelines for the short period mode are covered in two documents. Both will be addressed in this section.

7.4.4.1 MIL-F-8785C. MIL-F-8785C requires that the short period mode meet both a damping ratio and natural frequency requirement. The equivalent damping ratio requirements are presented in Table 7.7 and are a function of

Source from Yechout, T.R. "Introduction to Aircraft Flight Mechanics", AIAA education Series, 2003

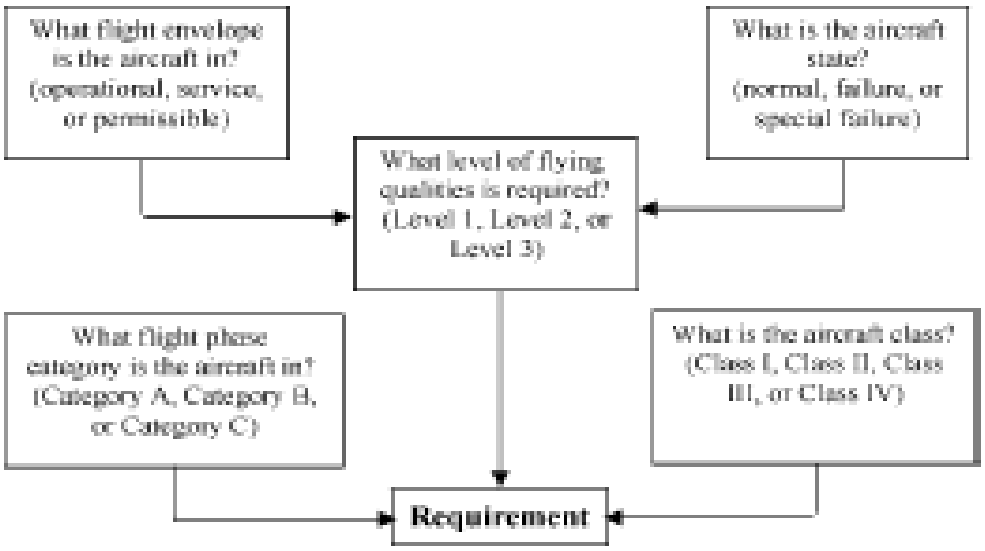

Fig. 7.18 Simplified decision process for using MIL-F-8785C.

category. The term equivalent is used so that aircraft with high authority augmentation systems or fly-by-wire systems can also be included. These aircraft have dynamic response characteristics (by design) that are significantly different from those of the basic airframe.

MIL-F-8785C requires that the short period natural frequency fall within an upper and lower limit as a function of the aircraft's n/α ratio and flight phase category. Figures 7.19–7.21 present the Level 1, 2, and 3 regions for short period natural frequency by category. Notice the logarithmic scale for n/α. This parameter can be estimated for an aircraft using

$$\frac{n}{\alpha} \approx -\frac{Z_\alpha}{g} \tag{7.59}$$

n/α can be thought of as a load factor (n) sensitivity parameter. It increases with increases in C_{L_α} and wing area, and it decreases as weight increases.

The MIL-F-8785C short period requirement will be satisfied if the roots of the short period mode fall within a region on the s plane. In general terms, this region is presented as the crosshatched area in Fig. 7.22.

Table 7.7 Short period damping ratio (ζ_{sp}) limits

	Category A and C flight phases		Category B flight phases	
	Minimum	Maximum	Minimum	Maximum
Level 1	0.35	1.30	0.30	2.00
Level 2	0.25	2.00	0.20	2.00
Level 3	0.15*	no maximum	0.15*	no maximum

*May be reduced at altitudes above 20,000 ft if approved by the procuring activity.

Source from Yechout, T.R. "Introduction to Aircraft Flight Mechanics", AIAA education Series, 2003

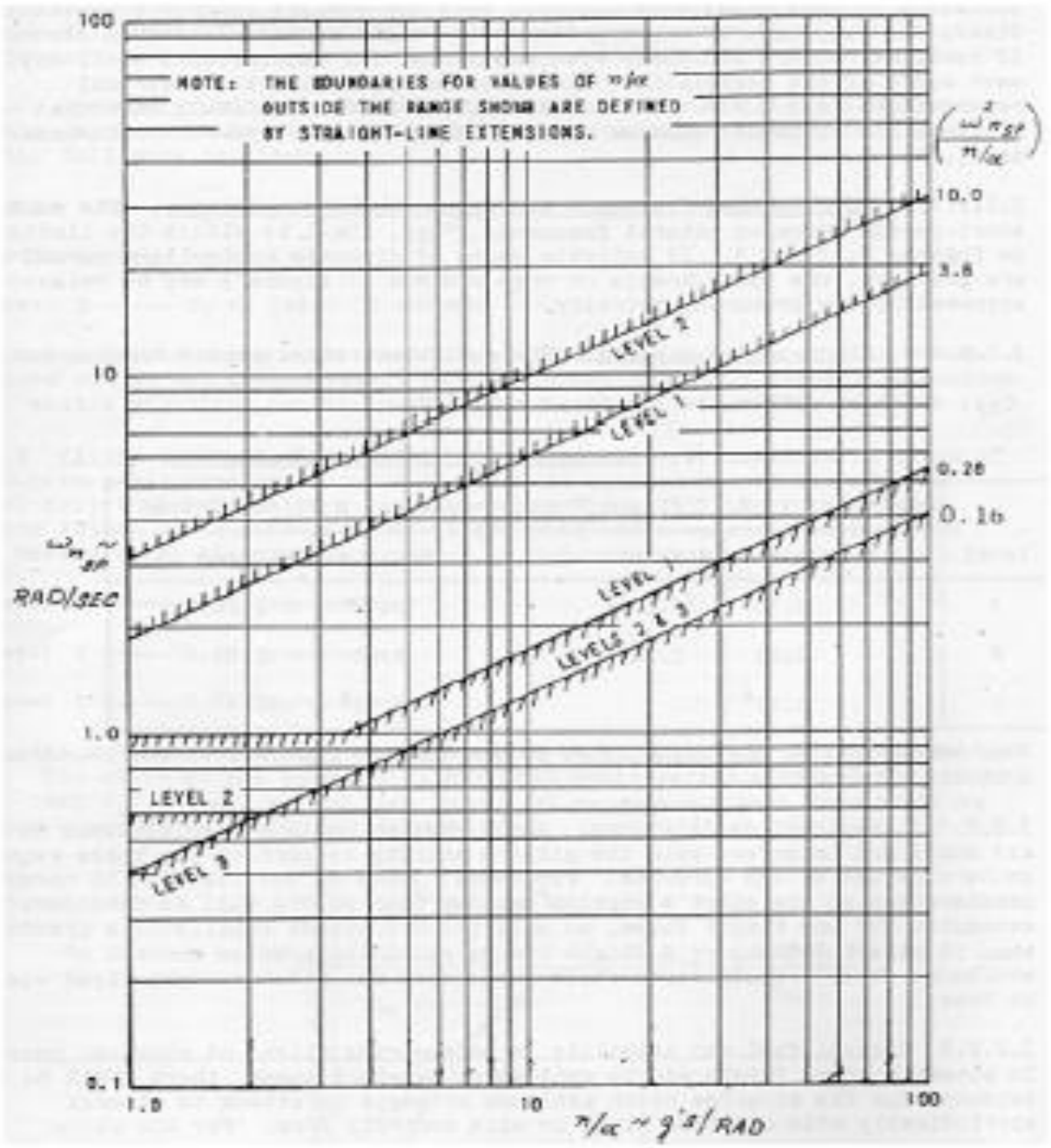

Fig. 7.19 MIL-F-8785C short period natural frequency requirements—Category A flight phases.

7.4.4.2 MIL-STD-1797A. MIL-STD-1797A provides almost identical requirements for the short period mode to those presented in MIL-F-8785C. The terms "equivalent frequency" and "equivalent damping ratio" are used, as with MIL-F-8785C, to account for the dynamics experienced by highly augmented aircraft. The concepts of short period natural frequency and damping ratio are retained when using these guidelines. The MIL-STD-1797A short period requirements are recast in terms of the control anticipation parameter (CAP) over an

Source from Yechout, T.R. "Introduction to Aircraft Flight Mechanics", AIAA education Series, 2003

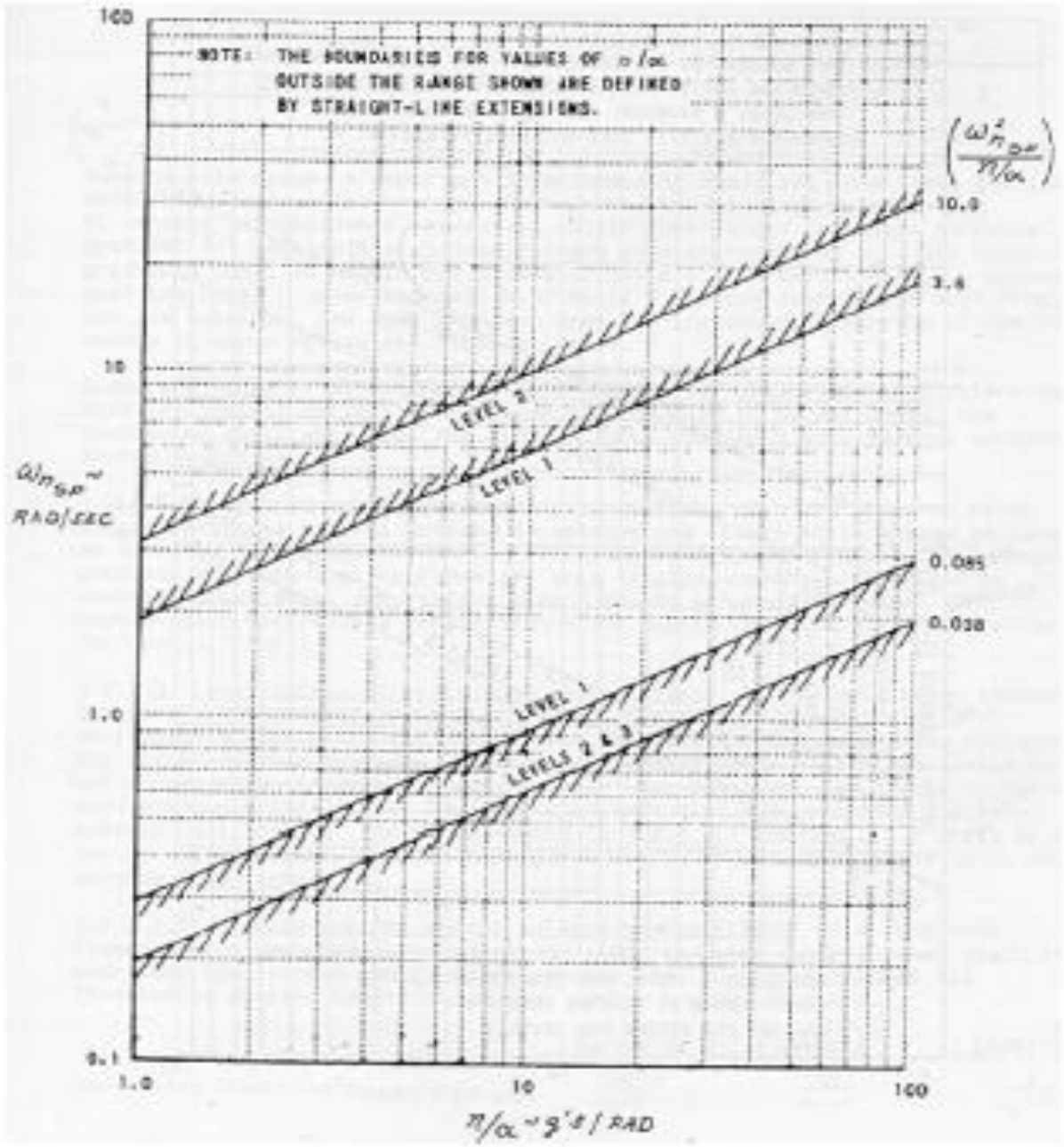

Fig. 7.20 MIL-F-8785C short period natural frequency requirements—Category B flight phases.

acceptable range of damping ratios. The CAP is estimated as

$$\text{CAP} \approx \frac{\omega_{n_{sp}}^2}{n/\alpha} \tag{7.60}$$

The CAP is represented on Figs. 7.19, 7.20, and 7.21 as the sloped boundaries of the Level 1, 2, and 3 regions. MIL-STD-1797A presents short-period compliance regions in terms of the CAP (which is directly proportional to the

Source from Yechout, T.R. "Introduction to Aircraft Flight Mechanics", AIAA education Series, 2003

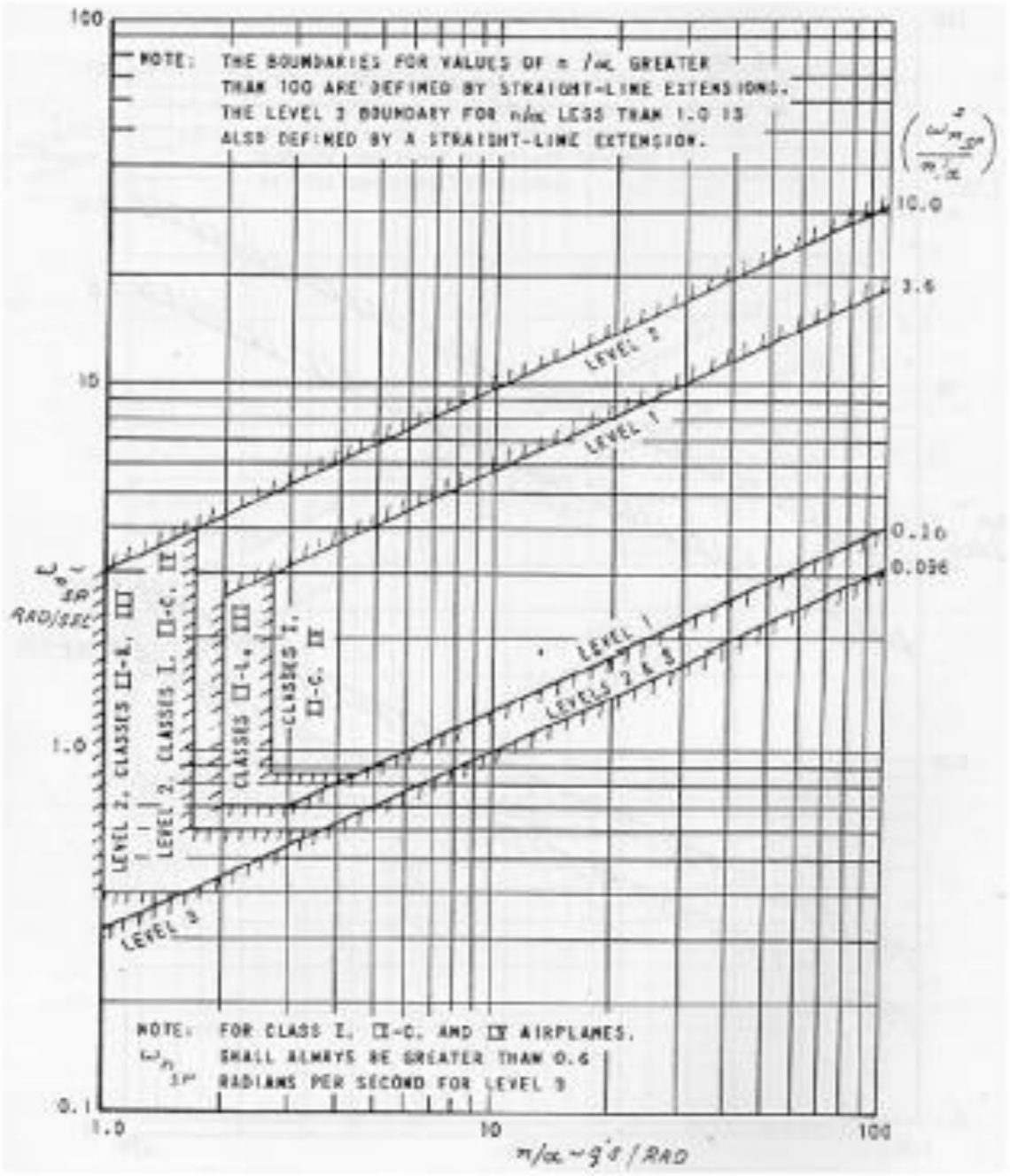

Fig. 7.21 MIL-F-8785C short period natural frequency requirements—Category C flight phases.

square of short period natural frequency) and damping ratio using Fig. 7.23. The only difference between the MIL-F-8785C requirements and those presented in Fig. 7.23 is that MIL-STD-1797A has dropped the lower Level 3 CAP limit. For the short period, these equivalent system requirements work well for highly augmented aircraft as long as the aircraft has a classical-looking response such as with an α-command, q-command, or g-command system (see Chapter 9). They do not work well for nonclassical response types such as

Source from Yechout, T.R. "Introduction to Aircraft Flight Mechanics", AIAA education Series, 2003

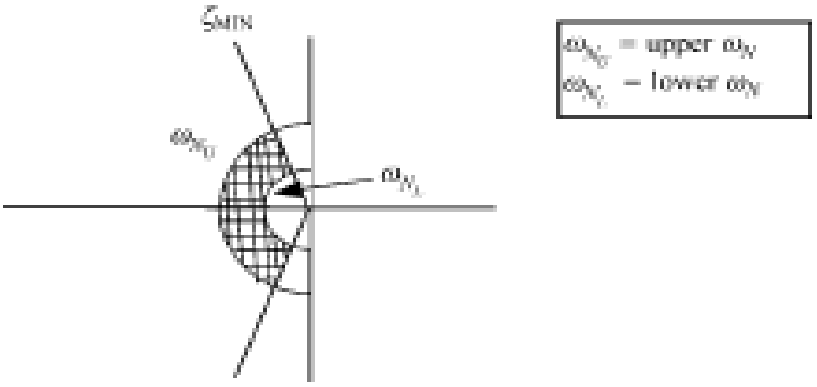

Fig. 7.22 S-plane MIL-F-8785C short period compliance region.

θ-command or flight path command systems. Consequently, MIL-STD-1797A also contains requirements on frequency-response shape that are not defined as a function of the classical dynamic modes discussed in this text.[3]

The level boundaries in Figs. 7.19–7.21 are specified in MIL-STD-1797A using Table 7.8.

In practice, the parameter of equivalent time delay must be considered when applying either MIL-F-8785C or MIL-STD-1797A. Only a snapshot of MIL-STD-1797A has been presented in this section. A detailed reading of this document is necessary for application to an actual aircraft design or flight test evaluation.

7.4.5 Phugoid

MIL-F-8785C has only a requirement on damping ratio for the phugoid mode. This requirement is independent of class and category and is presented in Table 7.9.

For Level 3, the phugoid mode is allowed to be unstable as long as the time to double amplitude is greater than or equal to 55 s. Equation (7.49) can be used to compute T_2. Under Level 3 conditions, a phugoid with neutral or positive stability will always satisfy the Level 3 requirement. The phugoid requirement is not very demanding because the phugoid is a low-frequency mode that generally has little effect on precision tasks. The pilot typically has sufficient time to correct for any undesirable phugoid characteristics. However, it can be important during unattended or divided-attention operation of the aircraft. Figure 7.24 presents the acceptable region for Level 1 phugoid roots on the s plane.

7.4.6 Roll

MIL-F8785C specifies maximum limits on the roll mode time constant (τ_r) which depend on class and category. Table 7.10 presents these requirements.

Source from Yechout, T.R. "Introduction to Aircraft Flight Mechanics", AIAA education Series, 2003

Table 7.10 Maximum roll mode time constant (seconds)

Flight phase category	Class	Level 1	Level 2	Level 3
A	I and IV	1.0	1.4	10
	II and III	1.4	3.0	10
B	All	1.4	3.0	10
C	I, II-C, and IV	1.0	1.4	10
	II-L and III	1.4	3.0	10

Recalling Eq. (7.48), the roll mode root of the characteristic equation is

$$s = -\frac{1}{\tau_r}$$

and the compliance region for the roll mode root becomes

$$s < -\frac{1}{\tau_{r_{max}}}$$

Because the roll mode is first order, the root will lie on the negative real axis and the compliance region as shown in Fig. 7.25.

By specifying a maximum roll mode time constant, MIL-F-8785C is essentially specifying that the step response of the roll mode must be faster than or equal to the time constant value specified.

7.4.7 Spiral

MIL-F-8785C specifies that the spiral mode meet the requirements for the time to double amplitude of the bank angle as presented in Table 7.11 for bank angle disturbances of up to 20 deg. Therefore, an unstable spiral is acceptable if the time to double amplitude is slow enough. Obviously, any stable spiral (negative root of the characteristic equation) is Level 1. The normal flight test

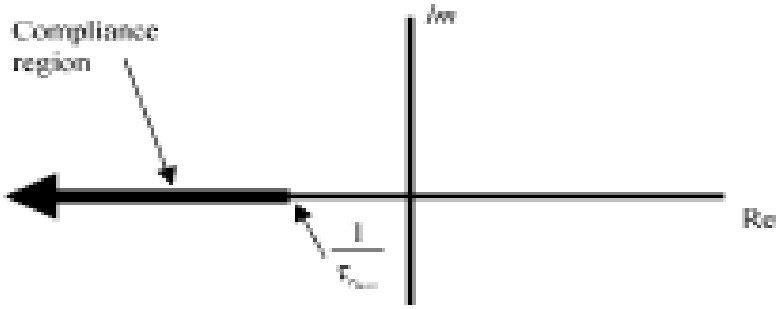

Fig. 7.25 S-plane MIL-F-8785C roll mode compliance region.

Source from Yechout, T.R. "Introduction to Aircraft Flight Mechanics", AIAA education Series, 2003

Table 7.11 MIL-F-8785C spiral mode minimum time to double amplitude

Flight phase category	Level 1	Level 2	Level 3
A and C	12 s	8 s	4 s
B	20 s	8 s	4 s

approach to evaluate the spiral is to trim the aircraft for wings-level, zero-yaw rate flight and then bank the aircraft to a 20-deg roll angle and neutralize the controls. If the time to 40 deg is less than the time specified in Table 7.11, then the spiral requirements of MIL-F-8785C are not met.

Recalling Eq. (7.49), the spiral mode root of the characteristic for an unstable spiral is equal to:

$$s = \frac{0.693}{T_2}$$

Therefore, the compliance region for the spiral root in the s plane becomes everything on the real axis to the left of:

$$s = \frac{0.693}{T_{2_{min}}}$$

The spiral compliance region is shown in Fig. 7.26.

7.4.8 Dutch Roll

The MIL-F-8785C requirements for the dutch roll consist of a minimum ζ, a minimum ω_N, and a minimum $\zeta\omega_N$, as shown in Table 7.12. The table must

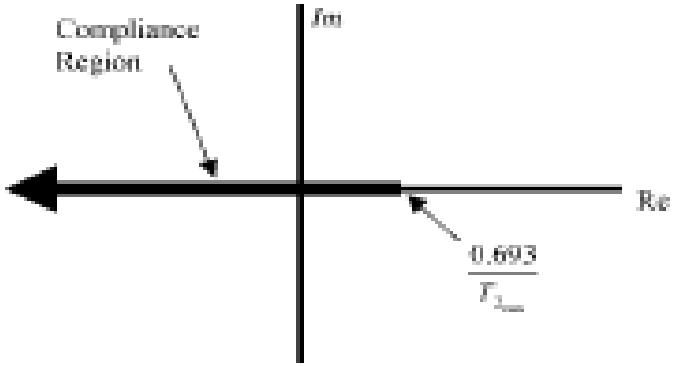

Fig. 7.26 MIL-F-8785C spiral compliance region.

Source from Yechout, T.R. "Introduction to Aircraft Flight Mechanics", AIAA education Series, 2003

Table 7.12 Minimum dutch roll frequency and damping

Level	Flight phase category	Class	Minimum ζ*	Minimum $\zeta\omega_N$,* rad/s	Minimum ω_N, rad/s
	A (CO, GA, RR, TF, RC, FF, and AS)	I, II, III, and IV	0.4	0.4	1.0
	A	I and IV	0.19	0.35	1.0
1		II and III	0.19	0.35	0.4
	B	All	0.08	0.15	0.4
	C	I, II-C, and IV	0.08	0.15	1.0
		II-L and III	0.08	0.10	0.4
2	All	All	0.02	0.05	0.4
3	All	All	0	—	0.4

* The governing damping requirement is that yielding the larger value of ζ_d, except that a ζ_d of 0.7 is the maximum required for Class III aircraft.

be modified if $\omega_D^2|\phi/\beta|_{DR} > 20$ rad$^2/s^2$ by increasing the $\zeta\omega_N$ requirement (details are provided in MIL-F-8785C).

A generalized compliance region for dutch roll roots is presented as the shaded area of Fig. 7.27.

Example 7.15

For the Lear Jet in cruise using the same flight condition (40,000 ft and $M = 0.7$) and data used in Examples 7.10 and 7.12, determine if the aircraft satisfies the dynamic stability requirements of MIL-F-8785C for Level 1.

To start the evaluation, we must first determine the aircraft class and category:

Class II, Category B (Cruise)

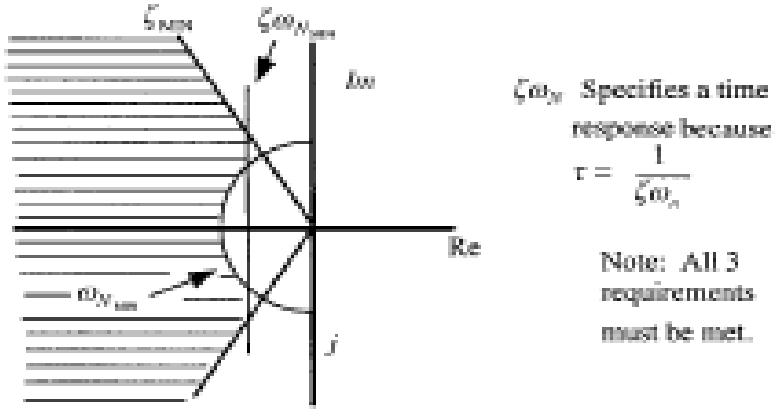

Fig. 7.27 S-plane MIL-F-8785C dutch roll compliance region.

Source from Yechout, T.R. "Introduction to Aircraft Flight Mechanics", AIAA education Series, 2003

Longitudinal Modes of Motion:

Short Period:

From Example 7.10,

$$\omega_{n_{sp}} = 2.836 \text{ rad/s}$$
$$\zeta_{sp} = 0.335$$

Referring to Table 7.7, because $\zeta_{sp} > 0.3$ and $\zeta_{sp} < 2.0$, the Lear Jet passes the damping ratio requirement at Level 1.

To evaluate $\omega_{n_{sp}}$ for compliance, we need to determine n/α. From Eq. (7.59), and knowing that Z_α is equal to -451.7 ft/s^2 for this aircraft and flight condition, we have

$$\frac{n}{\alpha} = -\frac{Z_\alpha}{g} = \frac{451.7}{32.2} = 14.03 \text{ g/rad}$$

Using Fig. 7.20 for a Category B Flight Phase, we plot $\omega_{n_{sp}}$ at an $n/\alpha = 14.03$. The point falls within the Level 1 compliance region and therefore passes the Level 1 short period natural frequency requirement. Because the Lear Jet passes both short period dynamic stability requirements at Level 1, the Lear Jet's short period dynamic characteristics are considered Level 1.

Phugoid:

From Example 7.10,

$$\zeta_{PH} = 0.076$$

Referring to Table 7.9, $\zeta_{PH} > 0.04$ and the Level 1 phugoid requirement is passed.

The Lear Jet (at this flight condition), therefore, meets the MIL-F-8785C Level 1 dynamic stability requirements for the longitudinal modes of motion (short period and phugoid).

Lateral-Directional Modes of Motion:

Roll:

From Example 7.12,

$$\tau_r = 1.972 \text{ s}$$

Using Table 7.10 for Category B, $\tau_r > 1.4$ s and it fails the Level 1 requirement. Because $\tau_r < 3$ s, it passes Level 2. Therefore, the roll mode is Level 2.

Spiral:

From Example 7.12, the spiral mode is stable ($s = -0.00101$) with a time constant of

$$\tau_s = 991.8 \text{ s}$$

Source from Yechout, T.R. "Introduction to Aircraft Flight Mechanics", AIAA education Series, 2003

Because the spiral is stable, the time-to double-amplitude requirements of Table 7.11 are automatically met. Therefore the Lear Jet spiral mode passes the Level 1 MIL-F-8785C dynamic stability requirement.

Dutch Roll:

From Example 7.12,

$$\omega_{N_{DR}} = 1.168 \text{ rad/s}$$
$$\zeta_{DR} = 0.036$$

Referring to Table 7.12, we will look at the dutch roll damping ratio requirement first.

$$\zeta_{DR} = 0.036 < 0.08,$$

so it *fails* Level 1. Because

$$\zeta_{DR} = 0.036 > 0.02$$

it passes Level 2.

We will next look at the Table 7.12 requirement for $\zeta_{DR}\omega_{N_{DR}}$. This product must be greater than 0.15 to pass Level 1. For our case,

$$\zeta_{DR}\omega_{N_{DR}} = 0.0582 < 0.15$$

therefore, it *fails* Level 1 for this requirement. Because $\zeta_{DR}\omega_{N_{DR}} > 0.05$ it barely passes Level 2.

Finally, we must look at the dutch roll natural frequency requirement in Table 7.12. We have

$$\omega_{N_{DR}} = 1.618 \text{ rad/s} > 0.4 \text{ rad/s}$$

therefore, the Lear Jet meets the Level 1 dutch roll natural frequency requirement.

The Lear Jet dutch roll mode is rated Level 2 based on failing the Level 1 $\zeta_{DR}\omega_{N_{DR}}$ dynamic stability requirement in MIL-F-8785C.

The Lear Jet lateral-directional mode is rated Level 2 based on both the dutch roll and roll mode characteristics being rated Level 2.

Overall, the Lear Jet meets MIL-F-8785C Level 2 dynamic stability requirements because of the dutch roll and roll mode characteristics.

Source from Yechout, T.R. "Introduction to Aircraft Flight Mechanics", AIAA education Series, 2003

Dynamic stability

The dynamic stability of an aircraft refers to how the aircraft behaves after it has been disturbed following steady non-oscillating flight,

Types of dynamic stability

It has two types

a) Longitudinal mode

i) Phugoid (longer period) oscillations
ii) Short period oscillations

b) Lateral- directional modes

i) Roll subsidence mode
ii) Dutch roll mode
iii) Spiral divergence

a) Longitudinal mode

Oscillating motions can be described by two parameters, the period of time required for one complete oscillation, and the time required to damp to half-amplitude, or the time to double the amplitude for a dynamically unstable motion. The longitudinal motion consists of two distinct oscillations, a long-period oscillation called a phugoid mode and a short-period oscillation referred to as the short-period mode.

i) Phugoid (longer period) oscillations

The longer period mode, called the "phugoid mode" is the one in which there is a large-amplitude variation of air-speed, pitch angle, and altitude, but almost no angle-of-attack variation. The phugoid oscillation is really a slow interchange of kinetic energy (velocity) and potential energy (height) about some equilibrium energy level as the aircraft attempts to re-establish the equilibrium level-flight condition from which it had been disturbed. The motion is so slow that the effects of inertia forces and damping forces are very low. Although the damping is very weak, the period is so long that the pilot usually corrects for this motion without being aware that the oscillation even exists. Typically the period is 20–60 seconds. This oscillation can generally be controlled by the pilot.

Source from Yechout, T.R. "Introduction to Aircraft Flight Mechanics", AIAA education Series, 2003

ii) Short period oscillations

With no special name, the shorter period mode is called simply the "short-period mode". The short-period mode is a usually heavily damped oscillation with a period of only a few seconds. The motion is a rapid pitching of the aircraft about the center of gravity. The period is so short that the speed does not have time to change, so the oscillation is essentially an angle-of-attack variation. The time to damp the amplitude to one-half of its value is usually on the order of 1 second. Ability to quickly self damp when the stick is briefly displaced is one of the many criteria for general aircraft certification.

b) Lateral- directional modes

"Lateral-directional" modes involve rolling motions and yawing motions. Motions in one of these axes almost always couples into the other so the modes are generally discussed as the "Lateral-Directional modes".

There are three types of possible lateral-directional dynamic motion: roll subsidence mode, spiral mode, and Dutch roll mode.

i) Roll subsidence mode

Roll subsidence mode is simply the damping of rolling motion. There is no direct aerodynamic moment created tending to directly restore wings-level, i.e. there is no returning "spring force/moment" proportional to roll angle. However, there is a damping moment (proportional to roll *rate*) created by the slewing-about of long wings. This prevents large roll rates from building up when roll-control inputs are made or it damps the roll *rate* (not the angle) to zero when there are no roll-control inputs.

Roll mode can be improved by **dihedral** effects coming from design characteristics, such as high wings, dihedral angles or sweep angles.

ii) Dutch roll mode

The second lateral motion is an oscillatory combined roll and yaw motion called Dutch roll,perhaps because of its similarity to an ice-skating motion of the same name made by Dutch skaters; the origin of the name is unclear. The Dutch roll may be described as a yaw and roll to the right, followed by a recovery towards the equilibrium condition, then an overshooting of this condition and a yaw and roll to the left, then back past the equilibrium attitude, and so on. The period is usually on the order of 3–15

seconds, but it can vary from a few seconds for light aircraft to a minute or more for airliners. Damping is increased by large directional stability and small dihedral and decreased by small directional stability and large dihedral. Although usually stable in a normal aircraft, the motion may be so slightly damped that the effect is very unpleasant and undesirable. In swept-back wing aircraft, the Dutch roll is solved by installing a **yaw damper**, in effect a special-purpose automatic pilot that damps out any yawing oscillation by applying rudder corrections. Some swept-wing aircraft have an unstable Dutch roll. If the Dutch roll is very lightly damped or unstable, the yaw damper becomes a safety requirement, rather than a pilot and passenger convenience. Dual yaw dampers are required and a failed yaw damper is cause for limiting flight to low altitudes, and possibly lower Mach numbers, where the Dutch roll stability is improved.

iii) Spiral divergence

Spiraling is inherent. Most aircraft trimmed for straight-and-level flight, if flown stick-fixed, will eventually develop a tightening spiral-dive.[3] If a spiral dive is entered unintentionally, the result can be fatal.

A spiral dive is not a spin; it starts, not with a stall or from torque but with a random, increasing roll and airspeed. Without prompt intervention by the pilot, this can lead to structural failure of the airframe, either as a result of excess aerodynamic loading or flight into terrain. The aircraft initially gives little indication that anything has changed. The pilot's "down" sensation continues to be with respect to the bottom of the airplane, although the aircraft actually has increasingly rolled off the true vertical. Under VFR conditions, the pilot corrects for this deviation from level automatically using the true horizon, while it is very small; but in IMC or dark conditions it can go unnoticed: the roll will increase and the lift, no longer vertical, is insufficient to support the airplane. The nose drops and speed increases: the spiral dive has begun

The forces involved

Say the roll is to the right. A sideslip develops, resulting in a slip-flow which is right-to-left. Now examine the resulting forces one at a time, calling any rightward influence yaw-in, leftward yaw-out, or roll-in or -out, whichever applies. The slip-flow will:

- push the fin, rudder, and other side areas aft of c.g. to the left, causing a right yaw-in,
- push side areas ahead of the c.g. to the left, causing a left yaw-out,
- push the right wingtip up, the left down, a left roll-out owing to the dihedral angle,
- cause the left wing to go faster, the right wing slower, a roll-in,
- push the side areas of the aircraft above the c.g. to the left, a roll-out,

- push the side areas of the aircraft below the c.g. to the left, a roll-in,

  Also, an aerodynamic force is imposed by the relative vertical positions of the fuselage and the wings, creating a roll-in leverage if the fuselage is above the wings, as in a low wing configuration; or roll-out if below, as in a high-wing configuration.

  A propeller rotating under power will influence the airflow passing it. Its effect depends on throttle setting (high at high rpm, low at low) and the attitude of the aircraft.

  Thus, a spiral dive results from the netting-out of many forces depending partly on the design of the aircraft, partly on its attitude, and partly on its throttle setting (a susceptible design will spiral dive under power but may not in the glide).

Recovery

A diving aircraft has more kinetic energy (which varies as the square of speed) than when straight-and-level. To get back to straight-and-level, the recovery must get rid of this excess energy safely. The sequence is: Power all off; level the wings to the horizon or, if horizon has been lost, to the instruments; reduce speed using gentle back-pressure on the controls until a desired speed is reached; level off and restore power. The pilot should be alert to a pitch up tendency as the aircraft is rolled to wings level.

The End